

# **Mechanisms underlying bypass of the essential telomere-capping protein Cdc13**

(1 volume)

Kate Rosalind Mary Clark

Thesis submitted for the degree of Doctor of Philosophy

Institute for Cell and Molecular Biosciences

Newcastle University

February 2016



## Abstract

In *S. cerevisiae*, Cdc13-Stn1-Ten (CST) caps chromosome ends (telomeres). Cdc13 binds telomeric single-stranded DNA and with Stn1 and Ten1 protects the telomere end from attack by DNA damage response (DDR) factors. All three CST genes are essential for cell viability, however the requirement for *CDC13* can be bypassed in strains lacking the nonsense-mediated mRNA decay (NMD) gene *NMD2* and the DDR genes *EXO1* (encoding a 3'-5' exonuclease) and *RAD24* (encoding a DNA damage checkpoint protein).

This PhD aimed to determine the mechanisms underlying Cdc13 bypass. One mechanism identified was that Stn1 is at telomeres in the absence of Cdc13, suggesting that Stn1 has a telomere protection role separate from Cdc13. To uncover the mechanisms underlying Cdc13 bypass, a synthetic genetic array (SGA) screen was conducted using an *nmd2Δ exo1Δ cdc13Δ* query strain crossed with a library of single gene deletion mutants. Rif1, which has telomeric and genome-wide roles, was found to be an absolute requirement for Cdc13 bypass. This result was confirmed by low-throughput methods. By analysing the phenotypes of *rif1* mutant alleles in a viable *cdc13Δ* strain it was possible to deduce the functions of Rif1 required for Cdc13 bypass. Remarkably, the putative HEAT-repeat domain and Glc7 (Protein Phosphatase 1) interaction sites were found to be essential. It is proposed that Rif1 uses this domain to interact with Ten1 to link CST with Rif1/Rap1/Rif2 to form a shelterin-like complex. Finally, evidence was found that Rad52-mediated recombination and long telomeres, with extended TG<sub>1-3</sub> repeats, promote Cdc13 bypass. Overall, multiple mechanisms underlie Cdc13 bypass: Stn1 activity, Rif1 interactions and recombination of telomeric TG<sub>1-3</sub> repeats.

## **Dedication**

This PhD is dedicated to my family.

## Acknowledgements

I would like to thank my supervisor, David Lydall for accepting me as a PhD student, for encouraging me to be ambitious, for giving me the opportunity to speak at two conferences and for his invaluable guidance during my PhD. Also, Eva-Maria Holstein, who discovered the Cdc13-bypass strains lacking Nmd2 and Exo1 or Rad24 and with whom I published a joint-first author paper (the work presented in this thesis is my own contribution to the paper, Eva's work is omitted). Thanks to Richard Knox and Morvus Technology, with whom I started a CASE studentship during my MRes year. I would like to thank David Shore, who provided *rif1* truncation strains and Anne Donaldson, who provided *rif1* truncation plasmids (and offered me a postdoc which I gratefully accepted!). These contributions are detailed in full in the Appendices. I would like to thank Peter Banks and Adrian Blackburn from the High Throughput Service for carrying out my *cdc13*Δ screen. I would like to thank the BBSRC for funding my PhD; I am very fortunate to receive their support. Also a special mention to Alan Leake, who provided invaluable technical support in the lab, and all members of the Lydall Lab for their good advice and friendship.



## Table of contents

<i>List of Figures</i> .....	x
<i>List of Tables</i> .....	xii
<i>Publications</i> .....	xiii
<i>Yeast Nomenclature</i> .....	xiv
<i>List of Abbreviations</i> .....	xv
<b>Chapter 1. Introduction</b> .....	<b>1</b>
1.1 Telomere function.....	1
1.2 Telomeres in cancer and ageing .....	7
1.2.1 <i>Telomere maintenance</i> .....	7
1.2.2 <i>Alternative lengthening of telomeres</i> .....	7
1.3 Telomere end protection: distinguishing telomeres from double-strand breaks.....	9
1.3.1 <i>Double strand breaks</i> .....	9
1.3.2 <i>DNA damage response</i> .....	10
1.3.3 <i>Telomere end protection</i> .....	13
1.3.4 <i>Telomeric repeat-containing non-coding RNA (TERRA)</i> .....	14
1.3.5 <i>Ku</i> .....	15
1.3.6 <i>Rif1, Rap1 and Rif2</i> .....	16
1.4 Cdc13, Stn1 and Ten1 telomere end protection .....	19
1.4.1 <i>CST function</i> .....	19
1.4.2 <i>Cdc13</i> .....	21
1.4.3 <i>The cdc13-1 mutation</i> .....	23
1.4.4 <i>Cdc13 bypass in a pif1<math>\Delta</math> exo1<math>\Delta</math> strain</i> .....	24
1.4.5 <i>Cdc13 bypass in a rad9<math>\Delta</math> sgs1<math>\Delta</math> exo1<math>\Delta</math> strain</i> .....	24
1.4.6 <i>Cdc13 bypass in an nmd2<math>\Delta</math> and exo1<math>\Delta</math> or rad24<math>\Delta</math> strain</i> .....	26
1.4.7 <i>CTC1 mutations and disease</i> .....	28
1.4.8 <i>Stn1</i> .....	29
1.4.9 <i>Ten1</i> .....	31
1.4.10 <i>A new model of CST function</i> .....	33
<b>Chapter 2. Materials &amp; Methods</b> .....	<b>35</b>
2.1 Yeast strains.....	35
2.2 Plasmids .....	35
2.3 Media.....	35
2.4 Sporulation .....	36
2.5 Tetrad dissection .....	36
2.6 Random spore analysis .....	37
2.7 Growth assay ('spot-testing') .....	38
2.8 Genomic DNA preparation.....	38
2.9 Genomic/Plasmid DNA PCR .....	39
2.10 Colony PCR.....	40
2.11 Lithium acetate transformation .....	41
2.12 Gene deletion .....	41
2.13 Epitope tagging.....	42
2.14 <i>In vivo</i> cloning.....	42
2.15 <i>In vitro</i> cloning .....	44
2.16 Transformation of plasmids into budding yeast .....	44

2.17	Southern blotting .....	45
2.18	Quantitative reverse transcriptase PCR .....	46
2.19	Chromatin immunoprecipitation (ChIP).....	48
2.20	Co-immunoprecipitation (Co-IP) .....	51
2.21	Western blotting.....	52
2.22	Trichloroacetic acid protein extraction .....	53
2.23	Synthetic Genetic Array .....	54
2.24	Growth of yeast strains in ethanol .....	56
<b>Chapter 3.</b>	<b>Stn1 protects the telomere without Cdc13 .....</b>	<b>57</b>
3.1	Viable <i>cdc13Δ</i> strains resemble telomerase-deficient survivors .....	57
3.2	Viable <i>cdc13Δ</i> strains can survive without telomerase .....	60
3.3	Cdc13 bypass is not dependent on Stn1 or Ten1 overexpression.....	64
3.4	The stoichiometry of CST components at telomeres can be altered ..	66
3.5	Stn1 is at telomeres without Cdc13 .....	69
3.6	Telomeric RPA is increased in the absence of Cdc13.....	71
3.7	<i>STN1</i> genetically interacts with <i>RFA3</i> .....	74
3.8	No evidence of a physical interaction between Stn1 and Rfa1, Rfa2 or Rfa3.....	77
3.9	Discussion .....	79
<b>Chapter 4.</b>	<b>Rif1 is required for Cdc13 bypass .....</b>	<b>83</b>
4.1	Genome-wide single gene deletion screens using <i>cdc13Δ</i> and <i>CDC13<sup>+</sup></i> query strains .....	83
4.2	Gene deletions for a number of known complexes behaved similarly in both <i>cdc13Δ</i> and <i>CDC13<sup>+</sup></i> genome-wide screens.....	85
4.3	Viable <i>cdc13Δ yfgΔ</i> strains resemble telomerase-deficient survivors .	87
4.4	Rif1 is required for Cdc13 bypass.....	90
4.5	Evidence that Rif1 DNA damage checkpoint repression is not required for Cdc13 bypass.....	94
4.6	The two most N-terminal Protein Phosphatase I (Glc7) interaction sites on Rif1 are not required for Cdc13 bypass .....	97
4.7	The Rif1 N terminus promotes Cdc13 bypass .....	100
4.8	Rif1 C-terminal interactions with Rap1 or Dbf4 are not required for Cdc13 bypass.....	102
4.9	Domains within the Rif1 HEAT repeats are required for Cdc13 bypass .	105
4.10	Discussion .....	109
<b>Chapter 5.</b>	<b>Rad52 is required for Cdc13 bypass .....</b>	<b>112</b>
5.1	Rad51-dependent recombination is not required for Cdc13 bypass .	112
5.2	Rad52 is required for Cdc13 bypass .....	114
5.3	Discussion .....	118
<b>Chapter 6.</b>	<b>Long telomeres promote Cdc13 bypass.....</b>	<b>121</b>
6.1	Generation of <i>cdc13Δ</i> strains not previously known to be viable .....	121
6.2	Long telomeres promote growth of <i>cdc13Δ</i> strains that are not normally viable .....	123
6.3	Ethanol exposure alters the telomere length of diploids .....	127
6.4	Diploids grown in ethanol produce <i>cdc13Δ</i> strains that are not normally viable .....	131
6.5	The frequency of Cdc13 bypass strains increases with telomere length .....	135
6.6	Discussion .....	138



<b>Chapter 7. General Discussion .....</b>	<b>141</b>
<b>Appendix A. Yeast strains by figure number.....</b>	<b>145</b>
<b>Appendix B. Yeast strains by strain number.....</b>	<b>151</b>
<b>Appendix C. Plasmids .....</b>	<b>157</b>
<b>Appendix D. PCR primers .....</b>	<b>159</b>
<b>References .....</b>	<b>161</b>

## List of Figures

Figure 1. <i>S. cerevisiae</i> telomere phenotypes.....	2
Figure 2. The telomere end replication problem. ....	4
Figure 3. Telomere structure in yeast and humans.....	6
Figure 4. Double-strand break repair .....	11
Figure 5. RPA and CST .....	12
Figure 6. Nonsense-mediated mRNA decay.....	27
Figure 7. Telomeres of viable <i>cdc13Δ</i> strains resemble those of telomerase-deficient survivors .....	59
Figure 8. Viable <i>cdc13Δ</i> strains can survive without telomerase .....	63
Figure 9. <i>STN1</i> and <i>TEN1</i> mRNA are not overexpressed in a <i>pif1Δ exo1Δ</i> background .....	65
Figure 10. Stn1 and Ten1 binding to telomeres increases in the absence of Nmd2 .....	68
Figure 11. Stn1 is at telomeres in the absence of Cdc13.....	70
Figure 12. Telomere-bound RPA is increased in the absence of Cdc13.....	73
Figure 13. <i>stn1-13</i> and <i>rfa3-313</i> conditional alleles are synthetic lethal .....	76
Figure 14. No evidence of a physical interaction between Stn1 and RPA .....	78
Figure 15. Hypothetical model of telomere end protection in the absence of Cdc13 .....	82
Figure 16. SGA protocols for <i>cdc13Δ</i> and <i>CDC13<sup>+</sup></i> screens .....	84
Figure 17. Single gene deletions and complexes affecting Cdc13 bypass .....	86
Figure 18. <i>cdc13Δ</i> strains generated by SGA had abnormal telomeres by passage 6 .....	89
Figure 19. Rif1 is required for Cdc13 bypass: evidence from tetrad dissections .....	91
Figure 20. Rif1 is required for Cdc13 bypass: evidence from random spore analysis.....	93

Figure 21. Absence of the Rad24 checkpoint protein does not permit Cdc13 bypass without Rif1 .....	96
Figure 22. Rif1 interaction with PP1 via two N-terminal PP1 interaction motifs is not required for Cdc13 bypass .....	99
Figure 23. The N terminus of Rif1 promotes Cdc13 bypass .....	101
Figure 24. The Rif1 C terminus promotes Cdc13 bypass .....	104
Figure 25. Domains within the Rif1 HEAT repeats are required for Cdc13 bypass .....	108
Figure 26. Hypothetical model in which Rif1 interacts with Ten1 at the telomere end to form a shelterin-like complex .....	111
Figure 27. Cdc13 bypass occurs without Rad51 .....	113
Figure 28. Rad52 is required for Cdc13 bypass (tetrad dissection) .....	115
Figure 29. Rad52 is required for Cdc13 bypass (random spore analysis) .....	117
Figure 30. Generation of unexpected Cdc13 bypass strains .....	122
Figure 31. Diploids with a Cdc13 bypass strain parent have long telomeres ..	126
Figure 32. Ethanol exposure lengthens diploid telomeres .....	130
Figure 33. Genotypes obtained after diploid growth in 1% ethanol .....	132
Figure 34. Genotypes obtained after diploid growth in 3% ethanol .....	134
Figure 35. Percentage of Cdc13 bypass strains obtained after diploid growth in ethanol .....	137

## List of Tables

Table 1. Gene deletions permitting Cdc13 bypass .....	25
Table 2. Ethanol increases the time taken for diploids to complete 50 generations .....	129

## Publications

Holstein, E. M.\*, Clark, K. R.\* and Lydall, D. (2014) 'Interplay between nonsense-mediated mRNA decay and DNA damage response pathways reveals that Stn1 and Ten1 are the key CST telomere-cap components', *Cell Rep*, 7(4), pp. 1259-69.

\*Joint first author

Data from this paper are presented in Chapter 3. The data in this thesis is my own contribution to the paper. Eva's work is omitted from this thesis.

## Yeast Nomenclature

<i>YFG</i>	Wild-type gene
<i>yfg</i> $\Delta$	Gene has been deleted
<i>yfg</i> $\Delta$ <i>C</i>	C-terminal truncation allele
<i>yfg</i> $\Delta$ <i>N</i>	N-terminal truncation allele
<i>yfg::XXX</i>	Denotes that the gene <i>yfg</i> has been disrupted by the integration of gene <i>XXX</i>
<i>Yfg</i>	Denotes that this is a protein
<i>yfg-m</i>	Denotes a conditional mutation of <i>YFG</i> (e.g. <i>cdc13-1</i> )

## List of Abbreviations

5-FOA	5-fluoroorotic acid
aa	amino acids
ALT	Alternative lengthening of telomeres
ARG	Arginine
BIR	Break induced replication
BSA	Bovine serum albumin
bp	base pairs (nucleotides)
ChIP	Chromatin immunoprecipitation
Chr VI-R	Chromosome VI, right arm
Co-IP	Co-immunoprecipitation
CST	Cdc13/Stn1/Ten1
DAmP	Decreased abundance by perturbation of mRNA
DDR	DNA damage response
DEPC	Diethyl pyrocarbonate
DMSO	Dimethyl sulfoxide
DNA	Deoxyribonucleic acid
DSB	Double-strand break
dsDNA	Double-stranded DNA
DTT	DT-dithiothreitol
EGS	Ethylene glycol-bis(succinic acid N-hydroxysuccinimide ester)
ESM	Enriched sporulation medium
g	gramme
HEAT	Huntingtin, elongation factor 3, Protein Phosphatase 2A, and yeast kinase TOR1
HIS	Histidine
HR	Homologous recombination
IP	Immunoprecipitation
kb	Kilobases (nucleotides)
kDa	KiloDaltons
Ku	Yku70/Yku80 complex
L	Litre
LEU	Leucine
LiAc	Lithium acetate

LYS	Lysine
M	Molar
µg	Microgrammes
µL	Microlitre
mg	Milligrammes
mL	Millilitre
MRN	Mre11/Rad50/Nbs1 complex
MRX	Mre11/Rad50/Xrs2 complex
ng	nanogrammes
NHEJ	Non-homologous end joining
NMD	Nonsense mediated mRNA decay
PBS	Phosphate-buffered saline pH 7.5
PBST	PBS with 0.1% (v/v) Tween-20
PCR	Polymerase chain reaction
PDs	Population doublings
PEG	Polyethylene glycol
PMSF	Phenylmethyl sulfonamide
PP1	Protein phosphatase 1
QFA	Quantitative fitness analysis
qPCR	Quantitative polymerase chain reaction
qRT-PCR	Quantitative reverse-transcriptase polymerase chain reaction
RNA	Ribonucleic acid
RPA	Rfa1/Rfa2/Rfa3 (yeast); RPA1/RPA2/RPA3 (humans)
SGA	Synthetic genetic array
ssDNA	Single-stranded DNA
TBE	Tris-borate EDTA pH 8.3 (Bio-Rad)
TCA	Trichloroacetic acid
TERRA	Telomeric repeat-containing non-coding RNA
TPE	Telomere position effect
TRP	Tryptophan
URA	Uracil
YPD	Yeast extract, peptone, dextrose



# Chapter 1. Introduction

## 1.1 Telomere function

Telomeres are the ends of eukaryotic chromosomes and typically contain tracts of repeated, non-coding nucleotide sequences. Telomeres protect DNA at the chromosome end from degradation and so stabilize chromosome ends. The length of telomeres varies between species, for example human telomeres can be from 5,000-15,000 base pairs of TTAGGG repeats whereas budding yeast (the unicellular eukaryotic organism *Saccharomyces cerevisiae*) telomeres are typically  $300 \pm 75$  bp and consist of series of TG<sub>1-3</sub> repeats (Larrivée *et al.*, 2004). Yeast also contains subtelomeric Y' elements (5.2 kb repeats) and X repeats (0.3-0.375 kb; Figure 1) (Chan and Tye, 1983).

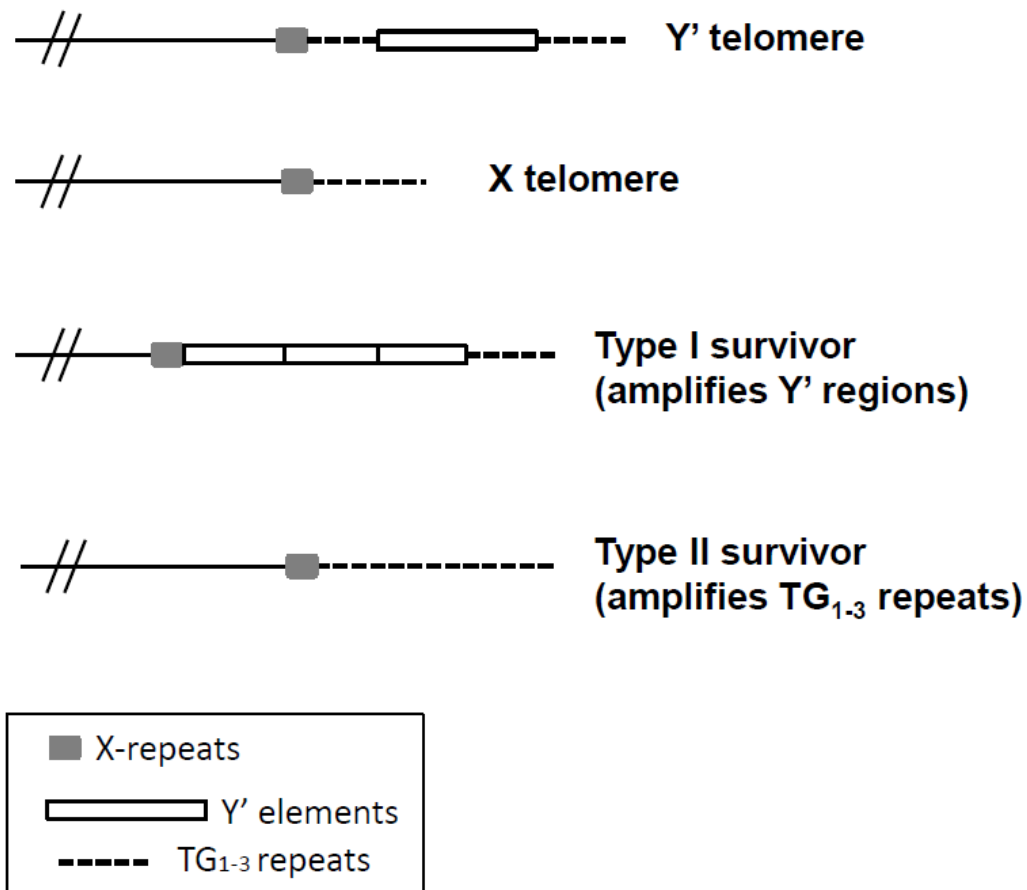


**Figure 1. *S. cerevisiae* telomere phenotypes.**

Normal yeast telomeres contain subtelomeric X repeats and Y' elements and terminate with G-rich (TG) repeats (Y' telomere and X telomere) (Lydall, 2003). Type I survivors amplify Y' elements, which contain autonomous replication sequences, using homologous recombination (Lydall, 2003). Type II survivors amplify G-rich repeats using homologous recombination (Lydall, 2003).

When telomeric DNA is replicated, the 'end replication problem' is encountered (Watson, 1972; Olovnikov, 1973). Replication of the C-rich leading strand occurs continuously such that no overhang is generated (Figure 2). Replication of the G-rich lagging strand occurs discontinuously in Okazaki fragments, using RNA primers (Figure 2). However, when the end of the 5'-3' template strand is reached, the RNA primer cannot bind and thus the final tract of DNA cannot be replicated. This leaves a tract of single-stranded DNA (ssDNA), the 3' overhang, caused by the parental strand overhanging the daughter strand (Figure 2). In mammalian somatic cells the 'end replication problem' means that telomeres shorten every time DNA is replicated, protecting protein-coding DNA from degradation (Harley *et al.*, 1990). When telomere length becomes critically short cells senesce or die (Blackburn, 2000).

Human germ cells and stem cells can maintain telomere length using the telomerase enzyme, which is not expressed in somatic cells. Telomerase is a ribonucleoprotein complex, containing both RNA and protein components, and is a reverse transcriptase that adds telomeric repeats to telomere ends (Greider and Blackburn, 1987). In humans, telomerase comprises a template RNA sequence (TER) (Feng *et al.*, 1995) and a catalytic subunit (TERT), which uses TER as a template to add telomeric repeats (dTTAGGG) to the 3' end of the telomere (Figure 3) (Meyerson *et al.*, 1997; Nakamura *et al.*, 1997). Extension of the 5'-3' strand facilitates fill-in of the 3'-5' strand by DNA polymerase alpha and telomere length is maintained.

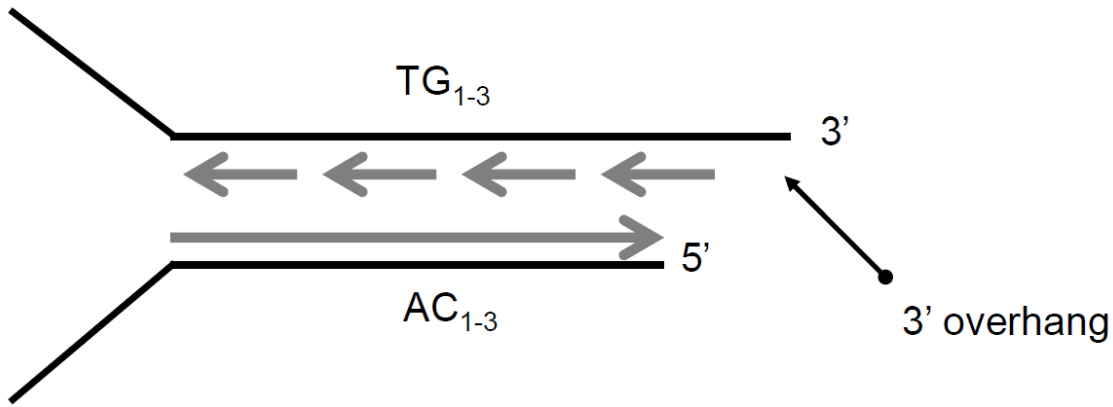


**Figure 2. The telomere end replication problem.**

Eukaryotic telomeres all contain a G-rich strand and a C-rich strand; the G-rich strand overhangs the C-rich strand. During telomere replication, the leading  $C_{1-3}A$  strand is synthesized continuously and the lagging  $TG_{1-3}$  strand is synthesized discontinuously (short arrows) via Okazaki fragments (Lydall, 2003). Lagging strand replication results in a 3' overhang once the RNA primer of the final Okazaki fragment has been removed (Lydall, 2003).

Telomerase is conserved across eukaryotes, for example budding yeast expresses telomerase and so maintains telomere length. The 5'-3' TG<sub>1-3</sub> strand of the budding yeast telomere terminates in a 3' overhang over the C<sub>1-3</sub>A strand at the telomere end. The length of this overhang alters depending on the cell cycle phase; in most phases the overhang is 10-15 nucleotides long, however in late S/G2 phase the overhang is longer (Larrivée *et al.*, 2004). Telomerase maintains telomere length throughout the budding yeast cell cycle and consists of the subunits Est1, Est2, Est3 and Tlc1 (Figure 3). Est2 is the reverse transcriptase element of yeast telomerase (Lingner *et al.*, 1997a; Lingner *et al.*, 1997b) and uses the template RNA provided by Tlc1 to add telomeric repeats to the 3' end of the telomere (Singer and Gottschling, 1994).

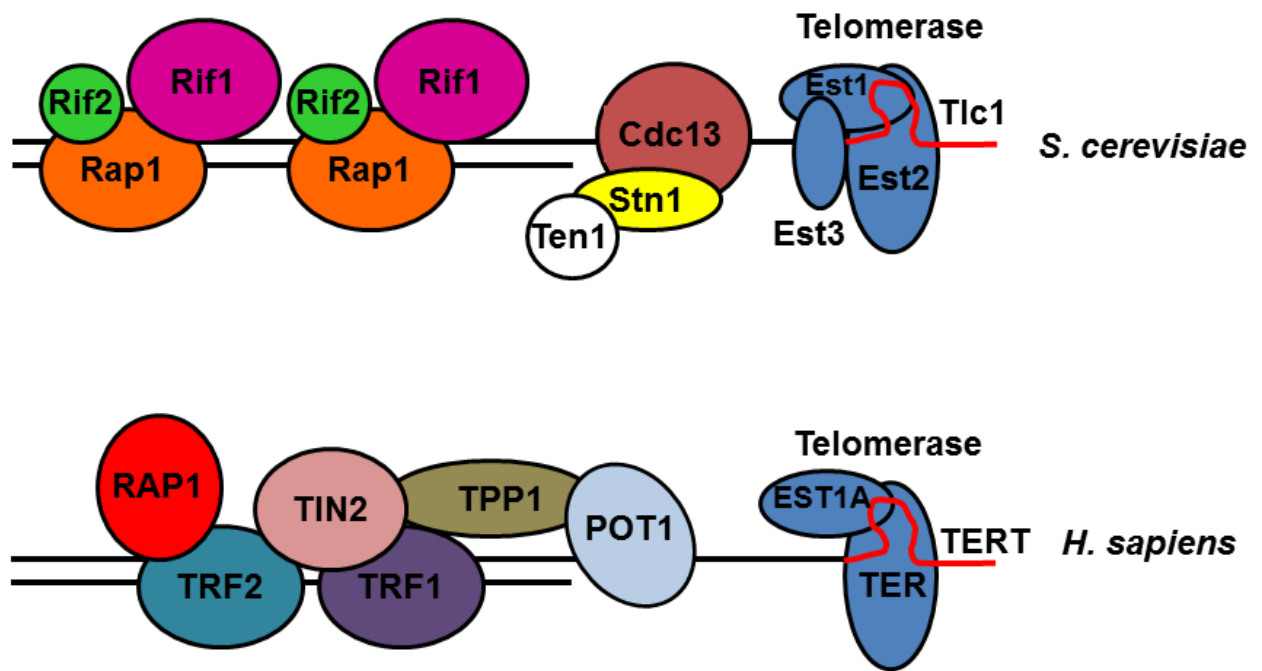


**Figure 3. Telomere structure in yeast and humans.**

*S. cerevisiae* telomeric double-stranded DNA is bound by Rap1, which recruits Rif1 and Rif2. Single-stranded telomeric DNA is capped by CST (Cdc13, Stn1, Ten1) (Lydall, 2009). In *H. sapiens*, telomeric DNA is capped by the Shelterin complex (TRF2, RAP1, TIN2, TPP1, TRF1, POT1), which binds double- and single-stranded DNA. Yeast telomerase consists of Est1, Est2 (telomerase reverse transcriptase, orthologous to human TERT), Est3 and Est4 (telomerase RNA, orthologous to human TER) (Lue, 2010). Human telomerase consists of EST1A, TER, and TERT subunits (Lue, 2010).

## 1.2 Telomeres in cancer and ageing

### 1.2.1 *Telomere maintenance*

Telomerase is not normally expressed in human somatic cells, but telomerase is active in the majority (85%) of cancerous tumours (Günes and Rudolph, 2013). Cancer cells use telomerase to maintain telomere length, this allows cells to escape replicative senescence and divide indefinitely (Kim *et al.*, 1994). Telomere length may be inversely correlated with age, since a number of epidemiological studies have shown that telomere length decreases as age increases (Sanders and Newman, 2013). This is likely to be a function of the end replication problem, in which telomeres shorten with each successive round of replication (Sanders and Newman, 2013). Also, short telomere length is reported in age-related disorders, e.g. arteriosclerosis, and premature ageing disorders e.g. Werner syndrome, Coats plus and *Dyskeratosis congenita* (Blasco, 2005).

### 1.2.2 *Alternative lengthening of telomeres*

15% of cancerous tumours have long, heterogeneous telomeres maintained by a telomerase-independent mechanism termed 'alternative lengthening of telomeres' (ALT) (Bryan *et al.*, 1995; Grobelny *et al.*, 2001). Telomere-capping appears to be defective in ALT cells, which may have decreased levels of TRF2 and other shelterin components relative to the level of telomeric DNA in the cell (Conomos *et al.*, 2013). Defects in the telomere cap promote homologous recombination (HR), which is used to copy telomeric repeats from the same telomere, the sister chromatid or a non-homologous chromosome (Dunham *et al.*, 2000; Muntoni *et al.*, 2009; Conomos *et al.*, 2013). The nuclei of ALT cells contain promyelocytic nuclear bodies that contain the Mre11-Rad50-Nbs1 (MRN) complex, which facilitates HR (van den Bosch *et al.*, 2003; Conomos *et al.*, 2013). The budding yeast MRX complex (Mre11-Rad50-Xrs2) is a functional orthologue of the MRN complex and Mre11 and Rad50 are highly conserved. MRX functions include telomerase recruitment, HR, Rad51-

independent repair of double-strand breaks (DSBs) and non-homologous end joining (Symington, 2002; Faure *et al.*, 2010).

Yeast cells can also maintain telomeres without telomerase (e.g. *tlc1* $\Delta$  mutants) using a mechanism similar to break-induced replication (BIR) (Lundblad and Blackburn, 1993). During BIR at a DSB, 5' DNA ends are resected to form a 3' overhanging tract of ssDNA, to which Rad51 binds (Wu *et al.*, 2008). Rad51-coated 3' ended ssDNA searches for homology in another chromosome and invades the homologous dsDNA (Aylon and Kupiec, 2004). The DNA replication machinery then proceeds to copy the missing genetic information (Wu *et al.*, 2008). Rad51 is highly conserved between yeast and humans (59% homology) (McEachern and Haber, 2006). Rad51-dependent recombination also requires Rad52, Rad54, Rad55 and Rad57. In Rad51-independent recombination, complementary DNA either side of the DSB is annealed together (single-strand annealing) in a process catalysed by Rad52 in the presence of RPA (Wu *et al.*, 2008). The process also involves Rad50, Mre11, Xrs2, Rad59 and Tid1 (McEachern and Haber, 2006).

Yeast cells in which telomeres have been amplified without telomerase are classed as Type I survivors (which amplify subtelomeric Y' regions) and Type II survivors (which amplify TG<sub>1-3</sub> repeats; see Figure 1) (Lundblad and Blackburn, 1993; Chen *et al.*, 2001). Type I survivors require Rad51, Rad52, Rad54, Rad55 and Rad57 and recombination between Y' regions and telomeric TG repeats occurs since Y' regions contain homologous TG repeats (Lundblad and Blackburn, 1993; Paques and Haber, 1999; McEachern and Haber, 2006). Type II survivors require Rad52 in budding yeast and also MRX and Rad59 (Symington, 2002; McEachern and Haber, 2006).

In budding yeast the generation of survivors is dependent on Rad52, which is essential to BIR (Lundblad and Blackburn, 1993; Chen *et al.*, 2001). Rad52 both facilitates the binding of Rad51 to ssDNA and facilitates annealing of ssDNA during DSB repair by homologous recombination (Symington, 2002). When Rad51-dependent recombination occurs the *rad51* $\Delta$  mutants are defective in Rad51-dependent HR but the effects on fitness is mild since the Rad51-independent pathway takes over. At the telomere, single-strand



annealing may occur by the 3' telomeric overhang being annealed to another telomere end (McEachern and Haber, 2006). Since Rad52 is involved in both Rad51-dependent and Rad51-independent DSB repair by HR, *rad52* $\Delta$  mutants are severely defective in DNA repair by HR/BIR and thus *tlc1* $\Delta$  *rad52* $\Delta$  strains fail to form survivors and they senesce rapidly (Lundblad and Blackburn, 1993; Wu *et al.*, 2008).

### **1.3 Telomere end protection: distinguishing telomeres from double-strand breaks**

#### *1.3.1 Double strand breaks*

Double-strand breaks may occur during DNA replication and must be repaired faithfully to ensure genome stability. At a double strand break (DSB), the DNA damage response (DDR) is initiated and involves repair of the lesion with concurrent inhibition of the cell cycle; or apoptosis if the lesion is irreparable (Lydall, 2009). Lesion repair can occur via either non-homologous end joining (NHEJ), in which the ends of the DSB are joined together, or homologous recombination (HR), which allows faithful replication of the chromosome by using homologous template DNA and is the major repair pathway in budding yeast (Li and Heyer, 2008; Lydall, 2009).

Rad24 is involved in the DDR for DSBs at G1, S and G2/M phases and in meiosis (Siede *et al.*, 1994; Lydall *et al.*, 1996; Paulovich *et al.*, 1997). When a DSB occurs (which contains ssDNA tracts), Rad24-Replication Factor C (RFC) complex loads the Rad17/Mec3/Ddc1 sliding clamp. Upon clamp loading, Ddc1-dependent activation of Mec1 occurs, the Dpb11 checkpoint sensor is recruited and Rad24-RFC promotes resection of the DSB end to promote repair by homologous recombination (the major DNA repair pathway in budding yeast) (Ngo and Lydall, 2015). A second pathway, independent of Rad24, involves Rad9, which activates Rad53 and Chk1 and is active at DSBs throughout the cell cycle (Weinert and Hartwell, 1988; Weinert and Hartwell, 1989; Siede *et al.*, 1993; Paulovich *et al.*, 1997). Rad9 stimulates Mec1 to phosphorylate Chk1

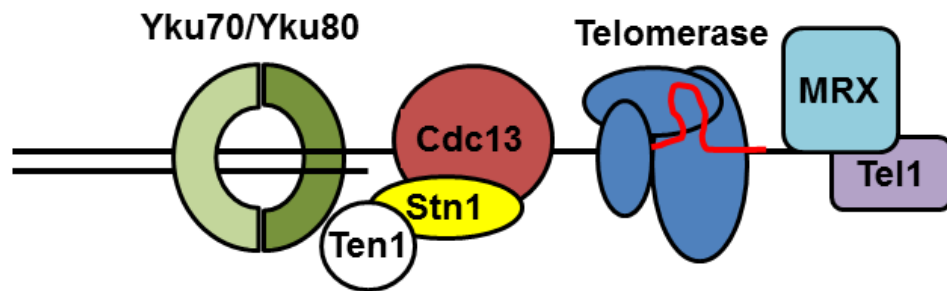
and Rad53, which causes a downstream signalling cascade leading to cell cycle arrest (Blankley and Lydall, 2004; Sweeney *et al.*, 2005; Ma *et al.*, 2006).

### 1.3.2 DNA damage response

During DSB repair in budding yeast (outlined in Figure 4), the MRX and the Ku complex (Yku70/Yku80) are recruited to the lesion and the 5'-3' strand of the DSB is resected by the co-ordinated action of helicases and nucleases (e.g. Exo1) (Tran *et al.*, 2002). MRX also has 3'-5' exonuclease activity at DSBs (Paull and Gellert, 1998). In addition, MRX binds telomeric ssDNA, where it generates ssDNA for the CST complex to bind to, but it may also have a role in recruiting telomeric proteins (Faure *et al.*, 2010). Similarly, Ku binds to telomeric double-stranded DNA (dsDNA) and has a number of roles at telomeres (discussed below).

RPA binds the region of ssDNA created by 5'-3' resection (Figure 5) and is highly conserved between yeast and other eukaryotes. It is formed from the subunits RPA1, RPA2 and RPA3 in mammals and in budding yeast the subunits are called Rfa1, Rfa2 and Rfa3 (Iftode *et al.*, 1999). RPA is functionally orthologous to CST, in that it is a heterotrimer that binds ssDNA (Krejci and Sung, 2002; Gao *et al.*, 2007; Miyake *et al.*, 2009; Sun *et al.*, 2009). Recently, it has been shown that RPA has a role at budding yeast telomeres, in that it binds to the two daughter strands during telomere replication and facilitates telomerase activity (Luciano *et al.*, 2012). At a DSB, RPA helps to recruit Rad51 and Rad52, which are required for lesion repair by HR, and also recruits Rad24 and the Rad17/Mec3/Ddc1 heterotrimer (9-1-1 complex) which are checkpoint proteins that are required to inhibit cell cycle progression during DNA damage repair (Plate *et al.*, 2008; Lydall, 2009; Sugiyama and Kantake, 2009). In addition, RPA binds Mec1 and Ddc2, which stimulate cell cycle arrest and the capping of the telomere by CST, preventing the telomere from being recognized as a DSB (Lydall, 2009).

## Telomere



## Double-strand break

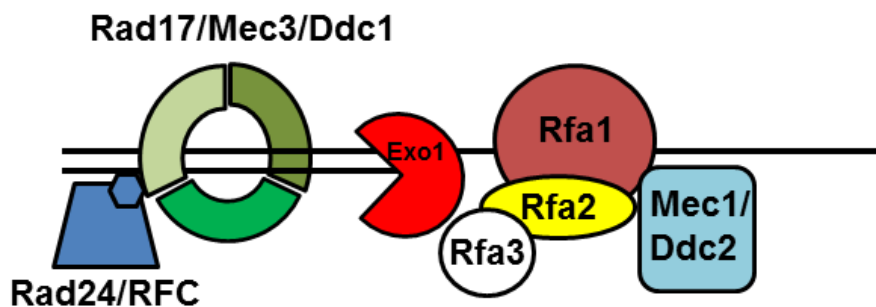


**Figure 4. Double-strand break repair**

Proteins recruited to the telomere end are shown in the top panel, proteins recruited to a double-strand break (DSB) end are shown in the bottom panel. At telomeres, the Mre11/Rad50/Xrs2 (MRX) complex resects DNA to produce single-stranded DNA for CST (Cdc13/Stn1/Ten1) to bind (Lydall, 2009). Yku70/Yku80 binds double-stranded DNA. CST recruits telomerase and Tel1 regulates telomere length. At a DSB, nucleases (such as Exo1, shown) resect DNA to produce overhanging ssDNA (Lydall, 2009). RPA (Rfa1/Rfa2/Rfa3) binds the single-stranded DNA and helps recruit the checkpoint proteins Rad24 (in complex with Replication Factor C), Rad17/Mec3/Ddc1 and Mec1/Ddc2 (Lydall, 2009). Recruitment of Rad9 then pauses the cell cycle at the G2/M checkpoint until the damage is repaired (Lydall, 2009).

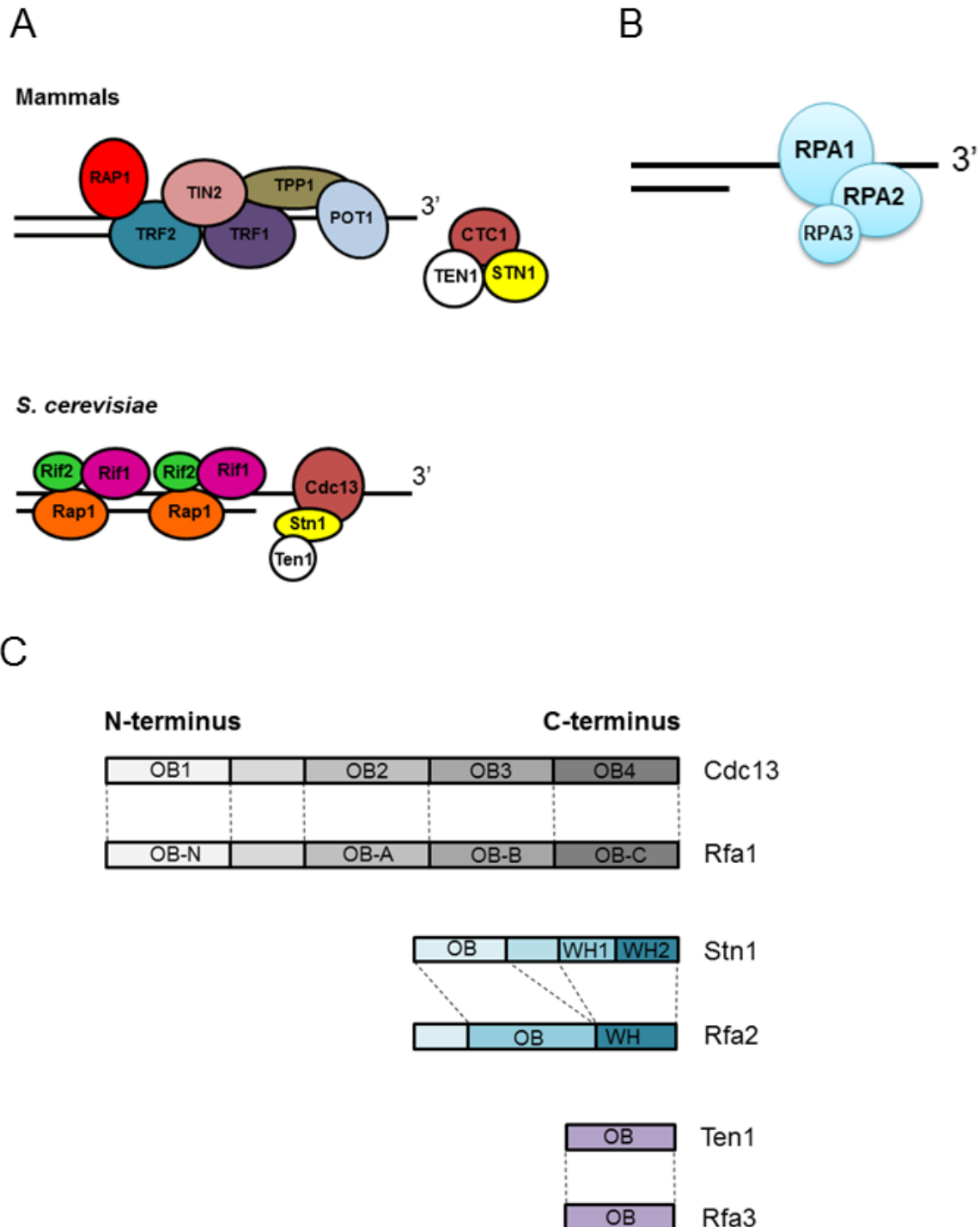


**Figure 5. RPA and CST**

(A) CST in mammals and budding yeast (*S. cerevisiae*). Mammalian CTC1 is the functional orthologue of Cdc13 (Miyake *et al.*, 2009). (B) RPA heterotrimer binds ssDNA and is highly conserved. (C) Structural homologies between CST and RPA (Rfa1/2/3 in budding yeast). OB folds and winged helix (WH) motifs are shown. Dashed lines indicate potential structural homologies between Cdc13 and Rfa1; Stn1 and Rfa2 and Ten1 and Rfa3. Not drawn to scale. Details of structures of RPA and CST were obtained from Sun *et al.* (2011) and Lewis *et al.* (2014).

RPA (Rfa1, Rfa2 and Rfa3) is detectable at budding yeast telomeres during S-phase, where it binds telomeric DNA to facilitate replication and loads the telomerase subunit Est1 onto telomeres (Schramke *et al.*, 2004). Also, Rfa2 (Rpa2) co-immunoprecipitates with Yku80, Est2 and Cdc13 and Rfa1 (Rpa1) co-immunoprecipitates with Cdc13 and Est1 and interacts with Tlc1, which may indicate that a transient Cdc13-Yku70/Yku80-RPA- Telomerase complex is formed during telomere replication (Luciano *et al.*, 2012). In both budding and fission yeasts, RPA genes are essential and mutations in Rfa1 in fission yeast leads to telomere shortening. Also in fission yeast, RPA has been shown to prevent the formation of G-quadruplex structures during lagging strand replication (Audry *et al.*, 2015). During lagging strand replication, the C-rich strand is filled in discontinuously which leaves the template G-rich strand vulnerable to G-quadruplex formation (Audry *et al.*, 2015). G-quadruplexes impede progression of the DNA replication machinery during C-rich strand synthesis.

### 1.3.3 *Telomere end protection*

Telomere ends resemble DSBs, but they are not recognized as such due to the presence of the Rif1-Rap1-Rif2 and the CST and Ku capping complexes in budding yeast (Figure 3). Ku, Rif1-Rap1-Rif2 and CST are discussed in detail in the following sections. In humans the telomere is protected by the shelterin complex, which comprises TRF1, TRF2, TIN2, RAP1, POT1 and TPP1 (Figure 3). RAP1 is highly conserved among eukaryotes, but human RAP1 does not directly bind telomeric DNA unlike budding yeast Rap1 (Li and de Lange, 2003). Pot1 is conserved in *Schizosaccharomyces pombe*. Due to the shelterin complex, human CST does not play as significant a role in telomere capping as it does in budding yeast (Palm and de Lange, 2008). In humans, telomere ends are also structurally protected from DSBs by telomeric t-loops and D-loops, in which the 3' overhang invades telomeric dsDNA (creating the t-loop), and displaces the G-rich strand at this location (creating the D-loop) (Palm and de Lange, 2008).

#### 1.3.4 *Telomeric repeat-containing non-coding RNA (TERRA)*

Protein complexes distinguish telomeres from DSBs to protect yeast and human telomeres (as well as T-loops in human cells). However, in human cells, a further mechanism of telomere protection may be employed: the telomeric C-rich strand is transcribed, from the subtelomeric region to the telomere end, by RNA Polymerase II into telomeric repeat-containing non-coding RNA (TERRA), where it forms a transient DNA:RNA hybrid (Azzalin *et al.*, 2007). TERRA is conserved in budding yeast where it is also transcribed from the telomeric C-rich strand by RNA polymerase II (Luke *et al.*, 2008), but currently it is unknown whether it protects the telomere end.

TERRA has a significant role in the formation of yeast survivors or human ALT cells, which lack telomerase but maintain telomeres by homologous recombination. Yeast cells deficient in the THO complex (involved in transcription elongation, mitotic recombination and mRNA export) and the telomerase RNA component *Tlc1*, formed Type II survivors due to defective telomere transcription (Yu *et al.*, 2014). Strains lacking THO components and *TLC1* also expressed higher levels of telomere-associated TERRA compared to wild-type cells and TERRA expression induced the formation of Type II survivors (Yu *et al.*, 2014). ALT-positive cancer cell lines show high levels of TERRA expression compared to telomerase-positive cancer cell lines (Ng *et al.*, 2009; Arora *et al.*, 2014). Induced TERRA transcription in an ALT cell line (U2OS-derived) elevated TERRA levels and caused telomere instability and increased recombination (Arora *et al.*, 2014). This suggests that TERRA expression can facilitate ALT initiation in cancer cells, similar to TERRA-induced Type II survivor formation in yeast.

Increased levels of TERRA lead to loss of telomeric tracts in human cells and hinder DNA replication in budding yeast, which fail to complete S-phase in a *rat1-1* mutant (Luke *et al.*, 2008). TERRA levels therefore need to be regulated by the cell. In yeast, Rat1 is a 5'-3' exonuclease that directly degrades TERRA and terminates the activity of RNA polymerase II, which transcribes TERRA from the telomeric C-rich strand (Luke *et al.*, 2008; Park *et al.*, 2015). TERRA is also regulated by Ribonuclease H (H1 and H2) in both yeast and humans (Balk

*et al.*, 2013; Arora *et al.*, 2014; Balk *et al.*, 2014; Chan *et al.*, 2014). In human ALT cancer cell lines, Ribonuclease H1 depletion increased TERRA levels and stabilized DNA:RNA hybrids (Arora *et al.*, 2014). Overexpressing Ribonuclease H1 reduced telomere recombination and increased the number of telomere signal-free ends in ALT cells (Arora *et al.*, 2014). Deleting *RNH1* and *RNH201* (the catalytic subunit of yeast Ribonuclease H2) increased the levels of DNA:RNA hybrids globally and at telomeres (Balk *et al.*, 2013; Chan *et al.*, 2014). Overexpressing *RNH1* in yeast reduced Rad52-dependent telomere recombination and caused telomerase-negative yeast cells to senesce at a faster rate, providing further evidence that TERRA is important for survivor formation in yeast (Balk *et al.*, 2013).

### 1.3.5 *Ku*

The Ku complex (Yku70 and Yku80 heterodimer) has a major role in NHEJ but also has a separate role at telomeres (Boulton and Jackson, 1996; Gravel *et al.*, 1998). Unlike Rap1, Ku binds DNA non-specifically, using its ring structure to slide onto DNA termini (i.e. a DSB or telomere end, Figure 4, right panel) (Walker *et al.*, 2001; Pflingsten *et al.*, 2012). When Ku is non-functional (i.e. a *yku70* $\Delta$  or *yku80* $\Delta$  mutant), cells exhibit short telomeres and increased ssDNA (Boulton and Jackson, 1996; Polotnianka *et al.*, 1998). Ku interacts with Cdc13 and Tlc1 (telomerase RNA) and facilitates the localization of telomerase to the nucleus (Stellwagen *et al.*, 2003; Gallardo *et al.*, 2008). When the Ku binding site in Tlc1 is deleted, cells have shorter telomeres; on the other hand when multiple copies of the Ku binding site are present, the abundance of telomerase increased indicating that Ku plays a role in regulating telomerase levels (Peterson *et al.*, 2001; Zappulla *et al.*, 2011). Ku also has a role in the TPE as there is evidence that Yku80 binds to Sir3 and helps to form telomeric heterochromatin-like structures (Roy *et al.*, 2004). It was previously thought that Ku tethered telomerase to the telomere in order to initiate fill-in of the C-strand, however more recent evidence has indicated that Ku regulates nuclear levels of telomerase instead (Pflingsten *et al.*, 2012).

### 1.3.6 *Rif1, Rap1 and Rif2*

Rap1 binds Rif1, which silences subtelomeric transcription and regulates telomere length (Levy and Blackburn, 2004). *rif1* $\Delta$  mutants have abnormally long telomeric TG<sub>1-3</sub> repeats and replicate telomeres early, indicating that Rif1 is required to count TG<sub>1-3</sub> repeats and delay telomere replication until S-phase (Hardy *et al.*, 1992; Levy and Blackburn, 2004; Lian *et al.*, 2011). Rif2 is functionally similar to Rif1 and binds to both Rif1 and Rap1, which suggests that Rap1 recruits Rif1 and Rif2 (Figure 3, Figure 5) to regulate telomere length (Wotton and Shore, 1997). Interestingly, RIF1 is only at damaged telomeres in human cells. At unprotected telomere ends the DDR is activated and telomeric RIF1 foci increase (Silverman *et al.*, 2004). This suggests that RIF1 has a role in DNA damage signalling (Kumar and Cheok, 2014).

Rif1 regulates genome-wide DNA replication as well as having a telomeric role. Rif1 inhibits pre-replication complex activators, namely Cdc7, Dbf4, Dpb11 and Sld3 (but not pre-replication complex assembly) by recruiting the PP1 phosphatase Glc7 to replication origins (Hiraga *et al.*, 2014; Mattarocci *et al.*, 2014). Rif1 interacts with Glc7, through its RVxF and SILK motifs, and uses these motifs to recruit Glc7 to telomeres, where Rif1-Glc7 controls firing of telomere-proximal origins (Hiraga *et al.*, 2014; Mattarocci *et al.*, 2014). During replication initiation, the MCM pre-replication complex (Mcm2-7) is loaded onto replication origins and is phosphorylated by the Dbf4-dependent kinase, DDK (Cdc7-Dbf4 complex). Glc7 is directed by Rif1 to dephosphorylate MCM and counteract DDK phosphorylation, in order to control the timing of replication origin firing (Labib, 2010). Rif1 also controls the timing of telomere replication by recruiting Glc7 to telomeres to control telomeric origin firing: at two telomeres studied, telomeric origins fired earlier in the absence of Rif1 (Hiraga *et al.*, 2014; Mattarocci *et al.*, 2014). Overall, yeast Rif1 represses origin firing in order to orchestrate timely DNA replication both throughout the genome and at telomeres. Recently, it was reported that human RIF1 has a role in controlling sister chromatid cohesion during replication. RIF1 binds ultrafine DNA bridges, which form between sister chromatids during DNA replication. Binding of RIF1,



along with PICH, BLM and RPA1 resolves ultrafine DNA bridges such that sister chromatids can fully separate at the end of replication (Hengeveld *et al.*, 2015).

Rif1 plays a role in resecting dsDNA and there is evidence regarding that it both promotes and inhibits resection in budding yeast. In wild-type cells, Rif1 promotes resection of DSBs, to promote repair by HR, and in the absence of Sae2 and MRX, Rif1 promotes resection (Martina *et al.*, 2014). Therefore deletion of Rif1 inhibits resection in these conditions. Also, Rif1 appears to inhibit resection in cells with defective Cdc13. A *rif1Δ cdc13-1* strain had severe fitness defects above 20°C, and one underlying cause was the accumulation of ssDNA (resulting from enhanced resection) (Anbalagan *et al.*, 2011). It was shown that deletion of the 5'-3' exonuclease *EXO1* reduced ssDNA accumulation and increased strain fitness at restrictive temperatures, as in *cdc13-1 exo1Δ* strains (Zubko *et al.*, 2004; Anbalagan *et al.*, 2011). Deletion of *RIF2* or the C-terminus of Rap1 was shown to significantly increase resection at a *de novo* telomere, but deletion of *RIF1* only marginally increased resection, indicating that Rif1 may only be a weak promoter of telomere resection (Martina *et al.*, 2012; Martina *et al.*, 2014).

Rif1 is thought to stimulate CST activity, since *rif1Δ cdc13-1* strains lose viability above at temperatures above 23°C and a *rif1Δ stn1ΔC* strain is inviable, whereas *rif2Δ cdc13-1* and *rif2Δ stn1ΔC* strains are viable (Anbalagan *et al.*, 2011). Expressing only the N-terminal portion of Stn1, (the N Terminal is used for Ten1 interaction), leads to ssDNA accumulation at the telomere end but not in subtelomeric regions (Puglisi *et al.*, 2008). Moreover, cells expressing Stn1-N terminal show no alternations in subtelomeric gene silencing (the TPE), suggesting that the effects of Stn1-N occur at the telomere end, independently of the Rap1-mediated TPE (Puglisi *et al.*, 2008).

Conversely, human RIF1, together with 53BP1, inhibits resection of DSBs by BRCA1 in G1 phase, to promote NHEJ at DSBs (Chapman *et al.*, 2013). Rif1 is of increasing interest in understanding cancer, given that human RIF1 and 53BP1 inhibit BRCA1, to inhibit resection of DSBs in G1. BRCA1 inhibition promotes NHEJ in G1 rather than repair by HR (class switching), which occurs in G2 (Silverman *et al.*, 2004). BRCA1 mutations carry a high risk of breast and

ovarian cancer in humans, since mutations lead to defective DNA damage repair and hence genome instability. Human RIF1 is only present at dysfunctional telomeres, however this may indicate a DDR signalling role in addition to DNA repair class switching (Kumar and Cheek, 2014). Another recently identified role of RIF1 in DNA replication is that it resolves ultrafine DNA bridges between sister chromatids after replication, to ensure timely separation (Hengeveld *et al.*, 2015). RIF1 therefore appears to be directly involved in maintaining genome stability in human cells, by regulating DNA damage repair, signalling DNA damage at telomeres and ensuring sister chromatid separation.

There is evidence that Rif1 controls the threshold at which ssDNA accumulation, caused by telomere uncapping, activates the DDR at telomeres. Significantly, Rif1 represses the DDR by independently associating with ssDNA lesions to stop DDR proteins such as RPA, Mec1, Rad24, Ddc1, Ddc2 and Rad9 sensing the damage and inducing cell cycle arrest (Xue *et al.*, 2011; Ribeyre and Shore, 2012). It has been proposed that Rif1 stimulates CST activity, by perhaps making contacts with Stn1 or Cdc13 to form a shelterin-like dsDNA-ssDNA telomere capping complex, since *rif1* $\Delta$  *cdc13-1* strains have poor viability and *rif1* $\Delta$  and *stn1* $\Delta$ C mutations are synthetic lethal (Anbalagan *et al.*, 2011). However, temperature-sensitive *cdc13-1* strains (discussed below) accumulate long tracts of ssDNA at restrictive temperatures (Zubko *et al.*, 2004). It is conceivable that in *cdc13-1* strains, grown at permissive temperatures (<25°C), ssDNA is generated at the telomere due to telomere capping defects and DDR activation is inhibited by Rif1 (Xue *et al.*, 2011).

At restrictive temperatures, ssDNA tracts extend beyond the telomere and the reach of Rif1, which activates the DDR and causes cell cycle arrest (Xue *et al.*, 2011). Therefore, rather than stimulating Cdc13/CST activity, Rif1 could protect against damage caused by Cdc13/CST dysfunction. Rif1 and Rif2 have been shown to block DNA damage checkpoint activation at short tracts (80 bp) of telomeric TG repeats by binding to ssDNA to form a protective cap (Ribeyre and Shore, 2012). However, Rif1 and Rif2 do not cap longer TG tracts (250 bp) or block accumulation of DDR factors, yet the tracts do not undergo resection (Ribeyre and Shore, 2012). In fact, at long and short TG tracts, Rif1 blocks

Cdc13 binding (Rif2 has no effect) and Cdc13 protects against resection (Ribeyre and Shore, 2012). There is clearly still much debate over the roles of Rif1 in resection, CST activity and DNA damage checkpoint activation. This thesis hopes to contribute to these debates in Chapter 4.

## **1.4 Cdc13, Stn1 and Ten1 telomere end protection**

### *1.4.1 CST function*

Budding yeast CST is thought to be a heterotrimer formed by Cdc13, Stn1 and Ten1 (Figure 5) and is conserved between yeast, plants and vertebrates (Jain and Cooper, 2010). Yeast CST binds telomeric ssDNA, which is the 3' overhang at the telomere end. CST is structurally analogous to the highly conserved RPA (Replication Protein A) heterotrimer (Figure 5), in that both are heterotrimers with ssDNA binding capability and subunits contain a similar number of OB folds in both yeast and humans (Gao *et al.*, 2007; Miyake *et al.*, 2009; Sun *et al.*, 2011). Binding of CST to telomeric ssDNA stops the chromosome end from being recognised as a DSB and therefore stops induction of the DNA damage response (Garvik *et al.*, 1995). It is essential that telomeres are not treated as DSBs, since repair of telomere ends by HR or NHEJ can lead to telomere end-to-end fusions, circular chromosomes and genomic instability (Larrivé and Wellinger, 2006; Lopez *et al.*, 2015).

CST was first identified in budding yeast and components are conserved between yeasts and mammals (Figure 5) (Giraud-Panis *et al.*, 2010). In humans and other mammals CST consists of CTC1, STN1 and TEN1, which are functional orthologues of budding yeast Cdc13, Stn1 and Ten1 respectively (Miyake *et al.*, 2009; Surovtseva *et al.*, 2009). Evidence that CST is a heterotrimer is that CST purifies as a trimeric complex from human cells (Chen *et al.*, 2012) and Stn1, Ten1 and Cdc13 associate in budding yeast in yeast-two hybrid experiments (Grandin *et al.*, 2000; Grandin *et al.*, 2001b). Interestingly, budding yeast CST subunits have not yet been co-purified. Both CTC1 and STN1 (also called OBFC1) in humans have been shown to regulate telomere length, similar to budding yeast Cdc13 and Stn1 (Nugent *et al.*, 1996; Puglisi *et*

*al.*, 2008; Wan *et al.*, 2009; Mangino *et al.*, 2012). Human CST has an affinity for telomeric ssDNA and binds using OB folds 1 and 2 of CTC1, whereas Cdc13 binds ssDNA using the OB3 fold (Mitton-Fry *et al.*, 2004; Miyake *et al.*, 2009).

There is evidence from budding yeast and humans that the CST subunits also have distinct roles at telomeres. In humans, CTC1-, STN1- and TEN1-depleted cells exhibit different phenotypes. TEN1-depleted cells showed a larger increase in chromosome ends lacking telomeres compared to STN1- and CTC1-depleted cells, and both TEN1- and STN1-depleted cells have increased levels of aberrant T-loops compared to CTC1-depleted cells (Stewart *et al.*, 2012; Kasbek *et al.*, 2013). In budding yeast, Cdc13 recruits telomerase to telomere ends (Nugent *et al.*, 1996; Chandra *et al.*, 2001) whereas Stn1 can inhibit telomerase (Puglisi *et al.*, 2008). Both Cdc13 and Stn1 bind to DNA polymerase alpha to promote C-strand fill-in (after G-strand extension) at the telomere end. Cdc13 binds to Pol1, the DNA polymerase subunit of DNA Polymerase alpha (Qi and Zakian, 2000), and Stn1 also directly binds to the Pol12 regulatory subunit of DNA Polymerase alpha at its C-terminus (Petreaca *et al.*, 2006; Puglisi *et al.*, 2008). The other two subunits of DNA Polymerase alpha are Pri1 and Pri2, primase subunits involved in the synthesis of a short RNA primer (7-10 nt), which allows DNA Polymerase alpha to initiate synthesis of Okazaki fragments. This is required for replication of the telomeric lagging strand (Figure 2), in which the C-rich strand is synthesised discontinuously. In *Candida glabrata*, CST stimulates the primase activity of DNA Polymerase alpha and stimulates the switch to polymerase activity (Lue *et al.*, 2014). Specifically, CST was found to shorten the RNA primers and promote elongation of DNA synthesised by DNA polymerase alpha (Lue *et al.*, 2014).

CST components also co-purify with DNA Polymerase alpha in mammalian cells (Casteel *et al.*, 2009). Recently it has been shown that in mouse and human telomeres, CST has a role in filling in the C-rich strand of the telomere, perhaps through DNA Polymerase alpha recruitment (Casteel *et al.*, 2009; Gu *et al.*, 2012; Wang *et al.*, 2012). Mouse and human CST also facilitated the progression of the DNA replication fork at telomeres (Gu *et al.*, 2012; Stewart *et al.*, 2012). Human STN1, and mouse CTC1, has a role in restarting stalled replication forks throughout the genome, which may indicate a role for CST

outside the telomere (Gu *et al.*, 2012; Stewart *et al.*, 2012). A non-telomeric role for CST has also been reported in the yeast *Candida glabrata*, where Cdc13 and CST have been shown to have a low affinity for non-telomeric DNA (Lue *et al.*, 2013). As yet, a non-telomeric role for budding yeast CST has not been identified.

Deletion of *CDC13*, *STN1* or *TEN1* is lethal in budding yeast. However, in *S. pombe*, deletion of *STN1* is lethal but *ten1* $\Delta$  strains are viable; in *C. glabrata*, *cdc13* $\Delta$  strains are inviable but *stn1* $\Delta$  and *ten1* $\Delta$  strains are viable (Sun *et al.*, 2009). Several studies have been conducted using human cell lines depleted for CST subunits, however these are telomerase-positive or ALT cell lines that have abnormal telomere maintenance. Depletion of STN1 in somatic cells (fibroblasts) that lack telomerase activity, leads to telomere dysfunction, erosion of telomeric tracts and acceleration of senescence (Boccardi *et al.*, 2015). Mutations in human CTC1 result in diseases associated with short telomeres and premature ageing, such as Coat's plus and *Dyskeratosis congenita* (Savage, 2012). Given the severity of the CTC1-null phenotype in mice, the premature ageing diseases caused by heterozygous CTC1 mutations and the severity of STN1 depletion in somatic cells, it seems reasonable to conclude that CST is an essential telomere-related complex in higher eukaryotes. Since deletion of any CST component is lethal to budding yeast, it is arguable that budding yeast is a good model to understand the essential functions of CST.

#### 1.4.2 *Cdc13*

Cdc13 is the most extensively studied component of the budding yeast CST complex. Along with Stn1 and Ten1, Cdc13 is essential and cells cannot survive without it. Cdc13 binds strongly to single-stranded TG<sub>1-3</sub> repeats and tethers the CST complex to telomeric ssDNA (Lin and Zakian, 1996; Nugent *et al.*, 1996). Cdc13 then recruits telomerase by interacting with Est1, a regulatory element of telomerase, using its recruitment domain (Figure 5 C) (Chandra *et al.*, 2001; Wu and Zakian, 2011). Cdc13 is both a positive and negative regulator of telomere length, in that Cdc13 first recruits telomerase for G-rich strand extension then recruits Stn1 to a binding site overlapping with Est1

(Nugent *et al.*, 1996; Chandra *et al.*, 2001). Recruitment of Stn1 inhibits telomerase G-rich strand extension and promotes C-rich strand fill-in by DNA polymerase alpha, facilitated by Stn1-Cdc13 (Chandra *et al.*, 2001).

Intriguingly, Cdc13 is less conserved than Stn1 and Ten1, since *S. pombe* has no Cdc13 homologue. There is some debate as to whether Pot1 in *S. pombe* and POT1 in mammals, which is the ssDNA binding protein of the shelterin-like/shelterin complex of these organisms, is the Cdc13 homologue. POT1 suppresses the DNA damage response at human telomeres, which is similar to Cdc13 function, and possesses OB folds for DNA binding (Theobald and Wuttke, 2004; Churikov *et al.*, 2006). Whilst Stn1 has significant sequence homology to human STN1, the two STN1 binding proteins identified in humans (CTC1 and TEN1) show little significant sequence homology to Cdc13 and Ten1 (Miyake *et al.*, 2009). However, both CTC1 and TEN1 contain 3 and 1 OB folds, respectively, which is similar to the 4 OB folds of Cdc13 and 1 OB fold of Ten1 (Miyake *et al.*, 2009; Sun *et al.*, 2011).

Yeast Cdc13 contains 4 OB (DNA-binding) folds (Figure 5) (Sun *et al.*, 2011). OB1 is situated at the N terminus of Cdc13 and binds transiently to the elongated 3' overhangs of S/G2 phase, where it helps to recruit the Pol1 subunit of DNA Polymerase alpha for fill-in of the AC<sub>1-3</sub> strand (Qi and Zakian, 2000; Hsu *et al.*, 2004; Mitchell *et al.*, 2010). The OB3 fold is the DNA binding domain of Cdc13 and binds strongly to telomeric ssDNA (Mitton-Fry *et al.*, 2004). The function of OB4 is currently unknown. It has been postulated that Cdc13 shares homology with Rfa1, since it contains 4 OB folds (Gao *et al.*, 2007; Gelinas *et al.*, 2009), however the structures of the Cdc13 OB folds are markedly different from those of Rfa1 and Cdc13 binds ssDNA with a single OB fold (OB3) unlike Rfa1 which uses two (Sun *et al.*, 2011; Lewis *et al.*, 2014).

A further difference between Cdc13 and Rfa1 is that Cdc13 undergoes homodimerization using the N-terminal OB fold (OB1) to bind to the Pol1 subunit of DNA Polymerase alpha (Sun *et al.*, 2011). Rfa1 is not known to homodimerize (Lewis *et al.*, 2014). Cells expressing Cdc13 defective in OB1-mediated homodimerization have wild-type fitness at temperatures up to 30 °C, however slight fitness defects are apparent at 37 °C (Sun *et al.*, 2011). More

recently it has been shown that OB2-mediated dimerization is required for efficient Stn1 binding to Cdc13 (Mason *et al.*, 2013). The OB2 domain does not bind telomeric DNA or Stn1, which suggests that OB2 dimerization is required for the assembly of the CST complex (Mason *et al.*, 2013). Cdc13 dimerization has no effect on ssDNA binding, since both wild-type and monomer forms bound with DNA equal affinity (Lewis *et al.*, 2014).

### 1.4.3 *The cdc13-1 mutation*

In genetic studies of Cdc13 function, conditional mutants of the *CDC13* gene are used. The most extensively studied conditional mutant is *cdc13-1*, which caps telomeres at 23 °C but is defective in capping at temperatures above 25 °C (Culotti and Hartwell, 1971; Garvik *et al.*, 1995). The *cdc13-1* mutation is a P371S mutation, which disrupts Cdc13-Stn1 binding (and hence CST assembly) (Grandin *et al.*, 2001a; Mason *et al.*, 2013). There is evidence that within the CST complex, Stn1 is primarily responsible for telomere protection, since budding yeast *cdc13Δ* strains are viable when they express Stn1 fused to the Cdc13 DNA binding domain (the strain is defective in telomerase recruitment, however) (Pennock *et al.*, 2001).

At restrictive temperatures, *cdc13-1* cells accumulate telomeric ssDNA and cell-cycle arrest occurs at G2 phase (Garvik *et al.*, 1995). The 5'-3' exonuclease Exo1 generates ssDNA in *cdc13-1* mutants, by resecting telomeric DNA at the chromosome end (Tsubouchi and Ogawa, 2000). Deleting *EXO1* reduces ssDNA levels and increases the fitness of *cdc13-1* strains at 27 °C (Zubko *et al.*, 2004). It is evident therefore that Cdc13 (together with Stn1 and Ten1) protects telomere ends from Exo1 nuclease activity. The DDR occurs at telomeres when telomere uncapping is induced in *cdc13-1* mutants. Rad24, which loads the Rad17/Mec3/Ddc1 checkpoint clamp during the DNA damage response, also helps generate ssDNA in *cdc13-1* mutants and, along with the Rad9 checkpoint protein, induces cell cycle arrest at restrictive temperatures (Lydall and Weinert, 1995; Zubko and Lydall, 2006). Deleting the checkpoint genes *RAD24* or *RAD9* partially restores fitness of the *cdc13-1* mutant at 28 °C (Lydall and Weinert, 1995; Zubko *et al.*, 2004).

#### 1.4.4 *Cdc13* bypass in a *pif1Δ* *exo1Δ* strain

Although *CDC13* is an essential gene, its function may be bypassed if *cdc13Δ* is combined with deletions of genes associated with the DDR (see Table 1 for a complete list). It has been previously reported that a small fraction of *cdc13-1* *exo1Δ* *rad24Δ* cells formed colonies at 36°C, and that *CDC13* could be completely deleted from these strains (Zubko and Lydall, 2006). *CDC13* can be deleted from a *pif1Δ* *exo1Δ* strain, although *cdc13Δ* *pif1Δ* *exo1Δ* spores only form small colonies compared to *CDC13*<sup>+</sup> strains (Dewar and Lydall, 2010). Pif1 is a DNA helicase that unwinds dsDNA during replication, and there is evidence to suggest that along with Exo1, it regulates nuclease activity at telomeres. That is, *cdc13Δ* *pif1Δ* *exo1Δ* mutants do not senesce or generate telomerase-independent survivors and they are dependent on telomerase to maintain their telomeres (Dewar and Lydall, 2010). This supports the model of DDR induction at uncapped telomeres, since attenuation of the DDR by deleting *EXO1* and *PIF1* appears to allow telomerase to access telomere ends.

#### 1.4.5 *Cdc13* bypass in a *rad9Δ* *sgs1Δ* *exo1Δ* strain

Another genetic background in which Cdc13 function can be bypassed is *rad9Δ* *sgs1Δ* *exo1Δ* (Ngo and Lydall, 2010). Rad9, Sgs1 and Exo1 are DDR proteins; Rad9 is a cell cycle checkpoint protein associated with the DDR, Sgs1 is a DNA helicase involved in ALT and, along with Exo1, regulates resection of dsDNA to ssDNA at telomeres (Huang *et al.*, 2001; Johnson *et al.*, 2001; Ngo and Lydall, 2010). *cdc13-1* *rad9Δ* *sgs1Δ* *exo1Δ* strains were viable at 36°C, furthermore *cdc13Δ* *rad9Δ* *sgs1Δ* *exo1Δ* spores formed colonies, indicating that telomere capping counteracts specific proteins associated with the DDR (Ngo and Lydall, 2010). After many passages, a proportion of *cdc13Δ* *rad9Δ* *sgs1Δ* *exo1Δ* strains escaped senescence and resembled telomerase-deficient survivors (Ngo and Lydall, 2010). Viability of *cdc13Δ* *rad9Δ* *sgs1Δ* *exo1Δ* strains indicates that Cdc13 is not required for telomere capping in the absence of DDR proteins Rad9, Sgs1 and Exo1.



Genetic manipulation	Gene function	Reason for Cdc13 bypass	Reference
<i>pif1Δ exo1Δ</i>	<p><u>PIF1</u>: DNA helicase, regulates nuclease activity at telomeres.</p> <p><u>EXO1</u>: Exonuclease associated with DDR, resects DNA at telomeres to produces ssDNA.</p>	Deleting <i>PIF1</i> and <i>EXO1</i> attenuates the DDR and allows telomerase to access the telomere end	Dewar and Lydall (2010)
<i>sgs1Δ exo1Δ rad9Δ</i>	<p><u>SGS1</u>: DNA helicase, involved in ALT, regulates resection at telomeres.</p> <p><u>EXO1</u>: As above.</p> <p><u>RAD9</u>: Checkpoint protein activated by the DDR.</p>	Deleting <i>SGS1</i> and <i>EXO1</i> attenuates the DDR, reducing the treatment of telomeres as DSBs. Deleting the DDR checkpoint protein Rad9 stops cell cycle arrest in response to DNA damage (e.g. an uncapped telomere that resembles a DSB).	Ngo and Lydall (2010)
<p><i>nmd2Δ exo1Δ</i></p> <p><i>nmd2Δ rad24Δ</i></p> <p><i>nmd2Δ exo1Δ rad24Δ</i></p>	<p><u>NMD2</u>: Part of the NMD pathway, which regulates levels of telomeric proteins such as Stn1 and Ten1.</p> <p><u>EXO1</u>: As above.</p> <p><u>RAD24</u>: Checkpoint protein associated with the DDR and repair of DSBs.</p>	<p>Deleting <i>NMD2</i> increases levels of Stn1 and Ten1, which may cap the telomere in the absence of Cdc13. <i>NMD2</i> deletion also attenuates ssDNA production. Deleting <i>EXO1</i> along with <i>NMD2</i> attenuates the DDR by reducing ssDNA production.</p> <p>Deleting <i>RAD24</i> alongside <i>NMD2</i> inhibits the initiation of cell cycle arrest in response to telomere uncapping.</p> <p>Deleting <i>EXO1</i> and <i>RAD24</i> along with <i>NMD2</i> attenuates the DDR and cell cycle arrest.</p>	Holstein <i>et al.</i> (2014)

**Table 1. Gene deletions permitting Cdc13 bypass**

#### 1.4.6 *Cdc13* bypass in an *nmd2Δ* and *exo1Δ* or *rad24Δ* strain

Recently it was reported that cells could survive without *CDC13* in an *nmd2Δ* and *exo1Δ* or *rad24Δ* background (Holstein *et al.*, 2014). Nmd2 is required for the nonsense-mediated mRNA decay (NMD) pathway and interacts with Nam7 and Upf3 (Figure 6). NMD is conserved between yeast and humans (where the major factors are UPF1, UPF2 and UPF3) and degrades mRNA that contains premature stop codons (nonsense mutations) to stop production of truncated proteins (Isken and Maquat, 2008). By degrading aberrant mRNA, NMD regulates cellular levels of 1-10% of proteins in yeast and humans (Isken and Maquat, 2008). NMD also regulates levels of telomeric proteins through degradation of mRNA, for example NMD regulates Stn1 and Ten1 levels (Enomoto *et al.*, 2004). When *NMD2* is deleted, over 200 proteins are overexpressed, including Stn1 and Ten1 (Dahlseid *et al.*, 2003; Guan *et al.*, 2006). Overexpression of Stn1 and Ten1 appears to cause the short telomere phenotype of *nmd2Δ* cells but delays their senescence by perhaps reinforcing CST telomere capping and blocking nuclease access (Dahlseid *et al.*, 2003; Enomoto *et al.*, 2004).

*STN1* and *TEN1* deletion mutants are inviable in an *nmd2Δ* and *exo1Δ* or *rad24Δ* background (Holstein *et al.*, 2014). This indicates that Cdc13 function can be bypassed in certain circumstances but Stn1 and Ten1 functions cannot. The lethal phenotype of *ten1Δ* and *stn1Δ* strains is rescued by expression of the wild-type genes on plasmids (Holstein *et al.*, 2014). Bypass of Cdc13 in an *nmd2Δ* and *exo1Δ* or *rad24Δ* background is supported by previous reports that overexpression of truncated or full-length Stn1 and Ten1 bypasses the requirement for Cdc13 (Petreaca *et al.*, 2006; Petreaca *et al.*, 2007; Gasparyan *et al.*, 2009).

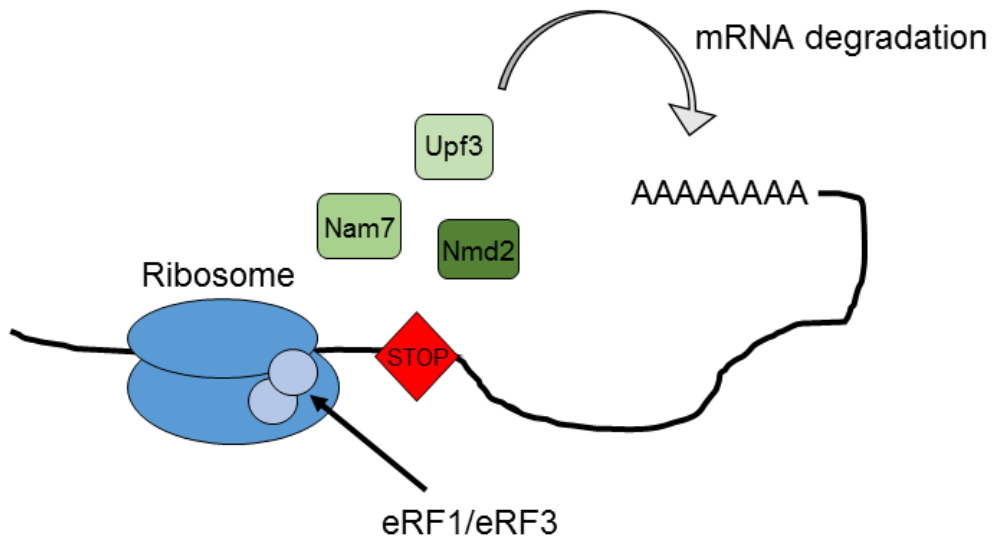


**Figure 6. Nonsense-mediated mRNA decay**

mRNA (shown as a black line with a poly-A tail) can contain premature translation termination (nonsense) codons (indicated by 'STOP'). When the ribosome reaches a nonsense codon, eukaryotic release factors eRF1 and eRF3 bind to the ribosome and recruit Nam7 (Upf1), Nmd2 (Upf2) and Upf3 to initiate degradation of the mRNA (Ikken and Maquat, 2007). This prevents synthesis of a truncated or mutated protein.

#### 1.4.7 *CTC1 mutations and disease*

There is recent evidence that mutations in *CTC1*, the mammalian functional orthologue of *Cdc13*, are tolerated in humans and mice. *CTC1*-null mice have been generated, however they die prematurely from bone marrow failure due to G2/M checkpoint arrest. *CTC1*-null mice exhibit telomere loss, chromosome end-to-end fusions and ssDNA from an enlarged telomeric G-rich overhang, caused by defective C-rich strand fill-in.

Bone marrow failure has been reported in Coats plus patients, which concurs with evidence from mice (Bisserbe *et al.*, 2015). Patients inherit a *CTC1* allele containing a frameshift mutation and the other allele containing a missense mutation, and therefore are heterozygous for *CTC1* mutations (Gu and Chang, 2013). Presumably, homozygous deletions are lethal, given the short lifespan of *CTC1*-null mice (Gu and Chang, 2013). So far, 14 missense mutations, 8 frameshift mutations and 3 in-frame deletions have been identified in *CTC1* in humans (Gu and Chang, 2013). A number of point mutations and in-frame deletions have been shown to interfere with STN1-TEN1 binding or DNA Polymerase alpha recruitment (Chen *et al.*, 2013; Gu and Chang, 2013).

Mutations in *CTC1* have been reported in patients with Coats plus, Cerebroretinal microangiopathy with calcifications and cysts (CRMCC) and *Dyskeratosis congenita*, which are diseases associated with telomere defects (Anderson *et al.*, 2012; Polvi *et al.*, 2012; Romaniello *et al.*, 2012; Walne *et al.*, 2013). *CTC1* frameshift mutations associated with these diseases abolished interaction with STN1 and TEN1 and reduced STN1 interaction with DNA polymerase alpha *in vivo* (Gu and Chang, 2013). Interestingly, no mutations in *STN1* and *TEN1* have been reported in the same sets of patients, indicating that in mammals, as in yeast, STN1 and TEN1 may be more important for telomere maintenance than *CTC1*. In mice, *CTC1* knockouts are viable but do not survive into adulthood; however no *STN1* or *TEN1* knockouts have been reported as yet (Gu *et al.*, 2012).

Although no STN1 or TEN1 mutations have been reported in diseases with telomere defects, single nucleotide polymorphisms (SNPs) have been found in STN1 (and CTC1), although it is unknown what effects these have on protein function. Large-scale genome-wide association studies have shown that SNPs in human STN1 (OBFC1) correlate with shorter telomere length, as do SNPs in CTC1 (Levy *et al.*, 2010; Burnett-Hartman *et al.*, 2012; Mangino *et al.*, 2012; Codd *et al.*, 2013). As yet, no SNPs or other mutations have been reported for Ten1. Two studies have knocked down STN1 and TEN1 in human cells by as much as 95%, however the cells were immortalised tumour cell lines expressing telomerase (Bryan *et al.*, 2013; Kasbek *et al.*, 2013). A more recent study examined the effect of STN1 depletion in normal somatic cells (human fibroblasts) and found that STN1 depletion resulted in telomere erosion and rapid entry into senescence (Boccardi *et al.*, 2015). Interestingly, fibroblasts overexpressing telomerase and depleted for STN1 maintained telomere length and did not rapidly senesce, indicating that telomerase can compensate for deficits in STN1 (hence the effects of STN1 depletion may be masked in telomerase-positive cells) (Boccardi *et al.*, 2015).

#### 1.4.8 *Stn1*

*Stn1* physically associates with Cdc13 and Ten1 in yeast two-hybrid experiments (Grandin *et al.*, 1997; Grandin *et al.*, 2001b). *Stn1* also physically interacts with the Pol12 subunit of DNA polymerase alpha to stimulate fill-in of the C-rich telomeric lagging strand in yeast and higher eukaryotes (Grossi *et al.*, 2004; Petreaca *et al.*, 2006; Gasparyan *et al.*, 2009; Derboven *et al.*, 2014; Lue *et al.*, 2014). *Stn1* is more highly conserved than Cdc13, since homologues are present in *S. pombe* as well as in higher eukaryotes, and human STN1 has significant sequence homology to yeast *Stn1* (Miyake *et al.*, 2009). *Stn1* has an N-terminal OB fold and two winged helix motifs at the C terminus (Sun *et al.*, 2011) whereas human STN1 has an N-terminal OB fold but no winged helix motifs (Miyake *et al.*, 2009). In yeast, the N-terminus of *Stn1* is required for interaction with Ten1 whilst the C-terminus is required for interaction with Cdc13 (Petreaca *et al.*, 2006; Petreaca *et al.*, 2007). Expressing the N-terminus of *Stn1* (amino acids 1-281) was sufficient to rescue the lethality of *stn1Δ*, however

expressing the C-terminal of Stn1 was insufficient (Puglisi *et al.*, 2008). This indicates that Stn1-Ten1 interaction is essential for cell viability but Stn1-Cdc13 interaction is dispensable (Puglisi *et al.*, 2008).

The *stn1-13* mutation (T101S, D134V, T203A, I209V, S393R, M416T) disrupts Stn1 binding to Ten1 and Cdc13 at restrictive temperatures and is synthetic lethal with the *cdc13-1* temperature-sensitive mutation (Grandin *et al.*, 1997; Grandin *et al.*, 2001b). Studying the phenotype of the *stn1-13* temperature-sensitive allele at a restrictive temperature (38°C) showed that *stn1-13* cells accumulate ssDNA, activate the Rad9 and Mec3 G2/M DNA damage checkpoints and undergo cell cycle arrest, similar to *cdc13-1* mutants (Grandin *et al.*, 1997). At semi-permissive temperatures, *stn1-13* cells exhibit long, heterogeneous telomeres perhaps because the *stn1-13* mutations interrupt Stn1-Cdc13 interaction (Grandin *et al.*, 1997). Lack of Stn1 binding to Cdc13 may lead to higher levels of Est1 recruitment, since Est1 competes for Cdc13 binding with Stn1 (Chandra *et al.*, 2001). This may result in longer telomeres, since telomerase has more access to the telomere end. The *stn1-63* mutation is a D99E substitution in the Stn1 N-terminus that leads to telomere uncapping and ssDNA accumulation at restrictive temperatures, although the phenotype is milder than *cdc13-1* grown at restrictive temperatures. This implies that Stn1-Ten1 interaction is important for telomere capping and prevention of DDR activation at the telomere end.

A growing body of evidence suggests that Stn1 is more important for telomere protection and replication than Cdc13. Stn1 fused to the DNA-binding domain of Cdc13 rescues the lethality of a *CDC13* deletion, however telomere replication is defective as Cdc13 is required to recruit telomerase (Pennock *et al.*, 2001). Overexpression of Stn1 or the Stn1 N-terminal and Ten1 together suppresses the temperature-sensitivity of a *cdc13-1* strain and permits growth of 16% of cells deleted for *CDC13*. However, cells deleted for *CDC13* senesced without telomerase (Grandin *et al.*, 1997; Petreaca *et al.*, 2006). Overexpression of the Stn1 C-terminus, which interacts with Cdc13, only partially rescued the *cdc13-1* phenotype (Petreaca *et al.*, 2006). Given that *cdc13-1* disrupts Stn1 binding (Mason *et al.*, 2013) it is perhaps unsurprising that there was only partial rescue. Conversely, overexpression of Cdc13 does

not rescue the *stn1-13* mutation at restrictive temperatures (Grandin *et al.*, 1997). Overexpression of *stn1-13* rescues the *cdc13-1* phenotype up to 30°C (the permissive temperature for *cdc13-1* is below 25°C) and partially rescues *cdc13-1* up to 32°C (Grandin *et al.*, 1997).

Stn1 binds to telomeric ssDNA with higher affinity compared to non-telomeric DNA (Gao *et al.*, 2007), which indicates that Stn1 may not require Cdc13 binding to access telomeric DNA. Indeed, it has been reported that Stn1 is at telomeres in the absence of Cdc13, in a strain defective in NMD and the DDR (Holstein *et al.*, 2014). Furthermore, in *Candida glabrata*, Stn1 alone is responsible for stimulating the primase activity of DNA Polymerase alpha and the OB fold domain or the winged-helix domains on their own can stimulate primase activity (Lue *et al.*, 2014). However, only winged helix 2 interacted with the Pol12, the regulatory subunit of DNA polymerase alpha (Lue *et al.*, 2014). Human STN1 also stimulates DNA Polymerase alpha alone and remarkably, intra-species interactions between Stn1/STN1 and Pol12 are observed using purified proteins from *Candida glabrata* and humans (Lue *et al.*, 2014).

Stn1 appears to share homology with the Rpa2 subunit, since it has a single OB fold and complexes with a larger and smaller subunit (Figure 5) (Gao *et al.*, 2007; Gelinas *et al.*, 2009; Sun *et al.*, 2009). However, the multiple roles of Stn1 in negatively regulating telomerase and regulating DNA polymerase alpha fill-in of the telomeric C-strand would suggest that Stn1 is functionally different. Also, as discussed above, Stn1 and Cdc13 carry out multiple separate roles, which would indicate that they are not necessarily always acting together in a complex.

#### 1.4.9 *Ten1*

Ten1 is an essential protein yet is the smallest component of CST and is conserved in *S. pombe* and in higher eukaryotes (although, as mentioned above, human TEN1 shares no significant sequence homology with yeast Ten1). It has been proposed that Ten1 is analogous to Rpa3, the smallest Rpa subunit, since both share a single OB fold (Gao *et al.*, 2007). In humans, TEN1 depletion has a different phenotype to either STN1 or CTC1 depletion. As

mentioned above, in TEN1-depleted cells there is a larger increase in telomere signal-free chromosomes compared to STN1 and CTC1-depleted cells (Kasbek *et al.*, 2013) indicating that TEN1 may carry out separate telomeric roles to STN1 and CTC1 and may not solely act in complex with its partner proteins.

Ten1 interacts physically with both Stn1 and Cdc13 and Stn1-Ten1 binding is not disrupted by the *cdc13-1* mutation, which disrupts Cdc13-Stn1 binding (Grandin *et al.*, 2001b; Mason *et al.*, 2013). Overexpression of Stn1 and Ten1 together suppress the temperature sensitivity of a *cdc13-1* strain, indicating that Ten1 binding is important for Stn1 activity in either inhibiting telomerase recruitment or stimulating fill-in of the telomeric C-rich lagging strand by DNA polymerase alpha (Grandin *et al.*, 2001b; Petreaca *et al.*, 2006). Interestingly, in *Arabidopsis thaliana*, TEN1 represses telomerase activity but STN1 has little effect (Song *et al.*, 2008; Leehy *et al.*, 2013). Mutants deleted for *STN1* or *CTC1*, or with mutated TEN1, rapidly lose telomeric tracts.

In budding yeast, there is evidence that Ten1 represses telomerase activity. At semi-permissive temperatures, *ten1* temperature-sensitive alleles (*ten1-3* (Q107R), *ten1-6* (K12E) and *ten1-13* (F94L)) had very long, heterogeneous telomeres similar to *stn1-13* mutants at semi-permissive temperatures (Grandin *et al.*, 2001b). Telomere elongation in the *ten1-3*, *ten1-6* and *ten1-13* strains was dependent on telomerase (Grandin *et al.*, 2001b), indicating that (similar to Stn1) Ten1 may negatively regulate telomerase activity.

Ten1 overexpression does not rescue the temperature-sensitive phenotype of *cdc13-1*, however overexpression of Stn1 and Ten1 together does rescue the lethality of *cdc13-1* at restrictive temperatures (Grandin *et al.*, 1997; Petreaca *et al.*, 2006). Mild overexpression (2-fold) of Ten1 in a *stn1* $\Delta$  strain does not restore viability, nor does mild overexpression of Stn1 in a *ten1* $\Delta$  strain (Holstein *et al.*, 2014). However, overexpression of Ten1 in a *stn1-13* strain does reduce the elongated telomeres of a *stn1-13* mutant. Similar to *stn1-13* and *cdc13-1*, two temperature-sensitive alleles of *TEN1*, *ten1-16* (F154I) and *ten1-31* (E58K, L76P, E91V, V115A) accumulate ssDNA, activate the Rad9-mediated G2/M DNA damage checkpoint and undergo cell cycle arrest (Grandin *et al.*, 2001b).



Interestingly, *ten1-16* and *ten1-31* are not rescued by overexpression of either Stn1 or Cdc13 (Grandin *et al.*, 2001b), indicating that neither Stn1 nor Cdc13 can compensate for the role(s) of Ten1. Given that overexpression of Stn1-N terminus and Ten1 together can bypass the requirement for Cdc13 in 16% of cells; Stn1-N terminus expression rescues *stn1Δ* lethality and expression of a Stn1-13-Ten1 fusion protein rescued the telomere elongation phenotype of *stn1-13* mutants (Grandin *et al.*, 2001b; Petreaca *et al.*, 2006; Puglisi *et al.*, 2008), it seems likely that Ten1-Stn1 interaction is important for the function of both proteins. Indeed, Stn1 and Ten1 together can perhaps orchestrate aspects of their telomere-capping activity independently of Cdc13 (Petreaca *et al.*, 2006; Holstein *et al.*, 2014). Temperature-sensitive alleles of Ten1 accumulated ssDNA and activated the Rad9 G2/M checkpoint at restrictive temperatures, similar to *cdc13-1* and *stn1-13* alleles (Grandin *et al.*, 2001b). However, *ten1-3*, *ten1-6* and *ten1-13* strains were not defective in Cdc13 and Stn1 binding (Grandin *et al.*, 2001b), which suggests novel additional role(s) independent of Stn1 and Cdc13.

#### 1.4.10 A new model of CST function

CST in yeast has long been assumed to be an obligate heterotrimer, existing in a 1:1:1 ratio of Cdc13/Stn1/Ten1. The recent research discussed above, both in yeast and humans, has shown that Stn1 and Ten1 have individual roles that may be independent in Cdc13. Furthermore, in *C. glabrata*, CST exists in a 2:4:2 or 2:6:2 arrangement and in budding yeast, the stoichiometry of CST components at telomeres can be altered (Lue *et al.*, 2013; Holstein *et al.*, 2014). The evidence indicates that CST is not necessarily a heterotrimer, as previously thought, and that CST components have separate roles.

Three modes of Cdc13 bypass have been discovered so far (*pif1Δ exo1Δ*; *sgs1Δ exo1Δ rad9Δ* and *nmd2Δ exo1Δ rad24Δ*), but no genetic manipulations that generate *stn1Δ* or *ten1Δ* strains have been found. Therefore, Stn1 and Ten1 appear to be more important for telomere end protection than their partner protein Cdc13. It is possible that Stn1 and Ten1 interact with telomeric proteins

other than Cdc13 in order to protect the telomere end. Candidate proteins are Rfa1/2/3 (RPA), which form an ssDNA-binding heterotrimer.

This thesis investigates the role of Stn1 and Ten1 in Cdc13 bypass using genetic and biochemical methods (Chapter 3). Chapter 4 investigates the cellular mechanisms underlying Cdc13 bypass using a genome-wide screen of single gene deletions that stop Cdc13 bypass. Chapter 5 investigates whether TERRA has a role in Cdc13 bypass, since TERRA may protect the telomere end and promote telomere recombination in the absence of telomerase (which is recruited to the telomere end by Cdc13 interactions). Chapter 6 reports a discovery that diploids with elongated telomere rearrangements can produce *cdc13* $\Delta$  strains with genotypes not previously known to be viable. It is hoped that these results will cast new light on how cells with telomere dysfunction, a hallmark of cancer, evade cell death or senescence. Through further understanding of Cdc13 bypass, it is hoped that promising strategies for future cancer therapies can be developed.

## Chapter 2. Materials & Methods

### 2.1 Yeast strains

*S. cerevisiae* strains used are given in the Appendices, listed by figure (Appendix A) and by strain number (Appendix B). All strains are in the W303 *RAD5* genetic background, apart from strains used for Synthetic Genetic Array screening (see below, 2.23) which are S288C.

### 2.2 Plasmids

Plasmids are listed in Appendix C.

### 2.3 Media

Yeast extract, peptone, dextrose, adenine (YPD) was 10g/L yeast extract, 20g/L bactopectone, 2% (w/v) dextrose and 0.0075% (w/v) adenine. Selective dropout (SD) media lacking uracil (-URA), tryptophan (-TRP), leucine (-LEU), histidine (-HIS), arginine (-ARG) or lysine (-LYS) or combinations thereof was 1.3 g/L dropout powder lacking the specified amino or nucleic acids (detailed below), 6.7 g/L yeast nitrogen base, 5 g/L ammonium sulphate and 2% (w/v) dextrose. Enriched sporulation media (ESM) was 1 g/L yeast extract, 0.05% (w/v) dextrose, 1% (w/v) potassium acetate, 12.5 mg/L histidine, 62.5mg/L leucine, 12.5 mg/L lysine, 12.5 mg/L uracil. Antibiotics were added to media, where specified, at the following concentrations: G418 (200 mg/L), clonNAT (100 mg/L), hygromycin B (300 mg/L). Canavanine and/or thialysine were added to media, where specified, at 50 mg/L. 5-fluoroorotic acid (5-FOA) plates were made with -URA dropout powder (1.3 g/L), yeast nitrogen base (1.7 g/L), uracil (50 mg/L), 5-FOA (1 g/L) and dextrose (2% w/v).

Solid agar plates were made from the same media but with the addition of 2% (w/v) agar.

### Amino/nucleic acids dropout powder recipe

Adenine	2.5g
L-arginine (HCl)	1.2g
L-aspartic acid	6.0g
L-glutamic acid (monosodium salt)	6.0g
L-histidine	1.2g
L-leucine	3.6g
L-lysine (mono-HCl)	1.8g
L-methionine	1.2g
L-phenylalanine	3.0g
L-serine	22.5g
L-threonine	12.0g
L-tryptophan	2.4g
L-tyrosine	1.8g
L-valine	9.0g
Uracil	1.2g

Amino/nucleic acid dropout powder was made by omitting the relevant amino acids from the dropout mix.

## **2.4 Sporulation**

Single diploid colonies were inoculated into 2 mL selective media and incubated overnight in a rotating wheel at 30°C. The culture was then resuspended in 2 mL YPD and incubated overnight at 30°C. 0.3-0.5 mL of culture were extracted, washed twice in 5 mL sterile water, and were resuspended in 2 mL ESM. Cultures were incubated at 23°C for 3-5 days in a wheel, until tetrads of spores were visible.

## **2.5 Tetrad dissection**

Sporulated culture was washed twice in sterile water and resuspended in 500  $\mu$ L sterile water. 20  $\mu$ L of cells were incubated with 1.2  $\mu$ L glusulase (Perkin Elmer) for 11-13 minutes at 30°C. Digestion of the asci were monitored by microscopy. Cells were resuspended in 1 mL water and 50  $\mu$ L of cell suspension were applied, in a line, to a YPD plate and allowed to dry. Standard tetrad dissection techniques were used, using a microscope with a 10X magnification lens and a microneedle to dissect spores onto YPD plates.

Spores were germinated at 23°C for 5 days before photographing and were then patched to YPD for replica-plating to appropriate selective media to determine genotype. Spore viability was determined by counting the number of strains with a given genotype and by counting the number of spores (of the given genotype) that failed to germinate. The genotypes of spores that failed to germinate were determined by inference from a group of three spores from a tetrad (the inference could be made in all cases) or from a group of two spores from a tetrad (the inference could be made in some cases where, for example, two out of four tetrads had the same genotype).

## **2.6 Random spore analysis**

Spores were washed 3 times in sterile water. The pellet was resuspended in 0.5 ml Zymolyase-20T solution (1 mg/mL in sterile water) and 10 µL of β-mercaptoethanol. Cells were transferred to a 15 mL screw-cap conical tube incubated overnight at 30°C on a wheel to preferentially lyse the diploid cells. 5 ml of 1.5% (v/v) NP-40 were added and cells were vortexed. Spores were pelleted at 3000 rpm for 5 minutes. Most of the supernatant was poured off, leaving 1 mL. Spores were resuspended in the remaining 1 mL and transferred to a 1.5mL microcentrifuge tube. Samples were incubated on ice for 15 minutes and were then sonicated (Sanyo Soniprep) on ice for 30 seconds at 10 microns power. Samples were cooled on ice and sonicated again as before. Spores were centrifuged for 30 seconds at 13,000 rpm and the supernatant was removed. Spores were resuspended in 1 mL of 1.5% (v/v) NP-40 and were vortexed and sonicated twice as before. Spores were centrifuged for 30 seconds at 13,000 rpm. The supernatant was removed and spores were resuspended in 1 mL sterile water and vortexed. Spores were sonicated once as before and a 1/10 dilution was counted using a haemocytometer. Spore suspensions were diluted to 1000 spores/mL and 100 µL spores were plated onto YPD (or appropriate selective media if spores contained a plasmid). Spores were germinated at 23°C for 5 days then strains were patched out onto YPD (or selective media if spores contained a plasmid). Strains were genotyped by replica-plating to selective media.

## 2.7 Growth assay ('spot-testing')

Cultures were inoculated from YPD plates into 2 mL YPD (or selective media if the strain had a plasmid) and incubated in a wheel at 23°C if temperature sensitive, otherwise 30°C, until saturated. Serial 1 in 6 dilutions in water were performed using a 96-well plate and multichannel pipette. Dilutions were spotted onto agar plates, YPD or selective media as appropriate, using either a sterilised 8 x 6 pin tool (Sigma Aldrich) for round plates or a sterilised 8 x 12 pin tool (Sigma Aldrich) for rectangular plates. Plates were incubated at 23°C or a range of temperatures, as appropriate, for 3 days.

For growth assays where a strain expressed two plasmids (i.e. *RIF1-URA3* and mutant alleles of *RIF1* on a *TRP1* plasmid), culture densities were equalised by counting with a haemocytometer and diluting down to  $2 \times 10^7$  cells/mL in selective media (i.e. –TRP –URA) and samples were sonicated for 30 seconds (5 microns power, 6 seconds; Sanyo Soniprep) prior to spotting. Plates were incubated for 5 days at 23°C before photographing.

## 2.8 Genomic DNA preparation

For polymerase chain reaction (PCR), genomic DNA was prepared using phenol extraction using the Dewar and Lydall (2012b) method. 2 mL of stationary phase culture were washed twice in water and the cell pellets were stored at -80°C. Pellets were thawed and resuspended in 400 µL of lysis buffer (2% (v/v) Triton X-100, 1% (w/v) SDS, 100 mM NaCl, 10 mM Tris–HCl, pH 8.0, 100 mM EDTA, pH 8.0) and 0.6 g glass beads were added. 400 µL phenol:chloroform:isoamyl alcohol (25:24:1, v/v/v) were added and cells were lysed using a Precellys 24 ribolyser on 5.5 power setting for 6 x 10 seconds (2 minutes pause where samples chilled on ice water between each 10 second lysis). 400 µL Tris-EDTA (10 mM Tris–HCl, pH 8.0, 1 mM EDTA pH 8.0) were added and samples were spun at 13,000 rpm, 4°C, for 5 minutes to separate aqueous and organic phases. 2 mL light phase lock gel tubes (5-Prime) were centrifuged at 13,000 rpm for 1 minute. 750 µL of aqueous phase were transferred to the phase lock tubes and 750 µL phenol:chloroform:isoamyl alcohol (25:24:1, v/v/v) were added. Tubes were centrifuged at 13,000 rpm for

5 minutes. The aqueous (upper) phase were transferred to a 2 mL microcentrifuge tube and 100% (v/v) ethanol was added to fill the tube. Tubes were left for 5 minutes at room temperature. Nucleic acids were harvested by centrifuging at 13,000 rpm for 3 minutes. The pellet was air-dried for 5 minutes and was then resuspended in 806  $\mu$ L TE/RNase solution (7.5  $\mu$ g/mL RNaseA) with incubation at 37°C for 30 minutes. 26  $\mu$ L of 3 M sodium acetate (pH 5.2) were added along with 100% (v/v) ethanol (to fill the tube) to precipitate DNA for 15 minutes. DNA was harvested by centrifugation at 13,000 rpm for 3 minutes and pellets were air-dried. DNA was resuspended in 40  $\mu$ L TE and incubated at 37 °C for 20 minutes. DNA yield and purity was determined using a Nanodrop 2000 (Thermo Scientific).

For Southern blotting and also PCR, genomic DNA was prepared using the Yale method (Maringele and Lydall, 2004). 2 mL saturated cultures were spun down, resuspended in 250  $\mu$ L of 0.1M EDTA (pH7.5), 1:1000  $\beta$ -mercaptoethanol and 2.5 mg/mL zymolyase 20T (Sigma Aldrich) and incubated at 37°C for one hour. 55  $\mu$ L of 0.25M EDTA (pH 8.5), 0.5M Tris, 2.5% (w/v) SDS) were added and samples were incubated at 65°C for 30 minutes. 68  $\mu$ L of 5M potassium acetate (KAc) were added and samples were incubated on ice for 30 minutes. Samples were spun for 20 minutes at 13,000 rpm and the supernatant transferred to a new tube, which was filled with 100% (v/v) ethanol. Samples were inverted and spun for 10 minutes as before. The supernatant was removed and pellets were briefly dried before being resuspended in 130  $\mu$ L TE containing 1 mg/mL RNAase A and incubated at 37°C for 35 minutes. 150  $\mu$ L isopropanol were added, samples were inverted and spun for 20 minutes as before. Samples were washed with 100  $\mu$ L 70% (v/v) ethanol by centrifuging for 5 minutes as before. The ethanol was removed and pellets were dried for 30 minutes. Pellets were resuspended in 40  $\mu$ L TE by incubation at 37°C for 30 minutes.

## **2.9 Genomic/Plasmid DNA PCR**

PCR was performed using genomic DNA or plasmid DNA for gene/cassette amplification. Oligonucleotides used for PCR are listed in Appendix D. Primers used for gene amplification from genomic DNA were 500bp upstream and

downstream of the target gene. Primers for amplification from plasmid DNA had 20bp homology upstream/downstream of the target plasmid insert and 40bp homology to the genomic DNA site in which the target plasmid DNA was to be inserted. 20  $\mu$ L PCR reactions using genomic or plasmid DNA comprised 0.3  $\mu$ M each primer, 0.5 units ExTaq polymerase (TaKaRa Bio Inc), 0.2 mM dNTPs, 1x ExTaq buffer, 4 ng genomic or plasmid DNA and molecular-biology grade water. PCR conditions were 5 minutes 95°C, 35 cycles of 94°C (1 minute) 55°C (1 minute) 72°C (1 minute per kb DNA amplified), then 10 minutes 72°C. The size of PCR products were verified by running samples on 1% (w/v) agarose gels made with 0.5x Tris-Borate-EDTA pH 8.3 (Bio-Rad) and 1x SyBr Safe (1/10,000 dilution; Life Technologies). Gels were imaged using a FujiFilm LAS Image 4000. If to be subsequently used for transformation, PCR products were pooled and purified using a QIAquick PCR purification kit (Qiagen), otherwise products were used without purification.

## **2.10 Colony PCR**

Colony PCR was used to confirm antibiotic/amino acid marker integration after lithium acetate transformation (see below). PCR primers were designed such that the forward primer was within the inserted marker and the reverse primer was around 800bp downstream of the insert location. 10  $\mu$ L PCR reactions using fresh colonies comprised 0.3  $\mu$ M each primer, 25 mM MgCl<sub>2</sub>, 0.5 units GoTaq HotStart polymerase (Promega), 0.25 mM dNTPs, 1x green GoTaq buffer, 1  $\mu$ L cell suspension (in sterile water) and molecular biology-grade water. PCR conditions were 15 minutes 95°C, 35 cycles of 94°C (1 minute) 55°C (1 minute) 72°C (1 minute per kb DNA amplified), then 10 minutes 72°C. The size of PCR products were verified by running samples on 1% (w/v) agarose gels made with 0.5x tris-borate-EDTA pH 8.3 (TBE: Bio-Rad) and 1x SyBr Safe (Life Technologies). Gels were imaged using a FujiFilm LAS Image 4000.



## 2.11 Lithium acetate transformation

Single colonies were inoculated into 2 mL YPD and incubated overnight in a wheel at 23°C (if temperature-sensitive) or 30°C. 1 mL of culture was added to 49 mL YPD and cultures were incubated in a shaking water bath at 23°C/30°C until the cell concentration was  $2 \times 10^7$  cells/mL. Cultures were washed once in 25 mL water and were resuspended in 1 mL 100 mM lithium acetate pH 7.5 (LiAc). The cell pellet was resuspended in 100 mM LiAc to a final concentration of  $2 \times 10^9$  cells/mL. The cell suspension was divided into 50  $\mu$ L aliquots, cells were spun down and the supernatant removed. The following were added to the cell pellets: 240  $\mu$ L 50% (v/v) polyethylene glycol (PEG)-4000, 36  $\mu$ L 1 M LiAc pH 7.5, 50  $\mu$ L salmon sperm DNA (2 mg/mL), 30  $\mu$ L purified PCR product or linearised vector (60 ng/ $\mu$ L), 20  $\mu$ L water. 50  $\mu$ L water were used for a no-DNA control. Cells were resuspended and incubated at 23°C for 30 minutes. Cells were heat-shocked at 42°C for 20 minutes and then spun down and resuspended in 200  $\mu$ L sterile water. Cells were plated onto appropriate selective media and incubated at 23°C /30°C until single colonies were visible. If strains were transformed with an antibiotic-resistance marker (e.g. *KANMX*, *HPHMX* or *NATMX*), transformants were grown on YPD plates overnight before replica-plating to media containing the appropriate antibiotic. Individual colonies were picked and streaked for single colonies on selective media. A single colony was picked and patched onto selective media. Transformants were verified by colony PCR as described above.

## 2.12 Gene deletion

Forward primers contained 40bp homology to immediately upstream of the gene start codon and 20bp homology to a plasmid containing an antibiotic resistance or auxotrophy marker (pAG25 or pAG32, details in Appendix C). Reverse primers contained 40bp homology to immediately downstream of the gene stop codon and 20bp homology to the same plasmid as before. Alternatively, genomic DNA was prepared as described below and PCR primers homologous to 500 bp upstream and downstream of a single gene deletion mutant from the Synthetic Gene Deletion Library, Version 4 (Tong *et al.*, 2001) were used. PCR was conducted as above. PCR products were pooled and

purified in 30µL molecular biology-grade water using a PCR purification kit (Qiagen). 30µL of purified PCR product were used for LiAc transformation of the required yeast strain, as described above. Transformants were plated onto selective media (or YPD overnight then replica-plated to selective media if transformed with an antibiotic resistance marker). Transformant colonies were streaked for single colonies on selective media. Single colonies were picked and checked for correct insertion of the deletion cassette by colony PCR (as described above), using a forward primer recognising inside the deletion cassette and a reverse primer recognising 600+bp downstream of the gene that had been deleted.

### **2.13 Epitope tagging**

Forward primers contained 40 bp homology to immediately upstream of the gene stop codon and 20 bp homology to a plasmid containing an epitope tag with an antibiotic resistance or auxotrophy marker (Longtine *et al.*, 1998). Reverse primers contained 40 bp homology to immediately downstream of the gene stop codon and 20 bp homology to the same plasmid as before. PCR using the tagging plasmids was conducted as above. LiAc transformation of yeast strains, transformant selection and verification was conducted as above. Transformants were further verified using Western blot (see below).

### **2.14 *In vivo* cloning**

0.3-1 µg plasmid vector were cut with 10 units of appropriate restriction enzymes (New England Biolabs), 2 µL 10x bovine serum albumin (BSA; New England Biolabs), 4 µL 5x NEBuffer4 (New England Biolabs) and 10 µL water (20 µL total volume). Digestion was confirmed by running cut and uncut vector on a 1% (w/v) agarose gel made with 0.5x TBE (Bio-Rad) and stained with 1x Sybr Safe (Life Technologies).

The vector insert was obtained by PCR (described above) using genomic DNA from a wild-type strain (DLY640) and primers to amplify ±500 bp upstream and downstream side of the target gene (for genes expressed under native

promoter). Alternatively, primers contained 40bp homology to the linearised plasmid vector and 20 bp homology to the target gene (forward primer starting at the initial ATG and reverse primer starting from the stop codon).

The LiAc method of transformation was used (see above) except 20  $\mu\text{L}$  purified PCR product (60 ng/ $\mu\text{L}$ ), 12.5  $\mu\text{L}$  digested plasmid (300 ng/ $\mu\text{L}$ ), 17.5  $\mu\text{L}$  water were used in the transformation. A no-DNA control contained 50  $\mu\text{L}$  water and no plasmid. A vector control contained 12.5  $\mu\text{L}$  digested plasmid and 37.5  $\mu\text{L}$  water. Transformant selection and verification was conducted as described above.

2 mL saturated cultures of transformants were centrifuged at 3000 x *g* for 5 minutes and resuspended in 100  $\mu\text{L}$  STET (8% (v/v) sucrose, 50 mM Tris-HCl pH 8, 50 mM EDTA pH 8, 5% (v/v) Triton X-100). 0.2g glass beads were added and samples were vortexed for 5 minutes. 100  $\mu\text{L}$  STET were added and samples were incubated at 100°C for 3 minutes then cooled on ice. Samples were centrifuged at 13,000 rpm for 10 minutes at 4°C. The top 100  $\mu\text{L}$  were transferred to 50  $\mu\text{L}$  7.5 M ammonium acetate and samples were freeze-precipitated at -20°C for 1 hour. Samples were centrifuged at 13,000 rpm for 10 minutes at 4°C and 100  $\mu\text{L}$  were transferred to 200  $\mu\text{L}$  ice-cold ethanol (100% v/v). Samples were centrifuged at 13,000 rpm for 10 minutes. Pellets were resuspended in 300  $\mu\text{L}$  70% (v/v) ethanol and were centrifuged for 5 minutes at 13,000 rpm. DNA pellets were air-dried for 5 minutes and then resuspended in 30  $\mu\text{L}$  water. 100  $\mu\text{L}$  *E.coli* DH5 $\alpha$  competent cells were transformed with 15  $\mu\text{L}$  of plasmid DNA (300 ng/ $\mu\text{L}$ ). Cells and DNA were incubated on ice for 20 minutes in 14 mL round-bottomed tubes. Cells were heat-shocked in a 42°C water bath for 45 seconds and then incubated on ice for 5 minutes. 0.9 mL pre-warmed (42°C) SOC medium (20g Bactotryptone, 5g yeast extract, 0.585 g NaCl, 0.166 g KCl, 10 mL 1M MgCl<sub>2</sub>, 10 mL 1M MgSO<sub>4</sub>, 3.6g glucose, in 1 litre) were added to the cells, which were then incubated in a rotating wheel for 30 minutes at 37°C. Cells were then transferred to 1.5 mL microcentrifuge tube and spun for 5 minutes at 5,000 rpm. 750  $\mu\text{L}$  of supernatant were removed and the cells were resuspended by gentle pipetting in the remaining supernatant. Cells were spread onto LB+ampicillin plates (10 g Bactopeptone, 5 g yeast extract, 10 g NaCl, 20 g agar, 100 mg Ampicillin, in 1 litre) and incubated

overnight at 37°C. Transformants were inoculated into 5 mL LB + ampicillin (100 mg/L) and incubated overnight at 37°C. Plasmid DNA was recovered using a QIAprep Spin Miniprep Kit (Qiagen).

Plasmids were verified by restriction digest, 0.2 µg plasmid DNA were cut with 10 units restriction enzyme (New England Biolabs), 1x restriction enzyme buffer (New England Biolabs), 1x BSA and sterile water. Digests were incubated at 37°C (or other temperature, as appropriate for enzyme) for 2-3 hours. Samples were run on a 1% (w/v) agarose gel made with 0.5x TBE (Bio-Rad) 1x Sybr Safe (Life Technologies).

### **2.15 *In vitro* cloning**

2.5 µg plasmid vector DNA were cut with 15 units of the appropriate restriction enzyme (New England Biolabs) and the appropriate restriction enzyme buffer (New England Biolabs) in a 20 µL volume digest for 90 minutes at 37°C. 2.5 µg plasmid DNA containing the required insert were digested as before. Then 2.2 µL 10x CIP phosphatase (New England Biolabs) were added to the digested vector. 1 µL of each digest was run on a 1% (w/v) agarose gel made with 0.5x TBE (Bio-Rad) and 1x SyBr Safe (Life Technologies) to check that the digest was complete. The cut vector and insert bands were removed from the gel using a scalpel and a SafeLight box (Life Technologies). DNA was purified from the gel using a Biomiga Gel Purification kit. Vector and insert were ligated by adding 400 units T4 DNA ligase (New England Biolabs) to 2 µL purified vector and 6 µL purified insert in a 10 µL reaction containing 1x T4 DNA ligase buffer (New England Biolabs). Ligation was carried out by incubating for 1 hour at 16°C (sticky ends) or overnight at 16°C (blunt ends). Digested vector-only and insert-only ligations were performed as negative controls. 5 µL of the ligated DNA was transformed into 100 µL *E.coli* DH5α competent cells as in 2.14, above.

### **2.16 Transformation of plasmids into budding yeast**

Fresh cells were scraped from an agar plate using a toothpick end and

resuspended in 100  $\mu$ L of one-step buffer (0.2M LiAc, 40% (v/v) PEG, 100 mM DL-dithiothreitol (DTT)). 300 ng of plasmid DNA were added along with 5.3  $\mu$ L salmon sperm DNA (10 mg/mL), boiled at 100°C for 5 minutes then cooled rapidly in iced water) and the cells were vortexed. Cells were incubated at 45°C for 30 minutes and were then plated onto the appropriate selective media. Transformants were streaked for single colonies and a single colony was picked for further experiments.

## 2.17 Southern blotting

10  $\mu$ L plasmid pDL987, containing 120bp of TG repeats and 752bp of the upstream Y' element from telomere VIII-R, were cut with 10 units *Bam*HI and 10 units *Xho*I in a 20  $\mu$ L digest containing 2  $\mu$ L 10x NEBuffer 4, 2  $\mu$ L 10x BSA, 5 $\mu$ L sterile water. The plasmid was digested for 2-3 hours at 37°C. Digested plasmid was run on a 1% (w/v) agarose gel made with 0.5x TBE and 1x Sybr Safe (Life Technologies) and the 1kb band, containing the TG repeats and Y' element, was cut out to use as the Southern blot probe. Probe DNA was purified from the agarose using a Qiaprep Gel Extraction Kit (Qiagen). The probe was Digoxigenin-dUTP (DIG) labelled using random oligonucleotide primers as per the DIG High Prime Labelling and Detection Starter Kit II (Roche).

2.5  $\mu$ L of DNA (prepared by the Yale method) was run on a 1% (w/v) agarose gel made with 0.5x TBE (Bio-Rad) and 1x Sybr Safe (Life Technologies) and samples were equalized for loading using ImageJ analysis of band intensity. 2.5  $\mu$ L equalized DNA were digested with 0.5  $\mu$ L *Xho*I (20 units/ $\mu$ L), 2  $\mu$ L 5x NEBuffer 4, 1  $\mu$ L 10x BSA, 4  $\mu$ L water for 3 hours at 37°C. Samples were run on a 1% (w/v) agarose gel (made with 0.5x TBE (Bio-Rad) and 1x SybrSafe (Life Technologies)) at 22 volts for 15 hours 30 minutes. The gel was photographed using a Fuji LAS 4000 imager to determine loading. The gel was depurinated in 0.25M hydrochloric acid for 15 minutes, rinsed twice in sterile water then denatured in 0.5M sodium hydroxide for 30 minutes. The gel was blotted to positively-charged nylon membrane (Roche) using a vacuum blotter (Model 785, BioRad) at 5 inches Hg in 10x saline-sodium citrate (SSC; 0.15M sodium citrate; 1.5M NaCl) for 90 minutes. DNA was cross-linked to the wet

membrane using auto UV cross-linking (Stratalinker). The membrane was rinsed briefly in sterile water and allowed to air-dry. The probe was hybridized to the membrane using the labelled probe and the DIG High Prime Labelling and Detection Starter Kit II (Roche). The probe was detected using the same kit and the membrane was imaged using a Fuji LAS 4000 imager for chemiluminescence, for 20 minutes.

## **2.18 Quantitative reverse transcriptase PCR**

RNA was isolated as follows. 25 mL of exponentially growing yeast culture were centrifuged for 2 minutes and 3,000 rpm at 4°C. The supernatant was removed, cells were resuspended in 0.5 mL ice-cold diethyl pyrocarbonate (DEPC)-treated water (Sigma Aldrich) and transferred to a 1.5 mL microcentrifuge tube. Samples were centrifuged for 30 seconds at 13,000 rpm in a benchtop centrifuge, the supernatant was removed and the cell pellet was washed again in 0.5 mL DEPC-treated water. Samples were centrifuged for 30 seconds at 13,000 rpm and the supernatant was removed completely. Pellets were frozen at -80°C. Pellets were thawed on ice for 1 hour and then resuspended in 300 µL RNA buffer (0.5M NaCl, 0.2M Tris-HCl pH 7.5, 10 mM EDTA pH 8.0). The cell suspension was transferred to a 2 mL skirted screw cap tube containing 200 µg acid-washed glass beads (ice cold). 300 µL phenol:chloroform:isoamyl alcohol (25:24:1 (v/v/v)) saturated with RNA buffer were added and the samples were mixed with the beads by inverting the tube gently. Cells were lysed in a Precellys 24 ribolyser (Bertin Technologies) using two cycles of 30 seconds at 6500 rpm with a 15 seconds pause between cycles. Samples were centrifuged at 13,000 rpm for 1 minute at 4°C in a benchtop centrifuge. The upper phase was transferred to a new 1.5 mL microcentrifuge tube and 300 µL phenol:chloroform:isoamyl alcohol (25:24:1 (v/v/v)) saturated with RNA buffer were added. Samples were vortexed briefly then centrifuged for 1 minute at 13,000 rpm at 4°C. The upper phase was transferred to a new 1.5 mL microcentrifuge tube and 900 µL of 100% (v/v) ethanol were added. Samples were incubated at -80°C for 2 hours and were then centrifuged for 2 minutes at 13,000 rpm at 4°C. The supernatant was removed and the sample was centrifuged for 10 seconds at 4°C and the remaining supernatant was removed. Pellets were air-dried for 15 minutes then

the RNA was dissolved in 50  $\mu\text{L}$  RNase-free water (Gibco). RNA concentrations were determined using the Nanodrop 2000 (Thermo Scientific). A 1/50 dilution of each RNA sample was run on a 1% (w/v) 0.5x TBE (Bio-Rad) agarose gel containing 1 x SyBr Safe (Life Technologies) to verify the integrity of the RNA and the presence of the 28S and 18S ribosomal RNA bands.

100  $\mu\text{g}$  of RNA sample was made up to 100  $\mu\text{L}$  volume by adding the appropriate amount of RNase-free water. Samples were purified by column using the Qiagen RNEasy Mini kit, following the RNA Cleanup protocol. RNA samples were eluted in 30  $\mu\text{L}$  RNase free water, the eluate was then re-applied to the column and eluted again to maximize RNA concentration. RNA concentrations were determined using the Nanodrop 2000 (Thermo Scientific) and samples were diluted to 1  $\mu\text{g}/\mu\text{L}$ . 5  $\mu\text{L}$  of 1  $\mu\text{g}/\mu\text{L}$  RNA sample were digested with 1 unit of DNase I (Amplification Grade; Life Technologies), 2  $\mu\text{L}$  10X DNase I buffer (Life Technologies) and 10  $\mu\text{L}$  DEPC-treated water (Sigma Aldrich), at 37°C for 30 minutes. The digestion was stopped by adding 2  $\mu\text{L}$  of 25 mM EDTA pH 7.5 (Life Technologies) and incubating samples at 65°C for 10 minutes in a heat block. 40  $\mu\text{L}$  of DEPC-treated water (Sigma Aldrich) were added to each sample to make a final RNA concentration of 82  $\text{ng}/\mu\text{L}$ .

RNA transcript levels were analysed by quantitative reverse-transcriptase PCR (qRT-PCR), using the Superscript III Platinum SyBr green one-step qRT-PCR kit (Life Technologies) and an ABI Systems StepOne Plus thermocycler. Primers were used that amplified a 100bp region within the gene of interest and measurements were performed in triplicate for each sample. The qRT-PCR mastermix per reaction contained 0.2  $\mu\text{L}$  Superscript III Platinum Taq Mix, 5  $\mu\text{L}$  2x SyBr Green Reaction Mix, 0.2  $\mu\text{L}$  forward primer (10  $\mu\text{M}$ ), 0.2  $\mu\text{L}$  reverse primer (10  $\mu\text{M}$ ), 0.2  $\mu\text{L}$  ROX reference dye and 0.2  $\mu\text{L}$  DEPC-treated water (Sigma Aldrich). Per reaction, 6  $\mu\text{L}$  master mix were added to 4  $\mu\text{L}$  RNA sample (82  $\text{ng}/\mu\text{L}$ ) in a 96-well reaction plate. The no-template control contained 4  $\mu\text{L}$  DEPC-treated water (Sigma Aldrich) instead of RNA. A standard curve of DNA concentrations was generated from 2  $\text{ng}/\mu\text{L}$ , 0.2  $\text{ng}/\mu\text{L}$  and 0.02  $\text{ng}/\mu\text{L}$  wild-type (DLY640) genomic DNA standards. 6  $\mu\text{L}$  master mix were added to 4  $\mu\text{L}$  of genomic DNA standard and each standard was measured in triplicate. The qRT-PCR programme was 50°C for 3 minutes,

95°C for 5 minutes, 40 cycles of 95°C for 15 seconds and 60°C for 30 seconds, then 40°C for 1 minute followed by melting curve analysis, using an ABI Systems StepOnePlus thermal cycler. As a loading control, RNA concentrations were normalized according to *BUD6* mRNA expression levels.

## **2.19 Chromatin immunoprecipitation (ChIP)**

Strains were inoculated into 2 mL YPD and incubated at 23°C or 30°C (as appropriate for the strain) overnight in a wheel. The following evening, 5-20 $\mu$ L of overnight culture were added to 100 mL YPD and incubated at 23°C or 30°C overnight. In the morning, cultures were diluted to  $2.5 \times 10^6$  cells/mL and grown at the same temperature until  $1 \times 10^7$  cells/mL.

For chromatin immunoprecipitation (ChIP) of Cdc13-Myc, Stn1-Myc and Ten1-Myc, strains 40 mL culture were washed twice with either 40 mL tris-buffered saline pH7.5 (TBS) (1.5 M sodium chloride, 100 mM Tris-HCl pH 7.5) or phosphate-buffered saline pH 7.5 (PBS) when ethylene glycol-bis(succinic acid N-hydroxysuccinimide ester) (EGS) was used as an additional crosslinking agent. Cells were resuspended in 40 mL TBS, then mixed with 1.1 mL 36.5% (w/v) formaldehyde (Sigma) and incubated at room temperature for 15 minutes. For ChIP of Stn1-Myc and Ten1-Myc, 160  $\mu$ L of 500 mM EGS (Pierce) in dimethyl sulfoxide (DMSO; Sigma Aldrich) were also added and cultures were incubated at room temperature for 30 minutes, prior to crosslinking with formaldehyde. 6 mL of 2.5 M glycine were added to quench the formaldehyde and samples were incubated for 5 minutes at room temperature.

Samples were then spun for 5 minutes at 3000 rpm at 4°C and the supernatant was discarded. Cell pellets were washed twice in 20-40 mL ice-cold TBS and spun at 3000 rpm at 4°C for 5 minutes. The supernatant was poured off and samples were resuspended in the residual supernatant before being transferred to a 2 mL Sarstedt tube. Tubes were spun for 1 minute at 13,000 rpm at 4°C and the supernatant was discarded. Cell pellets were frozen at -80°C.



Protein G dynabeads (Life Technologies; 30  $\mu$ L per immunoprecipitation) were washed twice in 500  $\mu$ L PBS-BSA (125 mg BSA fraction V (Sigma Aldrich)/25 mL PBS) and resuspended in a volume of PBS 1.15x the initial volume of beads. 1.8-5  $\mu$ g antibody per 30  $\mu$ L dynabeads were added and beads were incubated overnight in a wheel at 4°C. Antibodies used were: for ChIP of Myc-tagged proteins, monoclonal mouse anti-c-myc 9E10 (AbCam, ab32; 1.8  $\mu$ g/30 mL dynabeads); for ChIP of RPA, rabbit polyclonal anti-*Saccharomyces cerevisiae* RPA (Agrisera, AS07 214; 5  $\mu$ g/30  $\mu$ L dynabeads). For all ChIPs rabbit anti goat IgG (Abcam, ab97096; 1.8  $\mu$ g or 5  $\mu$ g) was used as a non-specific antibody control.

Cell pellets were thawed on ice for 30 minutes. Pellets from 40 mL cultures were resuspended in 1000  $\mu$ L of lysis buffer (20 mM Hepes-KOH pH 7.5, 140 mM NaCl, 1 mM EDTA, 1% (v/v) Triton X-100, 0.1% (w/v) Na-deoxycholate) and 5  $\mu$ L of protease inhibitors (P1860, Sigma Aldrich). Pellets from 20 mL cultures were resuspended in 500  $\mu$ L lysis buffer and 2.5  $\mu$ L protease inhibitors. Samples from 40 mL cultures were split into two 500  $\mu$ L aliquots, one for specific antibody immunoprecipitation (IP) and one for non-specific antibody immunoprecipitation (background). 0.5 mL cold acid-washed glass beads (0.5 mm) were added to the tubes and cells were ribolysed for three cycles of 6200 rpm for 30 seconds, with a 3 minute pause on ice water between cycles (Precellys 24, Bertin Technologies). The bottom of the tube was punctured using an incandescent needle (Microlance 3, Becton Dickinson) and placed in a 1.5 mL microcentrifuge tube with the lid removed. The tube assembly was placed in a 15 mL conical tube and samples were centrifuged at 1000 rpm for 1 minute at 4°C. The tube assembly was removed from the 15 mL conical tube and the lid was replaced on the 1.5 mL microcentrifuge tube containing the sample. Samples were vortexed briefly. Samples were sonicated using a Bioruptor (Diagenode) for 4 x 5 minutes of 30 seconds off, 30 seconds on, highest power setting, to generate chromatin fragments of 100-200 bp. Samples were then spun for 5 minutes at 12,000 rpm, 4°C. The supernatant (450  $\mu$ L) was removed to a fresh 1.5 mL microcentrifuge tube and 10  $\mu$ L were extracted for 'input' samples. The input samples were stored at 4°C overnight. The remaining lysate (440  $\mu$ L) was incubated with 30  $\mu$ L of dynabeads/antibody overnight at 4°C in a wheel.

The following morning, samples were washed as follows (all buffers were ice-cold):

1x with 1 mL lysis buffer

2x with 1 mL RIPA buffer

(0.1% (w/v) SDS, 10mM Tris-HCl pH7.5, 1mM EDTA, 0.1% (w/v) sodium deoxycholate, 1% (v/v) Triton X-100)

2x with 1 mL RIPA buffer containing 300mM NaCl

2x LiCl buffer (0.25M LiCl, 0.5% (v/v) NP40, 0.5% (w/v) sodium deoxycholate)

1x with 1 mL TE and 0.2% (v/v) Triton-X-100

Washing consisted of holding the beads with a magnet, removing the supernatant with a vacuum pump, and resuspending the beads in the appropriate washing solution by inverting tubes 20 times. After the final wash was removed, beads were resuspended in 200  $\mu$ L of 10% (w/v) Chelex (Bio-Rad) in sterile DNase/RNase free water (Sigma Aldrich). Samples were boiled in a heat block at 100°C for 10 minutes and then cooled to room temperature. Samples were spun for 2000 rpm for 7 seconds and 2.5  $\mu$ L proteinase K (10 mg/mL) were added. Samples were incubated for 30 minutes at 55°C and were then boiled for 10 minutes at 100°C to inactivate proteinase K. Tubes were spun for 7 seconds at 2000 rpm and 120  $\mu$ L of supernatant was extracted.

qPCR was used to determine the relative expression levels of proteins of interest at the specific loci (primers amplified a 100-150bp region within the target gene) using an ABI Systems StepOne Plus thermocycler. An internal control was *PAC2* on chromosome III (primers M1367, M1368). The qPCR reaction mix contained 5  $\mu$ L Platinum SyBr Green qPCR SuperMix-UDG with ROX (Life Technologies), 0.2  $\mu$ L forward primer (10  $\mu$ M), 0.2  $\mu$ L reverse primer (10  $\mu$ M) and 2.6  $\mu$ L sterile water. 2  $\mu$ L DNA was added to 8  $\mu$ L master mix in a 96-well plate. There were three replicates for each sample and a no template control contained 2  $\mu$ L sterile water rather than DNA. The qPCR programme was 50°C for 2 minutes, 95°C for 2 minutes, followed by 40 cycles of 95°C for 15 seconds and 60 °C for 30 seconds, then a melting curve analysis, using an ABI Systems StepOnePlus thermal cycler. The IP efficiency was defined as the

percentage of the input that was in the IP. This percentage was calculated using the following formula:  $2.273/2^{(IP\ CT - Input\ CT)}$  (the value 2.273 was used since input was 10  $\mu$ L, IP was 440  $\mu$ L. Ratio input:IP is 1:44;  $100/44 = 2.273$ ).

## 2.20 Co-immunoprecipitation (Co-IP)

Strains were inoculated into 2 mL YPD and incubated at 23°C or 30°C overnight in a wheel. The following evening, a sufficient volume of overnight culture was added to 100 mL YPD and incubated at 23°C or 30°C overnight, so that cultures were in mid-log phase by the following morning. 25 mL of each culture were washed once in 25 mL ice-cold water, transferred to a 1.5 mL microcentrifuge tube and washed in 1 mL ice-cold water. The supernatant was removed and samples were frozen at -80°C. Cell pellets were resuspended in 240  $\mu$ L lysis buffer (as used for ChIP, above) with 5  $\mu$ L protease inhibitors (P8215, Sigma Aldrich) and 5  $\mu$ L 100 mM phenylmethylsulfonyl fluoride (PMSF). 0.5 mL cold acid-washed glass beads (0.5 mm) were added and cells were ribolysed for 4 cycles of 2 x 20 seconds, 20 second pause, 5000 rpm (Precellys 24, Bertin Technologies). Samples were incubated for 2 minutes on ice water between cycles. The bottom of the tube was punctured using an incandescent needle (Microlance 3, Becton Dickinson) and placed in a 1.5 mL microcentrifuge tube with the lid removed. The assembly was placed in a 15 mL conical tube and samples were centrifuged at 2000 rpm for 2 minutes at 4°C. Samples were washed with 125  $\mu$ L of lysis buffer with protease inhibitors and PMSF (as before). The tube assembly was removed from the 15 mL conical tube and the lid was replaced on the 1.5 mL microcentrifuge tube containing the sample. Samples were spun at 13,000 rpm, 4°C, for 10 minutes and the supernatant was removed to a fresh tube (about 370  $\mu$ L). 15  $\mu$ L of cell lysate were taken for the 'input', to which 15  $\mu$ L Laemmli buffer (Bio-Rad) with 5% (v/v)  $\beta$ -mercaptoethanol were added. Samples were boiled for 5 minutes at 95°C, and then frozen at -20°C. The remainder of the cell lysates were incubated with 5  $\mu$ g of antibody (monoclonal mouse anti-c-myc antibody 9E10 (Abcam, ab32) or rabbit polyclonal anti-HA (Abcam, ab9110), whilst 25  $\mu$ L aliquots of protein G dynabeads (Life Technologies) were washed 3 x 10 minutes in 250  $\mu$ L lysis buffer on a wheel at 4°C. Protein G dynabeads (Life

Technologies) were then combined with cell lysates and incubated overnight on a wheel at 4°C.

The following morning, the cell lysate was removed from the beads using a magnet, and beads were washed 3 times by resuspending the beads in lysis buffer. The final wash was removed and the beads were resuspended in 40 µL Laemmli buffer with 5% (v/v) β-mercaptoethanol (Bio-Rad). The beads were then boiled at 95°C for 5 minutes in a heat block, and input samples were also reboiled at 95°C for 5 minutes. 10 µL of samples (input and immunoprecipitate) were loaded immediately onto a 7.5% (v/v) pre-cast SDS-PAGE gel (Bio-Rad Mini-Protean TGX) and run at 100V in Tris/Glycine/SDS running buffer (Bio-Rad). Gels were then western blotted (see below).

After anti c-Myc immunoprecipitation, western blot membranes were incubated first overnight (4°C, shaking) with polyclonal rabbit anti *Saccharomyces cerevisiae* Rfa1, Rfa2 (AgriSera AS07214). Antibody concentration was 2 µg in 11 mL 1% (w/v) skimmed milk powder in PBS with 0.1% (v/v) Tween-20 (PBST). After anti-HA immunoprecipitation, blots were incubated with mouse anti-c-myc antibody 9E10 (Abcam, ab32 5 µg/11 mL 1% (w/v) milk-PBST).

Membranes incubated with AS07214 were then probed with goat anti-rabbit-horseradish peroxidase (HRP; Dako P0448; 2 µg/10 mL 1% (w/v) milk-PBST). Membranes that were incubated with ab325 were probed with goat anti-mouse-HRP for two hours before detection (Dako P0447; 2 µg/10 mL 1% (w/v) milk-PBST). Before probing, membranes were washed for 2 x 5 minutes with PBST and were then incubated overnight (4°C, shaking) with the appropriate antibody solution, followed by chemiluminescent detection (see western blotting, below).

## **2.21 Western blotting**

Proteins were extracted using TCA extraction (see below) or were produced from Co-IP (see above) and were suspended in Laemmli buffer with 5% (v/v) β-mercaptoethanol (Bio-Rad). Protein extracts were loaded onto a 7.5% (v/v) pre-cast gel (Bio-Rad Mini-Protean TGX) and run at 100V in Tris/Glycine/SDS running buffer (Bio-Rad). The gel was transferred by the wet-transfer method to

a nitrocellulose membrane (Amersham Hybond ECL) in ice-cold transfer buffer (Tris-Glycine (Bio-Rad) with 20% (v/v) ethanol) for 1.5 hours at 100V. The membrane was washed in 50 mL 5% (w/v) milk-PBST (5% (w/v) skimmed milk powder dissolved in PBST) for 1 hour on a rocking stage at room temperature. The 5% (w/v) milk was removed and the membrane was covered with 11 mL 1% (w/v) milk in PBST with 5 µg primary antibody, overnight on a rocking stage at 4°C. The following morning the antibody solution was removed and the membrane was washed 4 x 15 minutes in PBST on a rocking stage. The membrane was then covered with 10 mL 1% (w/v) milk in PBST and 2 µg HRP-conjugated secondary antibody and was incubated for two hours at room temperature on a rocking stage. The membrane was washed 4 x 15 minutes with PBST. The membrane was removed from the PBST, laid on cling film, covered with 4 mL Thermo Scientific SuperSignal West Pico Chemiluminescent Substrate, covered with cling film and foil and incubated for 5 minutes. The membrane was then imaged using a Fujifilm LAS 4000 with chemiluminescent detection.

## **2.22 Trichloroacetic acid protein extraction**

25 mL mid log phase cells ( $1 \times 10^7$  cells/mL) were washed once with 25 mL water and resuspended in 2 mL water. 500 µL cells were centrifuged briefly (30 seconds, 13,000 rpm) and resuspended in 500 µL 10% (w/v) trichloroacetic acid (TCA). Cells were centrifuged as before and resuspended in 100 µL 10% (w/v) TCA. An equal volume (100 µL) of glass beads was added. Samples were vortexed for 4 minutes. The supernatant was transferred to a fresh tube (50-100 µL). The beads were washed twice with 100 µL 10% (w/v) TCA, the supernatant was extracted and added to the existing extract. Proteins were pelleted by centrifuging the sample at 13,000 rpm in a microcentrifuge for 10 minutes (4°C). The supernatant was discarded. 100 µL Laemmli loading buffer with 5% (v/v) β-mercaptoethanol (Bio-Rad) were added to the protein pellet. The sample was neutralized by adding 40 µL 1M Tris. The pellet was then resuspended by vortexing. Samples were boiled for 3 minutes at 95°C using a heat block before being centrifuged at 3,000 rpm (4°C) for 10 minutes. The

supernatant was removed to a fresh 2 mL skirted screw cap tube. 10  $\mu$ L of sample was used for a Western blot.

## 2.23 Synthetic Genetic Array

All *S. cerevisiae* yeast strains used for synthetic genetic array (SGA) high-throughput screens were in the S288C genetic background. The two SGA screens carried out have references SGA153 (*nmd2 $\Delta$  exo1 $\Delta$  cdc13 $\Delta$* ) and SGA156 (*nmd2 $\Delta$  exo1 $\Delta$* ). The *MAT $\alpha$*  query strain (containing the query mutations with *NATMX*, *HPHMX*, and *LEU2* markers, the *MAT $\alpha$* -specific *STE2* promoter cassette *can1delta::STE2pr-Sp\_his5* and *lyp1 $\Delta$* ) was cultured in YPD overnight at 23°C and spread onto YPD+clonNAT plates. Plates were incubated for two days at 23°C until a lawn of query culture was visible. All manipulations hereinafter described were conducted using a BM3 robot (S&P Robotics) and plates were photographed at each stage using a robotic plate imager (SPImager, S&P Robotics). The query plates were then pinned to 18 fresh YPD+clonNAT plates as 1536 individual colonies per plate and were incubated for 2 days at 20°C. The *MAT $\alpha$*  library of 5000 single deletion mutants (80% of all *S. cerevisiae* genes) and 842 strains where essential genes were depleted by mRNA perturbation (Decreased Abundance by mRNA Perturbation, DAmP) (Synthetic Deletion Library Version 4 (SDLV4); Tong and Boone, 2006) was pinned to YPD+G418 plates as 384 individual strains per plate and was incubated at 30°C for two days. The library was then pinned as 1536 colonies per plate (4 replicates of each strain from each 384-format plate) onto YPD+G418 plates and were incubated for 2 days at 30°C. The 1536-format query strains were then mated with the 1536-format library on YPD and diploids were formed during 24-48 hours at 23°C. Diploids were then pinned to YPD+G418+clonNAT and incubated for 1.5 days at 30°C before being pinned to sporulation media (ESM+G418) and sporulated for 5 days at 23°C. Plates were inspected visually for spore formation. Spores were pinned sequentially (and incubated for 2 days at 20°C) to:

- SD/MSG -HIS/ARG/LYS +canavanine/thialysine
- SD/MSG -HIS/ARG/LYS +canavanine/thialysine

- SD/MSG -HIS/ARG/LYS +canavanine/thialysine/G418
- SD/MSG -HIS/ARG/LYS/LEU +canavanine/thialysine/G418
- SD/MSG -HIS/ARG/LYS/LEU +canavanine/thialysine/G418/hygromycin
- SD/MSG -HIS/ARG/LYS/LEU  
+canavanine/thialysine/G418/hygromycin/clonNAT (final selection media)

in order to select *MATa* haploids harbouring both the query and library mutation (HIS is histidine; ARG is arginine; LYS is lysine; LEU is leucine). The robotic amino acid dropout recipe is given below. Canavanine concentration was 50 mg/L; thialysine concentration was 50 mg/L; G418 concentration was 200 mg/L; hygromycin concentration was 300 mg/L and clonNAT concentration was 100 mg/L. Photographs of the mutants on the final selection media were compared to a control SGA screen using a strain lacking the query mutation but harbouring *NATMX*, *HPHMX*, and *LEU2* markers, the *MATa*-specific *STE2* promoter cassette *can1delta::STE2pr-Sp\_his5* and *lyp1Δ*. Images were compared using COLONYZER image analysis software (Lawless *et al.*, 2010) to generate a Genetic Interaction Score (GIS).

#### Drop-out amino/nucleic acid recipe for robotic media

Adenine	3g
Inositol	2g
Para-aminobenzoic acid	0.2g
Alanine	2g
Arginine	2g
Asparagine	2g
Aspartic Acid	2g
Cysteine	2g
Glutamic acid	2g
Glutamine	2g
Glycine	2g
Histidine	2g
Isoleucine	2g
Leucine	10g
Lysine	2g
Methionine	2g
Phenylalanine	2g
Proline	2g
Serine	2g
Threonine	2g
Tryptophan	2g
Tyrosine	2g
Valine	2g
Uracil	2g

## **2.24 Growth of yeast strains in ethanol**

Single colonies of strains were grown overnight in 2 mL YPD at 30°C. Cultures were counted, using a haemocytometer, and were used to inoculate 5 mL fresh YPD media (containing 0%, 1%, 3% or 5% (v/v) ethanol) at a density of  $1 \times 10^5$  cells/mL. Cultures were grown in a wheel at 30°C until they had reached a density of  $1 \times 10^8$  cells/mL (= 10 population doublings). Fresh media was then inoculated with these cells at a density of  $1 \times 10^5$  cells/mL. Cells were then grown and passaged again as before.



## Chapter 3. Stn1 protects the telomere without Cdc13

### 3.1 Viable *cdc13Δ* strains resemble telomerase-deficient survivors

Cdc13 interacts with the Pol1 subunit of DNA Polymerase alpha and recruits telomerase via interaction with the Est1 subunit (Nugent *et al.*, 1996; Qi and Zakian, 2000). Moreover, Cdc13 may function as a loading complex for its partner proteins Stn1 and Ten1 since Stn1 fused to the Cdc13 DNA binding domain restores viability to a *cdc13Δ* strain, but has defective telomere replication because Cdc13 is required to load telomerase (Pennock *et al.*, 2001; Mitton-Fry *et al.*, 2004; Lewis *et al.*, 2014). Since Cdc13 recruits telomerase to extend the telomere end during replication, it is likely that in Cdc13 bypass cells (*cdc13Δ nmd2Δ exo1Δ* and/or *rad24Δ*) there is no telomerase recruitment. Cells that lack telomerase undergo telomere shortening and lose viability, until a small proportion of cells begin to maintain telomeres by recombination and form either Type I or Type II survivors (Lundblad and Blackburn, 1993). Viable *cdc13Δ* strains could be cultured for many passages and their fitness increased with passage (Holstein *et al.*, 2014). It was hypothesised therefore that Cdc13 bypass cells would be deficient in telomerase recruitment and would therefore maintain telomeres by recombination.

To test the hypothesis, telomere structure was determined for Cdc13 bypass strains after 1 and 9 passages. Telomeres were examined using Southern blotting with a Y' and TG repeat probe to detect terminal Y' telomeres, internal Y' elements and X telomeres (Figure 7 A; see also Figure 1 for a description of telomere subtypes). Figure 7 B, lane 1 shows a wild-type telomere, lane 2 is telomere from a strain lacking telomerase (*tlc1Δ*) and lane 3 is a telomerase-deficient strain that has lost Y' telomeres and has amplified TG repeats (a Type II survivor). At passage 1, *cdc13Δ* strains have short Y' telomeres (compare lanes 8-12 with lane 1) and their telomeres are similar to the corresponding *CDC13* strains in lanes 4-6 (these are independent strains from those in lanes

8-18). The *CDC13* strains in lanes 4-6 all have short Y' telomeres, most likely because they lack *NMD2*, which leads to short telomeres.

After 9 passages, the telomeres of *nmd2Δ exo1Δ cdc13Δ* strains (lanes 15 and 16) had amplified internal Y' elements and had lost X telomeres. The telomeres of these strains therefore bore some resemblance to Type I survivors, which amplify Y' elements and lose X telomeres (Lundblad and Blackburn, 1993; Chen *et al.*, 2001; Lydall, 2003). However, Type I survivors lose TG<sub>1-3</sub> repeats, which leads to very short Y' telomeres. In lanes 15 and 16 it is evident that there are both short and long TG<sub>1-3</sub> tracts present in *nmd2Δ exo1Δ cdc13Δ* strains. *nmd2Δ exo1Δ cdc13Δ* strains may therefore be attempting to amplify TG<sub>1-3</sub> repeats, perhaps in an attempt to switch to Type II recombination in which TG<sub>1-3</sub> repeats are amplified. Deletion of *EXO1* in telomerase-deficient strains suppresses Type II survivor formation (Maringele and Lydall, 2004), therefore *exo1Δ* may cause *nmd2Δ exo1Δ cdc13Δ* strains to become Type I survivors due to defective telomerase recruitment in the absence of Cdc13.

The telomeres of *nmd2Δ rad24Δ cdc13Δ* and *nmd2Δ exo1Δ rad24Δ cdc13Δ* strains resembled those of Type II survivors (compare lanes 13-14 and 17-18 with lane 3). Interestingly, telomerase-deficient strains deleted for *RAD24* have difficulty in forming Type II survivors (Grandin and Charbonneau, 2007) but *nmd2Δ rad24Δ cdc13Δ* still resemble Type II survivors. Therefore, perhaps Rad24 control of telomere recombination is overridden in *nmd2Δ rad24Δ cdc13Δ* and *nmd2Δ exo1Δ rad24Δ cdc13Δ* strains.

Taking the telomere phenotypes of *cdc13Δ* strains together, there is evidence that may indicate that *cdc13Δ* strains prefer Type II telomere recombination. However, there is currently no evidence that *nmd2Δ exo1Δ cdc13Δ* strains switch to Type II recombination, only that their telomeres are not classical Type I survivors. Therefore, future work should address whether *nmd2Δ exo1Δ cdc13Δ* strains become Type II survivors, perhaps by passaging the strains for longer. Also, examining the telomeres of a much larger number of independent *cdc13Δ* strains (over 50) would enable the survivor preference of the strains to be determined conclusively.

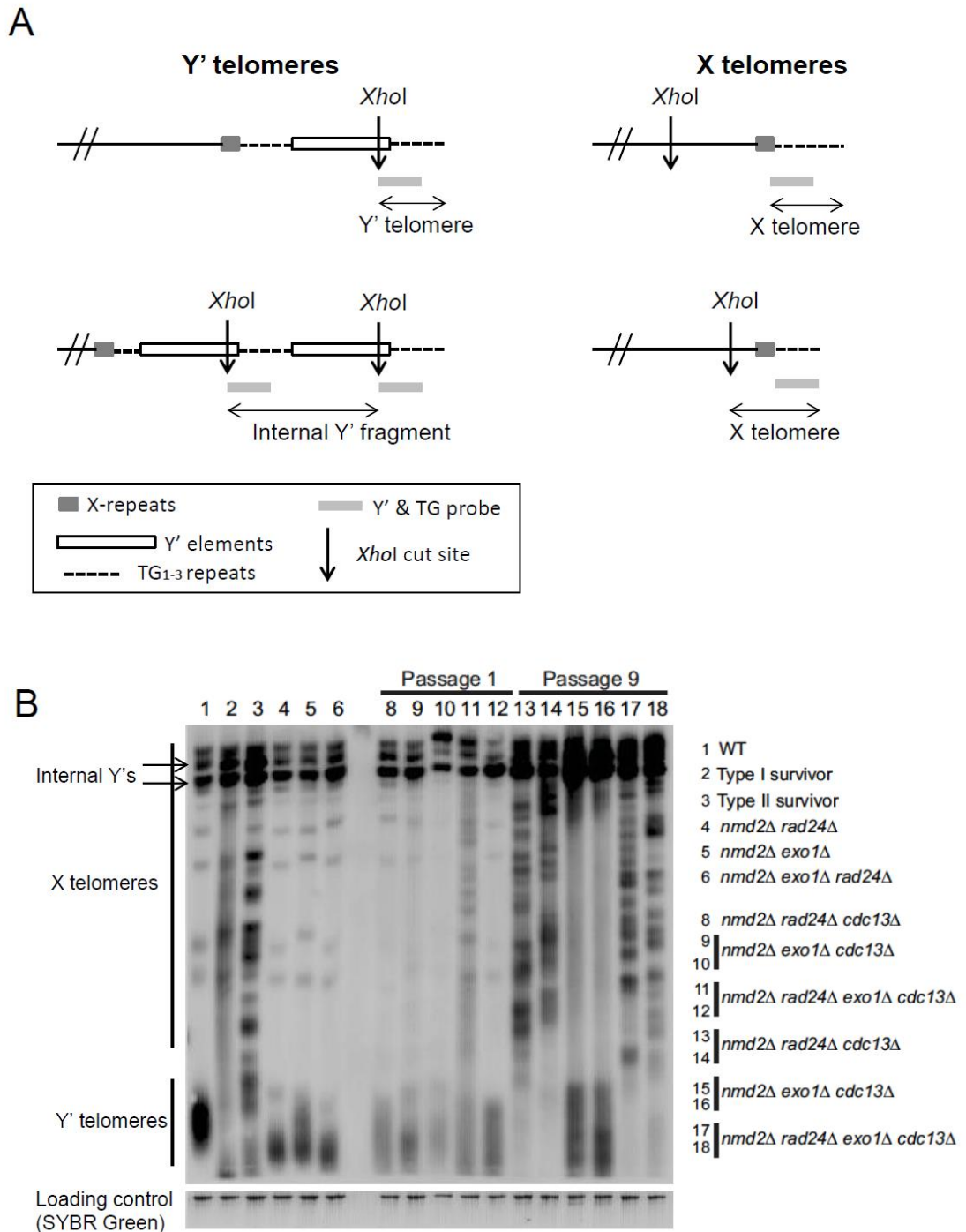


**Figure 7. Telomeres of viable *cdc13Δ* strains resemble those of telomerase-deficient survivors**

(A) Diagram showing how *Xho*I digestion of genomic DNA and Y' and TG<sub>1-3</sub> repeat probe generate Y' telomere, X telomere and internal Y' fragments for Southern blotting. Information regarding *Xho*I digestion of telomeric DNA obtained from Makovets *et al.*, 2008. (B) Genomic DNA was isolated from yeast strains indicated on the right. Strains in lanes 9-10 and 11-12 are independent strains of the same genotype. Strains in lanes 14-18 are the same strains in 8-12 but passaged 9 times. Telomere structures were analyzed by Southern blotting using the Y' and TG probe indicated. DNA was run on a 1% (w/v) agarose gel for Southern blotting was stained with SyBr Green and was used as a loading control.

### 3.2 Viable *cdc13* $\Delta$ strains can survive without telomerase

*Cdc13* bypass strains resembled telomerase-deficient survivors, therefore it was predicted that *cdc13* $\Delta$  strains would not require telomerase for viability. To test this theory, a diploid heterozygous for *NMD2*, *EXO1*, *RAD24*, *CDC13* and *TLC1* deletions was sporulated and tetrads were dissected to obtain haploids. Viable *cdc13* $\Delta$  genotypes previously observed were viable in the absence of *TLC1* (Figure 8 A). Viable *cdc13* $\Delta$  *tlc1* $\Delta$  strains were passaged 9 times and viability increased with passage, similar to a *tlc1* $\Delta$  strain (Figure 8 B).

Interestingly, *tlc1* $\Delta$  *nmd2* $\Delta$  *rad24* $\Delta$  *cdc13* $\Delta$  and *tlc1* $\Delta$  *nmd2* $\Delta$  *exo1* $\Delta$  *cdc13* $\Delta$  strains had very low initial fitness and could not be grown to a sufficient density in liquid culture. This contrasts with the fitness of the corresponding *CDC13*<sup>+</sup> strains, which could be grown in liquid culture from the first passage. However, fitness improved with passage such that even passage 2 for these strains could be grown in liquid culture for Southern blotting (Figure 8 C, lanes 5 and 6).

In Figure 8 C, the telomeres of *cdc13* $\Delta$  *tlc1* $\Delta$  strains (passage 1 or 2 and passage 9) were examined by Southern blotting, using the Y' and TG<sub>1-3</sub> probe described in Figure 7A. *cdc13* $\Delta$  *tlc1* $\Delta$  strains showed dramatic telomere rearrangements by passage 9, similar to the equivalent *TLC1*<sup>+</sup> strains (compare lanes 9-11, Figure 8 C, with lanes 13, 15 and 17, Figure 7 B). However, *cdc13* $\Delta$  *tlc1* $\Delta$  already showed dramatic telomere rearrangements at passage 1 or 2 (Figure 8, lanes 5-7), whereas at passage 1 *cdc13* $\Delta$  *TLC1* strains had short telomeres but did not yet exhibit dramatic telomere rearrangements (Figure 7 B, lanes 8, 9 and 11). Presumably *cdc13* $\Delta$  *tlc1* $\Delta$  strains underwent earlier telomere rearrangements because of the lack of functional telomerase to maintain telomere length.

*nmd2* $\Delta$  *rad24* $\Delta$  *cdc13* $\Delta$  *tlc1* $\Delta$  and *nmd2* $\Delta$  *exo1* $\Delta$  *rad24* $\Delta$  *cdc13* $\Delta$  *tlc1* $\Delta$  strains amplified TG repeats and resembled Type I survivors by passage 9, similar to the equivalent *TLC1* strains (compare lanes 9 and 11, Figure 8, with lanes 13-14 and 17-18, Figure 7). The *nmd2* $\Delta$  *exo1* $\Delta$  *cdc13* $\Delta$  *tlc1* $\Delta$  strain amplified internal Y' elements, contained no X telomeres, and compared to the equivalent

*TLC1* strain had shorter tracts of Y' telomeres with TG<sub>1-3</sub> repeats (compare lane 10, Figure 8, with lanes 15-16, Figure 7). Therefore the *nmd2Δ* *exo1Δ* *cdc13Δ* *tlc1Δ* strain more closely resembled a Type I survivor. In conclusion, strains lacking Cdc13 can survive without telomerase and it is probable that telomere rearrangements, resulting from recombination and amplification of TG<sub>1-3</sub> repeats, allow telomerase-mediated telomere lengthening to be bypassed.

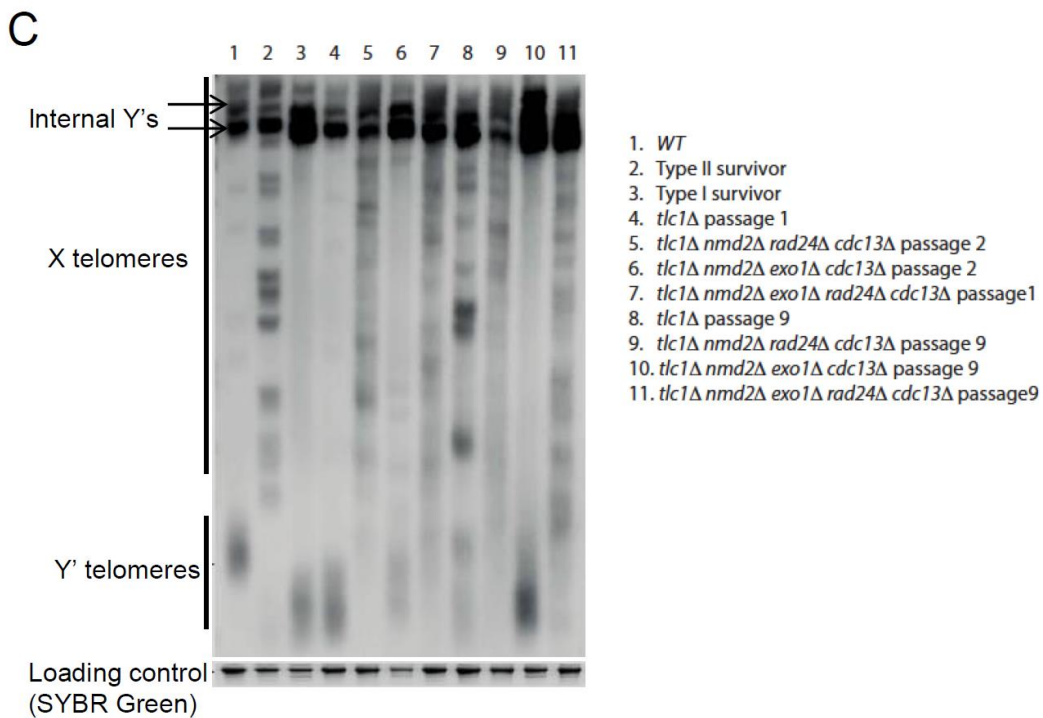
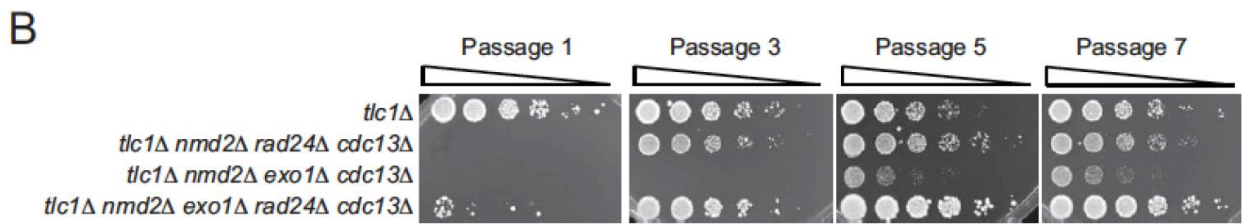
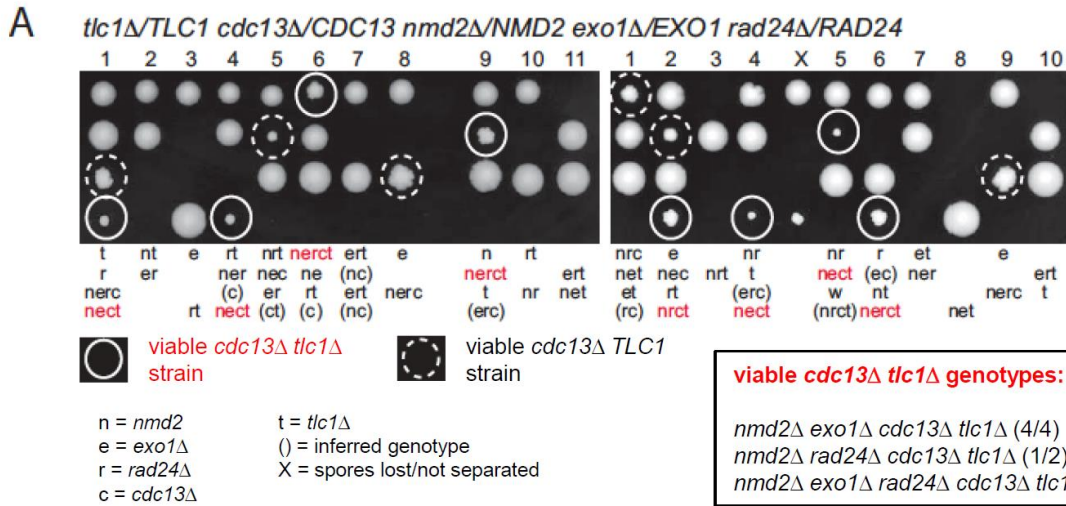


**Figure 8. Viable *cdc13*Δ strains can survive without telomerase**

(A) A diploid heterozygous for *TLC1*, *CDC13*, *NMD2*, *EXO1* and *RAD24* deletions was sporulated. Tetrads were dissected. Spores were allowed to form colonies for 5 days at 23°C before being photographed. Genotypes were determined by growth on appropriate selective plates. Viable *cdc13*Δ *tlc1*Δ genotypes are given and the spore viability is shown in brackets. (B) Strains of the genotypes indicated on the right were repeatedly passaged every 4 days at 23°C. 2 ml liquid cultures were grown overnight, serially diluted, spotted onto YPD plates and incubated for 2 days before being photographed. (C) Genomic DNA was isolated from yeast strains of the genotypes indicated (on the right) and telomere structures were analyzed by Southern blotting using the Y' and TG<sub>1-3</sub> probe as before (shown in Figure 7A).

### 3.3 Cdc13 bypass is not dependent on Stn1 or Ten1 overexpression

Stn1 and Ten1 are indispensable for cell survival in yeast (so far no genotypes allowing bypass of Stn1 or Ten1 have been discovered in either yeast or mice) but Cdc13 can be bypassed with certain genetic manipulations, which indicates that Stn1 and Ten1 may play essential roles in maintaining the viability of *cdc13* $\Delta$  strains. Stn1 may therefore carry out essential functions relating to telomere maintenance in the absence of a fully functional Cdc13, indeed it has been shown previously that overexpression of Stn1 and Ten1 together rescues the lethality of *cdc13* $\Delta$  (Petreaca *et al.*, 2006).

Given that deletion of *NMD2* results in the overexpression of Stn1 and Ten1 (Johansson *et al.*, 2007), it was hypothesised that overexpression of Stn1 and Ten1 alone explained the viability of *nmd2* $\Delta$  *exo1* $\Delta$  *cdc13* $\Delta$ , *nmd2* $\Delta$  *rad24* $\Delta$  *cdc13* $\Delta$  and *nmd2* $\Delta$  *exo1* $\Delta$  *rad24* $\Delta$  *cdc13* $\Delta$  strains. Another genetic background that permits *CDC13* deletion, but not *STN1* or *TEN1* deletion, is *pif1* $\Delta$  *exo1* $\Delta$  *cdc13* $\Delta$  (Dewar and Lydall, 2010; Holstein *et al.*, 2014) so mRNA levels of *STN1* and *TEN1* in *pif1* $\Delta$ , *exo1* $\Delta$  and *pif1* $\Delta$  *exo1* $\Delta$  strains were measured. In all three genotypes *STN1* and *TEN1* mRNA levels were similar to wild-type levels, in contrast with *nmd2* $\Delta$  strains (Figure 9), therefore Cdc13 bypass is not dependent on high levels of *STN1* and *TEN1* mRNA. However, future work needs to use western blotting to determine the expression levels of Stn1 and Ten1 proteins in *pif1* $\Delta$  *exo1* $\Delta$  strains, since protein expression and mRNA level are not necessarily linked.



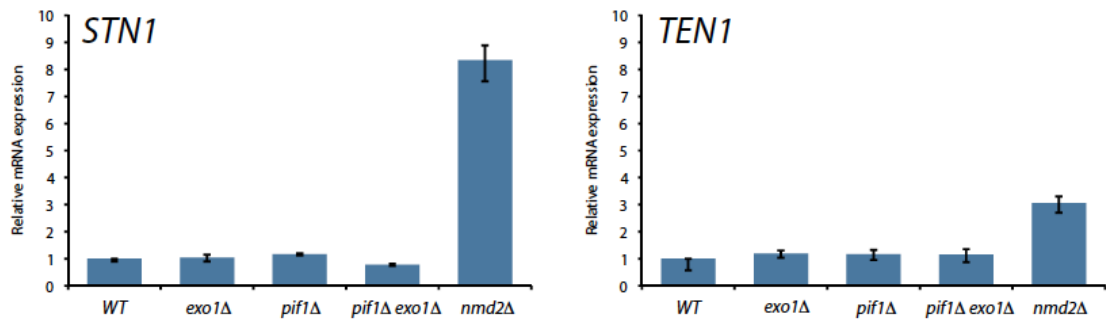


**Figure 9. *STN1* and *TEN1* mRNA are not overexpressed in a *pif1Δ exo1Δ* background**

Quantitative reverse-transcriptase PCR analysis of *Stn1* and *Ten1* mRNA expression levels in the strains indicated. All values were normalised to the control gene *BUD6*. A single wild-type strain was given a value of 1 and all other strains were expressed relative to this value. For each genotype, the mean of two independent strains is shown and error bars indicate the individual values for each strain.

### 3.4 The stoichiometry of CST components at telomeres can be altered

Deletion of *NMD2* increased the levels of *STN1* and *TEN1* mRNA (Figure 9) but it was unknown (in the published literature) whether increased expression of *STN1* and *TEN1* resulted in increased binding of Stn1 and Ten1 to the telomere end. To assay levels of Cdc13, Stn1 and Ten1 telomere binding in wild-type and *nmd2Δ* cells, chromatin immunoprecipitation (ChIP) was used to detect Stn1 and Ten1 binding to telomeric DNA. ChIP showed that Cdc13, Stn1 and Ten1 were bound to the end of the telomere of Chr. VI-R in a wild-type strain (Figure 10). Cdc13 has a much stronger ChIP signal than Stn1 and Ten1 in a wild-type strain, perhaps because it is a larger protein and also perhaps because it binds more tightly to ssDNA than Stn1 and Ten1 (therefore formaldehyde crosslinking to DNA is more effective).

In the absence of Nmd2, telomeric Cdc13 binding was only increased 1.8-fold, whereas Stn1 and Ten1 binding was increased 9-fold and 6-fold, respectively (Figure 10). Cdc13 is not known to be overexpressed in the absence of Nmd2 (Johansson *et al.*, 2007) but the slight increase in binding could indicate that increased Stn1 and Ten1 levels lead to a marginal increase in Cdc13 recruitment. Stn1 and Ten1 binding to the telomere increased dramatically in the absence of Nmd2 and this could simply be a result of overexpression. An alternative explanation is that *nmd2Δ* are known to have short telomeres (Figure 18, lane 5), therefore short telomeres may recruit higher levels of replication factors such as CST. However, since telomerase extends telomeres and Cdc13 recruits telomerase, it is surprising that Cdc13 is not more highly enriched at telomeres in the absence of Nmd2. Also, Stn1 represses telomerase recruitment therefore increased binding of Stn1 may actually explain why *nmd2Δ* cells have short telomeres.

It is possible that because the qPCR primers used recognise a unique sequence just upstream of the TG<sub>1-3</sub> repeats, this amplifies the qPCR signal when telomeres are short. This may be due to sonication of chromatin to 600bp fragments, in the ChIP protocol, which may increase the likelihood of obtaining fragments with TG<sub>1-3</sub> repeats and the unique upstream sequence. However,

Cdc13 levels are not known to increase in *nmd2Δ* cells and the increase in Cdc13 enrichment at *nmd2Δ* telomeres is less than twofold. This suggests that there may be a minor effect of the qPCR locus at short telomeres, but this does not wholly explain the large increases in telomeric Stn1 and Ten1.

Another explanation why increased telomeric Stn1 and Ten1 is seen in the absence Nmd2 is that *nmd2Δ* cells have an extended S-phase, the time at which CST is recruited to the telomere to facilitate replication. However, Stn1 is overexpressed in the absence of Nmd2 (Addinall *et al.*, 2011) and Stn1 overexpression overrides S-phase checkpoint signals (Gasparyan *et al.*, 2009), therefore it seems unlikely that *nmd2Δ* cells would have an extended S-phase. On the other hand, human cells arrest in S-phase when the NMD factor UPF1 is depleted (Azzalin and Lingner, 2006), therefore it would be informative to subject yeast *nmd2Δ* cells to FACS analysis to see whether S-phase is extended.

Overall, the simplest explanation for the increase in telomeric Stn1 and Ten1 in *nmd2Δ* cells is that overexpression of Stn1 and Ten1, in the absence of Nmd2, leads to more Stn1 and Ten1 binding to telomeres. If the increase in Cdc13 (1.8-fold), Stn1 (9-fold) and Ten1 (6-fold) binding in an *nmd2Δ* strain is expressed as a ratio, CST exists in a 1:5:3 ratio (Cdc13/Stn1/Ten1). Evidence from *Candida glabrata* has shown that CST is in a 2:4:2 or 2:6:2 arrangement (Lue *et al.*, 2013). The 1:5:3 ratio in budding yeast suggests that CST may be formed of repeated subunits when Stn1 and Ten1 are overexpressed.

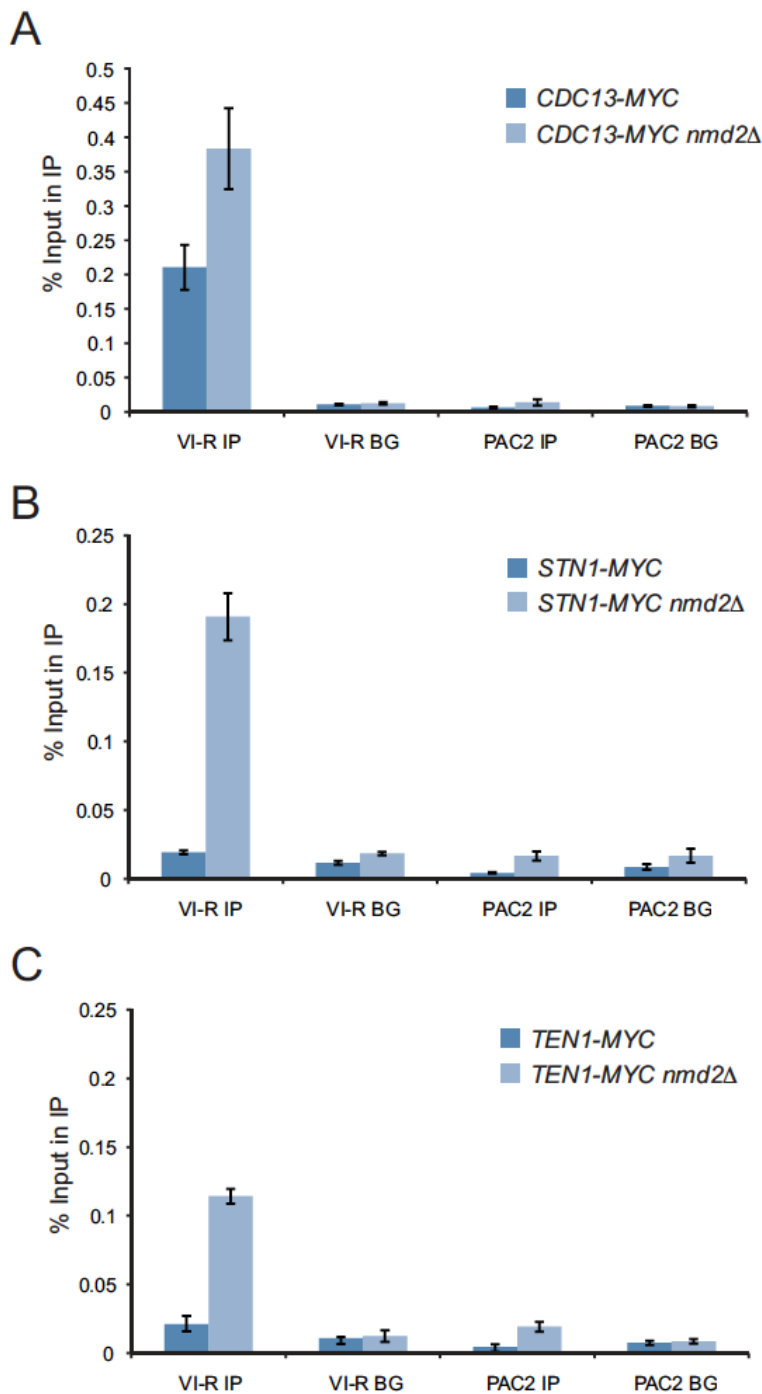


**Figure 10. Stn1 and Ten1 binding to telomeres increases in the absence of Nmd2**

ChIP analysis of (A) Cdc13-13Myc, (B) Stn1-13Myc and (C) Ten1-13Myc binding to the Chromosome VI-Right arm telomere (Chr VI-R) and the internal locus *PAC2* on Chromosome V in either wild-type or *nmd2Δ* strains. (A-C) Cultures of each genotype were grown at 23°C and cells were harvested in exponential phase. Duplicate samples were immunoprecipitated with an anti-Myc antibody (IP) or a non-specific IgG control (BG). ChIP samples were measured in triplicate by qPCR and group means are shown with error bars indicating standard deviation.

### 3.5 Stn1 is at telomeres without Cdc13

Since the genetic manipulations that allow bypass of Cdc13 do not allow bypass of Stn1 or Ten1, it was hypothesised that Stn1 and Ten1 carry out independent roles at the telomere. Similarly, although Cdc13 bypass strains can maintain telomeres by recombination, independently of telomerase, the same genetic manipulations do not allow bypass of Stn1 and Ten1. This implies that Stn1 and Ten1 still carry out essential roles at the telomere end in the absence of Cdc13.

To test whether Stn1 and Ten1 had telomeric roles separate from Cdc13, it was investigated whether Stn1 and Ten1 could still be located on telomeric DNA in the absence of Cdc13 using ChIP. In the absence of Cdc13, Stn1 was still enriched at telomeres (Chr. VI-R), but levels of DNA binding were lower (Figure 11 A). Levels of Ten1 binding in the absence of Cdc13 were below the detection limit of the ChIP assay (Figure 11 B). The drop in Stn1 DNA binding was perhaps because Cdc13 was not available to load Stn1 onto the telomere end (Stn1 competes for the Est1 binding site on Cdc13 (Chandra *et al.*, 2001)). An alternative explanation is that qPCR for a unique telomeric sequence (upstream of the TG<sub>1-3</sub> repeats), using sheared DNA from a strain maintaining telomeres by recombination, may affect enrichment for this locus due to extended TG<sub>1-3</sub> repeats in Type II survivors. Since chromatin was sheared to 600bp fragments, breaks may have occurred that separated Stn1, bound to single-stranded TG<sub>1-3</sub> repeats, from the upstream qPCR sequence. Also, since *cdc13*Δ strains maintain telomeres using recombination, it is possible that the qPCR sequence is lost to some degree, and this would also explain the drop in Stn1 enrichment in a *cdc13*Δ strain.

However, that Stn1 binding persists in the absence of Cdc13 indicates that either Stn1 has DNA-binding capability through its single OB fold and/or that Stn1 interacts with another DNA-binding protein to protect the telomere end and facilitate replication.

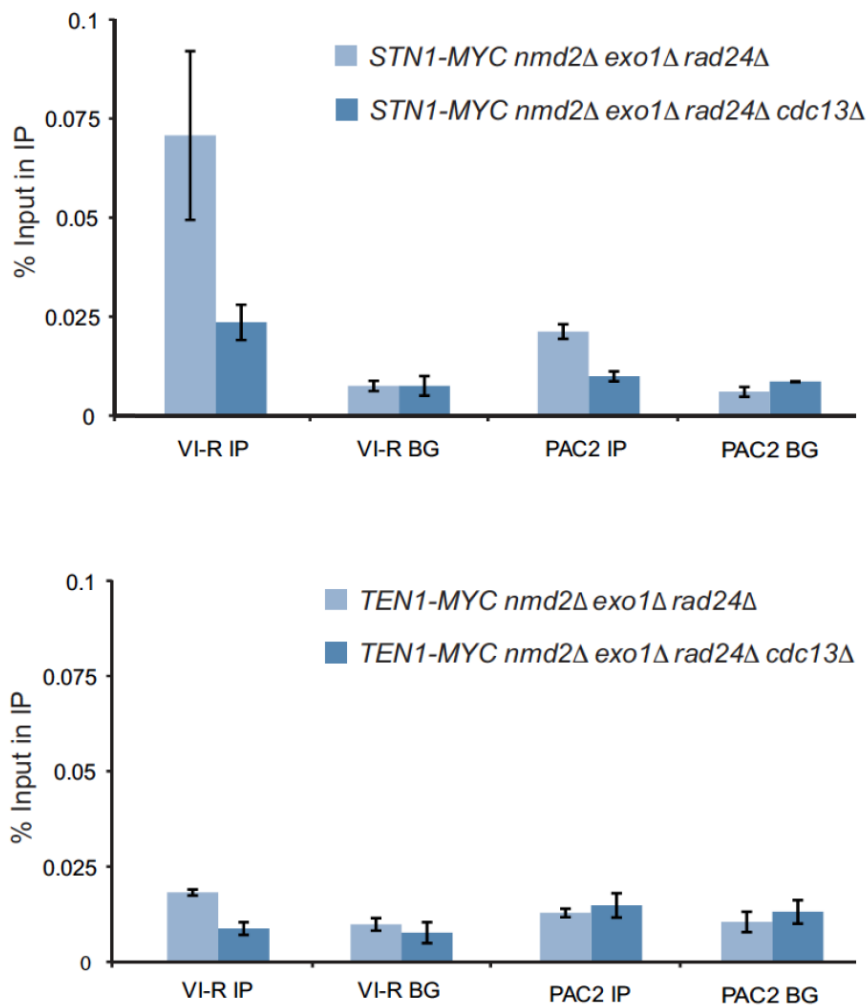


**Figure 11. Stn1 is at telomeres in the absence of Cdc13**

ChIP analysis of (A) Stn1-13Myc and (B) Ten1-13Myc binding to the Chromosome VI-Right arm telomere (Chr VI-R) and the internal locus *PAC2* on Chromosome V in strains with the genotypes indicated. (A & B) Cultures of each genotype were grown at 23°C and cells were harvested in exponential phase. Duplicate samples were immunoprecipitated with an anti-Myc antibody (IP) or a non-specific IgG control (BG). ChIP samples were measured in triplicate by qPCR and group means are shown with error bars indicating standard deviation.

### 3.6 Telomeric RPA is increased in the absence of Cdc13

Stn1 binds DNA more weakly than Cdc13 (Gao *et al.*, 2007), therefore it is possible that Stn1 might form a complex with RPA in order to bind telomeric DNA in the absence of Cdc13. RPA is a CST-like heterotrimer that binds ssDNA during replication and at DSBs. RPA also appears to have structural similarity to CST, in that the large subunit (Rfa1 in yeast) has strong DNA-binding capacity through an OB fold, similar to Cdc13 (Figure 5) (Maniar *et al.*, 1997; Gao *et al.*, 2007; Miyake *et al.*, 2009; Sun *et al.*, 2009). Similarly, both Stn1 and Rfa2 have a single OB fold and winged helix motifs, and Ten1 and Rfa3 have a single OB domain (Sun *et al.*, 2011). To see whether RPA bound to telomeres in the absence of Cdc13, RPA binding to telomeric DNA was measured by ChIP.

There were slightly elevated levels of RPA binding at the telomere (Chr VI-R) in an *nmd2Δ exo1Δ rad24Δ cdc13Δ* strain compared to wild-type levels (Figure 12). Elevated RPA binding in the *nmd2Δ exo1Δ rad24Δ cdc13Δ* strain may be because the strain is a Type II survivor (which has long TG<sub>1-3</sub> tracts that take longer to replicate) and this may cause RPA to bind for longer. Also, repetitive DNA tracts are more difficult to replicate, therefore there may be fork stalling and ssDNA generation, which leads to RPA binding to telomeric DNA for longer. Since the ChIP used a qPCR locus that is upstream of TG<sub>1-3</sub> repeats, it is not possible to determine whether telomeric RPA binding is at single-stranded TG<sub>1-3</sub> repeats at the telomere end. Therefore, it is not possible to determine whether RPA is co-localising with Stn1.

RPA bound strongly to telomeres in all genetic backgrounds tested, compared to the *PAC2* internal control locus. Telomeric RPA binding has been reported in a previous study, which showed that RPA was involved in the recruitment of telomerase during S-phase through Rfa2 interaction with Est1, which may promote Cdc13-Rfa2 interaction (Schramke *et al.*, 2004). In human cells and *S. pombe*, which have the POT1/Pot1 ssDNA binding protein in the shelterin/shelterin-like complex, there is a switch from Pot1 binding to RPA binding in S-phase to allow replication of the telomere (Flynn *et al.*, 2011; Audry

*et al.*, 2015). A similar switch may occur between RPA and Cdc13. In the absence of Cdc13, increased RPA binding may occur due to lack of Cdc13 recruitment of telomerase. Since Rfa2 interacts with Est1, Rfa2-mediated recruitment of telomerase may help to replicate telomeres in the absence of Cdc13.



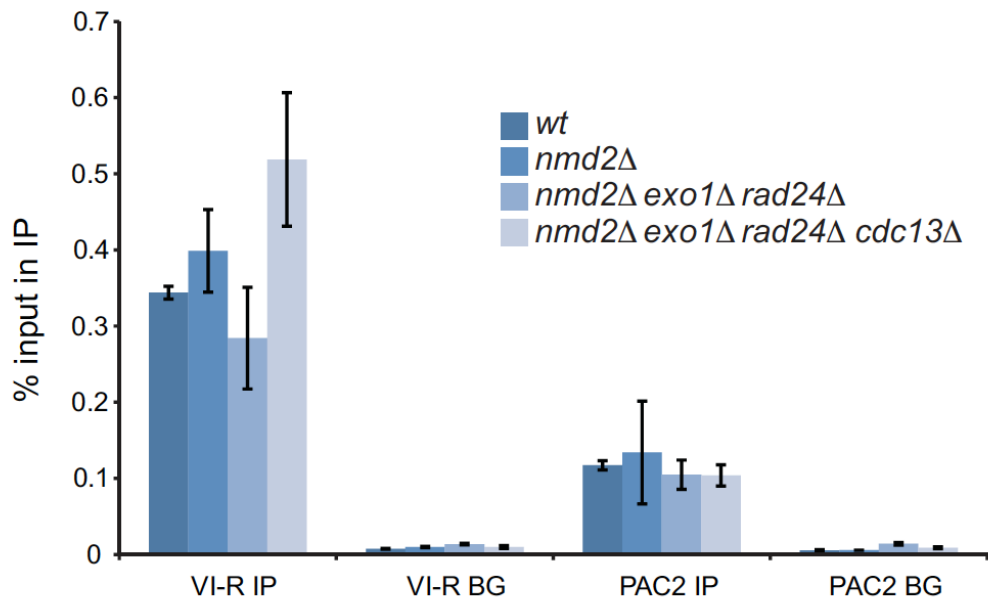


**Figure 12. Telomere-bound RPA is increased in the absence of Cdc13**

ChIP analysis of RPA binding to the Chromosome VI-Right arm telomere (ChrVI-R) and the internal locus *PAC2* on Chromosome V. Cultures of strains with the genotypes indicated were grown at 23°C and cells were harvested in exponential phase. Duplicate samples were immunoprecipitated with an anti-*S. cerevisiae* RPA antibody (IP) or a non-specific IgG control (BG). ChIP samples were measured in triplicate by qPCR and group means are shown with error bars indicating standard deviation.

### 3.7 *STN1* genetically interacts with *RFA3*

Since increased telomeric RPA was seen in the absence of Cdc13, this suggested that RPA might be important for Cdc13 bypass. Given that RPA is analogous to CST, it was hypothesised that RPA subunits could interact with Stn1, in order to recruit Stn1 to the telomere in the absence of Cdc13. All RPA genes (*RFA1/2/3*) deletions and *STN1* deletions are lethal in budding yeast so a *stn1-13* temperature-sensitive mutant was crossed with an *rfa3-313* temperature-sensitive mutant (both were taken from an S288C genetic background library of temperature-sensitive mutants, see Appendix B), the diploid was sporulated and tetrads were dissected. All colonies appeared sectorial, however this is normally observed for all S288C strains. *stn1-13* and *rfa3-313* mutations were synthetic lethal (Figure 13 A).

Rfa3 is the smallest subunit of RPA and is structurally analogous to Ten1 (Figure 5). Since the *rfa3-313* mutation has an additive effect to the *stn1-13* mutation (which disrupts Cdc13 and Ten1 binding to Stn1), this suggests that Rfa3 and Stn1 work in independent pathways. It is possible that when telomere end protection by Stn1 is sub-optimal, Rfa3 may compensate, perhaps by promoting RPA binding to the telomere end. Indeed, the *rfa3-313* mutant has Rfa1 aberrantly localized to the cytoplasm rather than the nucleus (Belanger *et al.*, 2011), which suggests that nuclear Rfa3 is required when Stn1 function is impaired. This suggests that Rfa3 may be able to compensate for telomere replication or end protection defects caused by the *stn1-13* mutation. When both Stn1 and Rfa3 function is compromised, damage to the telomere may activate the DDR, causing cell cycle arrest and ultimately cell death.

It is possible that Rfa1 might also be important for Stn1 activity. To investigate this possibility, the same *stn1-13* used previously was crossed to an *rfa1-M2* strain (from the same library as before). However, there was no synthetic lethality between *stn1-13* and *rfa1-M2* (Figure 13 B). Since there was no additive effect of *rfa1-M2*, this suggests that Rfa1 and Stn1 work together in the same pathway. Since Stn1 interacts with Cdc13 to inhibit telomerase access, perhaps Rfa1 has a similar role in inhibiting telomerase. Rfa2 is known to

promote Cdc13-Est1 interaction (Schramke *et al.*, 2004), therefore since Stn1 and Rfa1 appear to work in the same pathway, Rfa1 and Rfa2 may have an antagonistic role in regulating Cdc13 interaction with telomerase.

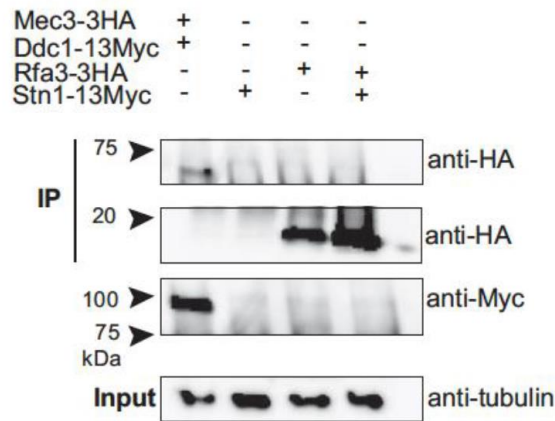


### 3.8 No evidence of a physical interaction between Stn1 and Rfa1, Rfa2 or Rfa3

Given that there was a genetic interaction between Stn1 and Rfa3 thermosensitive alleles, it was investigated whether Stn1 and Rfa3 interacted physically, using co-immunoprecipitation (co-IP). Rfa3-HA was immunoprecipitated but no Stn1-Myc could be detected (Figure 14 A). A control co-IP to detect interaction between Mec3-HA and Ddc1-Myc (which are known to physically interact) was successful, indicating that the co-IP method worked (Figure 14 A). There is evidence, therefore, of a genetic interaction between Stn1 and the RPA subunit Rfa3, but no evidence of a physical interaction.

As increased telomeric RPA was seen in the absence of Cdc13 (Figure 12) it was hypothesised that Stn1 or Ten1 might only interact with RPA in the absence of Cdc13. Also, since no interaction with Rfa3 was seen, Stn1 might interact physically with either Rfa1 or Rfa2. Stn1-Myc and Ten1-Myc were immunoprecipitated using an anti-Myc antibody and, as a control, Rfa1-Myc and Rfa2. Rfa2 could be detected in the Rfa1-Myc immunoprecipitate, therefore the co-IP method was successful. However, Stn1-Myc was successfully immunoprecipitated in the absence of Nmd2 (most likely because of a much higher level of expression when *NMD2* is deleted), but no Rfa1 or Rfa2 could be detected binding to Stn1-Myc (Figure 14 B). Therefore there is no evidence that Stn1 physically interacts with Rfa1 or Rfa2 in the absence of Cdc13. It was not possible to detect Stn1-Myc immunoprecipitation without the *NMD2* deletion, since wild-type expression of Stn1 is too low to detect by western blotting (Dahlseid *et al.*, 2003). Ten1-Myc expression is too low to detect by western blotting in the presence or absence of Nmd2 (Dahlseid *et al.*, 2003).

A



B

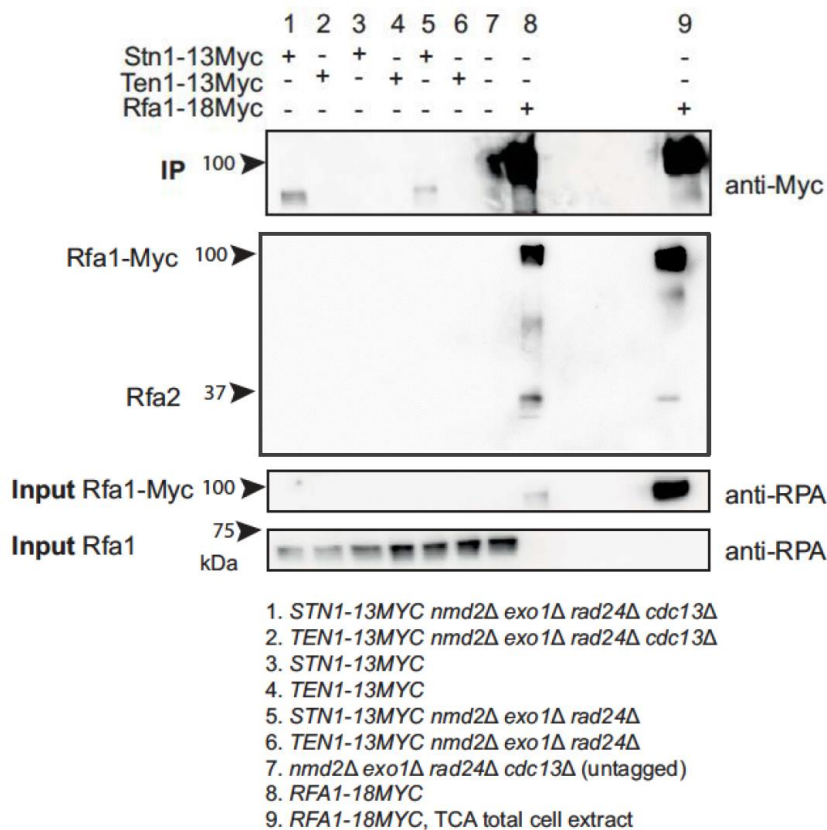


### Figure 14. No evidence of a physical interaction between Stn1 and RPA

(A) Lysate from strains with the genotypes shown was immunoprecipitated with anti-HA antibody. Immunoprecipitated proteins were analysed by Western blot, using anti-Myc antibody, anti-HA antibody and anti-tubulin antibody. (B) Lysate from strains with the genotypes shown was immunoprecipitated with anti-Myc antibody. Immunoprecipitated proteins were analysed by Western blot, using an anti-*S. cerevisiae* RPA antibody and an anti-Myc antibody. Lane 9 was a total cell extract control prepared using TCA extraction.

### 3.9 Discussion

The telomere-capping protein Cdc13 has long been a focus of budding yeast telomere research and it has been assumed that Cdc13 is the major telomeric ssDNA binding protein. In this chapter it has been demonstrated that Stn1 and Ten1, the partner proteins of Cdc13, play an important role in telomere protection independently of Cdc13. All three CST genes are essential, however the requirement for Cdc13 can be bypassed in the absence of Nmd2 and Exo1 or Rad24, but the requirement for Stn1 and Ten1 cannot be bypassed.

The telomeres of Cdc13 bypass strains resemble those of telomerase-deficient survivors. Whilst telomerase deficient survivors rapidly lose fitness with each passage, then enter 'crisis' and recover, viable *cdc13*Δ strains continually increase their fitness with passage and had no detectable 'crisis'. The lack of an observable crisis in *cdc13*Δ strains indicates that cells have no crisis, or that they undergo crisis much earlier than the first passage. When the telomerase RNA component *TLC1* was deleted from Cdc13 bypass strains, strains formed survivors at an early passage number but again increased in fitness with passage. Survivor formation at an early passage indicates that telomere crisis, occurred much earlier than passage 1, and perhaps earlier than in *cdc13*Δ *TLC1* strains.

It was found that the stoichiometry of CST components could be altered in the absence of Nmd2, when Stn1 and Ten1 are known to be overexpressed (Addinall *et al.*, 2011). It was found that in the absence of *NMD2*, Cdc13 telomere binding increased less than 2-fold, but Stn1 and Ten1 binding increased 9-fold and 6-fold, respectively (Figure 10). It is possible that ChIP analysis (by qPCR) amplified Stn1 and Ten1 binding to telomeres, because telomeres are short in *nmd2*Δ cells. Since the ChIP assay uses 600bp DNA fragments and a qPCR sequence in a unique sequence proximal to the TG<sub>1-3</sub> repeats, when telomeres are short there may be an increased likelihood of immunoprecipitating CST proteins bound to TG<sub>1-3</sub> repeats. Conversely, when telomeres are long and heterogeneous (as in strains bypassing Cdc13 in

Figures 11 and 12), the chances of obtaining TG<sub>1-3</sub> repeats proximal to the qPCR sequence may be reduced. This would reduce the levels of CST proteins detected by qPCR, e.g. in Figure 11, the drop in Stn1 binding to the telomere in the absence of Cdc13 could be due to telomere rearrangements affecting the qPCR signal or lack of Cdc13 to bind to (or both). However, there was no substantial increase in Cdc13 binding in *nmd2Δ* cells despite short telomeres, therefore it is difficult to judge the significance of the effect of short telomeres on the ChIP qPCR. The simplest explanation for increased enrichment of Stn1 and Ten1 at telomeric DNA, in *nmd2Δ* cells, is that more Stn1 and Ten1 binding increases when Stn1 and Ten1 are overexpressed.

Since *nmd2Δ* cells overexpress over 200 proteins, including Stn1 and Ten1 (Johansson *et al.*, 2007), it is possible that Stn1 and Ten1 overexpression solely explained Cdc13 bypass. However, it has previously been shown that it is impossible to obtain any *nmd2Δ cdc13Δ* cells (Holstein *et al.*, 2014).

Furthermore, in a *pif1Δ exo1Δ* strain, from which *CDC13* but not *STN1* or *TEN1* can be deleted (Holstein *et al.*, 2014), *STN1* and *TEN1* mRNA levels were not increased. Therefore, *STN1* and *TEN1* mRNA overexpression most likely does not explain Cdc13 bypass.

In the absence of Cdc13 it was found that Stn1 bound telomeric DNA (Ten1 binding was below the detection limit of the ChIP assay). The possibility that Stn1 bound to another ssDNA-binding protein, in the absence of Cdc13, was considered since Stn1 binds ssDNA more weakly than Cdc13 (Gao *et al.*, 2007; Sun *et al.*, 2009). Stn1 binding to the ssDNA-binding complex RPA was considered, however although increased levels of telomeric RPA were seen in the absence of Cdc13 and Stn1 appeared to work in the same pathway as Rfa1, no evidence of physical interaction between Stn1 and RPA subunits could be found. It is possible that without Cdc13, multiple units of Stn1-Ten1 bind telomeric ssDNA. Stn1-Ten1 may bind to telomeric DNA using the single OB fold of Stn1 when Cdc13 is absent. Also, RPA may bind telomeric ssDNA in the absence of Cdc13, since Rfa1 may act in the same pathway as Stn1 (Figure 15)



The Cdc13 orthologue CTC1 is mutated in diseases such as Coats plus and *dyskeratosis congenita* but no mutations have so far been reported in STN1 and TEN1 in the same sets of patients (Walne *et al.*, 2013). A CTC1-null mouse is viable but exhibits severe telomere defects and dies prematurely (Gu *et al.*, 2012). To date, no STN1 and TEN1-null mice have been produced. This suggests that in higher eukaryotes, as in yeast, STN1 and TEN1 are more important than CTC1 for cell viability. Since it has been demonstrated in this thesis that Stn1 and Ten1 can compensate for Cdc13 deficiency when NMD and the DDR are attenuated, it is possible that future therapies could stimulate and support STN1 and TEN1 activity to treat diseases involving CTC1 mutations. NMD inhibitors (e.g. inhibitors of UPF1) could be employed to overexpress STN1 and TEN1, together with suppression of the DDR. However, downsides to this treatment would be the expression of abnormal proteins containing a premature stop codon and accumulation of damaged DNA, which increases the risk of cancer.

In conclusion, Stn1 and Ten1 might be more important for telomere end protection than Cdc13 and are able to carry out their protective roles in the absence of Cdc13. CST in budding yeast is not an obligate heterotrimer and Stn1 and Ten1 are likely to carry out independent roles. STN1 and TEN1 may be similarly independent in humans, and their activities could be promoted in order to bypass faulty CTC1 in diseases such as Coat's plus and *dyskeratosis congenita*.

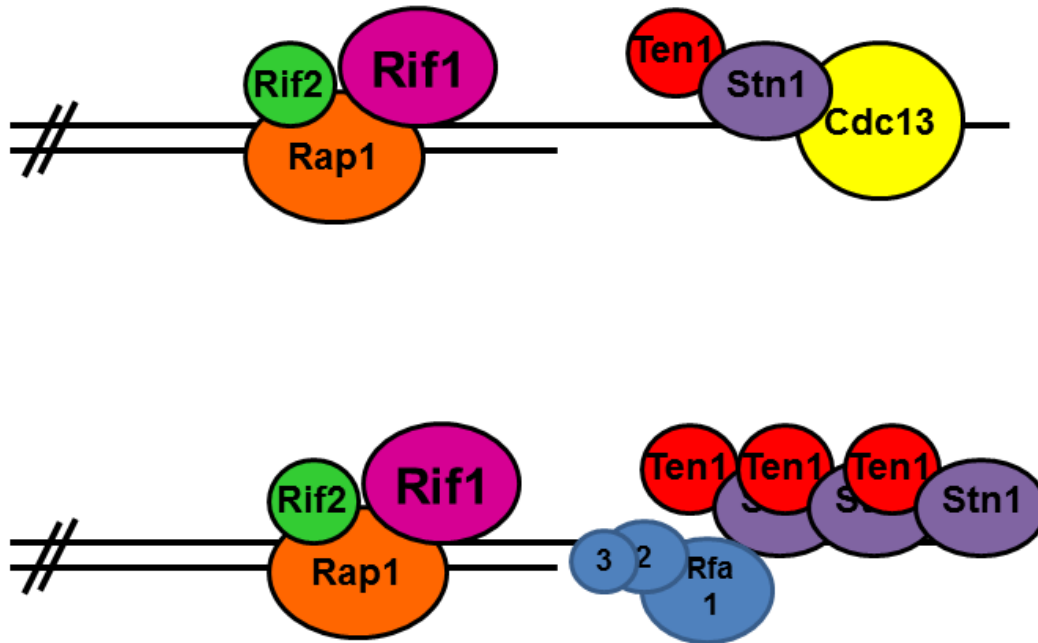


**Figure 15. Hypothetical model of telomere end protection in the absence of Cdc13**

(Top panel) In the presence of Cdc13, Stn1 and Ten1 bind Cdc13 to cap the telomere end and promote lagging strand fill-in. (Bottom panel) In the absence of Cdc13, Stn1 and Ten1 still maintain telomeric roles, perhaps by binding of multiple Stn1-Ten1 heterodimers to telomeric ssDNA. RPA (Rfa1, Rfa2, Rfa3) may also bind telomeric ssDNA in the absence of Cdc13.

## Chapter 4. Rif1 is required for Cdc13 bypass

### 4.1 Genome-wide single gene deletion screens using *cdc13Δ* and *CDC13<sup>+</sup>* query strains

In order to understand the cellular mechanisms allowing Cdc13 bypass, other than the roles of Stn1 and Ten1, yeast genetics was used to see which genes were important for the viability of a Cdc13 bypass strain. Robotic synthetic genetic array (SGA) technology allows for a single query strain to be mated with a single gene deletion library and DAmP (decreased abundance by mRNA perturbation) library of essential genes, totalling over 5,000 strains (Tong and Boone, 2006). In essence, the query strain is first mated with the library strains on agar plates using a robotic pin tool. This creates diploids, which are then sporulated to obtain haploid spores. Spores with the desired genotype are then selected by sequential pinning to selective media. Once haploids have been selected, the colony size is compared to a control screen conducted using the same media.

The SGA process is summarised graphically in Figure 16 A. The two SGA screens were performed (1) by mating an *nmd2Δ exo1Δ cdc13Δ* query strain (denoted '*cdc13Δ*') with a single gene deletion library and DAmP alleles (Figure 16 A) and (2) by mating an *nmd2Δ exo1Δ* query strain (denoted '*control*') with the same libraries (Figure 16 B). The single gene deletion library and query strain were in the *S. cerevisiae* S288C genetic background (rather than W303 which is used in this thesis). Each mating during the SGA screen had 4 replicates next to each other on the plate. The resulting diploids were sporulated to obtain haploid progeny and haploids with the genotype of (1) *nmd2Δ exo1Δ cdc13Δ yfgΔ* or (2) *nmd2Δ exo1Δ yfgΔ* were obtained using selective media.

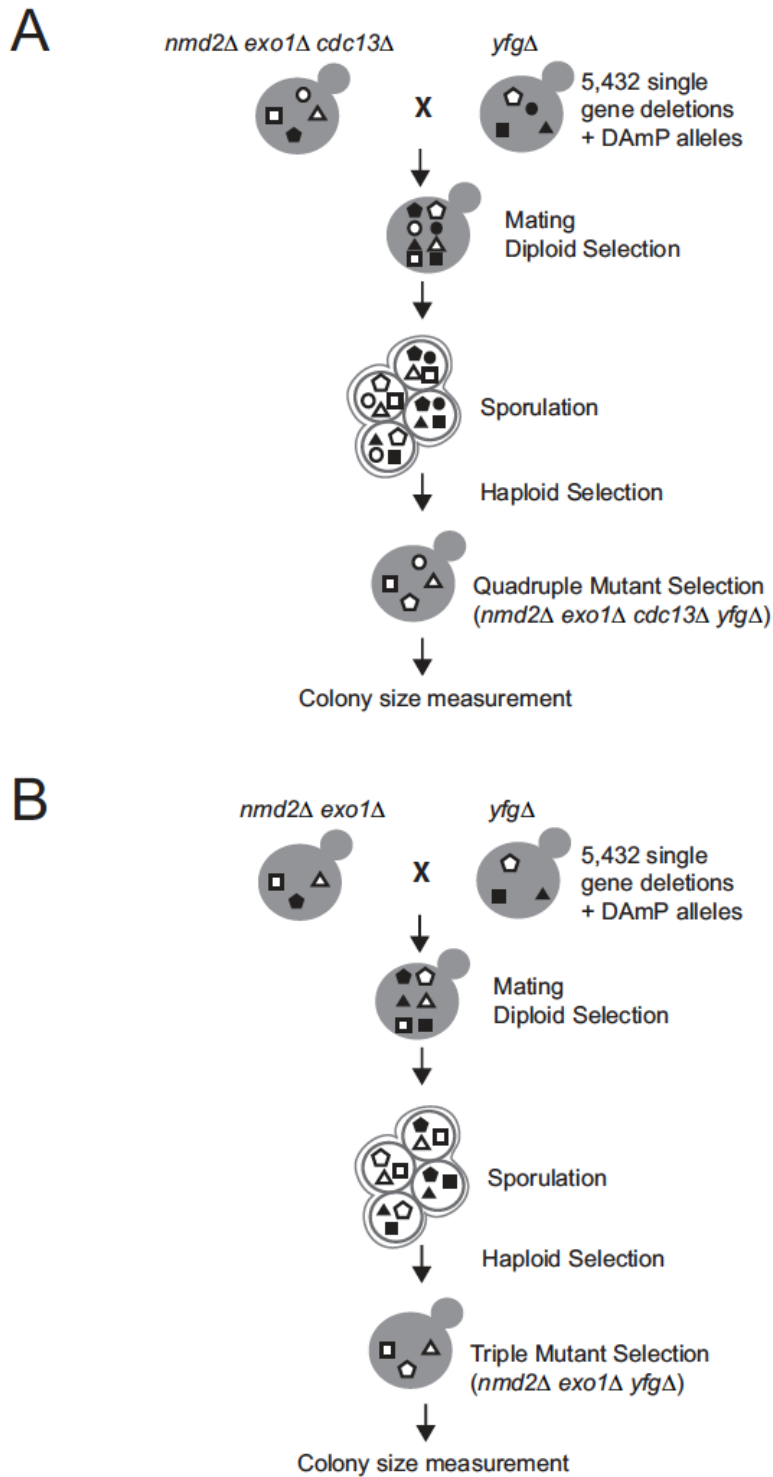


**Figure 16. SGA protocols for *cdc13Δ* and *CDC13<sup>+</sup>* screens**

(A) SGA protocol for crossing an *nmd2Δ exo1Δ cdc13Δ* query strain with single gene deletion and DAmP allele libraries, sporulating diploids and obtaining *nmd2Δ exo1Δ cdc13Δ yfgΔ* haploids. (B) SGA protocol for crossing an *nmd2Δ exo1Δ* query strain with single gene deletion and DAmP allele libraries, sporulating diploids and obtaining *nmd2Δ exo1Δ yfgΔ* haploids.

## 4.2 Gene deletions for a number of known complexes behaved similarly in both *cdc13* $\Delta$ and *CDC13*<sup>+</sup> genome-wide screens

Figure 17 shows the colony sizes from the *nmd2* $\Delta$  *exo1* $\Delta$  *cdc13* $\Delta$  and *nmd2* $\Delta$  *exo1* $\Delta$  SGAs plotted against each other. To remove genetic interactions due to linkage with the genes deleted in the screens, genes 20 kb upstream and downstream of the deleted genes were removed from the analysis.

One measure of the accuracy of an SGA screen is the clustering of complexes in similar locations on the plot of control versus query screen (Figure 17). To determine whether single gene deletions relating to complexes clustered together, the locations of a list of functional complexes (Benschop *et al.*, 2010) were determined. It was found that components of the Replication Factor C (RFC) complex *CTF8*, *CTF18* and *DCC1*; *RAD51* and *RAD55* which interact during DSB repair; the tRNA methyltransferase complex *TRM8* and *TRM82* and the DNA Polymerase Zeta complex *REV3* and *REV7* all clustered in similar locations to their partner genes (Figure 17). *CTF8*, *CTF18* and *DCC1* deletions are also synthetically sick with the *cdc13-1* allele (Addinall *et al.*, 2011), which provided further evidence that *CDC13* had been deleted in the SGA query strain. All complexes mentioned here reduced the fitness of a Cdc13 bypass strain when their genes were deleted. Since deleting genes within complexes has similar effects, this indicates that the SGAs conducted can accurately show genetic effects on Cdc13 bypass.

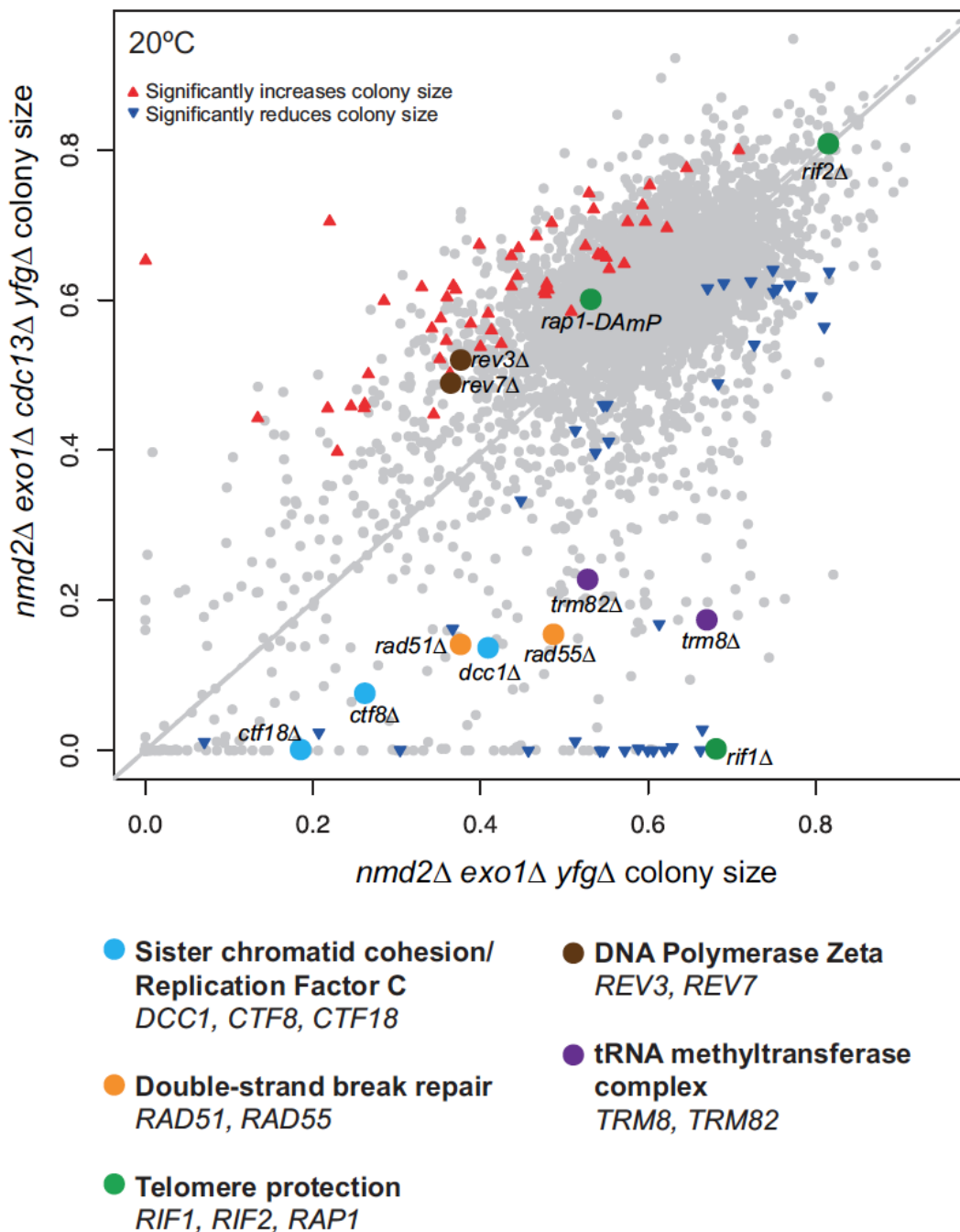


**Figure 17. Single gene deletions and complexes affecting Cdc13 bypass**

Mean colony sizes from the two SGA screens indicated were plotted against each other. Red upwards arrows indicate a single gene deletion/DAmP allele that significantly increases *nmd2Δ exo1Δ cdc13Δ* colony size (t-test on variance in colony size of 4 independent colonies,  $p < 0.05$ ). Blue downwards arrows indicate a single gene deletion/DAmP allele that significantly decreases *nmd2Δ exo1Δ cdc13Δ* colony size (t-test as before). The solid line is a regression line denoting the colony size expected on the y axis of each strain given its colony size on the x axis. The dashed line indicates 1:1 growth. The positions of gene deletions relating to complexes are indicated by coloured dots.

### 4.3 Viable *cdc13Δ yfgΔ* strains resemble telomerase-deficient survivors

It was surprising that there was no discernible fitness defect arising from *CDC13* deletion, since the lines of no interaction and 1:1 growth coincided. One possible explanation for this was that deletion of *CDC13* had not been selected for during the rounds of plating to selective media during the SGA. To confirm whether the *CDC13* had selected for, *nmd2Δ exo1Δ cdc13Δ yfgΔ* strains were picked at random from the upper fitness segment (above or on the line of no interaction) and passaged. The telomeres of some these strains resembled telomerase-deficient survivors by passage 6 (Figure 18 B, lanes 9-10, 13-15) and telomeres were short even at passage 1 (Figure 18, lanes 5-10 and 12-17). This concurred with previously published data that *cdc13Δ* strains resembled Type I and Type II survivors after 9 passages (Figure 7; Holstein *et al.* (2014)). Since S288C *nmd2Δ exo1Δ cdc13Δ yfgΔ* strains had abnormal telomeres, similar to W303 *nmd2Δ exo1Δ cdc13Δ* strains, it was evident that the *CDC13* deletion had been correctly selected for during the GA.

Perhaps the lack of a fitness defect in the *cdc13Δ* query strain resulted from the passages onto selective media during the haploid selection stage of the SGA. In this phase, strains are pinned sequentially onto selective media of increasing stringency to build up sufficient numbers of strains with the required genotype. It is known that W303 *nmd2Δ exo1Δ cdc13Δ* strains increase fitness with passage, therefore repeated passaging of the S288C strains may have resulted in a fitness increase. An alternative explanation for the lack of overall fitness defect, and most likely, is that the size of *nmd2Δ exo1Δ cdc13Δ* colonies are similar to wild-type colonies, although colonies are sectored (Holstein *et al.*, 2014). Since fitness was determined by colony size, similar *nmd2Δ exo1Δ cdc13Δ* and *nmd2Δ exo1Δ* colony size would lead to a similar estimation of fitness.

Interestingly, the *nmd2Δ exo1Δ cdc13Δ rif2Δ* strain maintained long Y' telomeres in passage 0 and passage 6 (Figure 18, lane 11 in A and B). Also, deleting *POL4* and *FOB1* increased Y' telomere length. It is possible that

absence of Rif2, Pol4 and Fob1 may be beneficial to Cdc13 bypass. Both *nmd2Δ* *exo1Δ* *cdc13Δ* *rif2Δ* and *nmd2Δ* *exo1Δ* *rif2Δ* strains appeared to have increased fitness (Figure 17). This suggests that elongated telomeres, caused by *RIF2* deletion, is beneficial in both strains – most likely because both strains have short telomeres.



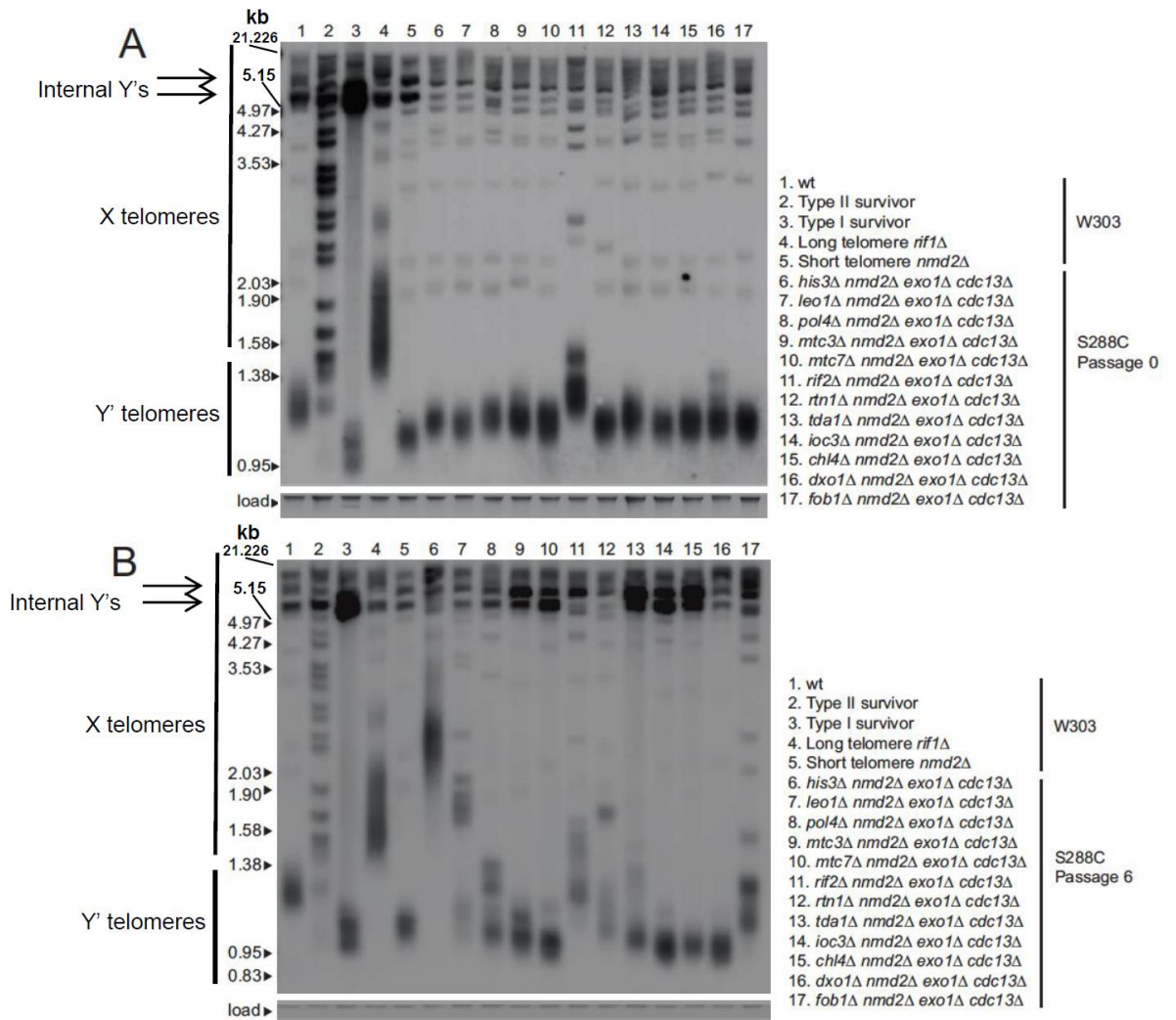


**Figure 18. *cdc13Δ* strains generated by SGA had abnormal telomeres by passage 6**

(A-B) SGA strains (genotypes given on the right) were passaged by repeated, sequential robotic pinning to selective media and analysed by Southern blotting using a Y' and TG<sub>1-3</sub> repeat probe as before (see Figure 7A). The loading control is SyBr green staining as before.

#### 4.4 Rif1 is required for Cdc13 bypass

One set of interacting proteins whose genes did not cluster together was Rif1, Rif2 and Rap1 (Figure 17). *rif2* $\Delta$  and *rap1-DAmP* had little effect on *cdc13* $\Delta$  colony size versus the control colony size (*rap1-DAmP* may not be effective, however, as mRNA abundance in this strain was not tested). However, deleting *RIF1* was completely lethal to the *cdc13* $\Delta$  strain (Figure 17). It has previously been shown that deleting *RIF1* is lethal in a *cdc13-1* temperature-sensitive mutant grown at 23°C (Anbalagan *et al.*, 2011), however at 20°C the double-mutant is viable (Addinall *et al.*, 2011; Anbalagan *et al.*, 2011). The *cdc13* $\Delta$  SGA was conducted at 20°C but *nmd2* $\Delta$  *exo1* $\Delta$  *cdc13* $\Delta$  *rif1* $\Delta$  was nonetheless inviable. To confirm that Rif1 was indeed required for Cdc13 bypass an *nmd2* $\Delta$  *exo1* $\Delta$  *cdc13* $\Delta$  strain was crossed with a *rif1* $\Delta$  strain in the *S. cerevisiae* W303 genetic background. The diploid strain was sporulated and spores were analysed using tetrad dissection and random spore analysis. 100% of *nmd2* $\Delta$  *exo1* $\Delta$  *cdc13* $\Delta$  strains were viable (14/14), however I obtained no *cdc13* $\Delta$  *rif1* $\Delta$  genotypes by tetrad dissection (Figure 19). 54 tetrads were analysed but only 1 inviable *nmd2* $\Delta$  *rif1* $\Delta$  *exo1* $\Delta$  *cdc13* $\Delta$  strain could be determined (Figure 19, tetrad 3c). All other inviable genotypes that could be determined were not quadruple mutants (among the inviable genotypes that could not be determined, there may have been quadruple mutants).

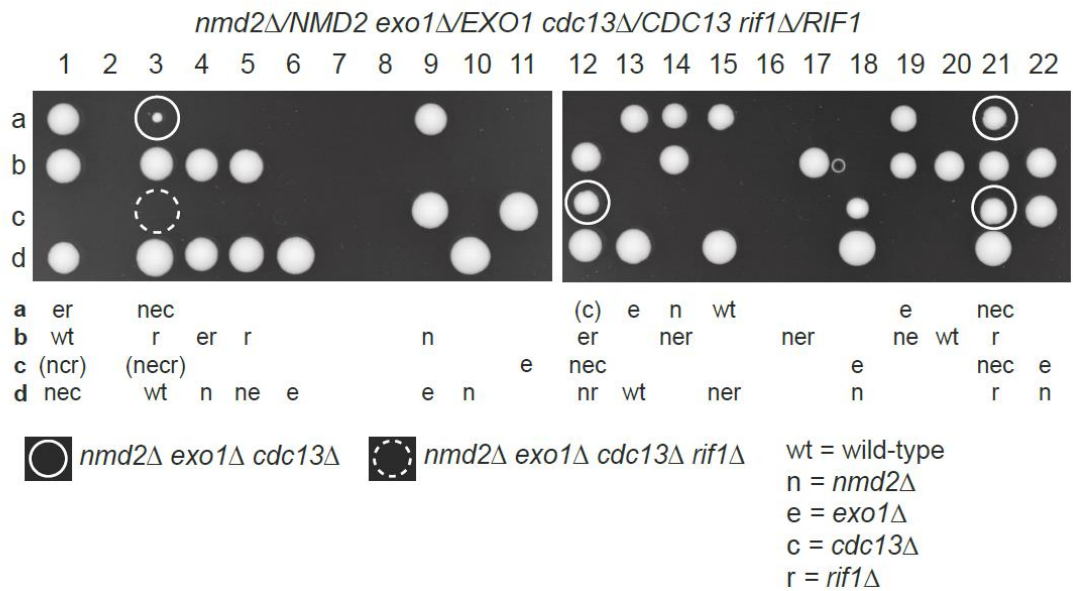


**Figure 19. Rif1 is required for Cdc13 bypass: evidence from tetrad dissections**

A diploid was generated by crossing a *rif1Δ* strain (DLY9697) with an *nmd2Δ* *exo1Δ* *cdc13Δ* strain (DLY8457). Spores were separated by tetrad dissection and plates were incubated for 5 days at 23°C before photographing. Two example plates are shown out of 54 tetrads analysed. Spore viability of the encircled genotypes is given in brackets after the genotype.

To generate larger numbers of spores, random spore analysis was conducted using the same spores. After determining the genotypes of 300 strains, no quadruple mutants were obtained. However, all other *rif1* $\Delta$  mutants that were *CDC13*<sup>+</sup> were obtained at or above the expected level (Figure 20). The expected number of spores (19) was calculated simply by dividing the number of strains analysed (302) by 16, the number of genotypes possible (assuming all genotypes were viable). Also, all other *RIF1*<sup>+</sup> *CDC13*<sup>+</sup> and *RIF1*<sup>+</sup> *cdc13* $\Delta$  strains (known previously to be viable) were obtained at or above the expected level. The finding that *RIF1*<sup>+</sup> *cdc13* $\Delta$  (i.e. *nmd2* $\Delta$  *exo1* $\Delta$  *cdc13* $\Delta$ ) strains were obtained above the expected level is supported by a previous publication in which *nmd2* $\Delta$  *exo1* $\Delta$  *cdc13* $\Delta$  strains had 100% viability (Holstein *et al.*, 2014). The fact that no *cdc13* $\Delta$  *rif1* $\Delta$  spores were obtained indicated that Rif1 is required for Cdc13 bypass (Figure 20).

Previously published data showed that a *rif1* $\Delta$  *cdc13-1* accumulated ssDNA, resulting from enhanced resection in the absence of Rif1 (Anbalagan *et al.*, 2011). Deleting *EXO1* reduced ssDNA accumulation to almost wild-type levels and increased *rif1* $\Delta$  *cdc13-1* fitness at restrictive temperatures (Anbalagan *et al.*, 2011). Therefore, Rif1 may be important for *cdc13-1* and Cdc13 bypass strain viability by repressing resection and ssDNA accumulation. However, Cdc13 bypass occurs in a strain deleted for *EXO1* and *NMD2* and deletion of either of these reduces ssDNA accumulation (Holstein *et al.*, 2014). Together with evidence that deletion of *RIF1* only slightly increases resection at a *de novo* telomere (Bonetti *et al.*, 2010), it would seem reasonable to assume that deletion of *RIF1* from an *nmd2* $\Delta$  *exo1* $\Delta$  *cdc13* $\Delta$  strain would not increase ssDNA accumulation enough to stop Cdc13 bypass. This is underlined by the SGA screen data, which showed that deletion of *RIF2* from an *nmd2* $\Delta$  *exo1* $\Delta$  *cdc13* $\Delta$  strain actually increased fitness (Figure 17) when *rif2* $\Delta$  cells degrade a *de novo* telomere more extensively than *rif1* $\Delta$  cells (Bonetti *et al.*, 2010). In conclusion, the role of Rif1 in preventing telomere resection may not be important for Cdc13 bypass.

<i>RIF1</i> genotypes	number	<i>rif1</i> $\Delta$ genotypes	number
<i>wt</i> ( <i>RIF1</i> )	21	<i>wt</i> ( <i>rif1</i> $\Delta$ )	45
<i>nmd2</i> $\Delta$	39	<i>nmd2</i> $\Delta$	31
<i>exo1</i> $\Delta$	30	<i>exo1</i> $\Delta$	21
<i>cdc13</i> $\Delta$	0	<i>cdc13</i> $\Delta$	0
<i>nmd2</i> $\Delta$ <i>exo1</i> $\Delta$	27	<i>nmd2</i> $\Delta$ <i>exo1</i> $\Delta$	34
<i>nmd2</i> $\Delta$ <i>cdc13</i> $\Delta$	0	<i>nmd2</i> $\Delta$ <i>cdc13</i> $\Delta$	0
<i>exo1</i> $\Delta$ <i>cdc13</i> $\Delta$	0	<i>exo1</i> $\Delta$ <i>cdc13</i> $\Delta$	0
<i>nmd2</i> $\Delta$ <i>exo1</i> $\Delta$ <i>cdc13</i> $\Delta$	54	<i>nmd2</i> $\Delta$ <i>exo1</i> $\Delta$ <i>cdc13</i> $\Delta$	0
<b>TOTAL</b>	<b>171</b>	<b>TOTAL</b>	<b>131</b>

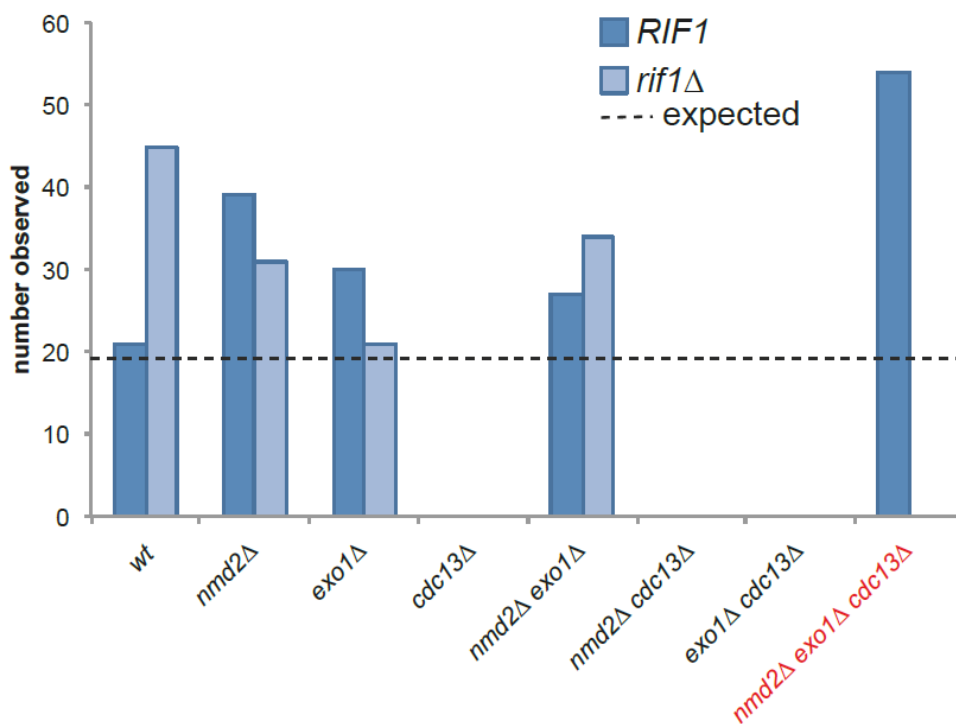


**Figure 20. Rif1 is required for Cdc13 bypass: evidence from random spore analysis**

The same spores from Figure 19 were analysed by random spore analysis. Numbers obtained per genotype are shown. Genotypes in red indicate that no *rif1* $\Delta$  spores were obtained for this genotype.

#### 4.5 Evidence that Rif1 DNA damage checkpoint repression is not required for Cdc13 bypass

A genetic background that permits Cdc13 bypass is absence of *NMD2* and the DNA damage checkpoint protein *RAD24*, which loads the Rad17-Mec3-Ddc1 sliding clamp and promotes DSB resection. It has been shown previously that Rif1 blocks Rad24 association with tracts of ssDNA (Xue *et al.*, 2011). In the absence of Cdc13, a degree of telomere uncapping may occur that generates ssDNA lesions. If these lesions are short and located at the telomere then Rif1 may mask these lesions from DDR factors such as Rad24, suppressing checkpoint activation and resection. It is possible that checkpoint suppression by Rif1 explains the requirement for Rif1 in an *nmd2Δ* *exo1Δ* *cdc13Δ* strain.

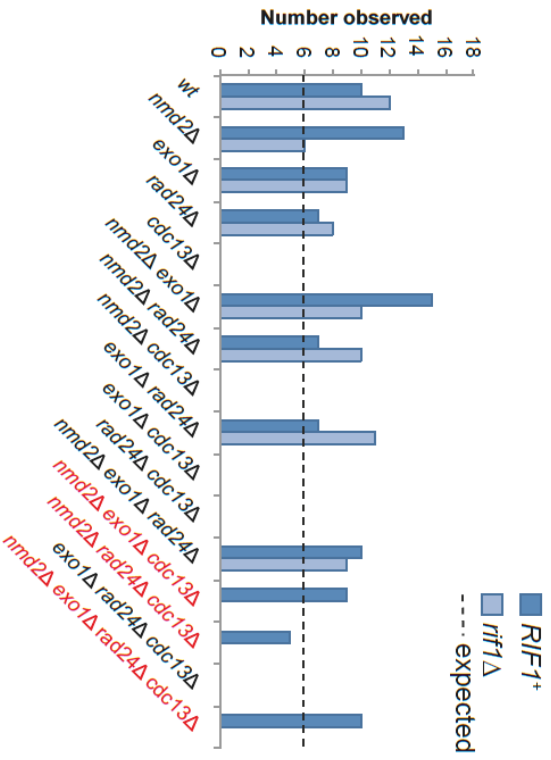
It was hypothesised that an *nmd2Δ* *rad24Δ* *cdc13Δ* *rif1Δ* strain was viable, since checkpoint suppression by *rad24Δ* might negate the anti-checkpoint role of Rif1. To test this hypothesis, two diploids heterozygous for *NMD2*, *EXO1*, *RAD24*, *CDC13* and *RIF1* deletions (two *nmd2Δ/NMD2* *rad24Δ/RAD24* *exo1Δ/EXO1* *cdc13Δ/CDC13* diploids transformed with *rif1::NATMX*) were sporulated and random spore analysis was conducted (Figure 21). No *cdc13Δ* *rif1Δ* genotypes were obtained (numbers of strains obtained for each genotype and the expected number are given in the upper panels and graphically in the lower panels). However, the expected number of *rif1Δ* *CDC13*<sup>+</sup> and viable *cdc13Δ* *RIF1*<sup>+</sup> strains were obtained (apart from *nmd2Δ* *rad24Δ* *cdc13Δ* where 5 strains were obtained instead of the expected 6). No strains were obtained for *cdc13Δ* genotypes previously known to be inviable (single and double mutants and triple mutants lacking *nmd2Δ*) which confirmed previously published data (Holstein *et al.*, 2014). The fact that no *nmd2Δ* *rad24Δ* *cdc13Δ* *rif1Δ* strains were viable indicates that inhibition of the Rad24 checkpoint by Rif1 is unimportant for Cdc13 bypass. This suggests that Rif1 has roles other than checkpoint repression (perhaps with Stn1 and Ten1) that allow Cdc13 bypass.

### DDY835

<i>RIF1+</i> genotypes	number	<i>rif1Δ</i> genotypes	number
wt	10	wt	12
<i>nmd2Δ</i>	13	<i>nmd2Δ</i>	6
<i>exo1Δ</i>	9	<i>exo1Δ</i>	9
<i>rad24Δ</i>	7	<i>rad24Δ</i>	8
<i>cdc13Δ</i>	0	<i>cdc13Δ</i>	0
<i>nmd2Δ</i> <i>exo1</i>	15	<i>nmd2Δ</i> <i>exo1Δ</i>	10
<i>nmd2Δ</i> <i>rad24Δ</i>	7	<i>nmd2Δ</i> <i>rad24Δ</i>	10
<i>nmd2Δ</i> <i>cdc13Δ</i>	0	<i>nmd2Δ</i> <i>cdc13Δ</i>	0
<i>exo1Δ</i> <i>rad24Δ</i>	7	<i>exo1Δ</i> <i>rad24Δ</i>	11
<i>exo1Δ</i> <i>cdc13Δ</i>	0	<i>exo1Δ</i> <i>cdc13Δ</i>	0
<i>rad24Δ</i> <i>cdc13Δ</i>	0	<i>rad24Δ</i> <i>cdc13Δ</i>	0
<i>nmd2Δ</i> <i>exo1Δ</i> <i>rad24Δ</i>	10	<i>nmd2Δ</i> <i>exo1Δ</i> <i>rad24Δ</i>	9
<i>nmd2Δ</i> <i>exo1Δ</i> <i>cdc13Δ</i>	9	<i>nmd2Δ</i> <i>exo1Δ</i> <i>cdc13Δ</i>	0
<i>nmd2Δ</i> <i>rad24Δ</i> <i>cdc13Δ</i>	5	<i>nmd2Δ</i> <i>rad24Δ</i> <i>cdc13Δ</i>	0
<i>exo1Δ</i> <i>rad24Δ</i> <i>cdc13Δ</i>	0	<i>exo1Δ</i> <i>rad24Δ</i> <i>cdc13Δ</i>	0
<i>nmd2Δ</i> <i>exo1Δ</i> <i>rad24Δ</i> <i>cdc13Δ</i>	10	<i>nmd2Δ</i> <i>exo1Δ</i> <i>rad24Δ</i> <i>cdc13Δ</i>	0
<b>TOTAL</b>	<b>102</b>	<b>TOTAL</b>	<b>75</b>

expected number per genotype = 6

(177 observed/32 genotypes)



### DDY836

<i>RIF1+</i> genotypes	number	<i>rif1Δ</i> genotypes	number
wt	15	wt	12
<i>nmd2Δ</i>	11	<i>nmd2Δ</i>	13
<i>exo1Δ</i>	8	<i>exo1Δ</i>	10
<i>rad24Δ</i>	17	<i>rad24Δ</i>	12
<i>cdc13Δ</i>	0	<i>cdc13Δ</i>	0
<i>nmd2Δ</i> <i>exo1Δ</i>	10	<i>nmd2Δ</i> <i>exo1Δ</i>	13
<i>nmd2Δ</i> <i>rad24Δ</i>	7	<i>nmd2Δ</i> <i>rad24Δ</i>	10
<i>nmd2Δ</i> <i>cdc13Δ</i>	0	<i>nmd2Δ</i> <i>cdc13Δ</i>	0
<i>exo1Δ</i> <i>rad24Δ</i>	7	<i>exo1Δ</i> <i>rad24Δ</i>	8
<i>exo1Δ</i> <i>cdc13Δ</i>	0	<i>exo1Δ</i> <i>cdc13Δ</i>	0
<i>rad24Δ</i> <i>cdc13Δ</i>	0	<i>rad24Δ</i> <i>cdc13Δ</i>	0
<i>nmd2Δ</i> <i>exo1Δ</i> <i>rad24Δ</i>	12	<i>nmd2Δ</i> <i>exo1Δ</i> <i>rad24Δ</i>	10
<i>nmd2Δ</i> <i>exo1Δ</i> <i>cdc13Δ</i>	8	<i>nmd2Δ</i> <i>exo1Δ</i> <i>cdc13Δ</i>	0
<i>nmd2Δ</i> <i>rad24Δ</i> <i>cdc13Δ</i>	8	<i>nmd2Δ</i> <i>rad24Δ</i> <i>cdc13Δ</i>	0
<i>exo1Δ</i> <i>rad24Δ</i> <i>cdc13Δ</i>	0	<i>exo1Δ</i> <i>rad24Δ</i> <i>cdc13Δ</i>	0
<i>nmd2Δ</i> <i>exo1Δ</i> <i>rad24Δ</i> <i>cdc13Δ</i>	9	<i>nmd2Δ</i> <i>exo1Δ</i> <i>rad24Δ</i> <i>cdc13Δ</i>	0
<b>TOTAL</b>	<b>112</b>	<b>TOTAL</b>	<b>88</b>

expected number per genotype = 6

(200 observed/32 genotypes)

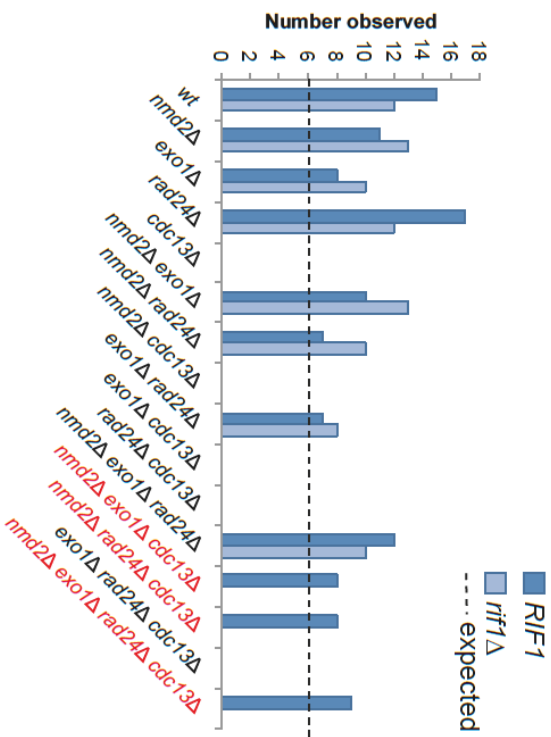


**Figure 21. Absence of the Rad24 checkpoint protein does not permit Cdc13 bypass without Rif1**

Two diploids (DDY835 and DDY836) heterozygous for *NMD2*, *RAD24*, *EXO1*, *CDC13* and *RIF1* deletions was sporulated and spores were analysed by random spore analysis. 177 (DDY835) and 200 (DDY836) haploid strains were genotyped and the numbers for each genotype are given in the tables and the graphs. Expected numbers of strains were calculated by dividing the number of spores analysed with the number of possible genotypes. Genotypes in red are where spores were obtained in a *RIF1*<sup>+</sup> background but not in a *rif1*Δ background.



#### 4.6 The two most N-terminal Protein Phosphatase I (Glc7) interaction sites on Rif1 are not required for Cdc13 bypass

Since neither the role of Rif1 in resection nor DNA damage checkpoint suppression were important for Cdc13 bypass, other roles of Rif1 were investigated using *rif1* mutants defective in other functions. Rif1 contains RVxF and SILK domains which are conserved between yeast and mammals, however in higher eukaryotes the domains are found in the C-terminus rather than the N terminus (Sreesankar *et al.*, 2012). It was previously shown that Rif1 represses initiation of replication origins, genome-wide, by recruiting the Protein phosphatase 1 (PP1) Glc7 (Hiraga *et al.*, 2014; Mattarocci *et al.*, 2014). *rif1* $\Delta$  strains also have very long telomeres and this is due to aberrantly early telomere replication and also lack of Rif1 counting of telomeric TG repeats (Levy and Blackburn, 2004).

Since Rif1 recruitment of PP1 is important for replication timing it was hypothesised that mutating the RVxF and SILK motifs would reduce the fitness of *nmd2* $\Delta$  *exo1* $\Delta$  *cdc13* $\Delta$  strains or make them inviable. To test this hypothesis, an *nmd2* $\Delta$  *exo1* $\Delta$  *cdc13* $\Delta$  strain was crossed with a *rif1-RVxF-SILK* mutant allele, which is defective in PP1 recruitment. The *rif1-RVxF-SILK* strain is mutated in the two most N-terminal RVxF (residues 114-118) and SILK (residues 147-149) motifs (referred to hereinafter as RVxF (1) and SILK (1)). The mutations were V116R, F118R, I147R, L148R, R149A and have been previously shown to interrupt Rif1 interaction with PP1 (Mattarocci *et al.*, 2014). 67 tetrads were dissected and *nmd2* $\Delta$  *exo1* $\Delta$  *cdc13* $\Delta$  *rif1-RVxF-SILK* strains were obtained with 100% viability although colony size was slightly reduced (10/10 strains; Figure 22 B). Some spore inviability was seen (Figure 22 B, tetrads 2, 5 and 7).

The fitness of the *nmd2* $\Delta$  *exo1* $\Delta$  *cdc13* $\Delta$  *rif1-RVxF-SILK* strains was compared with *nmd2* $\Delta$  *exo1* $\Delta$  *cdc13* $\Delta$  *RIF1* strains by spot-testing. *nmd2* $\Delta$  *exo1* $\Delta$  *cdc13* $\Delta$  *rif1-RVxF-SILK* strains were slightly less fit than *nmd2* $\Delta$  *exo1* $\Delta$  *cdc13* $\Delta$  *RIF1* strains (Figure 22 C). *rif1-RVxF-SILK* exhibit earlier firing of replication origins

(Hiraga *et al.*, 2014), therefore the fitness data suggests that early telomere replication moderately reduces the fitness of a Cdc13 bypass cell.

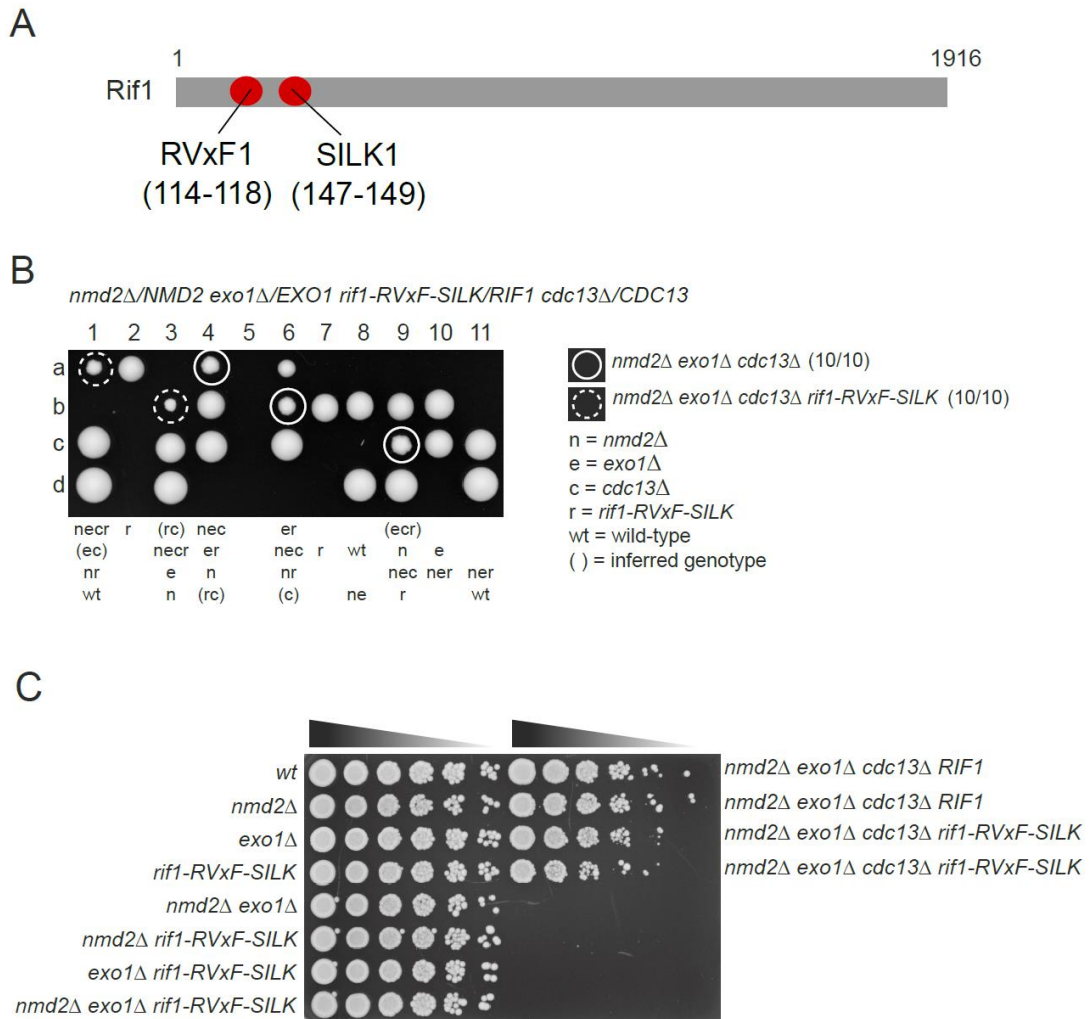


**Figure 22. Rif1 interaction with PP1 via two N-terminal PP1 interaction motifs is not required for Cdc13 bypass**

(A) Diagram of the Rif1 protein, showing the PP1 interaction motifs RVxF1 and SILK1. These motifs were mutated as follows in the *rif1-RVxF-SILK* strain: V116R, F118R, I147R, L148R, R149A. (B) Example tetrad dissection (67 tetrads dissected in total) from a sporulated diploid (DLY9699 x DLY8167). Spores were germinated for 5 days at 23°C before photographing. Spore viability is given for the encircled spore genotypes (in brackets). (C) Spot-test of serial 1 in 6 dilutions, in water, of the strains indicated. Cultures were spotted onto a YPD plate and incubated at 23°C for 3 days before photographing.

#### 4.7 The Rif1 N terminus promotes Cdc13 bypass

To see whether other, as yet unidentified, domains within the Rif1 N-terminus were important for Cdc13 bypass, a *rif1* $\Delta$ *N* strain ( $\Delta$ 2-176 residues, Figure 23 A) was crossed with an *nmd2* $\Delta$  *exo1* $\Delta$  *cdc13* $\Delta$ . After sporulating the diploid and dissecting 59 tetrads, I found that *nmd2* $\Delta$  *exo1* $\Delta$  *cdc13* $\Delta$  *rif1* $\Delta$ *N* strains were 100% viable (4/4 spores, Figure 23 B). The colony size of *nmd2* $\Delta$  *exo1* $\Delta$  *cdc13* $\Delta$  *rif1* $\Delta$ *N* strains was dramatically reduced compared to *nmd2* $\Delta$  *exo1* $\Delta$  *cdc13* $\Delta$  and *nmd2* $\Delta$  *exo1* $\Delta$  *cdc13* $\Delta$  *rif1*-RVxF-SILK strains. This indicated that there was a fitness defect in *nmd2* $\Delta$  *exo1* $\Delta$  *cdc13* $\Delta$  *rif1* $\Delta$ *N* strains. However, after streaking the strains to obtain more cells, fitness increased and cells could be grown to saturation in liquid media. Interestingly, far fewer *nmd2* $\Delta$  *exo1* $\Delta$  *cdc13* $\Delta$  *rif1* $\Delta$ *N* strains were obtained from tetrad dissection than *nmd2* $\Delta$  *exo1* $\Delta$  *cdc13* $\Delta$  strains (4 compared to 12) and significant spore inviability was seen (Figure 23, tetrads 5, 8 and 9). The spore inviability could potentially mask inviability of some *nmd2* $\Delta$  *exo1* $\Delta$  *cdc13* $\Delta$  *rif1* $\Delta$ *N* strains.

The relative fitness of *rif1* $\Delta$ *N* and *RIF1* strains was determined by spot-testing. This assay showed that *nmd2* $\Delta$  *exo1* $\Delta$  *cdc13* $\Delta$  *rif1* $\Delta$ *N* strains had dramatically reduced fitness compared to *nmd2* $\Delta$  *exo1* $\Delta$  *cdc13* $\Delta$  *RIF1* strains (Figure 23 C). In fact, *nmd2* $\Delta$  *exo1* $\Delta$  *cdc13* $\Delta$  *rif1* $\Delta$ *N* fitness appeared lower than *nmd2* $\Delta$  *exo1* $\Delta$  *cdc13* $\Delta$  *rif1*-RVxF-SILK fitness (Figure 22 C). This perhaps indicates that there are unknown domains within the N-terminus that are important for Cdc13 bypass, and hence the activity of Stn1 and Ten1. One possibility is the putative Rif1 nuclear localization sequence (NLS) that is very near the N terminus (Hiraga *et al.*, 2014). Without the NLS, Rif1 would be unable to interact with telomeres in the nucleus. It is therefore possible that *nmd2* $\Delta$  *exo1* $\Delta$  *cdc13* $\Delta$  *rif1* $\Delta$ *N* strains are less fit because Rif1 is not located at the telomere.

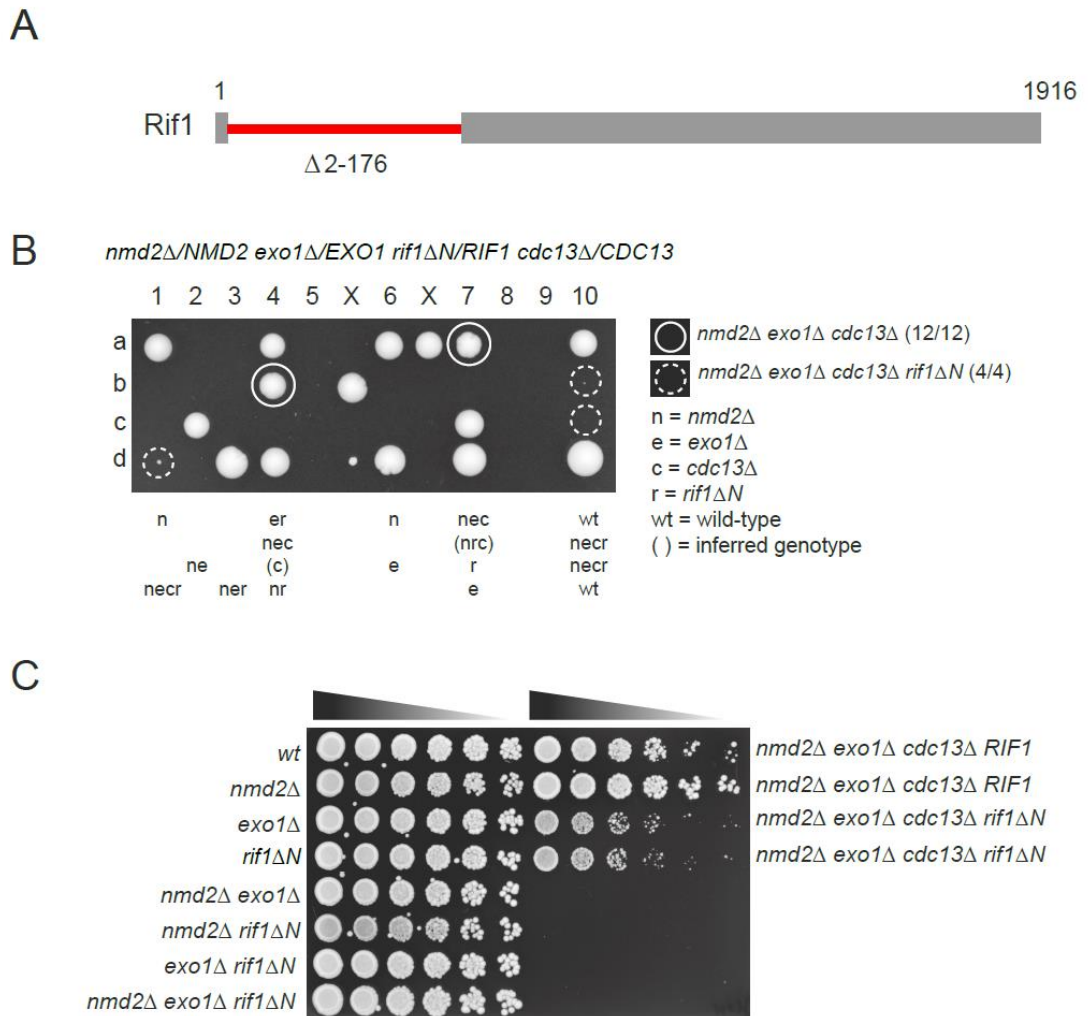


**Figure 23. The N terminus of Rif1 promotes Cdc13 bypass**

(A) Diagram of the Rif1 protein, with the red line showing the N terminal deletion. (B) Example tetrad dissection (59 tetrads dissected in total) from a sporulated diploid (DLY10255 x DLY10290). Spores were germinated for 5 days at 23°C before photographing. Spore viability is given for the encircled spore genotypes (in brackets). (C) Spot-test of serial 1 in 6 dilutions, in water, of the strains indicated. Cultures were spotted onto a YPD plate and incubated at 23°C for 3 days before photographing.

#### 4.8 Rif1 C-terminal interactions with Rap1 or Dbf4 are not required for Cdc13 bypass

The Rif1 C-terminal domain is conserved between yeast and humans and binds to the Rap1 C-terminal domain (Shi *et al.*, 2013). Rif1-Rap1-Rif2 forms a shelterin-like complex at telomeres, regulates telomere length and seems to promote CST activity, since Rif1 is essential for Cdc13 bypass (Anbalagan *et al.*, 2011). The complex also protects the telomere end from being recognised as a DSB and represses non-homologous end joining at the telomere to prevent circular chromosomes and hence genome instability. However, within the aforementioned activities, Rif1, Rap1 and Rif2 can carry out separate roles, for example Rap1 and Rif2 inhibit NHEJ at telomeres but Rif1 does not (Bonetti *et al.*, 2010; Anbalagan *et al.*, 2011). Rif1 C-terminus also binds to Dbf4, which is the regulatory subunit of the Cdc7 kinase that phosphorylates the MCM complex to initiate DNA replication (Hiraga *et al.*, 2014). The Dbf4 binding site overlaps with that of Rap1, therefore Rap1 and Dbf4 may compete to bind to Rif1 (Hiraga *et al.*, 2014).

The C terminus of Rif1 interacts with Rap1, thus it was hypothesised that deleting the Rif1 C-terminal would stop Cdc13 bypass since this would disrupt Rif1-Rap1 binding. A *rif1* $\Delta$ C strain (Figure 24 A) was crossed with an *nmd2* $\Delta$  *exo1* $\Delta$  *cdc13* $\Delta$  strain and tetrads were dissected. *nmd2* $\Delta$  *exo1* $\Delta$  *cdc13* $\Delta$  *rif1* $\Delta$ C strains were viable (5/6 possible spores) (Figure 24 B). One *nmd2* $\Delta$  *exo1* $\Delta$  *cdc13* $\Delta$  *rif1* $\Delta$ C was inviable and overall there was spore inviability seen similar to previous *nmd2* $\Delta$  *exo1* $\Delta$  *cdc13* $\Delta$  *rif1*-mutant dissections (e.g. tetrad 9, Figure 24 B).

Strain fitness analysis by spotting serial dilutions of saturated culture (in water) onto agar plates showed that *nmd2* $\Delta$  *exo1* $\Delta$  *cdc13* $\Delta$  *rif1* $\Delta$ C strains were much less fit than *nmd2* $\Delta$  *exo1* $\Delta$  *cdc13* $\Delta$  *RIF1* strains (Figure 24 C). Rif1 interaction with Rap1 may assist Cdc13 bypass since Rap1 tethers Rif1 to telomeric dsDNA. If Rif1 promotes CST activity (Anbalagan *et al.*, 2011) then in the absence of Cdc13 perhaps Rif1, whilst binding telomeric dsDNA, helps to

recruit Stn1 and Ten1 to the telomere or promotes Stn1-Ten1 interaction. Alternatively, or additionally, Rif1 interaction with the pre-replication complex activator Dbf4 (which occurs via the Rif1 C-terminus) may be important, since this regulates the timing of telomere replication.

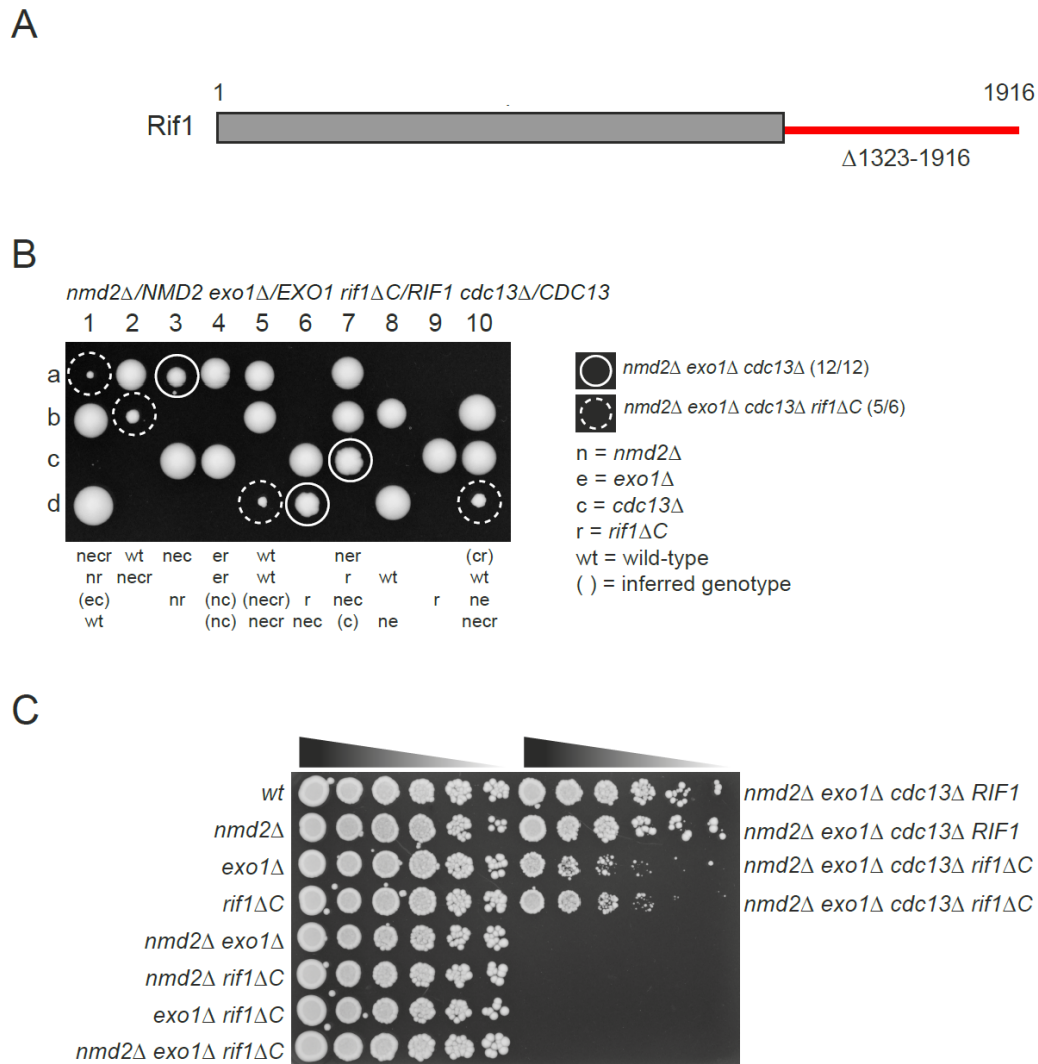


**Figure 24. The Rif1 C terminus promotes Cdc13 bypass**

(A) Diagram of the Rif1 protein, with the C-terminal deletion shown as a red line. (B) Tetrad dissection from a sporulated diploid (DLY10255 x DLY9714). Spores were germinated for 5 days at 23°C before photographing. Strains were patched to YPD and replica-plated to selective media for genotyping. Spore viability is given for the encircled spore genotypes (in brackets). (C) Spot-test of serial 1 in 6 dilutions, in water, of the strains indicated. Cultures were spotted onto a YPD plate and incubated at 23°C for 3 days before photographing.



#### 4.9 Domains within the Rif1 HEAT repeats are required for Cdc13 bypass

Rif1 contains HEAT (Huntingtin, elongation factor 3, Protein Phosphatase 2A, and yeast kinase TOR1) repeats, which are a conserved domain comprising around 50 amino acids found in a number of different proteins, although there is variable sequence homology (Sreesankar *et al.*, 2012; Hiraga *et al.*, 2014). It is thought that these residues become packed together to form super-helices ('solenoids' or 'springs') and that these structures mediate protein-protein interactions (Andrade *et al.*, 2001). HEAT repeats are an ill-defined domain in Rif1. In humans, the Rif1 HEAT repeats are thought to be located from the beginning of the N terminus; in yeast the Rif1 core HEAT repeats are amino acids 434-579, but the region is very likely to extend further from here towards the C and N termini (Xu *et al.*, 2010; Sreesankar *et al.*, 2012). In both yeast and humans the exact function of the Rif1 HEAT repeats is unknown. In yeast, there is evidence that the HEAT repeats are important for the regulation of DNA replication timing by Rif1 (Hiraga *et al.*, 2014).

It was hypothesized that Rif1 HEAT repeats were important for Cdc13 bypass, given that deletions of N (residues 2-176) and C (residues 1323-1916) terminal regions of Rif1 were not lethal to *nmd2Δ exo1Δ cdc13Δ*. The importance of the Rif1 HEAT repeats and domains within for Cdc13 bypass was determined by transforming a number of plasmids with Rif1 HEAT-repeat truncations into an *nmd2Δ exo1Δ cdc13Δ rif1Δ* strain expressing *RIF1* on a plasmid (Figure 25 A). Internal deletions were made by *in vitro* mutagenesis and cloning and had no linker inserted between N- and C-terminal truncations (Hiraga *et al.*, 2014). Loss of the *RIF1* plasmid left the Rif1 truncation plasmid only, therefore cells with Rif1 mutated in domains important for Cdc13 bypass would be inviable on 5-FOA.

When the *nmd2Δ exo1Δ cdc13Δ rif1Δ* had a *RIF1-URA3* plasmid and a vector only, the strain died on 5-FOA after losing the *RIF1-URA3* plasmid. This confirmed that Rif1 is essential for Cdc13 bypass and that *RIF1* had been correctly deleted from the strain used. When the strain had a *RIF1-URA3* and a

*RIF1-TRP1* plasmid, the strain was viable after losing the *RIF1-URA3* plasmid, since it could still express *RIF1*. This again confirmed that the strain used had *RIF1* correctly deleted and that Rif1 is required for Cdc13 bypass. The strain was quite sick on 5-FOA, indicating that perhaps the expression level of Rif1 was lower than optimal or that the plasmid was unstable. Future work could examine the expression levels of Rif1 in Cdc13 bypass, as these may be elevated to compensate for defects in telomere capping by Cdc13.

It was found that Cdc13 bypass strains containing only plasmids with the C-terminal domain of Rif1 deleted ( $\Delta 1790-1916$  and  $\Delta 997-1916$ ) were viable (Figure 25 B) which confirmed the previous finding that a strain with an integrated Rif1 C-terminal deletion was viable (Figure 24 B, C). Interestingly, deletion of the very end of the C-terminal ( $\Delta 1790-1916$ ) made the strain less fit than a strain expressing a much larger deletion ( $\Delta 997-1916$ ). 1790-1916 is required for Dbf4 binding (Hiraga *et al.*, 2014), however Rif1 can bind to Rap1 with a minimal binding region of 1752-1772. Therefore, one reason that Rif1  $\Delta 997-1916$  is fitter than  $\Delta 1790-1916$  in *cdc13* $\Delta$  strain is that Rif1-Rap1 interaction may be more persistent and this appears to be harmful. Alternatively, Rif1  $\Delta 1790-1916$  may be less stable than  $\Delta 997-1916$ , leading to lower levels of Rif1.

It was further found that the domain including the SILK2 motif (222-225 residues, Figure 25A) was important for Cdc13 bypass, since the  $\Delta 114-225$  plasmid led to complete loss of viability of the *nmd2* $\Delta$  *exo1* $\Delta$  *cdc13* $\Delta$  *rif1* $\Delta$  strain (Figure 25 B). The *rif1-RVxF-SILK* allele previously used, which allowed Cdc13 bypass, was mutated only in the RVxF (1) motif (residues 114-118) and the SILK (1) motif (147-149 residues) (Figure 22 A). However, Hiraga *et al.* (2014) identified two further RVxF/SILK motifs: SILK2 (residues 222-225) and RVxF2 (residues 316-320). Mutation of all four RVxF and SILK motifs (Rif1-PP1, Figure 25 B) were lethal. This indicates either that the SILK2 and RVxF2 motifs are required for Cdc13 bypass, or that there is redundancy between the motifs i.e. in the absence of RVxF1 and SILK1, Glc7 can bind to RVxF2 and SILK2. Triple, pairwise and single deletions of the four motifs are necessary to determine which motifs are essential for Rif1 function in Cdc13 bypass. Overall, SILK and RVxF motifs are important for Cdc13 bypass. These motifs are

thought to be required for interactions with PP1 (Glc7) (Hendrickx *et al.*, 2009). Rif1 recruitment of PP1 to the telomere, via the SILK2/RvXF2 motifs may therefore be important for Cdc13 bypass.

The SILK2 and RVxF2 motifs lie within a region thought to comprise HEAT repeats, which may extend into residues 213-836 (Hiraga *et al.*, 2014), although the strict HEAT repeat region is residues 434-579, which contain repeats conserved between yeast and higher eukaryotes (Andrade *et al.*, 2001). Interestingly, deletions of an N-terminal portion of the putative HEAT repeats ( $\Delta$ 321-455), the entire region of putative HEAT repeats ( $\Delta$ 213-836) and a C-terminal portion ( $\Delta$ 321-836) were all lethal (Figure 25 B). This suggests that the structure of the putative HEAT repeats (213-455) is important for Cdc13 bypass. Also, the fact that deletions within the 213-836 residues of Rif1 attenuate Cdc13 bypass suggests that this area has a common function, therefore it is likely that the HEAT repeats are as extensive as previously thought.

Since HEAT repeats across species promote protein-protein interactions (Andrade *et al.*, 2001), it is possible that Rif1 is interacting with another protein to maintain telomere protection in the absence of Cdc13. The protein interacting with Rif1 that is essential for Cdc13 bypass could be the essential protein Ten1, which binds to the N-terminus of Stn1. Co-IP between Rif1 and Ten1 could potentially uncover an interaction. Alternatively, the Rif1 HEAT repeats could promote interaction between Stn1 and Ten1, since both proteins are required for Cdc13 bypass.

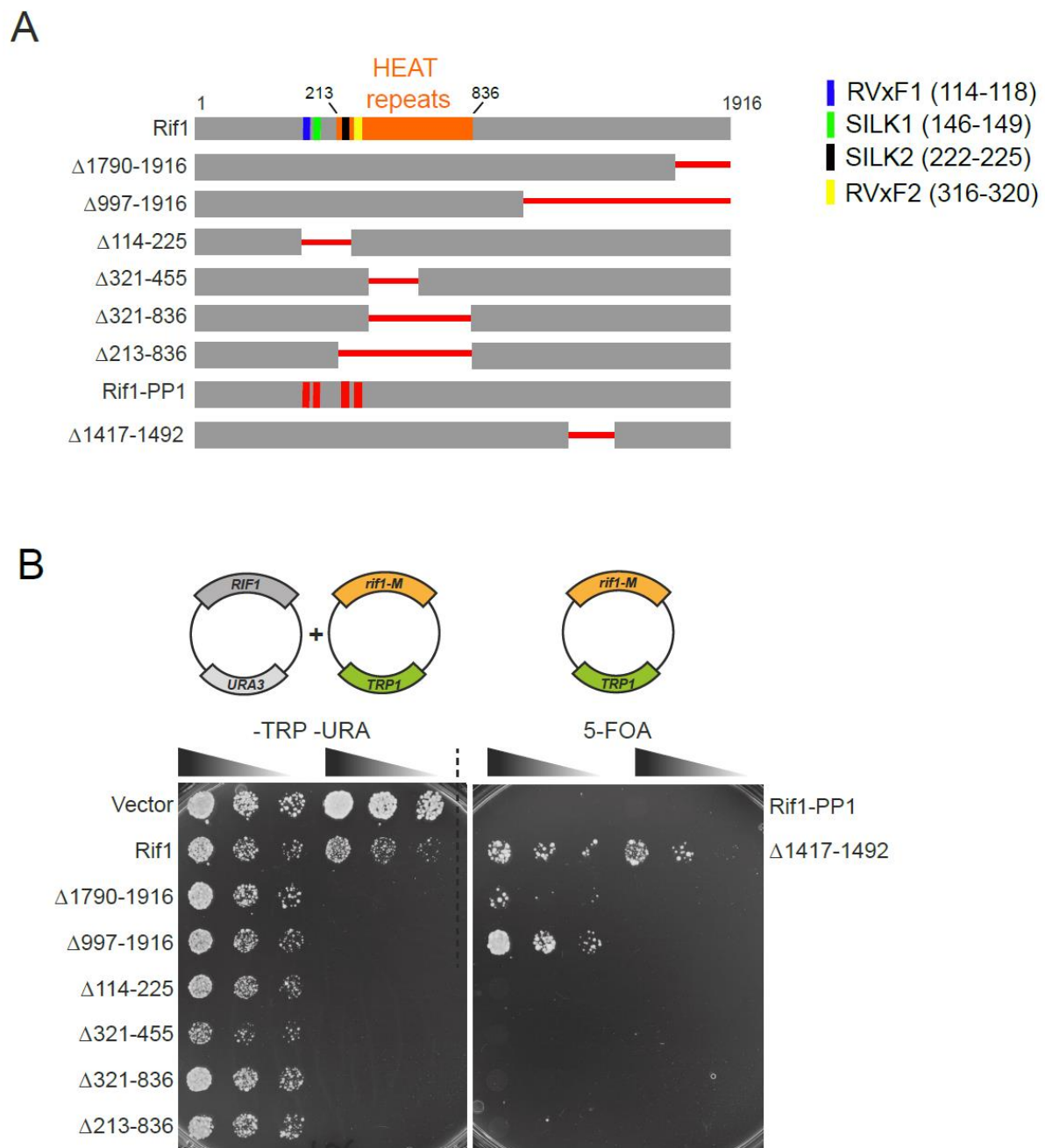


**Figure 25. Domains within the Rif1 HEAT repeats are required for Cdc13 bypass**

(A) An *nmd2Δ exo1Δ cdc13Δ rif1Δ* strain expressing *RIF1* on a *URA3* plasmid was transformed with *rif1* mutant alleles shown on a *TRP1* plasmid. HEAT repeats are from residues 213-836 (Hiraga *et al.*, 2014) and are shown in orange. Rif1-PP1 interaction motifs (RVxF/SILK motifs, as shown in Hiraga *et al.*, 2014) are shown by vertical blue, green, black and yellow lines. Red lines indicate the deletions made in Rif1. For the ‘Rif-PP1’ plasmid, each RvXF/SILK motif was mutated (red lines indicate mutations, details of mutations given in Hiraga *et al.*, 2014). (B) Cultures were serially diluted (1 in 4) and spotted onto –TRP –URA (control) and 5-FOA to lose the *RIF1-URA3* plasmid, leaving the mutant allele (*rif1-M*) on a *TRP1* plasmid.

## 4.10 Discussion

A genome-wide screen was conducted by crossing a single gene deletion/DAmP allele library with a Cdc13 bypass strain and a control *CDC13<sup>+</sup>* strain. It was found that Rif1 was essential for Cdc13 bypass. Rif1 is a multifunctional protein and its role in Cdc13 bypass was investigated. Mutating the two most N-terminal PP1 interaction sites did not affect Cdc13 bypass, however mutation of all four PP1 interaction sites was lethal, indicating that replication timing control by Rif1-PP1 interaction is important for cells to survive without Cdc13. Deleting the C or N-termini did not completely abolish Cdc13 bypass, but strain fitness was greatly reduced. This may be because the N terminus contains a putative NLS (Hiraga *et al.*, 2014) and the C-terminus is important for Rif1 binding to Rap1, which is important for telomere end protection (Hardy *et al.*, 1992).

It was found that the HEAT repeats are required for Cdc13 bypass. The function of the Rif1 HEAT repeats is currently unknown, however HEAT repeats across species promote protein-protein interactions (Andrade *et al.*, 2001). It is possible that Rif1 interacts with another protein using its HEAT repeats to promote Cdc13 bypass. A hypothetical model is that Rif1 interacts with CST at the telomere end by interacting with Ten1 – possibly using the HEAT repeats (Figure 26). Cdc13 binds tightly by itself to telomeric ssDNA, then recruits Stn1 (which binds ssDNA more weakly) and Ten1, to replicate the telomere and promote lagging strand fill-in. Rif1 and Ten1 may then interact to lead to the formation of a shelterin-like complex at the telomere end. Future work could address whether Rif1 interacts with Ten1-Stn1 by using co-IP.

An alternative explanation for the lethality of HEAT repeat deletions and mutation of the four PP1 interaction sites (Figure 25) is that such mutations render Rif1 unstable or misfolded. Similarly, the integrated *rif1-RVxF-SILK*,  $\Delta C$  and  $\Delta N$  alleles (Figures 22-24) may have reduced the fitness of Cdc13 bypass strains, due to these mutations producing unstable or misfolded Rif1. Since Rif1 is essential for Cdc13 bypass, unstable Rif1 would most likely to be lethal.

However, two of the Rif1 truncation plasmids ( $\Delta$ 114-225 and Rif1-PP1) are known to stably express Rif1 at levels that are similar to wild-type (Hiraga *et al.*, 2014), therefore in both cases lethality is most likely due to the attenuation of essential Rif1 functions. Future work could determine the effect of the other mutations on Rif1 function by Southern blotting of the telomeres of Cdc13 bypass strains with Rif1 truncations and *nmd2* $\Delta$  *exo1* $\Delta$  *cdc13* $\Delta$  *rif1* $\Delta$  strains expressing the plasmids used in Figure 25. Unstable or misfolded Rif1 would most likely lead to dramatic telomere lengthening in these strains. Also, western blotting could be used to determine Rif1 expression levels in strains carrying these plasmids.

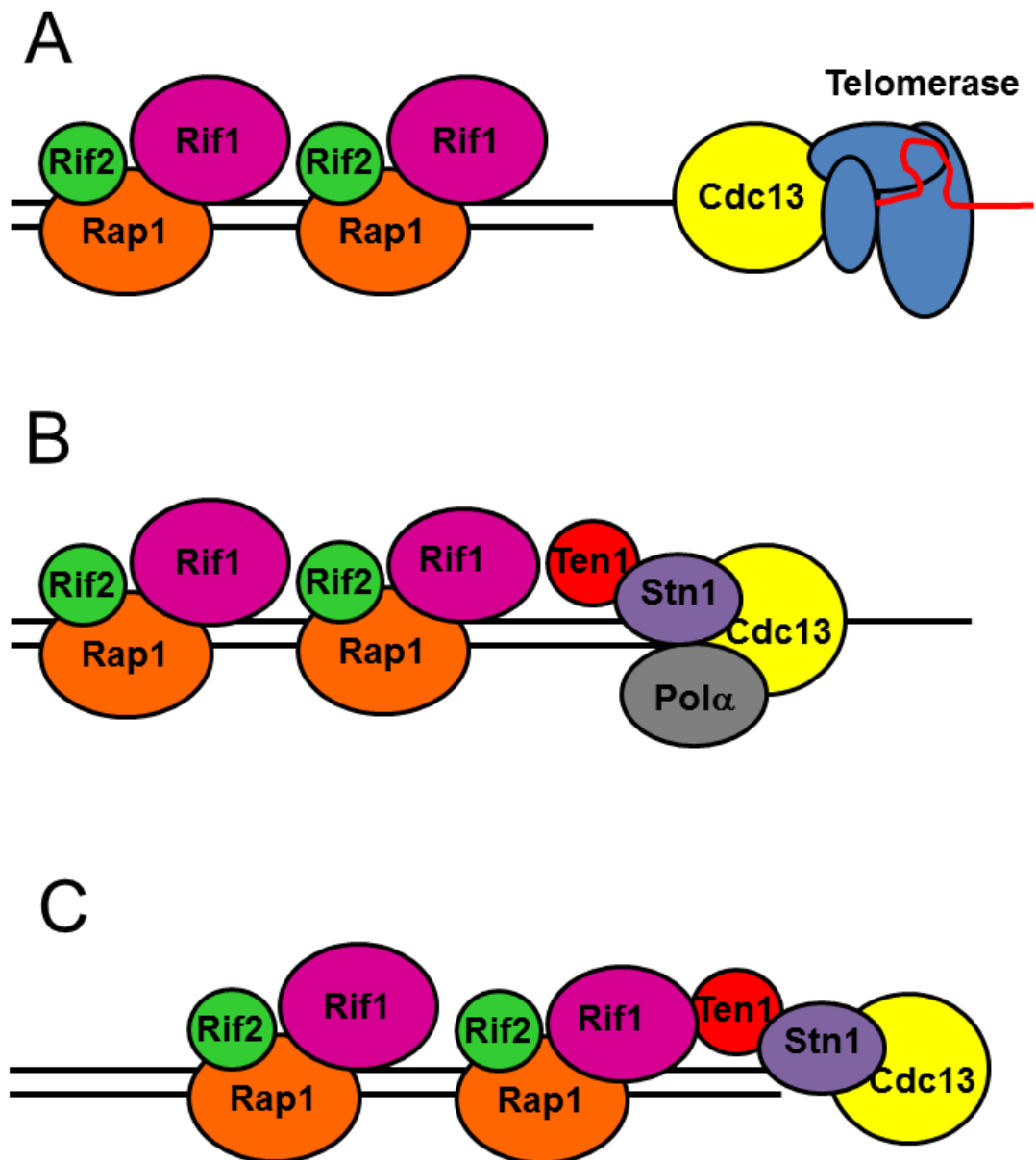


**Figure 26. Hypothetical model in which Rif1 interacts with Ten1 at the telomere end to form a shelterin-like complex**

(A) During telomere replication in late S-phase, Cdc13 binds telomeric ssDNA and recruits telomerase (Est1/Est2/Est3/Tlc1 RNA (red line)) to extend the leading strand. (B) Stn1 and Ten1 are recruited to repress telomerase and Pol  $\alpha$  is recruited to fill in the lagging strand after replication. (C) Ten1 interacts with Rif1 and Stn1 to form a shelterin-like complex to protect the telomere end.

## Chapter 5. Rad52 is required for Cdc13 bypass

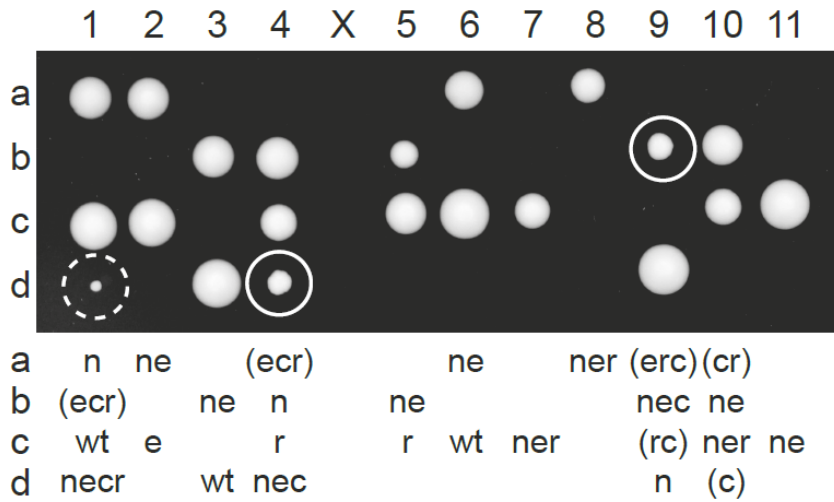
### 5.1 Rad51-dependent recombination is not required for Cdc13 bypass

Cdc13 bypass cells resemble telomerase-deficient survivors, which maintain telomeres by recombination. To determine whether telomere maintenance by homologous recombination was important for Cdc13 bypass, the effect of Rad51 on Cdc13 bypass was investigated. Deleting Rad51 reduced colony size in *nmd2Δ exo1Δ cdc13Δ* strains, when 56 tetrads were dissected from a diploid heterozygous for *NMD2*, *EXO1*, *CDC13* and *RAD51* deletions (Figure 27). *nmd2Δ exo1Δ cdc13Δ rad51Δ* strains had 100% viability (5/5 possible strains were viable). These data indicate that Rad51-dependent recombination is not required for Cdc13 bypass. Since Rad51 is required for the formation of Type I survivors and *rad51Δ* strains only form Type II survivors (Lundblad and Blackburn, 1993), perhaps *nmd2Δ exo1Δ cdc13Δ rad51Δ* cells only form Type II survivors. Future work could examine the telomere phenotypes of these cells using Southern blotting.

The SGA screen showed that *RAD50* deletion (and deletion of the two other MRX components *MRE11* and *XRS2*) severely reduced the colony size of both *nmd2Δ exo1Δ cdc13Δ* and *nmd2Δ exo1Δ* cells (data not shown). This is most likely because there is a negative genetic interaction between *exo1Δ* and MRX gene deletions (Collins *et al.*, 2007). Therefore, the effect of Rad51-independent (Rad50-dependent) recombination on Cdc13 bypass is difficult to analyse in an *nmd2Δ exo1Δ cdc13Δ* strain. However, in future work it could be analysed in an *nmd2Δ rad24Δ cdc13Δ* strain.



*nmd2Δ/NMD2* *exo1Δ/EXO1* *cdc13Δ/CDC13* *rad51Δ/RAD51*



○ *nmd2Δ* *exo1Δ* *cdc13Δ* (16/16)

○ *nmd2Δ* *exo1Δ* *cdc13Δ* *rad51Δ* (5/5)

n = *nmd2Δ*

c = *cdc13Δ*

wt = wild-type

e = *exo1Δ*

r = *rad51Δ*

X = not dissected

() = inferred genotype

### Figure 27. Cdc13 bypass occurs without Rad51

A diploid of the genotype indicated (made from crossing DLY3485 and DLY8167) was sporulated and 56 tetrads were dissected. Spores were germinated for 5 days at 23°C before photographing. The number of strains obtained, out of the number of possible strains, is given in brackets for the encircled genotypes.

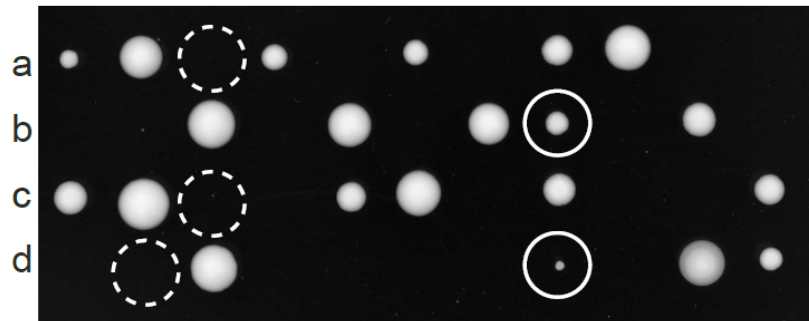
## 5.2 Rad52 is required for Cdc13 bypass

Rad52 is required for both Rad51-dependent and Rad50-dependent recombination, the two recombination pathways in budding yeast (Lundblad and Blackburn, 1993). Figure 27 showed that *nmd2Δ exo1Δ cdc13Δ* strains could survive without Rad51, therefore Rad51-independent recombination is not required for Cdc13 bypass. It was not to see whether Rad50-dependent recombination was required for Cdc13 bypass, since *RAD50* has a negative genetic interaction with *EXO1* (although future work could be to dissect tetrads from a sporulated diploid heterozygous for *rad50Δ nmd2Δ rad24Δ cdc13Δ*). However, Rad52 is required for both recombination pathways, therefore if *rad52Δ* was essential for Cdc13 bypass then this would suggest that Rad50-dependent recombination was important for Cdc13 bypass (since Rad51-dependent recombination is not essential).


To see whether Rad52 is required for Cdc13 bypass, a diploid heterozygous for *NMD2*, *EXO1*, *CDC13* and *RAD52* deletions was sporulated and 69 tetrads were dissected to determine whether *nmd2Δ exo1Δ cdc13Δ rad52Δ* strains were viable (Figure 28). It was found that *nmd2Δ exo1Δ cdc13Δ rad52Δ* strains were inviable, therefore it is likely that Rad50-dependent recombination is essential for Cdc13 bypass (Figure 28). Rad52 is essential for recombination pathways and is thus required for the formation of both Type I and Type II survivors, which maintain telomeres by recombination (Lundblad and Blackburn, 1993). As Rad51 is not essential for Cdc13 bypass, and Rad51 is required for the formation of Type I survivors, it is likely that Cdc13 bypass cells lacking Rad51 maintain telomeres by Type II recombination. The fact that deletion of *RAD52*, which is required for both Type I and Type II recombination, is lethal to Cdc13 bypass strains provides evidence that Type II recombination is necessary for cells to survive without Cdc13. However, it is possible that when Type II recombination is defective (e.g. in the absence of Rad50), Cdc13 bypass cells can switch to Type I recombination. Overall, telomere recombination (either Type I or Type II) is essential for Cdc13 bypass.


*nmd2Δ/NMD2* *exo1Δ/EXO1* *cdc13Δ/CDC13* *rad52Δ/RAD52*

1 2 3 4 5 6 7 8 9 10 11



a	nr	wt	(necr)	nr		er		r	wt		
b	(ec)	(ncr)	wt		ner	(rc)	ne	nec		r	
c	nr	e	(necr)		r	ne		r			nr
d	(c)	(necr)	wt			(nc)		nec		ne	ner

 *nmd2Δ* *exo1Δ* *cdc13Δ* (13/13)

 *nmd2Δ* *exo1Δ* *cdc13Δ* *rad52Δ* (0/11)

n = *nmd2Δ*

c = *cdc13Δ*

wt = wild-type

e = *exo1Δ*

r = *rad52Δ*

() = inferred genotype

### Figure 28. Rad52 is required for Cdc13 bypass (tetrad dissection)

A diploid of the genotype indicated (made from crossing DLY5872 and DLY8167) was sporulated and 69 tetrads were dissected. Spores were germinated for 5 days at 23°C before photographing. The number of strains obtained, out of the number of possible strains, is given in brackets for the encircled genotypes.

Some spore inviability was seen (e.g. tetrads 4 and 9, Figure 28), therefore to confirm that *nmd2Δ* *exo1Δ* *cdc13Δ* *rad52Δ* strains could not be generated, haploid strains were generated using random spore analysis. From analysing 250 strains, no *nmd2Δ* *exo1Δ* *cdc13Δ* *rad52Δ* strains were obtained (23 strains were expected (assuming 11 viable genotypes) or 15 strains were expected, assuming 16 viable genotypes) (Figure 29). This shows that Cdc13 bypass cells require Rad52 and that telomere maintenance by HR is essential for these cells.

Genotype	number
wt	30
<i>nmd2</i> Δ	33
<i>exo1</i> Δ	31
<i>cdc13</i> Δ	0
<i>rad52</i> Δ	35
<i>nmd2</i> Δ <i>exo1</i> Δ	19
<i>nmd2</i> Δ <i>rad52</i> Δ	27
<i>nmd2</i> Δ <i>cdc13</i> Δ	0
<i>exo1</i> Δ <i>cdc13</i> Δ	0
<i>exo1</i> Δ <i>rad52</i> Δ	25
<i>rad52</i> Δ <i>cdc13</i> Δ	0
<i>nmd2</i> Δ <i>exo1</i> Δ <i>cdc13</i> Δ	27
<i>nmd2</i> Δ <i>rad52</i> Δ <i>cdc13</i> Δ	0
<i>exo1</i> Δ <i>rad52</i> Δ <i>cdc13</i> Δ	0
<i>nmd2</i> Δ <i>exo1</i> Δ <i>rad52</i> Δ	15
<i>nmd2</i> Δ <i>exo1</i> Δ <i>rad52</i> Δ <i>cdc13</i> Δ	0
<b>TOTAL</b>	<b>242</b>

Expected number = 15 (242/16 genotypes)

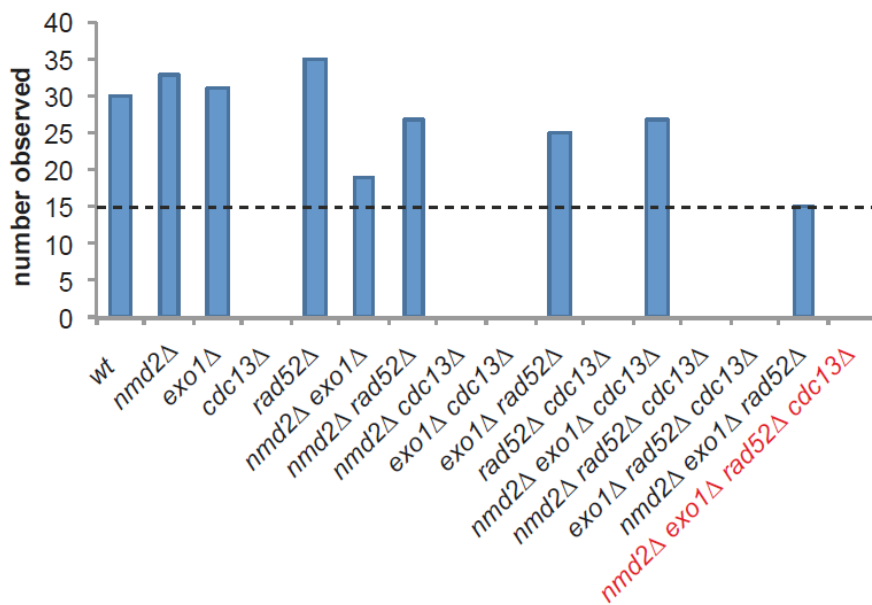


**Figure 29. Rad52 is required for Cdc13 bypass (random spore analysis)**

A diploid (DLY5872 x DLY8167) was sporulated and spores were separated by random spore analysis. Spores were germinated on YPD for 4 days before genotyping. The number of strains for each genotype are given in tabular and graphical form. The dashed line on the graph shows the expected number of spores, assuming all genotypes are viable (15). The genotype highlighted in red indicates that no strains were obtained for this genotype.

### 5.3 Discussion

Deletion of the HR gene *RAD51* reduces the colony size of Cdc13 bypass strains, and deletion of the HR gene *RAD52*, which is essential for both Rad51-dependent and Rad50-dependent HR, is lethal. The importance of Rad50 for Cdc13 bypass could be determined by crossing a *rad50* $\Delta$  strain with an *nmd2* $\Delta$  *rad24* $\Delta$  *cdc13* $\Delta$  strain, since *rad50* $\Delta$  is synthetic sick with *exo1* $\Delta$  (therefore an *nmd2* $\Delta$  *exo1* $\Delta$  *cdc13* $\Delta$  strain crossed with *rad50* $\Delta$  would not be informative).

Deleting *RAD51* was not lethal to *nmd2* $\Delta$  *exo1* $\Delta$  *cdc13* $\Delta$  strains, suggesting either that Type I recombination is not essential for Cdc13 bypass, or that Cdc13 bypass strains employing Type I recombination to maintain telomeres may be able to switch to Type II recombination instead. This could be tested by Southern blotting of the telomeres of *nmd2* $\Delta$  *exo1* $\Delta$  *cdc13* $\Delta$  *rad51* $\Delta$  strains. Furthermore, if future work showed that deleting *RAD50* from *nmd2* $\Delta$  *rad24* $\Delta$  *cdc13* $\Delta$  strains was not lethal (Rad50 is required for Type II recombination) then it is likely that Type II recombination is not essential for Cdc13 bypass and that Cdc13 bypass strains can switch between the two types of recombination.

Rad52 is required for both yeast recombination pathways (Rad51-dependent and Rad50-dependent) and thus is essential for both Type I and Type II survivors. Deleting *RAD52* is lethal to Cdc13 bypass strains, therefore it is likely either that availability of at least one recombination pathway is essential for these strains to survive, or that Type II recombination is essential (since absence of Rad51 is not lethal to Cdc13 bypass).

If it were the case that Type II recombination was required for Cdc13 bypass, then it would seem somewhat paradoxical that deletion of *Rif1*, which promotes Type I recombination and inhibits Type II recombination (Teng *et al.*, 2000), is lethal. Therefore, it is probably most likely that Cdc13 bypass strains require the availability of at least one recombination pathway, rather than primarily Type II recombination. The lethality of *RIF1* deletion for Cdc13 bypass, despite *rif1* $\Delta$

promoting Type II survivor formation, may support the conclusions of the previous chapter that it is Rif1 interactions with CST that are important for Cdc13 bypass.

Also, if Type II recombination was required for Cdc13 bypass, a second apparent paradox is that the *nmd2Δ exo1Δ cdc13Δ* strains tested (Figure 7) resembled Type I survivors more closely than Type II survivors. These strains did appear to have extended Y' telomeres indicating possible amplification of TG<sub>1-3</sub> repeats. It is plausible that *nmd2Δ exo1Δ cdc13Δ* strains may resemble Type II survivors more closely after extensive passaging. However, at face value the *nmd2Δ exo1Δ cdc13Δ* strains tested resemble Type I survivors more closely than Type II. Therefore, it is more likely that Cdc13 bypass strains require at least one recombination pathway, but does not require a specific pathway.

Overall, Rad52 is essential for Cdc13 bypass and Rad51 is not. Rad52 is required for Type I and Type II survivors, whereas Rad51 is required for Type I survivors, therefore Type II recombination may be essential for cells to survive without Cdc13. In Type II survivors, TG<sub>1-3</sub> repeats are amplified, therefore long tracts of TG repeats may promote survival without Cdc13, perhaps by allowing greater Rif1-Rif2-Rap1 binding or Stn1-Ten1 binding. To see whether Type II recombination is required, future work needs to address whether Rad50 (required for Type II survivors) is essential for Cdc13 bypass. However, there is evidence to suggest that Type II recombination may not be essential for Cdc13 bypass. Rif1 inhibits Type II recombination yet deletion of *RIF1* is lethal to Cdc13 bypass cells, also *nmd2Δ exo1Δ cdc13Δ* strains resembled Type I survivors more closely than Type II. In conclusion, the most likely explanation is that Cdc13 bypass cells require at least one recombination pathway to survive, but do not require a specific pathway.





## Chapter 6. Long telomeres promote Cdc13 bypass

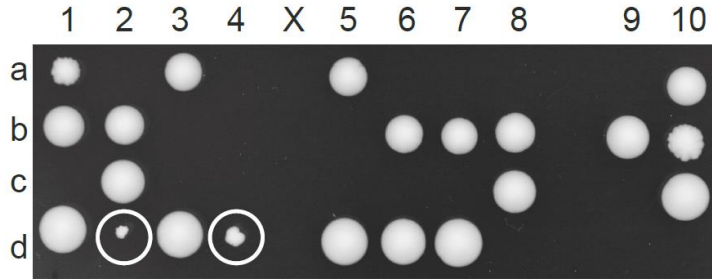
### 6.1 Generation of *cdc13*Δ strains not previously known to be viable

It was previously published that the only Cdc13 bypass strains that could be obtained from a diploid heterozygous for *NMD2*, *EXO1*, *RAD24*, *RIF1* and *CDC13* deletions were *nmd2*Δ *exo1*Δ *cdc13*Δ, *nmd2*Δ *rad24*Δ *cdc13*Δ and *nmd2*Δ *exo1*Δ *rad24*Δ *cdc13*Δ (Holstein *et al.*, 2014). Remarkably, however, it was possible to obtain *nmd2*Δ *cdc13*Δ strains from diploids created by mating a Cdc13 bypass strain with a single gene deletion strain.

When an *nmd2*Δ *rad24*Δ *cdc13*Δ strain was crossed with a *rif1*Δ strain, after the diploid was sporulated and 20 tetrads were dissected it was found that *nmd2*Δ *cdc13*Δ strains were obtained (Figure 30 A). Such strains have not been obtained from previous dissections of diploids heterozygous for *NMD2*, *EXO1*, *RAD24* and *CDC13* deletions (Holstein *et al.*, 2014). Furthermore, when an *nmd2*Δ *exo1*Δ *cdc13*Δ strain was crossed with a *dxo1*Δ strain and 33 tetrads were dissected, *nmd2*Δ *cdc13*Δ and *nmd2*Δ *cdc13*Δ *dxo1*Δ strains were obtained (Figure 30 B).

A

*nmd2Δ/NMD2 rad24Δ/RAD24 cdc13Δ/CDC13 rif1Δ/RIF1*



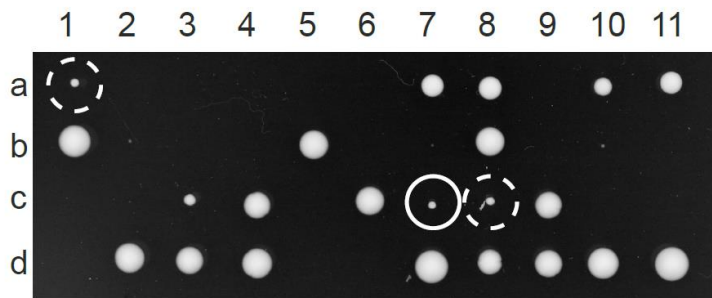
a nrc (nrc1) r n r  
b n1 r (rc1) nr1 nr1 1 wt nrc  
c (c1) 1 (rc1) nr  
d r nc nr1 nc n wt wt (c1)

○ *nmd2Δ cdc13Δ* (2/2)

n = *nmd2Δ* c = *cdc13Δ* wt = wild-type  
r = *rad24Δ* 1 = *rif1Δ*

B

*nmd2Δ/NMD2 exo1Δ/EXO1 cdc13Δ/CDC13 dxo1Δ/DXO1*



a ncd d d (c) ne ed  
b ed ed (ecd) e (ce)  
c nec nd ne nc ncd ned  
d nd nd ne ne nec nd d nd

○ *nmd2Δ cdc13Δ* (3/4) ○ *nmd2Δ cdc13Δ dxo1Δ* (3/3)

n = *nmd2Δ* c = *cdc13Δ* wt = wild-type  
e = *exo1Δ* d = *dxo1Δ*

**Figure 30. Generation of unexpected Cdc13 bypass strains**

(A) An *nmd2Δ rad24Δ cdc13Δ* strain (DLY8455) was crossed with a *rif1Δ* strain (DLY9697) and 20 tetrads were dissected. A representative dissection is shown. Viability is shown in brackets by the encircled genotypes. (B) An *nmd2Δ exo1Δ cdc13Δ* strain (DLY8167) was crossed with a *dxo1Δ* strain (DLY10209) and 33 tetrads were dissected. A representative dissection is shown. Viability is shown in brackets by the encircled genotypes.

The telomeres of Cdc13 bypass strains resemble those of telomerase-deficient survivors, which rearrange and maintain telomeres by recombination. Also, it is known that mating a strain with rearranged telomeres to another strain does not result in a diploid with wild-type telomeres, even when the diploid is heterozygous for all gene deletions (Zubko and Lydall, 2006). Furthermore, it has previously been shown that cells with telomeres resembling Type I and Type II survivors can adapt to the loss of Cdc13 (Larrivé and Wellinger, 2006). Therefore, perhaps the telomere structure of the resultant diploid allows unexpected Cdc13 bypass genotypes to arise in the haploid progeny.

## **6.2 Long telomeres promote growth of *cdc13*Δ strains that are not normally viable**

To test the hypothesis that unexpected Cdc13 bypass strains could be obtained by crossing a Cdc13 bypass strain with a single gene deletion strain, the telomere composition of diploids generated from these crosses were examined by Southern blotting. The diploids were passaged to see whether alterations in telomere composition occurred. It was hypothesised that diploids that produced unexpected Cdc13 bypass strains would have long telomeres.

*NMD2/nmd2*Δ *EXO1/exo1*Δ *RAD24/rad24*Δ *CDC13/cdc13*Δ diploids (DDY567 and DDY568), generated by transformation with a *cdc13*Δ cassette, had Y' telomeres of a similar length to a wild-type strain (Figure 31; compare lane 1 with lanes 4-5). However, diploids generated by crossing an *nmd2*Δ *exo1*Δ *cdc13*Δ strain with a *rif1*Δ strain initially had long, heterogeneous Y' and X telomeres but resembled wild-type telomeres more closely with passaging (Figure 31; compare lanes 6-7 with lanes 24-25). Interestingly, even though this diploid has long telomeres, no unexpected Cdc13 bypass strains were obtained from this cross (see Figure 20). These data are inconsistent with the hypothesis that unexpected Cdc13 bypass strains are obtained from diploids with long telomeres. However, it is possible that the telomere rearrangements are less severe than the other Cdc13 bypass diploids tested since telomeres recover with passage.

Diploids generated by crossing an *nmd2Δ rad24Δ cdc13Δ* strain with a *rif1Δ* strain maintained long, heterogeneous Y' and X telomeres with each passage and telomere length appeared to increase (Figure 31; compare lanes 8-9, 14-15 and 26-27). Diploids generated by crossing an *nmd2Δ exo1Δ cdc13Δ* strain with a *dxo1Δ* strain had terminal fragments that were of wild-type length but also appeared to have long, heterogeneous Y' and X telomeres. This structure also did not change with passage (Figure 31; compare lanes 10-11, 16-17 and 28-29). These data are consistent with the hypothesis that unexpected Cdc13 bypass strains are generated from long telomeres.

Overall, it appears that long telomeres are a contributing factor to Cdc13 bypass, but do not explain Cdc13 bypass overall. It is possible that extensive telomere rearrangements, which cannot be resolved by passaging, promote Cdc13 bypass. This is perhaps because such haploids already have telomeres maintained by recombination, which is known to occur in the Cdc13 bypass strains previously published (Holstein *et al.*, 2014).

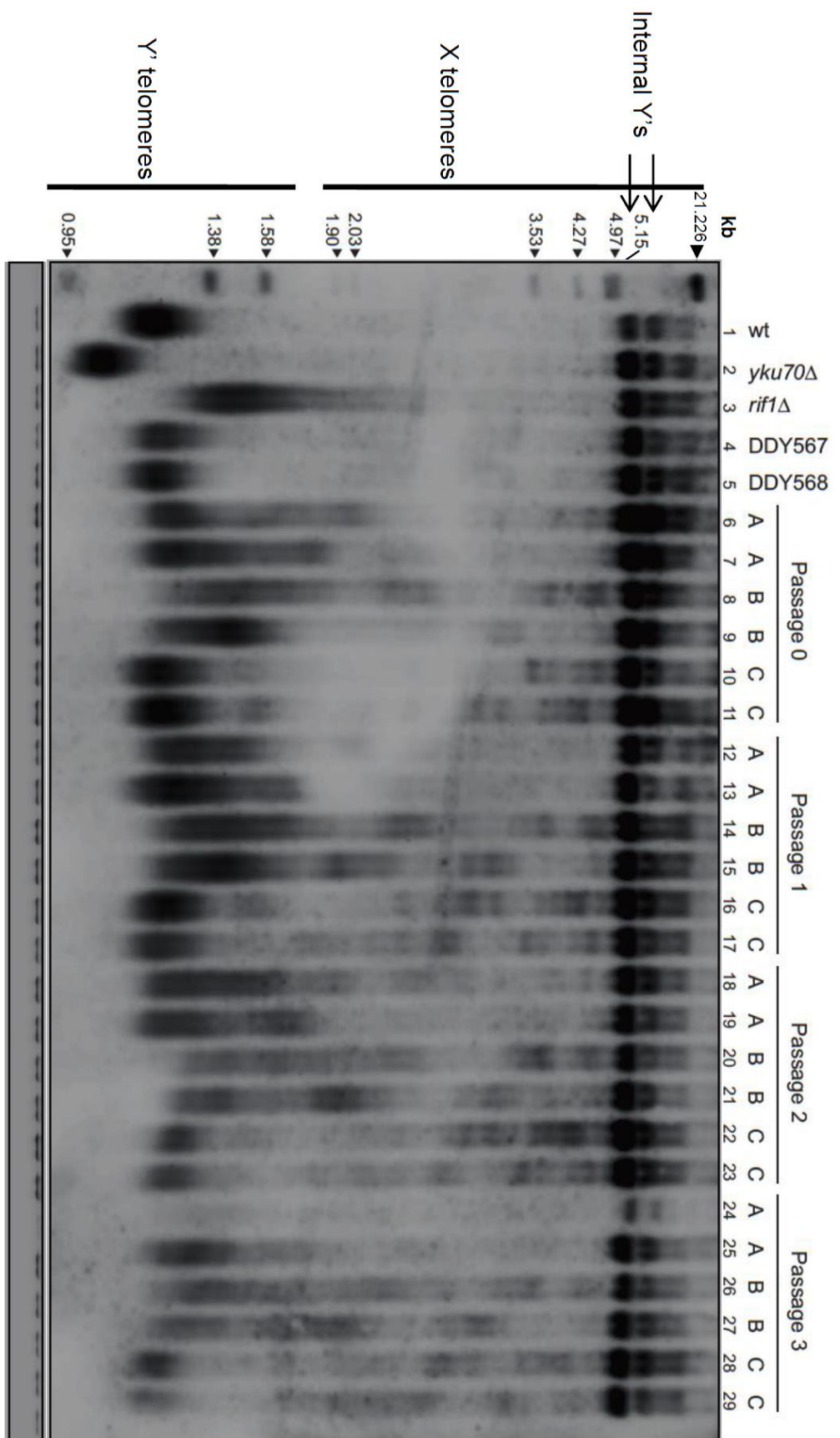


### **Figure 31. Diploids with a Cdc13 bypass strain parent have long telomeres**

The diploids indicated were passaged, genomic DNA was prepared and telomeres were analysed using Southern blotting and a Y' and TG<sub>1-3</sub> repeat probe as before (see Figure 7A). DDY567 and DDY568 (lanes 4 and 5) were diploids in which *CDC13* was deleted from the diploid using a deletion cassette. Diploids A-C were created by mating a Cdc13 bypass strain with a single gene deletion strain. 'A' diploids were DLY9697 x DLY8457; 'B' diploids were DLY9697 x DLY8455; 'C' diploids were DLY10209 x DLY8167. Replicates are independent colonies from each cross.

### 6.3 Ethanol exposure alters the telomere length of diploids

Growth in YPD with ethanol concentrations of up to 7% have previously been shown to lengthen the telomeres of budding yeast (Romano *et al.*, 2013). To further test whether telomere length was important for Cdc13 bypass, the telomeres of two *NMD2/nmd2Δ EXO1/exo1Δ RAD24/rad24Δ CDC13/cdc13Δ* diploids were lengthened by exposure to ethanol. The diploids were DDY567 and DDY568; independent strains made by transformation of a diploid with a *cdc13Δ* cassette. It was essential to use diploids where *CDC13* had been deleted by transformation of the diploid, since crossing a Cdc13 bypass strain with another haploid can produce heterogeneous telomeres (as shown in Figure 31).

The diploids were grown for 50 population doublings in 0%, 1%, 3% or 5% (v/v) ethanol. These concentrations were chosen because initial growth rates showed that both 0% and 1% cultures took 1 day to undergo 10 population doublings; 3% took two days and 5% took three days. Growth in 7% (v/v) ethanol was attempted but after inoculating at a density of  $1 \times 10^5$  cells/mL cultures only reached  $\approx 5 \times 10^7$  cells/mL after 4 days in culture and failed to double thereafter. This could be because the yeast genetic background being used (W303) was different to that used in Romano *et al.* (2013) (who used BY4741/2 haploids); or perhaps diploids are more sensitive to ethanol than haploids.

Table 2 shows the number of days in culture required for strains to undergo 50 population doublings. Diploids grown in 0% and 1% (v/v) ethanol underwent 50 population doublings after 5 days in culture, however strains in 3% and 5% (v/v) ethanol grew more poorly and required longer for 50 population doublings.

The telomere length of the strains grown in ethanol was examined by Southern blotting (Figure 32). It was found that increasing the percentage of ethanol increased Y' and X telomere length, similar to previously published data (Romano *et al.*, 2013). However, telomere length heterogeneity increased with ethanol concentration, such that strains grown in 5% ethanol also had very

short as well as very long Y' telomeres. This perhaps shows telomere degradation, since strains grown in 5% ethanol grew poorly compared to 0% ethanol growth.



<b>Ethanol %</b>	<b>Time taken to undergo 50 population doublings (days)</b>
0%	5
1%	5
3%	12
5%	17

**Table 2. Ethanol increases the time taken for diploids to complete 50 population doublings**

DDY567 and DDY568 diploids were grown in YPD with the given percentage of ethanol for 50 population doublings. Cells numbers were determined by counting with a haemocytometer.

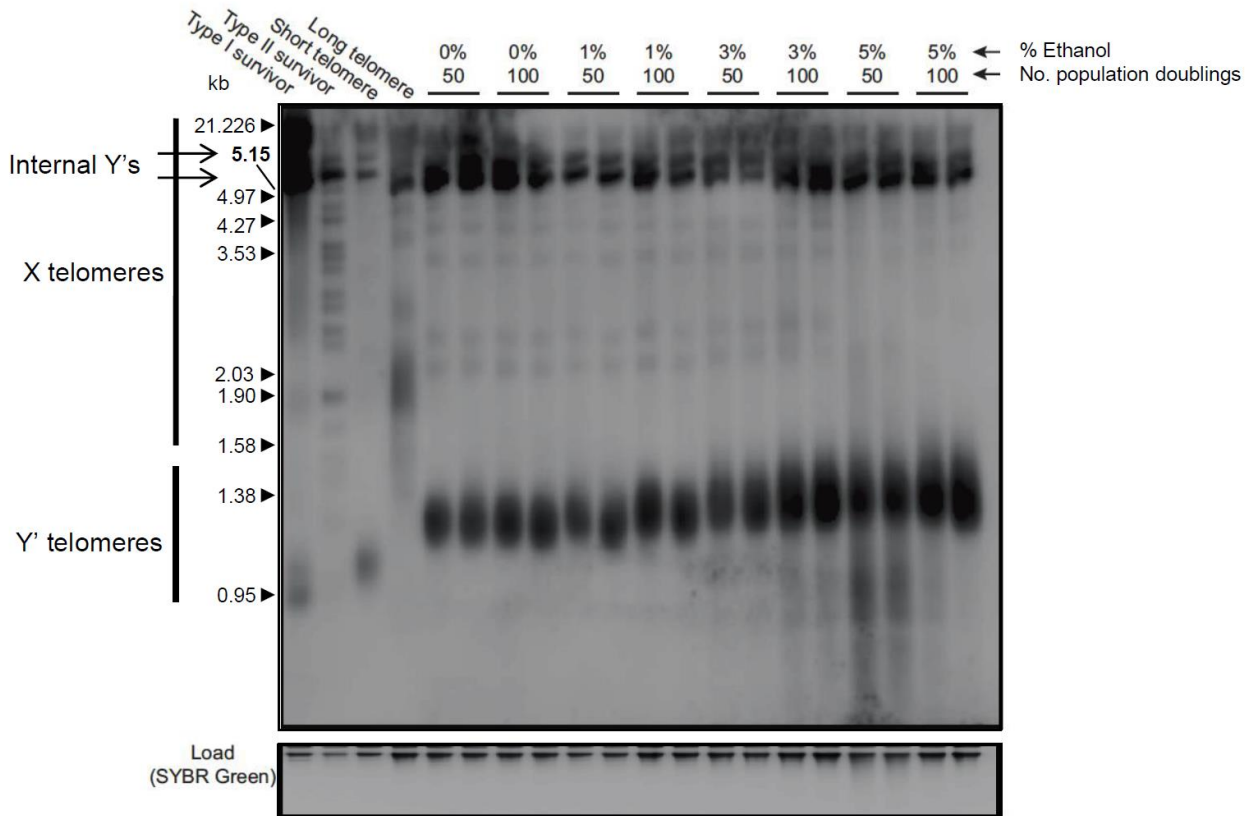


**Figure 32. Ethanol exposure lengthens diploid telomeres**

*nmd2Δ/NMD2 exo1Δ/EXO1 rad24Δ/RAD24 cdc13Δ/CDC13* diploids (DDY567 and DDY568) were grown in YPD with the ethanol concentrations shown and for the given number of population doublings. Genomic DNA was prepared and telomeres were analysed by Southern blotting using a Y' and TG<sub>1-3</sub> repeat probe as before (see Figure 7A). Type I survivor is DLY2146 (*tlc1Δ*), Type II survivor is DLY2148 (*tlc1Δ exo1Δ*), short telomere is DLY4528 (*nmd2Δ*), long telomere is DLY4451 (*rif1Δ*).

#### 6.4 Diploids grown in ethanol produce *cdc13Δ* strains that are not normally viable

To see whether long Y' and X telomeres caused the occurrence of *cdc13Δ* genotypes that are not normally viable, diploids grown in 0% and 1% ethanol were sporulated and spores were analysed using random spore analysis. Diploids grown in 5% ethanol were eliminated from the analysis as growth was very poor and telomeres showed evidence of degradation after Southern blot analysis.

Diploids grown in 0% ethanol for 50 population doublings produced above the expected number of all genotypes (previously known to be viable), apart from *nmd2Δ exo1Δ cdc13Δ* and *nmd2Δ rad24Δ cdc13Δ* genotypes, which were below the expected level (perhaps indicating spore inviability). Figure 33 shows the number of strains per genotype, after growth in 0% or 1% ethanol, in tables with the expected number per genotype given below the table (upper panel). The number of strains per genotype and condition are also shown in a bar graph (lower panel) with the expected number of spores given as a dashed line. Importantly, *cdc13Δ* genotypes that are not normally viable were not observed for diploids grown in YPD (0% ethanol), showing that in the absence of ethanol these strains behaved as previously published (Holstein *et al.*, 2014). However, diploids grown in 1% ethanol for 50 population doublings produced seven *cdc13Δ* genotypes that are not normally viable: two *exo1Δ cdc13Δ*, one *rad24Δ cdc13Δ*, two *exo1Δ rad24Δ cdc13Δ* and two *cdc13Δ* strains were obtained (Figure 33)

50 population doublings Genotype	0% ethanol			1% Ethanol		
	Number (I)	Number (II)	Average	Number (I)	Number (II)	Average
<i>wt</i>	22	42	32.0	28	46	37
<i>nmd2Δ</i>	26	36	31.0	14	24	19
<i>exo1Δ</i>	27	24	25.5	19	24	21.5
<i>cdc13Δ</i>	0	0	0.0	2	0	1
<i>rad24Δ</i>	17	12	14.5	8	20	14
<i>nmd2Δ exo1Δ</i>	31	19	25.0	22	27	24.5
<i>nmd2Δ rad24Δ</i>	24	19	21.5	14	15	14.5
<i>nmd2Δ cdc13Δ</i>	0	0	0.0	0	0	0
<i>exo1Δ cdc13Δ</i>	0	0	0.0	1	1	1
<i>exo1Δ rad24Δ</i>	19	17	18.0	18	17	17.5
<i>rad24Δ cdc13Δ</i>	0	0	0.0	1	0	0.5
<i>nmd2Δ exo1Δ cdc13Δ</i>	10	7	8.5	21	31	26
<i>nmd2Δ rad24Δ cdc13Δ</i>	8	7	7.5	4	10	7
<i>exo1Δ rad24Δ cdc13Δ</i>	0	0	0.0	1	1	1
<i>nmd2Δ exo1Δ rad24Δ</i>	20	22	21.0	23	12	17.5
<i>nmd2Δ exo1Δ rad24Δ cdc13Δ</i>	21	14	17.5	12	15	13.5
<b>TOTALS</b>	<b>225</b>	<b>219</b>	<b>222.0</b>	<b>188</b>	<b>243</b>	<b>215.5</b>

expected number = 14 (222/16) expected number = 14 (215.5/16)

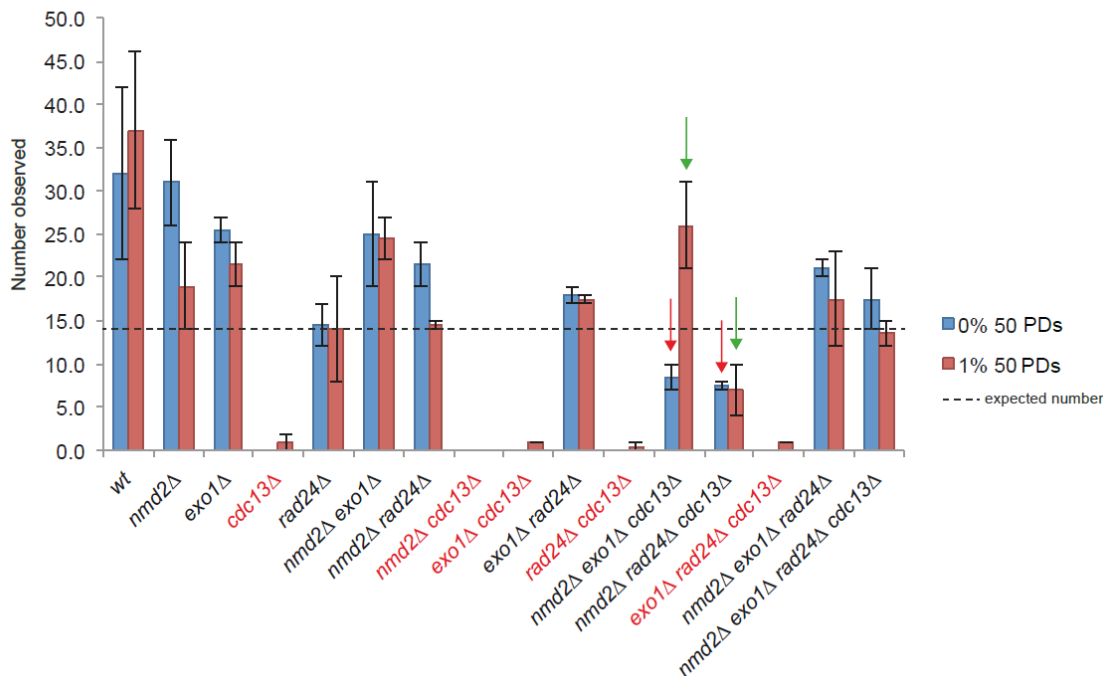


**Figure 33. Genotypes obtained after diploid growth in 1% ethanol**

(I) is DDY567 and (II) is DDY568. The numbers of each haploid genotype, obtained from the sporulation of the diploids, are given in the table and graph. Diploids were grown for 50 population doublings (PDs) in 1% ethanol. The bars of the graph show the average number of haploid genotypes obtained from the two independent diploid strains. The expected number of genotypes is given underneath the tables and as a dashed line in the bar graph. The upper and lower bounds of the error bars represent the numbers obtained from the individual diploid. *cdc13Δ* genotypes that are not normally viable are shown in red. Red and green arrows are to indicate genotypes of interest and are discussed in section 6.5.

Diploids that were grown in 3% ethanol for 50 population doublings produced fewer *cdc13Δ* genotypes (3 in total) that are not normally viable than diploids grown in 1% ethanol: one *cdc13Δ* and two *exo1Δ cdc13Δ* strains (Figure 34). The number of strains per genotype in 3% and 0% ethanol were compared (0% ethanol numbers are the same as in Figure 33). Taken together, there is evidence that elongated telomeres allow survival of a small proportion of *cdc13Δ* spores. However, the slightly longer telomeres of strains grown in 3% ethanol did not increase the frequency of *cdc13Δ* genotypes that are not normally viable, in fact the frequency decreased. This indicates that long telomeres promote Cdc13 bypass but do not wholly explain the existence of strains with *cdc13Δ* genotypes that are not normally viable.

50 population doublings Genotype	0% Ethanol			3% Ethanol		
	Number (I)	Number (II)	Average	Number (I)	Number (II)	Average
<i>wt</i>	22	42	32.0	27	29	28
<i>nmd2Δ</i>	26	36	31.0	19	23	21
<i>exo1Δ</i>	27	24	25.5	28	19	23.5
<i>cdc13Δ</i>	0	0	0.0	0	1	0.5
<i>rad24Δ</i>	17	12	14.5	12	14	13
<i>nmd2Δ exo1Δ</i>	31	19	25.0	32	32	32
<i>nmd2Δ rad24Δ</i>	24	19	21.5	18	15	16.5
<i>nmd2Δ cdc13Δ</i>	0	0	0.0	0	0	0
<i>exo1Δ cdc13Δ</i>	0	0	0.0	1	1	1
<i>exo1Δ rad24Δ</i>	19	17	18.0	20	11	15.5
<i>rad24Δ cdc13Δ</i>	0	0	0.0	0	0	0
<i>nmd2Δ exo1Δ cdc13Δ</i>	10	7	8.5	23	22	22.5
<i>nmd2Δ rad24Δ cdc13Δ</i>	8	7	7.5	9	10	9.5
<i>exo1Δ rad24Δ cdc13Δ</i>	0	0	0.0	0	0	0
<i>nmd2Δ exo1Δ rad24Δ</i>	20	22	21.0	25	21	23
<i>nmd2Δ exo1Δ rad24Δ cdc13Δ</i>	21	14	17.5	16	19	17.5
<b>TOTALS</b>	<b>225</b>	<b>219</b>	<b>222.0</b>	<b>230</b>	<b>217</b>	<b>223.5</b>

expected number = 14 (222/16)    expected number = 14 (223.5/16)

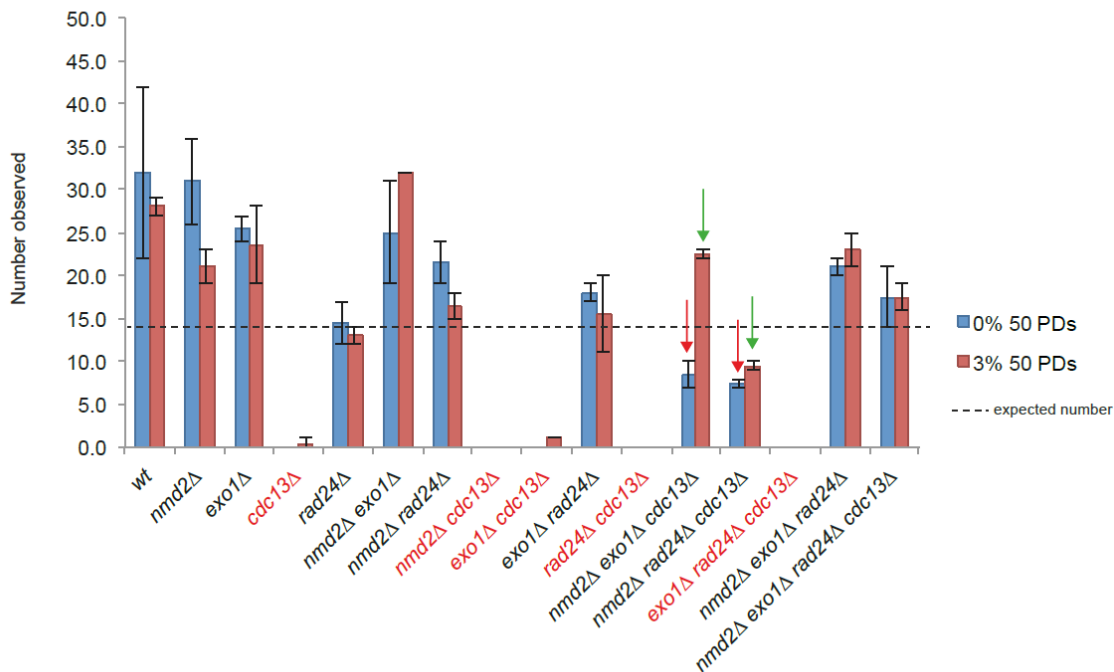


**Figure 34. Genotypes obtained after diploid growth in 3% ethanol**

As for Figure 33.

## 6.5 The frequency of Cdc13 bypass strains increases with telomere length

The number of expected Cdc13 bypass strains (*nmd2Δ exo1Δ cdc13Δ*; *nmd2Δ rad24Δ cdc13Δ*; *nmd2Δ exo1Δ rad24Δ cdc13Δ*) was below what was expected when diploids DDY567 and 568 were grown in YPD (0% ethanol) (see columns indicated by red arrows in Figure 33). However, it appeared that the number of *nmd2Δ exo1Δ cdc13Δ* and *nmd2Δ rad24Δ cdc13Δ* strains was increasing with the percentage of ethanol in the media (compare these genotypes for 0% (red arrow) and 1% (green arrow) in Figure 33 and for 0% (red arrow) and 3% (green arrow) in Figure 34). Since ethanol increases telomere length, I hypothesised that diploids with longer telomeres produced a higher frequency of Cdc13 bypass strains.

To test the hypothesis, genotype frequency was expressed as a percentage for each condition (i.e. 0% ethanol, 1% ethanol, 3% ethanol; 50 population doublings) (Figure 35). It was found that the percentage of *nmd2Δ exo1Δ cdc13Δ* strains obtained dramatically increased, relative to 0% ethanol, when grown in 1% and 3% ethanol (error bars for 0%, 1% and 3% did not overlap). The percentage of *nmd2Δ rad24Δ cdc13Δ* strains also increased, compared to growth in 0% ethanol, after exposure to 3% ethanol (error bars for 0% and 3% did not overlap). Furthermore, a diploid made from a *rif1Δ x nmd2Δ exo1Δ cdc13Δ* cross, which has long telomeres initially, produced similarly high frequency of *nmd2Δ exo1Δ cdc13Δ* spores (18%; Figure 20). Interestingly, there was no change in the frequency of *nmd2Δ exo1Δ rad24Δ cdc13Δ* strains between 0% to 1% and 3% ethanol, perhaps because these have higher spore viability.

It appears that longer diploid telomeres lead to an increased frequency of *nmd2Δ exo1Δ cdc13Δ* and *nmd2Δ rad24Δ cdc13Δ* strains. It is possible that there is a higher degree of spore inviability for *nmd2Δ exo1Δ cdc13Δ* and *nmd2Δ rad24Δ cdc13Δ* genotypes when grown in YPD (0% ethanol), perhaps

because of short telomeres. Indeed, absence of *nmd2* $\Delta$  leads to short telomeres, so perhaps this reduces spore viability in Cdc13 bypass strains. When diploids have longer telomeres this could increase the telomere length of the haploid progeny, allowing more Cdc13 bypass strains to form viable colonies.



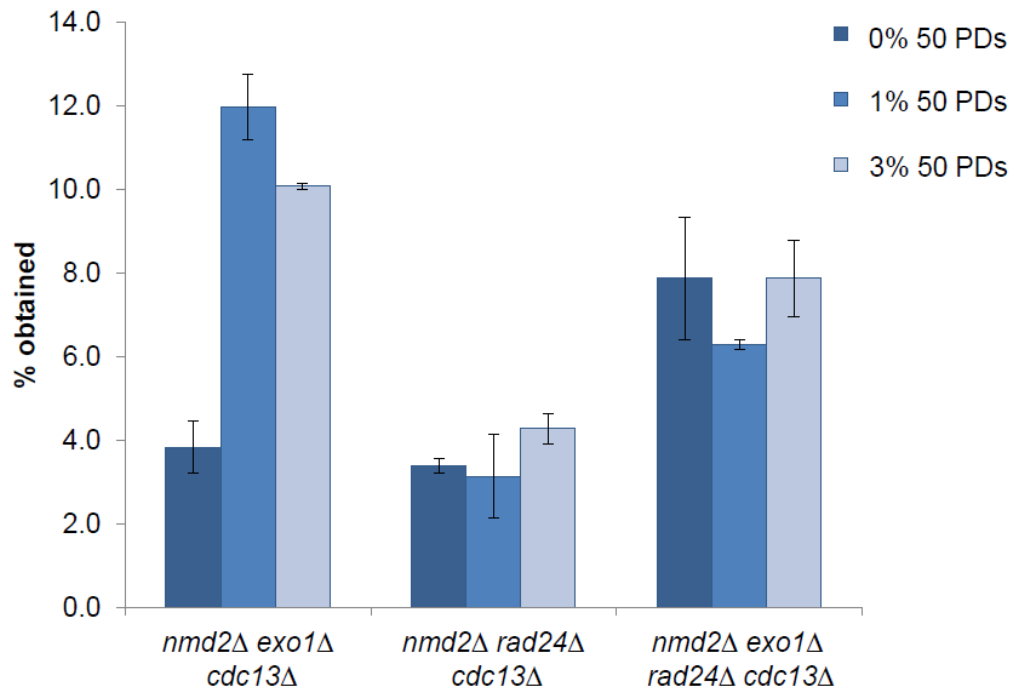


**Figure 35. Percentage of Cdc13 bypass strains obtained after diploid growth in ethanol**

% obtained is the percentage of the total number of haploid strains analysed (for each % ethanol condition after 50 population doublings (PDs)), using the data shown in Figure 33 and Figure 34. The bars show the average from two independent diploid strains (sporulated to produce the haploids), the upper and lower bounds of the error bars show the individual value for each strain.

## 6.6 Discussion

The data in this chapter has shown that diploids with long, heterogeneous telomeres can generate *cdc13*Δ genotypes that are not normally viable. Such diploids can be produced when crossing a Cdc13 bypass strain with another haploid. In addition, diploids with slightly elongated telomeres (after growth in ethanol) also produce *cdc13*Δ genotypes that are not normally viable when telomeres are of wild-type length. Also, the frequency of *nmd2*Δ *exo1*Δ *cdc13*Δ and *nmd2*Δ *rad24*Δ *cdc13*Δ strains, previously identified as Cdc13 bypass strains, increased with telomere length. This indicates that longer telomeres increase the spore viability of these genotypes, perhaps because deletion of *NMD2* leads to short telomeres which could lead to cell cycle arrest in strains lacking Cdc13. Since longer Y' and X telomeres occurs by extension of TG<sub>1-3</sub> repeats, it is possible that long tracts of these repeats promote survival without Cdc13. This hypothesis is supported by the fact that *cdc13*Δ cells are inviable without Rad52, which promotes Type II recombination in which TG<sub>1-3</sub> repeats are amplified.

Long telomeres do not wholly explain Cdc13 bypass since an *nmd2*Δ *exo1*Δ *cdc13*Δ strain crossed with a *rif1*Δ strain had long telomeres but did not produce any *cdc13*Δ genotypes that are not normally viable. Nonetheless, the telomeres of this diploid recovered with passage, resembling a wild-type diploid telomere more closely after three passages. Therefore, perhaps Type II recombination is partially inhibited in the diploids heterozygous for *NMD2*, *EXO1*, *CDC13* and *RIF1* deletions but is not inhibited in diploids heterozygous for *NMD2*, *RAD24*, *CDC13* and *RIF1* deletions. Moreover, strains with the longest telomeres produced fewer *cdc13*Δ genotypes (that are not normally viable) than those with slightly shorter telomeres.

Further work needs to be conducted to identify the other factors contributing to the growth of *cdc13*Δ genotypes that are not normally viable. One possible explanation for such genotypes is aneuploidy, when a strain has an extra chromosome carrying *CDC13* as well as the deletion. To determine whether this is the case, PCR of the *CDC13* gene in these strains could be carried out.

It would furthermore be informative to examine the telomere structure of haploid strains from diploids grown in ethanol compared to YPD. This would show whether telomere rearrangements and length are inherited by haploids. If so, this would provide further evidence that long telomeres promote Cdc13 bypass.

Long telomeres have been thought to be beneficial to health, since telomeres shorten with age and short telomeres may lead to genome instability and cancer (Lapham *et al.*, 2015; Needham *et al.*, 2015). Indeed, companies have been set up to offer telomere length assessment for individuals, for use as a biomarker for ageing and health. This is because shorter telomeres have been associated with alcohol consumption, smoking and obesity and it has been reported that healthy lifestyle changes increase telomere length in immune cells in individuals with cancer (Strandberg *et al.*, 2012; Ornish *et al.*, 2013; Joshi *et al.*, 2015; Verde *et al.*, 2015).

However, this chapter has provided evidence that long, heterogeneous telomeres contribute to cells surviving without the essential telomere-capping protein Cdc13. Furthermore, ethanol-lengthened telomeres in yeast lead to *cdc13Δ* genotypes not normally obtained and increases the frequency of Cdc13 bypass strains. Cell division in the absence of an essential telomere-capping protein is not necessarily beneficial, since the telomere end may have greater exposure to the DDR, which ultimately leads to genome instability. On the other hand, one cause of ageing is telomere shortening. Absence of a telomere capping protein may allow an ageing cell to maintain its viability by allowing telomeres to be extended and maintained by recombination. The disadvantage of telomere maintenance by recombination is that this can increase the risk of cancer, for example ALT cancer cells maintain telomeres by recombination.

Recent research has cast doubt on whether long telomeres are always beneficial to health. Shorter telomeres are not necessarily associated with an increased cancer risk, although they do reduce cancer survival rates (Weischer *et al.*, 2013). Also, it has been reported that subjects with a genetic predisposition to short telomeres (those with SNPs associated with short leukocyte telomere length, e.g. SNPs in OBFC1) have lower cancer mortality, therefore those with genetically long telomeres have higher cancer mortality (Rode *et al.*, 2015).

Interestingly, SNPs in OBFC1 (also known as human STN1) are associated with short telomeres but subjects do not have increased cancer mortality (Rode *et al.*, 2015). This suggests that maximally functional (or indeed over-active) human STN1 may actually be harmful, leading to telomere maintenance of cells that should senesce or die due to their age or accumulated mutations (Rode *et al.*, 2015). This appears to be the case in budding yeast, where increased Stn1 and Ten1 activity can allow Cdc13 bypass to occur, if the DDR is attenuated (Holstein *et al.*, 2014). Long telomeres appear to contribute to bypass of Cdc13 without any other gene deletions (shown in this chapter), and it has been further shown that cells resembling Type I and Type II survivors, with substantial telomere rearrangements, lose Cdc13 and maintain viability (Larrivé and Wellinger, 2006). It is possible that Stn1 and Ten1 provide sufficient telomere protection when telomeres are long, such that cells can survive without Cdc13.

## Chapter 7. General Discussion

My data suggests that Stn1 (and presumably Ten1) are at the telomere in the absence of Cdc13, and therefore carry out telomeric roles independently of Cdc13. CST has been described as a telomeric RPA, since RPA is an ssDNA-binding heterotrimer. However, the essential telomere protection roles of Stn1 and Ten1, in the absence of Cdc13, suggest that CST components act very differently to RPA components. Indeed, I propose that Ten1 may interact with Rif1, to form a shelterin-like complex after telomere replication.

Rif1 is of increasing interest in cancer research, since human RIF1 appears to be directly involved in maintaining genome stability in human cells, by regulating DNA damage repair through BRCA1 repression, signalling DNA damage at telomeres and ensuring timely sister chromatid separation (Silverman *et al.*, 2004; Chapman *et al.*, 2013; Hengeveld *et al.*, 2015). Since Rif1 is required for Cdc13 bypass, Rif1 activities may promote the survival of strains with damaged or rearranged telomeres. RIF1 may therefore have a role in promoting the formation or maintenance of ALT cancer cells and could be a potential therapeutic target in the treatment of cancer.

I found that Rad52, a key HR protein, was essential for Cdc13 bypass. Rad52 is required for Type I and Type II recombination, therefore at least one recombination pathway is required for cells to survive without Cdc13. Since Rad51 (which is required for the formation of Type I survivors) was not required for Cdc13 bypass, it is possible that cells lacking Cdc13 require Type II recombination. However, deletion of *RIF1* promotes Type II recombination (Teng *et al.*, 2000) but is lethal to Cdc13 bypass. Also, *nmd2Δ* *exo1Δ* *cdc13Δ* strains have telomeres that more closely resemble those of Type I survivors. Therefore, it seems most likely Cdc13 bypass requires recombination, but not a specific recombination pathway.

I found evidence that long telomeres promoted Cdc13 bypass, as diploids with telomeres elongated by ethanol exposure (Both Y' and X telomeres with extended TG repeats) produced *cdc13Δ* genotypes that were previously thought to be inviable (i.e. double mutants and triple mutants that were not deleted for *NMD2*). Therefore, there is evidence that extended tracts of TG repeats promote Cdc13 bypass. Furthermore, growth in ethanol led to an increased frequency of Cdc13 bypass genotypes (previously known to be viable). These data suggest that longer TG<sub>1-3</sub> repeats may promote the viability of Cdc13 bypass strains. Perhaps long tracts of TG<sub>1-3</sub> repeats promote telomere recombination, which is essential for the survival of cells lacking Cdc13.

However, diploids heterozygous for *NMD2*, *EXO1*, *CDC13* and *RIF1* deletions had long telomeres but produced no unexpected *cdc13Δ* genotypes. The telomeres of diploids heterozygous for *NMD2*, *EXO1*, *CDC13* and *RIF1* deletions did recover with passage, however. This suggests that their long, heterogeneous phenotype was not as severe as those of the other diploids tested and perhaps this explains why no unexpected *cdc13Δ* genotypes were obtained.

Promotion of human STN1 and TEN1 protein activity, perhaps by suppression of NMD and DDR, may be helpful to patients with CTC1-mutation diseases, since there is evidence that Stn1 and Ten1 have the most important telomere protection roles in CST. In ALT cancers, inhibition of RIF1 may reduce cell viability since in yeast Rif1 supports Cdc13 bypass, in which cells maintain telomeres by recombination in a manner similar to ALT cells. Finally, there is evidence that alcohol exposure is harmful to telomeres, since ethanol exposure allows the bypass of protective telomere capping in yeast.

Overall, this thesis concludes that Cdc13 bypass depends on Stn1 and Ten1 binding to the telomere end, Rif1 and Rad52-mediated Type II recombination. Perhaps extended TG<sub>1-3</sub> tracts encourage increased Stn1- Ten1 and Rif1 binding and this helps to protect the telomere without Cdc13. Since Stn1 and Ten1 appear to be more important for telomere end protection than Cdc13, and the fission yeast *S. pombe* has no Cdc13 orthologue, it is possible that Stn1

and Ten1 evolved earlier than Cdc13 and therefore have independent or overlapping telomere protection roles.





## Appendix A. Yeast strains by figure number

Strain numbers are prefixed DLY unless otherwise stated.

<b>Strain number</b>	<b>Genotype (all W303 <i>RAD5</i><sup>+</sup> unless otherwise stated)</b>	<b>Related figure</b>
1628	<i>MAT</i> alpha <i>tlc1::HIS3 pTLC1::URA3</i> (streaked until plasmid lost)	Figure 7
2148	<i>MAT</i> alpha <i>tlc1::HIS3 exo1::LEU2</i> (Type II survivor)	Figure 7
8167	<i>MAT</i> alpha <i>nmd2::HIS3 exo1::LEU2 cdc13::HPHMX</i> passage 1	Figure 7
8168	<i>nmd2::HIS3 exo1::LEU2 cdc13::HPHMX</i> passage 1	Figure 7
8169	<i>nmd2::HIS3 exo1::LEU2 rad24::TRP1 cdc13::HPHMX</i> passage 1	Figure 7
8170	<i>nmd2::HIS3 exo1::LEU2 rad24::TRP1 cdc13::HPHMX</i> passage 1	Figure 7
8171	<i>nmd2::HIS3 rad24::TRP1 cdc13::HPHMX</i> passage 1	Figure 7
8172	<i>nmd2::HIS3 rad24::TRP1 cdc13::HPHMX</i> passage 1	Figure 7
8193	<i>nmd2::HIS3 rad24::TRP1</i>	Figure 7
8195	<i>nmd2::HIS3 exo1::LEU2</i>	Figure 7
8197	<i>nmd2::HIS3 exo1::LEU2 rad24::TRP1</i>	Figure 7
8199	<i>nmd2::HIS3 exo1::LEU2 rad24::TRP1 cdc13::HPHMX</i> passage 9	Figure 7
8200	<i>nmd2::HIS3 exo1::LEU2 rad24::TRP1 cdc13::HPHMX</i> passage 9	Figure 7
8201	<i>nmd2::HIS3 rad24::TRP1 cdc13::HPHMX</i> passage 9	Figure 7
8202	<i>nmd2::HIS3 rad24::TRP1 cdc13::HPHMX</i> passage 9	Figure 7
8203	<i>nmd2::HIS3 exo1::LEU2 cdc13::HPHMX</i> passage 9	Figure 7
8204	<i>nmd2::HIS3 exo1::LEU2 cdc13::HPHMX</i> passage 9	Figure 7
8460	<i>MAT</i> a <i>ade2-1 trp1-1 can1-100 leu2-3,112 his3-11,15 ura3 GAL+ psi+ ssd1-d2 RAD5</i> (W303 wild-type)	Figure 7
8460	<i>MAT</i> a <i>ade2-1 trp1-1 can1-100 leu2-3,112 his3-11,15 ura3 GAL+ psi+ ssd1-d2 RAD5</i> (W303 wild-type)	Figure 8
2146	<i>MAT</i> a <i>tlc1::HIS3</i> (Type I survivor)	Figure 8
2148	<i>MAT</i> alpha <i>tlc1::HIS3 exo1::LEU2</i> (Type II survivor)	Figure 8
8462	<i>MAT</i> a <i>tlc1::NATMX</i> passage 1	Figure 8
8465	<i>MAT</i> a <i>tlc1::NATMX</i> passage 9	Figure 8

8467	<i>MATa tlc1::NATMX nmd2::HIS3 rad24::TRP1 cdc13::HPHMX</i> passage 2	Figure 8
8468	<i>MATa tlc1::NATMX nmd2::HIS3 exo1::LEU2 cdc13::HPHMX</i> passage 2	Figure 8
8472	<i>MATa tlc1::NATMX</i> passage 3	Figure 8
8473	<i>MATa tlc1::NATMX nmd2::HIS3 rad24::TRP1 cdc13::HPHMX</i>	Figure 8
8474	<i>MATa tlc1::NATMX nmd2::HIS3 exo1::LEU2 cdc13::hph</i>	Figure 8
8475	<i>MATa tlc1::NATMX nmd2::HIS3 exo1::LEU2 rad24::TRP1 cdc13::hph</i>	Figure 8
8509	<i>MATa tlc1::NATMX</i>	Figure 8
8510	<i>MATa tlc1::NATMX nmd2::HIS3 rad24::TRP1 cdc13::HPHMX</i>	Figure 8
8511	<i>MATa tlc1::NATMX nmd2::HIS3 exo1::LEU2 cdc13::HPHMX</i>	Figure 8
8512	<i>MATalpha tlc1::NATMX nmd2::HIS3 rad24::TRP1 exo1::LEU2 cdc13::hph</i>	Figure 8
8601	<i>MATa tlc1::NATMX nmd2::HIS3 rad24::TRP1 cdc13::HPHMX</i> passage 9	Figure 8
8602	<i>MATa tlc1::NATMX nmd2::HIS3 exo1::LEU2 cdc13::HPHMX</i> passage 9	Figure 8
8603	<i>MATalpha tlc1::NATMX nmd2::HIS3 rad24::TRP1 exo1::LEU2 cdc13::HPHMX</i> passage 9	Figure 8
8460	<i>MATa ade2-1 trp1-1 can1-100 leu2-3,112 his3-11,15 ura3 GAL+ psi+ ssd1-d2 RAD5</i> (W303 wild-type)	Figure 9
1272	<i>MATa exo1::LEU2</i>	Figure 9
1273	<i>MATalpha exo1::LEU2</i>	Figure 9
3001	<i>MATalpha ade2-1 trp1-1 can1-100 leu2-3,112 his3-11,15 ura3 GAL+ psi+ ssd1-d2 RAD5</i> (W303 wild-type)	Figure 9
4765	<i>MATa nmd2::HIS3</i>	Figure 9
4766	<i>MATalpha nmd2::HIS3</i>	Figure 9
4872	<i>MATa pif1::NATMX</i>	Figure 9
4873	<i>MATalpha pif1::NATMX</i>	Figure 9
5915	<i>MATa pif1::NATMX exo1::LEU2</i>	Figure 9
5916	<i>MATalpha pif1::NATMX exo1::LEU2</i>	Figure 9
5759	<i>MATa STN1-13MYC::TRP1 nmd2::HIS3</i>	Figure 10
5761	<i>MATa STN1-13MYC::TRP1</i>	Figure 10
7273	<i>MATalpha CDC13-13MYC::HIS3</i>	Figure 10
7274	<i>MATalpha CDC13-13MYC::HIS3 nmd2::URA3</i>	Figure 10
8100	<i>MATa TEN1-13MYC::KANMX nmd2::URA3</i>	Figure 10
8101	<i>MATa TEN1-13MYC::KANMX</i>	Figure 10
8432	<i>MATa STN1-13MYC::KANMX nmd2::HIS3 exo1::LEU2 rad24::TRP1</i>	Figure 11
8434	<i>MATalpha TEN1-13MYC::KANMX nmd2::HIS3 exo1::LEU2 rad24::TRP1</i>	Figure 11
8604	<i>MATalpha STN1-13MYC::KANMX nmd2::HIS3 exo1::LEU2 rad24::TRP1 cdc13::HPHMX</i>	Figure 11

8605	<i>MATa TEN1::Myc::KANMX nmd2::HIS3 exo1::LEU2 rad24::TRP1 cdc13::hph</i>	Figure 11
8460	<i>MATa ade2-1 trp1-1 can1-100 leu2-3,112 his3- 11,15 ura3 GAL+ psi+ ssd1-d2 RAD5 (W303 wild-type)</i>	Figure 12
4528	<i>MATa nmd2::HIS3</i>	Figure 12
8198	<i>nmd2::HIS3 exo1::LEU2 rad24::TRP1</i>	Figure 12
8461	<i>MATa nmd2::HIS3 exo1::LEU2 rad24::TRP1 cdc13::HPHMX</i>	Figure 12
8766	<i>MATalpha stn1-13::HPHMX lyp1::NATMX can1Δ::STE2pr-Sp_his5 (S288C)</i>	Figure 13
9101	<i>MATa rfa1-M2::KANMX (S288C)</i>	Figure 13
9102	<i>MATa rfa3-313::KANMX (S288C)</i>	Figure 13
5761	<i>MATa STN1-13MYC::TRP1</i>	Figure 14
8101	<i>MATa TEN1-13MYC::KANMX</i>	Figure 14
8432	<i>MATa STN1-13MYC::KANMX nmd2::HIS3 exo1::LEU2 rad24::TRP1</i>	Figure 14
8434	<i>MATalpha TEN1-13MYC::KANMX nmd2::HIS3 exo1::LEU2 rad24::TRP1</i>	Figure 14
8461	<i>MATa nmd2::HIS3 exo1::LEU2 rad24::TRP1 cdc13::HPHMX</i>	Figure 14
1098	<i>MATa rfa1::MYC18::RFA1 rad5-535</i>	Figure 14
8298	<i>MATalpha RFA3-3HA::KANMX</i>	Figure 14
8429	<i>MATalpha STN1-13MYC::KANMX nmd2::HIS3 exo1::LEU2 rad24::TRP1 cdc13::HPHMX</i>	Figure 14
8431	<i>MATa TEN1-13MYC::KANMX nmd2::HIS3 exo1::LEU2 rad24::TRP1 cdc13::HPHMX</i>	Figure 14
8989	<i>MATa cdc13-1 cdc15-2 int bar1 Ddc1-Myc- HIS3MX6 Mec3-3HA-KanMX</i>	Figure 14
9527	<i>MATalpha RFA3-3HA::KANMX STN1- 13MYC::TRP1</i>	Figure 14
9653	<i>MATalpha nmd2::HPHMX exo1::NATMX cdc13::LEU2 lyp1Δ can1Δ::STE2pr-Sp_his5 (S288C)</i>	Figure 17
9718	<i>MATalpha nmd2::HPHMX exo1::NATMX lyp1::LEU2 can1-ste2_pr_his5 (S288C)</i>	Figure 17
2146	<i>MATa tlc1::HIS3 (Type I survivor)</i>	Figure 18
2148	<i>MATalpha tlc1::HIS3 exo1::LEU2 (Type II survivor)</i>	Figure 18

4451	<i>MAT</i> alpha <i>rif1::URA3</i> (long telomere)	Figure 18
4528	<i>MAT</i> a <i>nmd2::HIS3</i> (short telomere)	Figure 18
8460	<i>MAT</i> a <i>ade2-1 trp1-1 can1-100 leu2-3,112 his3-11,15 ura3 GAL+ psi+ ssd1-d2 RAD5</i> (W303 wild-type)	Figure 18
8457	<i>MAT</i> a <i>nmd2::HIS3 exo1::LEU2 cdc13::HPHMX</i>	Figure 20
9697	<i>MAT</i> alpha <i>rif1::NATMX</i>	Figure 20
835 (DDY)	<i>nmd2::his3/NMD2 exo1::LEU2/EXO1 rad24::TRP1/RAD24 cdc13::HPHMX/CDC13 rif1::NATMX/RIF1</i>	Figure 21
836 (DDY)	<i>nmd2::his3/NMD2 exo1::LEU2/EXO1 rad24::TRP1/RAD24 cdc13::HPHMX/CDC13 rif1::NATMX/RIF1</i>	Figure 21
8167	<i>MAT</i> alpha <i>nmd2::HIS3 exo1::LEU2 cdc13::HPHMX</i> passage 1	Figure 22
8460	<i>MAT</i> a <i>ade2-1 trp1-1 can1-100 leu2-3,112 his3-11,15 ura3 GAL+ psi+ ssd1-d2 RAD5</i> (W303 wild-type)	Figure 22
1273	<i>MAT</i> alpha <i>exo1::LEU2</i>	Figure 22
4528	<i>MAT</i> a <i>nmd2::HIS3</i>	Figure 22
8457	<i>MAT</i> a <i>nmd2::HIS3 exo1::LEU2 cdc13::HPHMX</i>	Figure 22
8196	<i>nmd2::HIS3 exo1::LEU2</i>	Figure 22
9699	<i>MAT</i> a <i>rif1-RVxF-SILK</i>	Figure 22
10211	<i>MAT</i> a <i>nmd2::HIS3 rif1-RVxF-SILK</i>	Figure 22
10213	<i>MAT</i> alpha <i>exo1::LEU2 rif1-RVxF-SILK</i>	Figure 22
10215	<i>MAT</i> a <i>nmd2::HIS3 exo1::LEU2 rif1-RVxF-SILK</i>	Figure 22
10218	<i>MAT</i> a <i>nmd2::HIS3 exo1::LEU2 cdc13::HPHMX rif1- RVxF-SILK</i>	Figure 22
10219	<i>MAT</i> alpha <i>nmd2::HIS3 exo1::LEU2 cdc13::HPHMX rif1- rif1- RVxF-SILK</i>	Figure 22
10254	<i>MAT</i> alpha <i>nmd2::URA3 exo1::LEU2 cdc13::HPHMX</i>	Figure 22
8167	<i>MAT</i> alpha <i>nmd2::HIS3 exo1::LEU2 cdc13::HPHMX</i> passage 1	Figure 23
8460	<i>MAT</i> a <i>ade2-1 trp1-1 can1-100 leu2-3,112 his3-11,15 ura3 GAL+ psi+ ssd1-d2 RAD5</i> (W303 wild-type)	Figure 23
1273	<i>MAT</i> alpha <i>exo1::LEU2</i>	Figure 23
4528	<i>MAT</i> a <i>nmd2::HIS3</i>	Figure 23
8457	<i>MAT</i> a <i>nmd2::HIS3 exo1::LEU2 cdc13::HPHMX</i>	Figure 23
8196	<i>nmd2::HIS3 exo1::LEU2</i>	Figure 23
10290	<i>MAT</i> alpha <i>rif1Δ2-176-13MYC::HIS3MX6</i>	Figure 23
10757	<i>MAT</i> alpha <i>nmd2::URA3 rif1Δ2-176-13MYC::HIS3MX6</i>	Figure 23
10758	<i>MAT</i> a <i>exo1::LEU2 rif1Δ2-176-13MYC::HIS3MX6</i>	Figure 23
10760	<i>MAT</i> a <i>nmd2::URA3 exo1::LEU2 rif1Δ2-176-13MYC::HIS3MX6</i>	Figure 23

10795	<i>MAT</i> alpha <i>nmd2::URA3 exo1::LEU2 cdc13::HPHMX LEU2 rif1Δ2-176-13MYC::HIS3MX6</i>	Figure 23
10796	<i>MAT</i> alpha <i>nmd2::URA3 exo1::LEU2 cdc13::HPHMX LEU2 rif1Δ2-176-13MYC::HIS3MX6</i>	Figure 23
10813	<i>MAT</i> alpha <i>nmd2::HIS3 exo1::LEU2 cdc13::HPHMX rif1::NATMX pRIF1-URA3 (pDL1714)</i>	Figure 25
10255	<i>MAT</i> a <i>nmd2::URA3 exo1::LEU2 cdc13::HPHMX</i>	Figure 23
8167	<i>MAT</i> alpha <i>nmd2::HIS3 exo1::LEU2 cdc13::HPHMX passage 1</i>	Figure 24
8460	<i>MAT</i> a <i>ade2-1 trp1-1 can1-100 leu2-3,112 his3-11,15 ura3 GAL+ psi+ ssd1-d2 RAD5 (W303 wild-type)</i>	Figure 24
1273	<i>MAT</i> alpha <i>exo1::LEU2</i>	Figure 24
4528	<i>MAT</i> a <i>nmd2::HIS3</i>	Figure 24
8457	<i>MAT</i> a <i>nmd2::HIS3 exo1::LEU2 cdc13::HPHMX</i>	Figure 24
8196	<i>nmd2::HIS3 exo1::LEU2</i>	Figure 24
9714	<i>MAT</i> alpha <i>rif1Δ1323-1916-13MYC::HIS3MX6</i>	Figure 24
10255	<i>MAT</i> a <i>nmd2::URA3 exo1::LEU2 cdc13::HPHMX</i>	Figure 24
10291	<i>MAT</i> alpha <i>exo1::LEU2 rif1Δ1323-1916-13MYC::HIS3MX</i>	Figure 24
10293	<i>MAT</i> a <i>nmd2::URA3 rif1 rif1Δ1323-1916-13MYC::HIS3MX</i>	Figure 24
10295	<i>MAT</i> alpha <i>nmd2::URA3 exo1::LEU2 rif1Δ1323-1916-13MYC::HIS3MX</i>	Figure 24
10297	<i>MAT</i> alpha <i>nmd2::URA3 exo1::LEU2 cdc13::HPHMX rif1Δ1323-1916-13MYC::HIS3MX</i>	Figure 24
10298	<i>MAT</i> a <i>nmd2::URA3 exo1::LEU2 cdc13::HPHMX rif1Δ1323-1916-13MYC::HIS3MX</i>	Figure 24
10813	<i>MAT</i> alpha <i>nmd2::HIS3 exo1::LEU2 cdc13::HPHMX rif1::NATMX pRIF1-URA3 (pDL1714)</i>	Figure 25
8167	<i>MAT</i> alpha <i>nmd2::HIS3 exo1::LEU2 cdc13::HPHMX passage 1</i>	Figure 27
5872	<i>MAT</i> a <i>rad52::TRP1</i>	Figure 27
3485	<i>MAT</i> a <i>rad51::KANMX</i>	Figure 27
8167	<i>MAT</i> alpha <i>nmd2::HIS3 exo1::LEU2 cdc13::HPHMX passage 1</i>	Figure 29
5872	<i>MAT</i> a <i>rad52::TRP1</i>	Figure 29
8455	<i>MAT</i> a <i>nmd2::HIS3 rad24::LEU2 cdc13::HPHMX passage 1</i>	Figure 30
9697	<i>MAT</i> alpha <i>rif1::NATMX</i>	Figure 30
8167	<i>MAT</i> alpha <i>nmd2::HIS3 exo1::LEU2 cdc13::HPHMX passage 1</i>	Figure 30
10209	<i>MAT</i> a <i>dxo1::KANMX</i>	Figure 30
8455	<i>MAT</i> a <i>nmd2::HIS3 rad24::LEU2 cdc13::HPHMX passage 1</i>	Figure 31

9697	<i>MAT</i> alpha <i>rif1::NATMX</i>	Figure 31
8167	<i>MAT</i> alpha <i>nmd2::HIS3 exo1::LEU2 cdc13::HPHMX</i> passage 1	Figure 31
10209	<i>MAT</i> a <i>dxo1::KANMX</i>	Figure 31
225 (DDY)	wt/wt	Figure 31
812 (DDY)	<i>rif1::NATMX/rif1::URA3</i>	Figure 31
810 (DDY)	<i>yku70::LEU2/yku70::HIS3</i>	Figure 31
567 (DDY)	<i>nmd2::his3/NMD2 exo1::LEU2/EXO1 rad24::TRP1/RAD24 cdc13::HPHMX/CDC13</i>	Figure 31
568 (DDY)	<i>nmd2::his3/NMD2 exo1::LEU2/EXO1 rad24::TRP1/RAD24 cdc13::HPHMX/CDC13</i>	Figure 31
567 (DDY)	<i>nmd2::his3/NMD2 exo1::LEU2/EXO1 rad24::TRP1/RAD24 cdc13::HPHMX/CDC13</i>	Table 2
568 (DDY)	<i>nmd2::his3/NMD2 exo1::LEU2/EXO1 rad24::TRP1/RAD24 cdc13::HPHMX/CDC13</i>	Table 2
2146	<i>MAT</i> a <i>tlc1::HIS3</i> (Type I survivor)	Figure 32
2148	<i>MAT</i> alpha <i>tlc1::HIS3 exo1::LEU2</i> (Type II survivor)	Figure 32
4451	<i>MAT</i> alpha <i>rif1::URA3</i>	Figure 32
4528	<i>MAT</i> a <i>nmd2::HIS3</i>	Figure 32
567 (DDY)	<i>nmd2::his3/NMD2 exo1::LEU2/EXO1 rad24::TRP1/RAD24 cdc13::HPHMX/CDC13</i>	Figure 32
568 (DDY)	<i>nmd2::his3/NMD2 exo1::LEU2/EXO1 rad24::TRP1/RAD24 cdc13::HPHMX/CDC13</i>	Figure 32
567 (DDY)	<i>nmd2::his3/NMD2 exo1::LEU2/EXO1 rad24::TRP1/RAD24 cdc13::HPHMX/CDC13</i>	Figure 33
568 (DDY)	<i>nmd2::his3/NMD2 exo1::LEU2/EXO1 rad24::TRP1/RAD24 cdc13::HPHMX/CDC13</i>	Figure 33
567 (DDY)	<i>nmd2::his3/NMD2 exo1::LEU2/EXO1 rad24::TRP1/RAD24 cdc13::HPHMX/CDC13</i>	Figure 34
568 (DDY)	<i>nmd2::his3/NMD2 exo1::LEU2/EXO1 rad24::TRP1/RAD24 cdc13::HPHMX/CDC13</i>	Figure 34
567 (DDY)	<i>nmd2::his3/NMD2 exo1::LEU2/EXO1 rad24::TRP1/RAD24 cdc13::HPHMX/CDC13</i>	Figure 35
568 (DDY)	<i>nmd2::his3/NMD2 exo1::LEU2/EXO1 rad24::TRP1/RAD24 cdc13::HPHMX/CDC13</i>	Figure 35

## Appendix B. Yeast strains by strain number

Strain numbers are prefixed DLY unless otherwise stated

Strain number	Genotype (all W303 <i>RAD5</i> <sup>+</sup> unless otherwise stated)	Related figure	Origin
225 (DDY)	wt/wt	Figure 31	
567 (DDY)	<i>nmd2::his3/NMD2 exo1::LEU2/EXO1</i> <i>rad24::TRP1/RAD24</i> <i>cdc13::HPHMX/CDC13</i>	Figure 31, Figure 32, Figure 33, Figure 34, Figure 35, Table 2	
568 (DDY)	<i>nmd2::his3/NMD2 exo1::LEU2/EXO1</i> <i>rad24::TRP1/RAD24</i> <i>cdc13::HPHMX/CDC13</i>	Figure 31, Figure 32, Figure 33, Figure 34, Figure 35, Table 2	
810 (DDY)	<i>yku70::LEU2/yku70::HIS3</i>	Figure 31	This work
812 (DDY)	<i>rif1::URA3/rif1::NATMX</i>	Figure 31	This work
835 (DDY)	<i>nmd2::his3/NMD2 exo1::LEU2/EXO1</i> <i>rad24::TRP1/RAD24</i> <i>cdc13::HPHMX/CDC13 rif1::NATMX/RIF1</i>	Figure 21	This work
836 (DDY)	<i>nmd2::his3/NMD2 exo1::LEU2/EXO1</i> <i>rad24::TRP1/RAD24</i> <i>cdc13::HPHMX/CDC13 rif1::NATMX/RIF1</i>	Figure 21	This work
1098	<i>MATa rfa1::MYC18::RFA1 rad5-535</i>	Figure 14	
1272	<i>MATa exo1::LEU2</i>	Figure 9	
1273	<i>MATalpha exo1::LEU2</i>	Figure 9, Figure 22, Figure 23, Figure 24	
1628	<i>MATalpha tlc1::HIS3 pTLC1::URA3</i> (streaked until plasmid lost)	Figure 7	
2146	<i>MATa tlc1::HIS3</i>	Figure 8	
2148	<i>MATalpha tlc1::HIS3 exo1::LEU2</i>	Figure 8	
3001	<i>MATalpha ade2-1 trp1-1 can1-100 leu2-3,112 his3-11,15 ura3 GAL+ psi+ ssd1-d2 RAD5</i> (W303 wild-type)	Figure 9	
3485	<i>MATa rad51::KANMX</i>	Figure 27	
4451	<i>MATalpha rif1::URA3</i>	Figure 32	

4528	<i>MATa nmd2::HIS3</i>	Figure 12, Figure 22, Figure 23, Figure 24, Figure 32	
4765	<i>MATa nmd2::HIS3</i>	Figure 9	
4766	<i>MATalpha nmd2::HIS3</i>	Figure 9	
4872	<i>MATa pif1::NATMX</i>	Figure 9	
4873	<i>MATalpha pif1::NATMX</i>	Figure 9	
5759	<i>MATa STN1-13MYC::TRP1 nmd2::HIS3</i>	Figure 10	
5761	<i>MATa STN1-13MYC::TRP1</i>	Figure 10, Figure 14	
5872	<i>MATa rad52::TRP1</i>	Figure 27, Figure 29	
5915	<i>MATa pif1::NATMX exo1::LEU2</i>	Figure 9	
5916	<i>MATalpha pif1::NATMX exo1::LEU2</i>	Figure 9	
7273	<i>MATalpha CDC13-13MYC::HIS3</i>	Figure 10	
7274	<i>MATalpha CDC13-13MYC::HIS3 nmd2::URA3</i>	Figure 10	
8100	<i>MATa TEN1-13MYC::KANMX nmd2::URA3</i>	Figure 10	
8101	<i>MATa TEN1-13MYC::KANMX</i>	Figure 10, Figure 14	
8167	<i>MATalpha nmd2::HIS3 exo1::LEU2 cdc13::HPHMX passage 1</i>	Figure 7, Figure 22, Figure 23, Figure 24, Figure 27, Figure 29, Figure 30, Figure 31	
8168	<i>nmd2::HIS3 exo1::LEU2 cdc13::HPHMX passage 1</i>	Figure 7,	
8169	<i>nmd2::HIS3 exo1::LEU2 rad24::TRP1 cdc13::HPHMX passage 1</i>	Figure 7	
8170	<i>nmd2::HIS3 exo1::LEU2 rad24::TRP1 cdc13::HPHMX passage 1</i>	Figure 7	
8171	<i>nmd2::HIS3 rad24::TRP1 cdc13::HPHMX passage 1</i>	Figure 7	
8172	<i>nmd2::HIS3 rad24::TRP1 cdc13::HPHMX passage 1</i>	Figure 7	
8193	<i>nmd2::HIS3 rad24::TRP1</i>	Figure 7	
8195	<i>nmd2::HIS3 exo1::LEU2</i>	Figure 7	
8196	<i>nmd2::HIS3 exo1::LEU2</i>	Figure 22, Figure 23, Figure 24	
8197	<i>nmd2::HIS3 exo1::LEU2 rad24::TRP1</i>	Figure 7	
8198	<i>nmd2::HIS3 exo1::LEU2 rad24::TRP1</i>	Figure 12	
8199	<i>nmd2::HIS3 exo1::LEU2 rad24::TRP1 cdc13::HPHMX passage 9</i>	Figure 7	
8200	<i>nmd2::HIS3 exo1::LEU2 rad24::TRP1 cdc13::HPHMX passage 9</i>	Figure 7	



8201	<i>nmd2::HIS3 rad24::TRP1 cdc13::HPHMX</i> passage 9	Figure 7	
8202	<i>nmd2::HIS3 rad24::TRP1 cdc13::HPHMX</i> passage 9	Figure 7	
8203	<i>nmd2::HIS3 exo1::LEU2 cdc13::HPHMX</i> passage 9	Figure 7	
8204	<i>nmd2::HIS3 exo1::LEU2 cdc13::HPHMX</i> passage 9	Figure 7	
8298	<i>MATalpha RFA3-3HA::KANMX</i>	Figure 14	This work
8429	<i>MATalpha STN1-13MYC::KANMX</i> <i>nmd2::HIS3 exo1::LEU2 rad24::TRP1</i> <i>cdc13::HPHMX</i>	Figure 14	This work
8431	<i>MATa TEN1-13MYC::KANMX nmd2::HIS3</i> <i>exo1::LEU2 rad24::TRP1 cdc13::HPHMX</i>	Figure 14	This work
8432	<i>MATa STN1-13MYC::KANMX nmd2::HIS3</i> <i>exo1::LEU2 rad24::TRP1</i>	Figure 11, Figure 14	This work
8434	<i>MATalpha TEN1-13MYC::KANMX</i> <i>nmd2::HIS3 exo1::LEU2 rad24::TRP1</i>	Figure 11, Figure 14	This work
8455	<i>MATa nmd2::HIS3 rad24::TRP1</i> <i>cdc13::HPHMX</i>	Figure 30, Figure 31	This work
8457	<i>MATa nmd2::HIS3 exo1::LEU2</i> <i>cdc13::HPHMX</i>	Figure 20, Figure 22, Figure 23, Figure 24	This work
8460	<i>MATa ade2-1 trp1-1 can1-100 leu2-3,112</i> <i>his3-11,15 ura3 GAL+ psi+ ssd1-d2 RAD5</i> (W303 wild-type)	Figure 7, Figure 8, Figure 9, Figure 12, Figure 22, Figure 23, Figure 24	
8461	<i>MATa nmd2::HIS3 exo1::LEU2 rad24::TRP1</i> <i>cdc13::HPHMX</i>	Figure 12, Figure 14	This work
8462	<i>MATa tlc1::NATMX</i> passage 1	Figure 8	This work
8465	<i>MATa tlc1::NATMX</i> passage 9	Figure 8	This work
8467	<i>MATa tlc1::NATMX nmd2::HIS3</i> <i>rad24::TRP1 cdc13::HPHMX</i> passage 2	Figure 8	This work
8468	<i>MATa tlc1::NATMX nmd2::HIS3 exo1::LEU2</i> <i>cdc13::HPHMX</i> passage 2	Figure 8	This work
8472	<i>MATa tlc1::NATMX</i> passage 3	Figure 8	This work
8473	<i>MATa tlc1::NATMX nmd2::HIS3</i> <i>rad24::TRP1 cdc13::HPHMX</i>	Figure 8	This work
8474	<i>MATa tlc1::NATMX nmd2::HIS3 exo1::LEU2</i> <i>cdc13::hph</i>	Figure 8	This work
8475	<i>MATa tlc1::NATMX nmd2::HIS3 exo1::LEU2</i> <i>rad24::TRP1 cdc13::hph</i>	Figure 8	This work

8509	<i>MATa tlc1::NATMX</i>	Figure 8	This work
8510	<i>MATa tlc1::NATMX nmd2::HIS3 rad24::TRP1 cdc13::HPHMX</i>	Figure 8	This work
8511	<i>MATa tlc1::NATMX nmd2::HIS3 exo1::LEU2 cdc13::HPHMX</i>	Figure 8	This work
8512	<i>MATalpha tlc1::NATMX nmd2::HIS3 rad24::TRP1 exo1::LEU2 cdc13::hph</i>	Figure 8	This work
8601	<i>MATa tlc1::NATMX nmd2::HIS3 rad24::TRP1 cdc13::HPHMX passage 9</i>	Figure 8	This work
8602	<i>MATa tlc1::NATMX nmd2::HIS3 exo1::LEU2 cdc13::HPHMX passage 9</i>	Figure 8	This work
8603	<i>MATalpha tlc1::NATMX nmd2::HIS3 rad24::TRP1 exo1::LEU2 cdc13::HPHMX passage 9</i>	Figure 8	This work
8604	<i>MATalpha STN1-13MYC::KANMX nmd2::HIS3 exo1::LEU2 rad24::TRP1 cdc13::HPHMX</i>	Figure 11	This work
8605	<i>MATa TEN1::Myc::KANMX nmd2::HIS3 exo1::LEU2 rad24::TRP1 cdc13::hph</i>	Figure 11	This work
8766	<i>MATalpha stn1-13::HPHMX lyp1::NATMX can1Δ::STE2pr-Sp_his5 (S288C)</i>	Figure 13	
8989	<i>MATa cdc13-1 cdc15-2 int bar1 Ddc1-Myc-HIS3MX6 Mec3-3HA-KanMX</i>	Figure 14	
9101	<i>MATa rfa1-M2::KANMX (S288C)</i>	Figure 13	Newcastle University High Throughput Service
9102	<i>MATa rfa3-313::KANMX (S288C)</i>	Figure 13	Newcastle University High Throughput Service
9527	<i>MATalpha RFA3-3HA::KANMX STN1-13MYC::TRP1</i>	Figure 14	This work
9653	<i>MATalpha nmd2::HPHMX exo1::NATMX cdc13::LEU2 lyp1Δ can1Δ::STE2pr-Sp_his5 (S288C)</i>	Figure 17	This work
9697	<i>MATalpha rif1::NATMX</i>	Figure 20	David Shore
9699	<i>MATa rif1-RVxF-SILK</i>	Figure 22	David Shore
9714	<i>MATalpha rif1Δ1323-1916-13MYC::HIS3MX6</i>	Figure 24	David Shore
9718	<i>MATalpha nmd2::HPHMX exo1::NATMX lyp1::LEU2 can1-ste2_pr_his5 (S288C)</i>	Figure 17	This work
10209	<i>MATa dxo1::KANMX</i>	Figure 30, Figure 31	This work
10211	<i>MATa nmd2::HIS3 rif1-RVxF-SILK</i>	Figure 22	This work
10213	<i>MATalpha exo1::LEU2 rif1-RVxF-SILK</i>	Figure 22	This work

10215	<i>MATa nmd2::HIS3 exo1::LEU2 rif1-RVxF-SILK</i>	Figure 22	This work
10218	<i>MATa nmd2::HIS3 exo1::LEU2 cdc13::HPHMX rif1- RVxF-SILK</i>	Figure 22	This work
10219	<i>MATalpha nmd2::HIS3 exo1::LEU2 cdc13::HPHMX rif1- rif1- RVxF-SILK</i>	Figure 22	This work
10254	<i>MATalpha nmd2::URA3 exo1::LEU2 cdc13::HPHMX</i>	Figure 22	This work
10255	<i>MATa nmd2::URA3 exo1::LEU2 cdc13::HPHMX</i>	Figure 24, Figure 23	This work
10290	<i>MATalpha rif1Δ2-176-13MYC::HIS3MX6</i>	Figure 23	This work
10291	<i>MATalpha exo1::LEU2 rif1Δ1323-1916-13MYC::HIS3MX</i>	Figure 24	This work
10293	<i>MATa nmd2::URA3 rif1 rif1Δ1323-1916-13MYC::HIS3MX</i>	Figure 24	This work
10295	<i>MATalpha nmd2::URA3 exo1::LEU2 rif1Δ1323-1916-13MYC::HIS3MX</i>	Figure 24	This work
10297	<i>MATalpha nmd2::URA3 exo1::LEU2 cdc13::HPHMX rif1Δ1323-1916-13MYC::HIS3MX</i>	Figure 24	This work
10298	<i>MATa nmd2::URA3 exo1::LEU2 cdc13::HPHMX rif1Δ1323-1916-13MYC::HIS3MX</i>	Figure 24	This work
10757	<i>MATalpha nmd2::URA3 rif1Δ2-176-13MYC::HIS3MX6</i>	Figure 23	This work
10758	<i>MATa exo1::LEU2 rif1Δ2-176-13MYC::HIS3MX6</i>	Figure 23	This work
10760	<i>MATa nmd2::URA3 exo1::LEU2 rif1Δ2-176-13MYC::HIS3MX6</i>	Figure 23	This work
10795	<i>MATalpha nmd2::URA3 exo1::LEU2 cdc13::HPHMX LEU2 rif1Δ2-176-13MYC::HIS3MX6</i>	Figure 23	This work
10796	<i>MATalpha nmd2::URA3 exo1::LEU2 cdc13::HPHMX LEU2 rif1Δ2-176-13MYC::HIS3MX6</i>	Figure 23	This work
10813	<i>MATalpha nmd2::HIS3 exo1::LEU2 cdc13::HPHMX rif1::NATMX pRIF1-URA3 (pDL1714)</i>	Figure 25	This work



## Appendix C. Plasmids

Plasmid number	Construction	Related figure/ Notes	Reference
pDL508	pFA6a-13Myc-kanMX6	For Myc tagging	(Longtine <i>et al.</i> , 1998)
pDL987	pBluescriptII SK2 carrying 1.0-kb <i>XhoI</i> fragment of a yeast chromosomal end, which contains 120 base pairs of telomere repeats and part of the Y9 subtelomeric repeat	Figure 7; Figure 8	(Tsubouchi and Ogawa, 2000)
pDL1535	pAG32 <i>HPHMX4</i>	For gene deletions	(Goldstein and McCusker, 1999)
pDL1539	pRS314 <i>TRP1</i>	For cloning <i>rif1</i> truncations into/ amplifying <i>TRP1</i>	
pDL1599	pAG25 <i>NATMX4</i>	For gene deletions	(Goldstein and McCusker, 1999)
pDL1714	p <i>RIF1 URA3</i> (yeast centromeric)	Figure 25	Anne Donaldson (Hiraga <i>et al.</i> , 2014)
pDL1705	pRS316 <i>TRP1</i> swapped for <i>URA3</i>	Figure 25	This work
pDL1706	<i>rif1</i> $\Delta$ 114-225 <i>TRP1</i> (plasmid from A.D. was <i>URA3</i> , this was swapped for <i>TRP1</i> )	Figure 25	This work; Anne Donaldson (Hiraga <i>et al.</i> , 2014)
pDL1707	<i>rif1</i> $\Delta$ 997-1916 <i>TRP1</i> (plasmid from A.D. was <i>URA3</i> , this was swapped for <i>TRP1</i> )	Figure 25	This work; Anne Donaldson (Hiraga <i>et al.</i> , 2014)
pDL1708	<i>rif1</i> $\Delta$ 1790-1916 <i>TRP1</i> (plasmid from A.D. was <i>URA3</i> , this was swapped for <i>TRP1</i> )	Figure 25	This work; Anne Donaldson (Hiraga <i>et al.</i> , 2014)

pDL1709	<i>rif1</i> Δ321-455 <i>TRP1</i> (plasmid from A.D. was <i>URA3</i> , this was swapped for <i>TRP1</i> )	Figure 25	This work; Anne Donaldson (Hiraga <i>et al.</i> , 2014)
pDL1710	<i>rif1</i> Δ321-836 <i>TRP1</i> (plasmid from A.D. was <i>URA3</i> , this was swapped for <i>TRP1</i> )	Figure 25	This work; Anne Donaldson (Hiraga <i>et al.</i> , 2014)
pDL1711	<i>rif1</i> - <i>PP1</i> (RvXF1-2 and SILK1-2 motifs mutated) <i>TRP1</i> (plasmid from A.D. was <i>URA3</i> , this was swapped for <i>TRP1</i> )	Figure 25	This work; Anne Donaldson (Hiraga <i>et al.</i> , 2014)
pDL1712	<i>rif1</i> Δ213-836 <i>TRP1</i> (plasmid from A.D. was <i>URA3</i> , this was swapped for <i>TRP1</i> )	Figure 25	This work; Anne Donaldson (Hiraga <i>et al.</i> , 2014)
pDL1738	<i>RIF1</i> <i>TRP1</i> ( <i>RIF1</i> from A. D. <i>URA3</i> plasmid cloned into pDL1539)	Figure 25	This work; Anne Donaldson (Hiraga <i>et al.</i> , 2014)
pDL1739	<i>rif1</i> Δ1417-1492 <i>TRP1</i> ( <i>rif1</i> Δ1417-1492 from A. D. <i>URA3</i> plasmid cloned into pDL1539)	Figure 25	This work; Anne Donaldson (Hiraga <i>et al.</i> , 2014)
pDL1740	<i>rif1</i> Δ266-455 <i>TRP1</i> ( <i>rif1</i> Δ266-455 from A. D. <i>URA3</i> plasmid cloned into pDL1539)	Figure 25	This work; Anne Donaldson (Hiraga <i>et al.</i> , 2014)

## Appendix D. PCR primers

Ordered by gene target.

Ref. No.	Primer Sequence	Target	Usage and related figures
M1172	CAGACCGAACTCGGTGATT T	<i>BUD6</i>	qRT-PCR Figure 9
M1173	TTTTAGCGGGCTGAGACCT A	<i>BUD6</i>	qRT-PCR Figure 9
M2245	CGTATGCTAAAGTATATATT ACTTCACTCCATT	chrVI-R	ChIP/DNA-IP Figure 10, Figure 11, Figure 12
M2246	TCCGAACTCAGTTACTATTG ATGGAA	chrVI-R	ChIP/DNA-IP Figure 10, Figure 11, Figure 12
M1367	AATAACGAATTGAGCTATG ACACCAA	<i>PAC2</i>	ChIP/DNA-IP Figure 10, Figure 11, Figure 12
M1368	AGCTTACTCATATCGATTTT ATACGACTT	<i>PAC2</i>	ChIP/DNA-IP Figure 10, Figure 11, Figure 12
M3487	AAGTCAACAGAAGGCAGGT G	<i>RIF1</i>	For amplification of <i>rif1::NATMX</i> from DLY9697  Figure 21
M2822	GGTATGACACAAGAGGCTA A	<i>RIF1</i>	For amplification of <i>rif1::NATMX</i> from DLY9697  Figure 21
M1003	AGAGATGCGCCGTTATTGA CGATGCGAGTTTTCTAACA AAGAATTCGAGCTCGTTTA AAC	<i>STN1</i>	For C-terminal Myc- tagging of <i>STN1</i> Figure 10, Figure 11, Figure 14
M1734	TCGAGCAACTGCAAGAAGA A	<i>STN1</i>	qRT-PCR Figure 9

M1735	CGAAATGACAAGGAATGCA C	<i>STN1</i>	qRT-PCR Figure 9
M2752	TGGAATATTATTACATTTGG AATACGCAGCAGCATATTC ACGGATCCCCGGGTTAATT AA	<i>STN1</i>	For C-terminal Myc- tagging of <i>STN1</i> Figure 10, Figure 11, Figure 14
M1794	ATACACCAAAGTCCGCCAA T	<i>TEN1</i>	qRT-PCR Figure 9
M1795	CACCAAGTGGTGATTTGAC A	<i>TEN1</i>	qRT-PCR Figure 9
M2355	ATCACCACCTTGGTGAGAAG TTTCTGAACATCTCTAACTC CCGGATCCCCGGGTTAATT AA	<i>TEN1</i>	For C-terminal Myc- tagging of <i>TEN1</i> Figure 10, Figure 11, Figure 14
M2356	AAAGGTATTATATAATCTCA GTATATGCCAACGTCTGA CGAATTCGAGCTCGTTTAA AC	<i>TEN1</i>	For C-terminal Myc- tagging of <i>TEN1</i> Figure 10, Figure 11, Figure 14
M1803	CCAACGTCAACGCACC	<i>TLC1</i>	To confirm integration of <i>NATMX</i> cassette Figure 8
M1807	CGTGAGTCTGTGGAATCC	<i>TLC1</i>	To confirm integration of <i>NATMX</i> cassette Figure 8
M2013	CAATTAAGACCTTCTTTG TAGCTTTTAGTGTGATTTT CTGGTTTGAGCACATACGA TTTAGGTGACAC	<i>TLC1</i>	To integrate <i>NATMX</i> cassette at <i>TLC1</i> locus Figure 8
M2014	TGTATATTGTATATTCTAAA AAGAAGAAGCCATTTGGTG GGCTTTATTAATACGACTC ACTATAGGGAG	<i>TLC1</i>	To integrate <i>NATMX</i> cassette at <i>TLC1</i> locus Figure 8



## References

Addinall, S. G., Holstein, E. M., Lawless, C., Yu, M., Chapman, K., Banks, A. P., Ngo, H. P., Maringele, L., Taschuk, M., Young, A., Ciesiolka, A., Lister, A. L., Wipat, A., Wilkinson, D. J. and Lydall, D. (2011) 'Quantitative fitness analysis shows that NMD proteins and many other protein complexes suppress or enhance distinct telomere cap defects', *PLoS Genet*, 7(4), p. e1001362.

Anbalagan, S., Bonetti, D., Lucchini, G. and Longhese, M. P. (2011) 'Rif1 supports the function of the CST complex in yeast telomere capping', *PLoS Genet*, 7(3), p. e1002024.

Anderson, B. H., Kasher, P. R., Mayer, J., Szykiewicz, M., Jenkinson, E. M., Bhaskar, S. S., Urquhart, J. E., Daly, S. B., Dickerson, J. E., O'Sullivan, J., Leibundgut, E. O., Muter, J., Abdel-Salem, G. M., Babul-Hirji, R., Baxter, P., Berger, A., Bonafe, L., Brunstom-Hernandez, J. E., Buckard, J. A., Chitayat, D., Chong, W. K., Cordelli, D. M., Ferreira, P., Fluss, J., Forrest, E. H., Franzoni, E., Garone, C., Hammans, S. R., Houge, G., Hughes, I., Jacquemont, S., Jeannet, P. Y., Jefferson, R. J., Kumar, R., Kutschke, G., Lundberg, S., Lourenco, C. M., Mehta, R., Naidu, S., Nischal, K. K., Nunes, L., Ounap, K., Philippart, M., Prabhakar, P., Risen, S. R., Schiffmann, R., Soh, C., Stephenson, J. B., Stewart, H., Stone, J., Tolmie, J. L., van der Knaap, M. S., Vieira, J. P., Vilain, C. N., Wakeling, E. L., Wermenbol, V., Whitney, A., Lovell, S. C., Meyer, S., Livingston, J. H., Baerlocher, G. M., Black, G. C., Rice, G. I. and Crow, Y. J. (2012) 'Mutations in CTC1, encoding conserved telomere maintenance component 1, cause Coats plus', *Nat Genet*, 44(3), pp. 338-42.

Andrade, M. A., Petosa, C., O'Donoghue, S. I., Muller, C. W. and Bork, P. (2001) 'Comparison of ARM and HEAT protein repeats', *J Mol Biol*, 309(1), pp. 1-18.

Arora, R., Lee, Y., Wischnewski, H., Brun, C. M., Schwarz, T. and Azzalin, C. M. (2014) 'RNaseH1 regulates TERRA-telomeric DNA hybrids and telomere maintenance in ALT tumour cells', *Nat Commun*, 5, p. 5220.

Audry, J., Maestroni, L., Delagoutte, E., Gauthier, T., Nakamura, T. M., Gachet, Y., Saintome, C., Geli, V. and Coulon, S. (2015) 'RPA prevents G-rich structure formation at lagging-strand telomeres to allow maintenance of chromosome ends', *EMBO J*, 34(14), pp. 1942-58.

Aylon, Y. and Kupiec, M. (2004) 'New insights into the mechanism of homologous recombination in yeast', *Mutat Res*, 566(3), pp. 231-48.

Azzalin, C. M. and Linger, J. (2006) 'The human RNA surveillance factor UPF1 is required for S phase progression and genome stability', *Curr Biol*, 16(4), pp. 433-9

- Azzalin, C. M., Reichenbach, P., Khoraiuli, L., Giulotto, E. and Lingner, J. (2007) 'Telomeric repeat containing RNA and RNA surveillance factors at mammalian chromosome ends', *Science*, 318(5851), pp. 798-801.
- Balk, B., Dees, M., Bender, K. and Luke, B. (2014) 'The differential processing of telomeres in response to increased telomeric transcription and RNA-DNA hybrid accumulation', *RNA Biol*, 11(2), pp. 95-100.
- Balk, B., Maicher, A., Dees, M., Klermund, J., Luke-Glaser, S., Bender, K. and Luke, B. (2013) 'Telomeric RNA-DNA hybrids affect telomere-length dynamics and senescence', *Nat Struct Mol Biol*, 20(10), pp. 1199-205.
- Belanger, K. D., Griffith, A. L., Baker, H. L., Hansen, J. N., Kovacs, L. A., Seconi, J. S. and Strine, A. C. (2011) 'The karyopherin Kap95 and the C-termini of Rfa1, Rfa2, and Rfa3 are necessary for efficient nuclear import of functional RPA complex proteins in *Saccharomyces cerevisiae*', *DNA Cell Biol*, 30(9), pp. 641-51.
- Benschop, J. J., Brabers, N., van Leenen, D., Bakker, L. V., van Deutekom, H. W., van Berkum, N. L., Apweiler, E., Lijnzaad, P., Holstege, F. C. and Kemmeren, P. (2010) 'A consensus of core protein complex compositions for *Saccharomyces cerevisiae*', *Mol Cell*, 38(6), pp. 916-28.
- Bisserbe, A., Tertian, G., Buffet, C., Turhan, A., Lambotte, O., Nasser, G., Alvin, P., Tardieu, M., Riant, F., Bergametti, F., Tournier-Lasserre, E. and Denier, C. (2015) 'Cerebro-retinal microangiopathy with calcifications and cysts due to recessive mutations in the CTC1 gene', *Rev Neurol (Paris)*, 171(5), pp. 445-9.
- Blackburn, E. H. (2000) 'Telomere states and cell fates', *Nature*, 408(6808), pp. 53-6.
- Blankley, R. T. and Lydall, D. (2004) 'A domain of Rad9 specifically required for activation of Chk1 in budding yeast', *J Cell Sci*, 117(Pt 4), pp. 601-8.
- Blasco, M. A. (2005) 'Telomeres and human disease: ageing, cancer and beyond', *Nat Rev Genet*, 6(8), pp. 611-22.
- Boccardi, V., Razdan, N., Kaplunov, J., Mundra, J. J., Kimura, M., Aviv, A. and Herbig, U. (2015) 'Stn1 is critical for telomere maintenance and long-term viability of somatic human cells', *Aging Cell*, 14(3), pp. 372-81.
- Bonetti, D., Clerici, M., Anbalagan, S., Martina, M., Lucchini, G. and Longhese, M. P. (2010) 'Shelterin-like proteins and Yku inhibit nucleolytic processing of *Saccharomyces cerevisiae* telomeres', *PLoS Genet*, 6(5), p. e1000966.
- Boulton, S. J. and Jackson, S. P. (1996) 'Identification of a *Saccharomyces cerevisiae* Ku80 homologue: Roles in DNA double strand break rejoining and in telomeric maintenance', *Nucleic Acids Res*, 24(23), pp. 4639-48.
- Bryan, C., Rice, C., Harkisheimer, M., Schultz, D. C. and Skordalakes, E. (2013) 'Structure of the human telomeric Stn1-Ten1 capping complex', *PLoS ONE*, 8(6), p. e66756.

- Bryan, T. M., Englezou, A., Gupta, J., Bacchetti, S. and Reddel, R. R. (1995) 'Telomere elongation in immortal human cells without detectable telomerase activity', *EMBO J*, 14(17), pp. 4240-8.
- Burnett-Hartman, A. N., Fitzpatrick, A. L., Kronmal, R. A., Psaty, B. M., Jenny, N. S., Bis, J. C., Tracy, R. P., Kimura, M. and Aviv, A. (2012) 'Telomere-associated polymorphisms correlate with cardiovascular disease mortality in Caucasian women: the Cardiovascular Health Study', *Mech Ageing Dev*, 133(5), pp. 275-81.
- Casteel, D. E., Zhuang, S., Zeng, Y., Perrino, F. W., Boss, G. R., Goulian, M. and Pilz, R. B. (2009) 'A DNA polymerase-alpha primase cofactor with homology to replication protein A-32 regulates DNA replication in mammalian cells', *J Biol Chem*, 284(9), pp. 5807-18.
- Chan, C. S. M. and Tye, B.-K. (1983) 'Organization of DNA sequences and replication origins at yeast telomeres', *Cell*, 33(2), pp. 563-73.
- Chan, Y. A., Aristizabal, M. J., Lu, P. Y., Luo, Z., Hamza, A., Kobor, M. S., Stirling, P. C. and Hieter, P. (2014) 'Genome-wide profiling of yeast DNA:RNA hybrid prone sites with DRIP-chip', *PLoS Genet*, 10(4), p. e1004288.
- Chandra, A., Hughes, T. R., Nugent, C. I. and Lundblad, V. (2001) 'Cdc13 both positively and negatively regulates telomere replication', *Genes Dev*, 15(4), pp. 404-14.
- Chapman, J. R., Barral, P., Vannier, J. B., Borel, V., Steger, M., Tomas-Loba, A., Sartori, A. A., Adams, I. R., Batista, F. D. and Boulton, S. J. (2013) 'RIF1 Is Essential for 53BP1-Dependent Nonhomologous End Joining and Suppression of DNA Double-Strand Break Resection', *Mol Cell*, 49(5), pp. 858-71.
- Chen, L. Y., Majerska, J. and Lingner, J. (2013) 'Molecular basis of telomere syndrome caused by CTC1 mutations', *Genes Dev*, 27(19), pp. 2099-108.
- Chen, L. Y., Redon, S. and Lingner, J. (2012) 'The human CST complex is a terminator of telomerase activity', *Nature*, 488(7412), pp. 540-4.
- Chen, Q., Ijima, A. and Greider, C. W. (2001) 'Two survivor pathways that allow growth in the absence of telomerase are generated by distinct telomere recombination events', *Mol Cell Biol*, 21(5), pp. 1819-27.
- Churikov, D., Wei, C. and Price, C. M. (2006) 'Vertebrate POT1 restricts G-overhang length and prevents activation of a telomeric DNA damage checkpoint but is dispensable for overhang protection', *Mol Cell Biol*, 26(18), pp. 6971-82.
- Codd, V., Nelson, C. P., Albrecht, E., Mangino, M., Deelen, J., Buxton, J. L., Hottenga, J. J., Fischer, K., Esko, T., Surakka, I., Broer, L., Nyholt, D. R., Mateo Leach, I., Salo, P., Hagg, S., Matthews, M. K., Palmen, J., Norata, G. D., O'Reilly, P. F., Saleheen, D., Amin, N., Balmforth, A. J., Beekman, M., de Boer, R. A., Bohringer, S., Braund, P. S., Burton, P. R., Craen, A. J., Denniff, M., Dong, Y., Douroudis, K., Dubinina, E., Eriksson, J. G., Garlaschelli, K., Guo, D., Hartikainen, A. L., Henders, A. K., Houwing-Duistermaat, J. J., Kananen, L., Karssen, L. C., Kettunen, J., Klopp, N., Lagou, V., van Leeuwen, E. M., Madden, P. A., Magi, R., Magnusson, P. K., Mannisto, S., McCarthy, M. I.,

Medland, S. E., Mihailov, E., Montgomery, G. W., Oostra, B. A., Palotie, A., Peters, A., Pollard, H., Pouta, A., Prokopenko, I., Ripatti, S., Salomaa, V., Suchiman, H. E., Valdes, A. M., Verweij, N., Vinuela, A., Wang, X., Wichmann, H. E., Widen, E., Willemsen, G., Wright, M. J., Xia, K., Xiao, X., van Veldhuisen, D. J., Catapano, A. L., Tobin, M. D., Hall, A. S., Blakemore, A. I., van Gilst, W. H., Zhu, H., Consortium, C., Erdmann, J., Reilly, M. P., Kathiresan, S., Schunkert, H., Talmud, P. J., Pedersen, N. L., Perola, M., Ouwehand, W., Kaprio, J., Martin, N. G., van Duijn, C. M., Hovatta, I., Gieger, C., Metspalu, A., Boomsma, D. I., Jarvelin, M. R., Slagboom, P. E., Thompson, J. R., Spector, T. D., van der Harst, P. and Samani, N. J. (2013) 'Identification of seven loci affecting mean telomere length and their association with disease', *Nat Genet*, 45(4), pp. 422-7.

Collins, S. R., Miller, K. M., Maas, N. L., Roguev, A., Fillingham, J., Chu, C. S., Schuldiner, M., Gebbia, M., Recht, J., Shales, M., Ding, H., Xu, H., Han, J., Ingvarsdottir, K., Cheng, B., Andrews, B., Boone, C., Berger, S. L., Hieter, P., Zhang, Z., Brown, G. W., Ingles, C. J., Emili, A., Allis, C. D., Toczyski, D. P., Weissman, J. S., Greenblatt, J. F. and Krogan, N. J. (2007) 'Functional dissection of protein complexes involved in yeast chromosome biology using a genetic interaction map', *Nature*, 446(7137), pp. 806-10.

Conomos, D., Pickett, H. A. and Reddel, R. R. (2013) 'Alternative lengthening of telomeres: remodeling the telomere architecture', *Front Oncol*, 3, p. 27.

Culotti, J. and Hartwell, L. H. (1971) 'Genetic control of the cell division cycle in yeast. 3. Seven genes controlling nuclear division', *Exp Cell Res*, 67(2), pp. 389-401.

Cusanelli, E., Romero, C. A. and Chartrand, P. (2013) 'Telomeric noncoding RNA TERRA is induced by telomere shortening to nucleate telomerase molecules at short telomeres', *Mol Cell*, 51(6), pp. 780-91.

Dahlseid, J. N., Lew-Smith, J., Lelivelt, M. J., Enomoto, S., Ford, A., Desruisseaux, M., McClellan, M., Lue, N. F., Culbertson, M. R. and Berman, J. (2003) 'mRNAs encoding telomerase components and regulators are controlled by UPF genes in *Saccharomyces cerevisiae*', *Eukaryot Cell*, 2(1), pp. 134-42.

Derboven, E., Ekker, H., Kusenda, B., Bulankova, P. and Riha, K. (2014) 'Role of STN1 and DNA polymerase alpha in telomere stability and genome-wide replication in *Arabidopsis*', *PLoS Genet*, 10(10), p. e1004682.

Dewar, J. M. and Lydall, D. (2010) 'Pif1- and Exo1-dependent nucleases coordinate checkpoint activation following telomere uncapping', *EMBO J*, 29(23), pp. 4020-34.

Dewar, J. M. and Lydall, D. (2012a) 'Similarities and differences between "uncapped" telomeres and DNA double-strand breaks', *Chromosoma*, 121(2), pp. 117-30.

Dewar, J. M. and Lydall, D. (2012b) 'Simple, non-radioactive measurement of single-stranded DNA at telomeric, sub-telomeric, and genomic loci in budding yeast', *Methods Mol Biol*, 920, pp. 341-8.

- Dunham, M. A., Neumann, A. A., Fasching, C. L. and Reddel, R. R. (2000) 'Telomere maintenance by recombination in human cells', *Nat Genet*, 26(4), pp. 447-50.
- Enomoto, S., Glowczewski, L., Lew-Smith, J. and Berman, J. G. (2004) 'Telomere cap components influence the rate of senescence in telomerase-deficient yeast cells', *Mol Cell Biol*, 24(2), pp. 837-45.
- Faure, V., Coulon, S., Hardy, J. and Geli, V. (2010) 'Cdc13 and telomerase bind through different mechanisms at the lagging- and leading-strand telomeres', *Mol Cell*, 38(6), pp. 842-52.
- Feng, J., Funk, W. D., Wang, S. S., Weinrich, S. L., Avilion, A. A., Chiu, C. P., Adams, R. R., Chang, E., Allsopp, R. C., Yu, J. and et al. (1995) 'The RNA component of human telomerase', *Science*, 269(5228), pp. 1236-41.
- Flynn, R. L., Centore, R. C., O'Sullivan, R. J., Rai, R., Tse, A., Songyang, Z., Chang, S., Karlseder, J. and Zou, L. (2011) 'TERRA and hnRNPA1 orchestrate an RPA-to-POT1 switch on telomeric single-stranded DNA', *Nature*, 471(7339), pp. 532-6.
- Gallardo, F., Olivier, C., Dandjinou, A. T., Wellinger, R. J. and Chartrand, P. (2008) 'TLC1 RNA nucleo-cytoplasmic trafficking links telomerase biogenesis to its recruitment to telomeres', *EMBO J*, 27(5), pp. 748-57.
- Gao, H., Cervantes, R. B., Mandell, E. K., Otero, J. H. and Lundblad, V. (2007) 'RPA-like proteins mediate yeast telomere function', *Nat Struct Mol Biol*, 14(3), pp. 208-14.
- Garvik, B., Carson, M. and Hartwell, L. (1995) 'Single-stranded DNA arising at telomeres in cdc13 mutants may constitute a specific signal for the RAD9 checkpoint', *Mol Cell Biol*, 15(11), pp. 6128-38.
- Gasparyan, H. J., Xu, L., Petreaca, R. C., Rex, A. E., Small, V. Y., Bhogal, N. S., Julius, J. A., Warsi, T. H., Bachant, J., Aparicio, O. M. and Nugent, C. I. (2009) 'Yeast telomere capping protein Stn1 overrides DNA replication control through the S phase checkpoint', *Proc Natl Acad Sci USA*, 106(7), pp. 2206-11.
- Gelinas, A. D., Paschini, M., Reyes, F. E., Heroux, A., Batey, R. T., Lundblad, V. and Wuttke, D. S. (2009) 'Telomere capping proteins are structurally related to RPA with an additional telomere-specific domain', *Proc Natl Acad Sci U S A*, 106(46), pp. 19298-303.
- Giraud-Panis, M. J., Teixeira, M. T., Geli, V. and Gilson, E. (2010) 'CST meets shelterin to keep telomeres in check', *Mol Cell*, 39(5), pp. 665-76.
- Goldstein, A. L. and McCusker, J. H. (1999) 'Three new dominant drug resistance cassettes for gene disruption in *Saccharomyces cerevisiae*', *Yeast*, 15(14), pp. 1541-53.
- Grandin, N. and Charbonneau, M. (2007) 'Control of the yeast telomeric senescence survival pathways of recombination by the Mec1 and Mec3 DNA damage sensors and RPA', *Nucleic Acids Res*, 35(3), pp. 822-38

- Grandin, N., Damon, C. and Charbonneau, M. (2000) 'Cdc13 cooperates with the yeast Ku proteins and Stn1 to regulate telomerase recruitment', *Mol Cell Biol*, 20(22), pp. 8397-408.
- Grandin, N., Damon, C. and Charbonneau, M. (2001a) 'Cdc13 prevents telomere uncapping and Rad50-dependent homologous recombination', *EMBO J*, 20(21), pp. 6127-39.
- Grandin, N., Damon, C. and Charbonneau, M. (2001b) 'Ten1 functions in telomere end protection and length regulation in association with Stn1 and Cdc13', *EMBO J*, 20(5), pp. 1173-83.
- Grandin, N., Reed, S. I. and Charbonneau, M. (1997) 'Stn1, a new *Saccharomyces cerevisiae* protein, is implicated in telomere size regulation in association with Cdc13', *Genes Dev*, 11(4), pp. 512-27.
- Gravel, S., Larrivée, M., Labrecque, P. and Wellinger, R. J. (1998) 'Yeast Ku as a regulator of chromosomal DNA end structure', *Science*, 280(5364), pp. 741-4.
- Greider, C. W. and Blackburn, E. H. (1987) 'The telomere terminal transferase of tetrahymena is a ribonucleoprotein enzyme with two kinds of primer specificity', *Cell*, 51(6), pp. 887-98.
- Grobelny, J. V., Kulp-McEliece, M. and Broccoli, D. (2001) 'Effects of reconstitution of telomerase activity on telomere maintenance by the alternative lengthening of telomeres (ALT) pathway', *Hum Mol Genet*, 10(18), pp. 1953-61.
- Grossi, S., Puglisi, A., Dmitriev, P. V., Lopes, M. and Shore, D. (2004) 'Pol12, the B subunit of DNA polymerase alpha, functions in both telomere capping and length regulation', *Genes Dev*, 18(9), pp. 992-1006.
- Gu, P. and Chang, S. (2013) 'Functional characterization of human CTC1 mutations reveals novel mechanisms responsible for the pathogenesis of the telomere disease Coats plus', *Aging Cell*, 12(6), pp. 1100-9.
- Gu, P., Min, J. N., Wang, Y., Huang, C., Peng, T., Chai, W. and Chang, S. (2012) 'CTC1 deletion results in defective telomere replication, leading to catastrophic telomere loss and stem cell exhaustion', *EMBO J*, 31(10), pp. 2309-21.
- Guan, Q., Zheng, W., Tang, S., Liu, X., Zinkel, R. A., Tsui, K. W., Yandell, B. S. and Culbertson, M. R. (2006) 'Impact of nonsense-mediated mRNA decay on the global expression profile of budding yeast', *PLoS Genet*, 2(11), p. e203.
- Günes, C. and Rudolph, K. L. (2013) 'The Role of Telomeres in Stem Cells and Cancer', *Cell*, 152(3), pp. 390-3.
- Hardy, C. F., Sussel, L. and Shore, D. (1992) 'A RAP1-interacting protein involved in transcriptional silencing and telomere length regulation', *Genes Dev*, 6(5), pp. 801-14.
- Harley, C. B., Futcher, A. B. and Greider, C. W. (1990) 'Telomeres shorten during ageing of human fibroblasts', *Nature*, 345(6274), pp. 458-60.

- Hendrickx, A., Beullens, M., Ceulemans, H., Den Abt, T., Van Eynde, A., Nicolaescu, E., Lesage, B. and Bollen, M. (2009) 'Docking motif-guided mapping of the interactome of protein phosphatase-1', *Chem Biol*, 16(4), pp. 365-71.
- Hengeveld, R. C., de Boer, H. R., Schoonen, P. M., de Vries, E. G., Lens, S. M. and van Vugt, M. A. (2015) 'Rif1 Is Required for Resolution of Ultrafine DNA Bridges in Anaphase to Ensure Genomic Stability', *Dev Cell*, 34(4), pp. 466-74.
- Hiraga, S., Alvino, G. M., Chang, F., Lian, H. Y., Sridhar, A., Kubota, T., Brewer, B. J., Weinreich, M., Raghuraman, M. K. and Donaldson, A. D. (2014) 'Rif1 controls DNA replication by directing Protein Phosphatase 1 to reverse Cdc7-mediated phosphorylation of the MCM complex', *Genes Dev*, 28(4), pp. 372-83.
- Holstein, E. M. (2012) *Mechanisms for maintaining the telomere cap in eukaryotic cells*. PhD thesis. Newcastle University.
- Holstein, E. M., Clark, K. R. and Lydall, D. (2014) 'Interplay between nonsense-mediated mRNA decay and DNA damage response pathways reveals that Stn1 and Ten1 are the key CST telomere-cap components', *Cell Rep*, 7(4), pp. 1259-69.
- Hsu, C. L., Chen, Y. S., Tsai, S. Y., Tu, P. J., Wang, M. J. and Lin, J. J. (2004) 'Interaction of *Saccharomyces* Cdc13p with Pol1p, Imp4p, Sir4p and Zds2p is involved in telomere replication, telomere maintenance and cell growth control', *Nucleic Acids Res*, 32(2), pp. 511-21.
- Huang, P., Pryde, F. E., Lester, D., Maddison, R. L., Borts, R. H., Hickson, I. D. and Louis, E. J. (2001) 'SGS1 is required for telomere elongation in the absence of telomerase', *Curr Biol*, 11(2), pp. 125-9.
- Iftode, C., Daniely, Y. and Borowiec, J. A. (1999) 'Replication protein A (RPA): the eukaryotic SSB', *Crit Rev Biochem Mol Biol*, 34(3), pp. 141-80.
- Isken, O. and Maquat, L. E. (2008) 'The multiple lives of NMD factors: balancing roles in gene and genome regulation', *Nat Rev Genet*, 9(9), pp. 699-712.
- Jain, D. and Cooper, J. P. (2010) 'Telomeric strategies: means to an end', *Annu Rev Genet*, 44, pp. 243-69.
- Johansson, M. J., He, F., Spatrick, P., Li, C. and Jacobson, A. (2007) 'Association of yeast Upf1p with direct substrates of the NMD pathway', *Proc Natl Acad Sci USA*, 104(52), pp. 20872-7.
- Johnson, F. B., Marciniak, R. A., McVey, M., Stewart, S. A., Hahn, W. C. and Guarente, L. (2001) 'The *Saccharomyces cerevisiae* WRN homolog Sgs1p participates in telomere maintenance in cells lacking telomerase', *EMBO J*, 20(4), pp. 905-13.
- Joshu, C. E., Peskoe, S. B., Heaphy, C. M., Kenfield, S. A., Van Blarigan, E. L., Mucci, L. A., Giovannucci, E. L., Stampfer, M. J., Yoon, G., Lee, T. K., Hicks, J. L., De Marzo, A. M., Meeker, A. K. and Platz, E. A. (2015) 'Prediagnostic Obesity and Physical Inactivity Are Associated with Shorter Telomere Length in Prostate Stromal Cells', *Cancer Prev Res (Phila)*, 8(8), pp. 737-42.

- Kasbek, C., Wang, F. and Price, C. M. (2013) 'Human TEN1 Maintains Telomere Integrity and Functions in Genome-wide Replication Restart', *J Biol Chem*, 288(42), pp. 30139-50.
- Kim, N. W., Piatyszek, M. A., Prowse, K. R., Harley, C. B., West, M. D., Ho, P. L. C., Coviello, G. M., Wright, W. E., Weinrich, S. L. and Shay, J. W. (1994) 'Specific association of human telomerase activity with immortal cells and cancer', *Science*, 266(5193), pp. 2011-5.
- Krejci, L. and Sung, P. (2002) 'RPA Not that Different from SSB', *Structure*, 10(5), pp. 601-2.
- Kumar, R. and Cheek, C. F. (2014) 'RIF1: a novel regulatory factor for DNA replication and DNA damage response signaling', *DNA Repair (Amst)*, 15, pp. 54-9.
- Labib, K. (2010) 'How do Cdc7 and cyclin-dependent kinases trigger the initiation of chromosome replication in eukaryotic cells?', *Genes Dev*, 24(12), pp. 1208-19.
- Lapham, K., Kvale, M. N., Lin, J., Connell, S., Croen, L. A., Dispensa, B. P., Fang, L., Hesselton, S., Hoffmann, T. J., Iribarren, C., Jorgenson, E., Kushi, L. H., Ludwig, D., Matsuguchi, T., McGuire, W. B., Miles, S., Quesenberry, C. P., Jr., Rowell, S., Sadler, M., Sakoda, L. C., Smethurst, D., Somkin, C. P., Van Den Eeden, S. K., Walter, L., Whitmer, R. A., Kwok, P. Y., Risch, N., Schaefer, C. and Blackburn, E. H. (2015) 'Automated Assay of Telomere Length Measurement and Informatics for 100,000 Subjects in the Genetic Epidemiology Research on Adult Health and Aging (GERA) Cohort', *Genetics*, 200(4), pp. 1061-72.
- Larrivé, M., LeBel, C. and Wellinger, R. J. (2004) 'The generation of proper constitutive G-tails on yeast telomeres is dependent on the MRX complex', *Genes Dev*, 18(12), pp. 1391-6.
- Larrivé, M. and Wellinger, R. J. (2006) 'Telomerase- and capping-independent yeast survivors with alternate telomere states', *Nat Cell Biol*, 8(7), pp. 741-7.
- Lawless, C., Wilkinson, D. J., Young, A., Addinall, S. G. and Lydall, D. A. (2010) 'Colonyzer: automated quantification of micro-organism growth characteristics on solid agar', *BMC Bioinformatics*, 11, p. 287.
- Leehy, K. A., Lee, J. R., Song, X., Renfrew, K. B. and Shippen, D. E. (2013) 'MERISTEM DISORGANIZATION1 Encodes TEN1, an Essential Telomere Protein That Modulates Telomerase Processivity in Arabidopsis', *Plant Cell*, 25(4), pp. 1343-54.
- Levy, D., Neuhausen, S. L., Hunt, S. C., Kimura, M., Hwang, S. J., Chen, W., Bis, J. C., Fitzpatrick, A. L., Smith, E., Johnson, A. D., Gardner, J. P., Srinivasan, S. R., Schork, N., Rotter, J. I., Herbig, U., Psaty, B. M., Sastrasinh, M., Murray, S. S., Vasan, R. S., Province, M. A., Glazer, N. L., Lu, X., Cao, X., Kronmal, R., Mangino, M., Soranzo, N., Spector, T. D., Berenson, G. S. and Aviv, A. (2010) 'Genome-wide association identifies OBFC1 as a locus involved in human leukocyte telomere biology', *PLoS Genet*, 10(7), pp. 9293-8.



- Levy, D. L. and Blackburn, E. H. (2004) 'Counting of Rif1p and Rif2p on *Saccharomyces cerevisiae* telomeres regulates telomere length', *Mol Cell Biol*, 24(24), pp. 10857-67.
- Lewis, K. A., Pfaff, D. A., Earley, J. N., Altschuler, S. E. and Wuttke, D. S. (2014) 'The tenacious recognition of yeast telomere sequence by Cdc13 is fully exerted by a single OB-fold domain', *Nucleic Acids Res*, 42(1), pp. 475-84.
- Li, B. and de Lange, T. (2003) 'Rap1 affects the length and heterogeneity of human telomeres', *Mol Biol Cell*, 14(12), pp. 5060-8.
- Li, X. and Heyer, W. D. (2008) 'Homologous recombination in DNA repair and DNA damage tolerance', *Cell Res*, 18(1), pp. 99-113.
- Lian, H. Y., Robertson, E. D., Hiraga, S., Alvino, G. M., Collingwood, D., McCune, H. J., Sridhar, A., Brewer, B. J., Raghuraman, M. K. and Donaldson, A. D. (2011) 'The effect of Ku on telomere replication time is mediated by telomere length but is independent of histone tail acetylation', *Mol Biol Cell*, 22(10), pp. 1753-65.
- Lin, J. J. and Zakian, V. A. (1996) 'The *Saccharomyces* CDC13 protein is a single-strand TG1-3 telomeric DNA-binding protein in vitro that affects telomere behavior in vivo', *Proc Natl Acad Sci U S A*, 93(24), pp. 13760-5.
- Lingner, J., Cech, T. R., Hughes, T. R. and Lundblad, V. (1997a) 'Three Ever Shorter Telomere (EST) genes are dispensable for in vitro yeast telomerase activity', *Proc Natl Acad Sci U S A*, 94(21), pp. 11190-5.
- Lingner, J., Hughes, T. R., Shevchenko, A., Mann, M., Lundblad, V. and Cech, T. R. (1997b) 'Reverse transcriptase motifs in the catalytic subunit of telomerase', *Science*, 276(5312), pp. 561-7.
- Longtine, M. S., McKenzie, A., 3rd, Demarini, D. J., Shah, N. G., Wach, A., Brachat, A., Philippsen, P. and Pringle, J. R. (1998) 'Additional modules for versatile and economical PCR-based gene deletion and modification in *Saccharomyces cerevisiae*', *Yeast*, 14(10), pp. 953-61.
- Lopez, V., Barinova, N., Onishi, M., Pobiega, S., Pringle, J. R., Dubrana, K. and Marcand, S. (2015) 'Cytokinesis breaks dicentric chromosomes preferentially at pericentromeric regions and telomere fusions', *Genes Dev*, 29(3), pp. 322-36.
- Luciano, P., Coulon, S., Faure, V., Corda, Y., Bos, J., Brill, S. J., Gilson, E., Simon, M.-N. and Geli, V. (2012) 'RPA facilitates telomerase activity at chromosome ends in budding and fission yeasts', *EMBO J*, 31(8), pp. 2034-46.
- Lue, N. F. (2010) 'Plasticity of telomere maintenance mechanisms in yeast', *Trends Biochem Sci*, 35(1), pp. 8-17.
- Lue, N. F., Chan, J., Wright, W. E. and Hurwitz, J. (2014) 'The CDC13-STN1-TEN1 complex stimulates Pol alpha activity by promoting RNA priming and primase-to-polymerase switch', *Nat Commun*, 5, p. 5762.
- Lue, N. F., Zhou, R., Chico, L., Mao, N., Steinberg-Neifach, O. and Ha, T. (2013) 'The Telomere Capping Complex CST Has an Unusual Stoichiometry,

- Makes Multipartite Interaction with G-Tails, and Unfolds Higher-Order G-Tail Structures', *PLoS Genet*, 9(1), p. e1003145.
- Luke, B. and Lingner, J. (2009) 'TERRA: telomeric repeat-containing RNA', *EMBO J*, 28(17), pp. 2503-10.
- Luke, B., Panza, A., Redon, S., Iglesias, N., Li, Z. and Lingner, J. (2008) 'The Rat1p 5' to 3' exonuclease degrades telomeric repeat-containing RNA and promotes telomere elongation in *Saccharomyces cerevisiae*', *Mol Cell*, 32(4), pp. 465-77.
- Lundblad, V. and Blackburn, E. H. (1993) 'An alternative pathway for yeast telomere maintenance rescues est1- senescence', *Cell*, 73(2), pp. 347-60.
- Lydall, D. (2003) 'Hiding at the ends of yeast chromosomes: telomeres, nucleases and checkpoint pathways', *J Cell Sci*, 116(20), pp. 4057-65.
- Lydall, D. (2009) 'Taming the tiger by the tail: modulation of DNA damage responses by telomeres', *EMBO J*, 28(15), pp. 2174-87.
- Lydall, D., Nikolsky, Y., Bishop, D. K. and Weinert, T. (1996) 'A meiotic recombination checkpoint controlled by mitotic checkpoint genes', *Nature*, 383(6603), pp. 840-3.
- Lydall, D. and Weinert, T. (1995) 'Yeast checkpoint genes in DNA damage processing: implications for repair and arrest', *Science*, 270(5241), pp. 1488-91.
- Ma, J. L., Lee, S. J., Duong, J. K. and Stern, D. F. (2006) 'Activation of the checkpoint kinase Rad53 by the phosphatidylinositol kinase-like kinase Mec1', *J Biol Chem*, 281(7), pp. 3954-63.
- Makovets, S., Williams, T. L. and Blackburn, E. H. (2008) 'The telotype defines the telomere state in *Saccharomyces cerevisiae* and is inherited as a dominant non-Mendelian characteristic in cells lacking telomerase', *Genetics*, 178(1), pp. 245-57.
- Mangino, M., Hwang, S. J., Spector, T. D., Hunt, S. C., Kimura, M., Fitzpatrick, A. L., Christiansen, L., Petersen, I., Elbers, C. C., Harris, T., Chen, W., Srinivasan, S. R., Kark, J. D., Benetos, A., El Shamieh, S., Visvikis-Siest, S., Christensen, K., Berenson, G. S., Valdes, A. M., Vinuela, A., Garcia, M., Arnett, D. K., Broeckel, U., Province, M. A., Pankow, J. S., Kammerer, C., Liu, Y., Nalls, M., Tishkoff, S., Thomas, F., Ziv, E., Psaty, B. M., Bis, J. C., Rotter, J. I., Taylor, K. D., Smith, E., Schork, N. J., Levy, D. and Aviv, A. (2012) 'Genome-wide meta-analysis points to CTC1 and ZNF676 as genes regulating telomere homeostasis in humans', *Hum Mol Genet*, 21(24), pp. 5385-94.
- Maniar, H. S., Wilson, R. and Brill, S. J. (1997) 'Roles of replication protein-A subunits 2 and 3 in DNA replication fork movement in *Saccharomyces cerevisiae*', *Genetics*, 145(4), pp. 891-902.
- Maringele, L. and Lydall, D. (2004) 'Exo1 plays a role in generating Type I and Type II survivors in budding yeast', *Genetics*, 166(4), pp. 1641-1649

- Martina, M., Bonetti, D., Villa, M., Lucchini, G. and Longhese, M. P. (2014) 'Saccharomyces cerevisiae Rif1 cooperates with MRX-Sae2 in promoting DNA-end resection', *EMBO Rep*, 15(6), pp. 695-704.
- Martina, M., Clerici, M., Baldo, V., Bonetti, D., Lucchini, G. and Longhese, M. P. (2012) 'A balance between Tel1 and Rif2 activities regulates nucleolytic processing and elongation at telomeres', *Mol Cell Biol*, 32(9), pp. 1604-17.
- Mason, M., Wanat, J. J., Harper, S., Schultz, David C., Speicher, D. W., Johnson, F. B. and Skordalakes, E. (2013) 'Cdc13 OB2 Dimerization Required for Productive Stn1 Binding and Efficient Telomere Maintenance', *Structure*, 21, pp. 109-20.
- Mattarocci, S., Shyian, M., Lemmens, L., Damay, P., Altintas, D. M., Shi, T., Bartholomew, C. R., Thoma, N. H., Hardy, C. F. and Shore, D. (2014) 'Rif1 controls DNA replication timing in yeast through the PP1 phosphatase Glc7', *Cell Rep*, 7(1), pp. 62-9.
- McEachern, M. J. and Haber, J. E. (2006) 'Break-induced replication and recombinational telomere elongation in yeast', *Annu Rev Biochem*, 75, pp. 111-35.
- Meyerson, M., Counter, C. M., Eaton, E. N., Ellisen, L. W., Steiner, P., Caddle, S. D., Ziaugra, L., Beijersbergen, R. L., Davidoff, M. J., Liu, Q., Bacchetti, S., Haber, D. A. and Weinberg, R. A. (1997) 'hEST2, the Putative Human Telomerase Catalytic Subunit Gene, Is Up-Regulated in Tumor Cells and during Immortalization', *Cell*, 90(4), pp. 785-95.
- Mitchell, M. T., Smith, J. S., Mason, M., Harper, S., Speicher, D. W., Johnson, F. B. and Skordalakes, E. (2010) 'Cdc13 N-Terminal Dimerization, DNA Binding, and Telomere Length Regulation', *Mol Cell Biol*, 30(22), pp. 5325-34.
- Mitton-Fry, R. M., Anderson, E. M., Theobald, D. L., Glustrom, L. W. and Wuttke, D. S. (2004) 'Structural basis for telomeric single-stranded DNA recognition by yeast Cdc13', *J Mol Biol*, 338(2), pp. 241-55.
- Miyake, Y., Nakamura, M., Nabetani, A., Shimamura, S., Tamura, M., Yonehara, S., Saito, M. and Ishikawa, F. (2009) 'RPA-like Mammalian Ctc1-Stn1-Ten1 Complex Binds to Single-Stranded DNA and Protects Telomeres Independently of the Pot1 Pathway', *Mol Cell*, 36(2), pp. 193-206.
- Muntoni, A., Neumann, A. A., Hills, M. and Reddel, R. R. (2009) 'Telomere elongation involves intra-molecular DNA replication in cells utilizing alternative lengthening of telomeres', *Hum Mol Genet*, 18(6), pp. 1017-27.
- Nakamura, T. M., Morin, G. B., Chapman, K. B., Weinrich, S. L., Andrews, W. H., Lingner, J., Harley, C. B. and Cech, T. R. (1997) 'Telomerase catalytic subunit homologs from fission yeast and human', *Science*, 277(5328), pp. 955-9.
- Needham, B. L., Rehkopf, D., Adler, N., Gregorich, S., Lin, J., Blackburn, E. H. and Epel, E. S. (2015) 'Leukocyte telomere length and mortality in the National Health and Nutrition Examination Survey, 1999-2002', *Epidemiology*, 26(4), pp. 528-35.

- Ng, L. J., Cropley, J. E., Pickett, H. A., Reddel, R. R. and Suter, C. M. (2009) 'Telomerase activity is associated with an increase in DNA methylation at the proximal subtelomere and a reduction in telomeric transcription', *Nucleic Acids Res*, 37(4), pp. 1152-9.
- Ngo, H.-P. and Lydall, D. (2010) 'Survival and Growth of Yeast without Telomere Capping by Cdc13 in the Absence of Sgs1, Exo1, and Rad9', *PLoS Genet*, 6(8), p. e1001072.
- Ngo, H.-P. and Lydall, D. (2015) 'The 9-1-1 checkpoint clamp coordinates resection at DNA double strand breaks', *Nucleic Acids Res*, 43(10), pp. 5017-32.
- Nugent, C. I., Hughes, T. R., Lue, N. F. and Lundblad, V. (1996) 'Cdc13p: a single-strand telomeric DNA-binding protein with a dual role in yeast telomere maintenance', *Science*, 274(5285), pp. 249-52.
- Olovnikov, A. M. (1973) 'A theory of marginotomy. The incomplete copying of template margin in enzymic synthesis of polynucleotides and biological significance of the phenomenon', *J Theor Biol*, 41(1), pp. 181-90.
- Ornish, D., Lin, J., Chan, J. M., Epel, E., Kemp, C., Weidner, G., Marlin, R., Frenda, S. J., Magbanua, M. J., Daubenmier, J., Estay, I., Hills, N. K., Chainani-Wu, N., Carroll, P. R. and Blackburn, E. H. (2013) 'Effect of comprehensive lifestyle changes on telomerase activity and telomere length in men with biopsy-proven low-risk prostate cancer: 5-year follow-up of a descriptive pilot study', *Lancet Oncol*, 14(11), pp. 1112-20.
- Palm, W. and de Lange, T. (2008) 'How shelterin protects mammalian telomeres', *Annu Rev Genet*, 42, pp. 301-34.
- Paques, F. and Haber, J. E. (1999) 'Multiple pathways of recombination induced by double-strand breaks in *Saccharomyces cerevisiae*', *Microbiol Mol Biol Rev*, 63(2), pp. 349-404.
- Park, J., Kang, M. and Kim, M. (2015) 'Unraveling the mechanistic features of RNA polymerase II termination by the 5'-3' exoribonuclease Rat1', *Nucleic Acids Res*, 43(5), pp. 2625-37.
- Paull, T. T. and Gellert, M. (1998) 'The 3' to 5' exonuclease activity of Mre 11 facilitates repair of DNA double-strand breaks', *Mol Cell*, 1(7), pp. 969-79.
- Paulovich, A. G., Margulies, R. U., Garvik, B. M. and Hartwell, L. H. (1997) 'RAD9, RAD17, and RAD24 are required for S phase regulation in *Saccharomyces cerevisiae* in response to DNA damage', *Genetics*, 145(1), pp. 45-62.
- Pennock, E., Buckley, K. and Lundblad, V. (2001) 'Cdc13 delivers separate complexes to the telomere for end protection and replication', *Cell*, 104(3), pp. 387-96.
- Peterson, S. E., Stellwagen, A. E., Diede, S. J., Singer, M. S., Haimberger, Z. W., Johnson, C. O., Tzoneva, M. and Gottschling, D. E. (2001) 'The function of

a stem-loop in telomerase RNA is linked to the DNA repair protein Ku', *Nat Genet*, 27(1), pp. 64-7.

Petreaca, R. C., Chiu, H. C., Eckelhoefer, H. A., Chuang, C., Xu, L. and Nugent, C. I. (2006) 'Chromosome end protection plasticity revealed by Stn1p and Ten1p bypass of Cdc13p', *Nat Cell Biol*, 8(7), pp. 748-55.

Petreaca, R. C., Chiu, H. C. and Nugent, C. I. (2007) 'The role of Stn1p in *Saccharomyces cerevisiae* telomere capping can be separated from its interaction with Cdc13p', *Genetics*, 177(3), pp. 1459-74.

Pfingsten, J. S., Goodrich, K. J., Taabazuing, C., Ouenzar, F., Chartrand, P. and Cech, T. R. (2012) 'Mutually exclusive binding of telomerase RNA and DNA by Ku alters telomerase recruitment model', *Cell*, 148(5), pp. 922-32.

Plate, I., Hallwyl, S. C., Shi, I., Krejci, L., Muller, C., Albertsen, L., Sung, P. and Mortensen, U. H. (2008) 'Interaction with RPA is necessary for Rad52 repair center formation and for its mediator activity', *J Biol Chem*, 283(43), pp. 29077-85.

Polotnianka, R. M., Li, J. and Lustig, A. J. (1998) 'The yeast ku heterodimer is essential for protection of the telomere against nucleolytic and recombinational activities', *Curr Biol*, 8(14), pp. 831-4.

Polvi, A., Linnankivi, T., Kivela, T., Herva, R., Keating, J. P., Makitie, O., Pareyson, D., Vainionpaa, L., Lahtinen, J., Hovatta, I., Pihko, H. and Lehesjoki, A. E. (2012) 'Mutations in CTC1, encoding the CTS telomere maintenance complex component 1, cause cerebrotelomeric microangiopathy with calcifications and cysts', *Am J Hum Genet*, 90(3), pp. 540-9.

Puglisi, A., Bianchi, A., Lemmens, L., Damay, P. and Shore, D. (2008) 'Distinct roles for yeast Stn1 in telomere capping and telomerase inhibition', *EMBO J*, 27(17), pp. 2328-39.

Qi, H. and Zakian, V. A. (2000) 'The *Saccharomyces* telomere-binding protein Cdc13p interacts with both the catalytic subunit of DNA polymerase alpha and the telomerase-associated est1 protein', *Genes Dev*, 14(14), pp. 1777-88.

Ribeyre, C. and Shore, D. (2012) 'Anticheckpoint pathways at telomeres in yeast', *Nat Struct Mol Biol*, 19(3), pp. 307-13.

Rode, L., Nordestgaard, B. G. and Bojesen, S. E. (2015) 'Peripheral blood leukocyte telomere length and mortality among 64,637 individuals from the general population', *J Natl Cancer Inst*, 107(6), p. djv074.

Romaniello, R., Arrigoni, F., Citterio, A., Tonelli, A., Sforzini, C., Rizzari, C., Pessina, M., Triulzi, F., Bassi, M. T. and Borgatti, R. (2012) 'Cerebrotelomeric Microangiopathy With Calcifications and Cysts Associated With CTC1 and NDP Mutations', *J Child Neurol*, 28(12), pp. 1702-8.

Romano, G. H., Harari, Y., Yehuda, T., Podhorzer, A., Rubinstein, L., Shamir, R., Gottlieb, A., Silberberg, Y., Pe'er, D., Ruppin, E., Sharan, R. and Kupiec, M. (2013) 'Environmental stresses disrupt telomere length homeostasis', *PLoS Genet*, 9(9), p. e1003721.

- Roy, R., Meier, B., McAinsh, A. D., Feldmann, H. M. and Jackson, S. P. (2004) 'Separation-of-function Mutants of Yeast Ku80 Reveal a Yku80p-Sir4p Interaction Involved in Telomeric Silencing', *J Biol Chem*, 279(1), pp. 86-94.
- Sanders, J. L. and Newman, A. B. (2013) 'Telomere Length in Epidemiology: A Biomarker of Aging, Age-Related Disease, Both, or Neither?', *Epidemiol Rev*, 35(1), pp. 112-31.
- Savage, S. A. (2012) 'Connecting complex disorders through biology', *Nat Genet*, 44(3), pp. 238-40.
- Schramke, V., Luciano, P., Brevet, V., Guillot, S., Corda, Y., Longhese, M. P., Gilson, E. and Geli, V. (2004) 'RPA regulates telomerase action by providing Est1p access to chromosome ends', *Nat Genet*, 36(1), pp. 46-54.
- Shi, T., Bunker, R. D., Mattarocci, S., Ribeyre, C., Faty, M., Gut, H., Scrima, A., Rass, U., Rubin, S. M., Shore, D. and Thoma, N. H. (2013) 'Rif1 and Rif2 shape telomere function and architecture through multivalent Rap1 interactions', *Cell*, 153(6), pp. 1340-53.
- Siede, W., Friedberg, A. S., Dianova, I. and Friedberg, E. C. (1994) 'Characterization of G1 checkpoint control in the yeast *Saccharomyces cerevisiae* following exposure to DNA-damaging agents', *Genetics*, 138(2), pp. 271-81.
- Siede, W., Friedberg, A. S. and Friedberg, E. C. (1993) 'RAD9-dependent G1 arrest defines a second checkpoint for damaged DNA in the cell cycle of *Saccharomyces cerevisiae*', *Proc Natl Acad Sci U S A*, 90(17), pp. 7985-9.
- Silverman, J., Takai, H., Buonomo, S. B., Eisenhaber, F. and de Lange, T. (2004) 'Human Rif1, ortholog of a yeast telomeric protein, is regulated by ATM and 53BP1 and functions in the S-phase checkpoint', *Genes Dev*, 18(17), pp. 2108-19.
- Singer, M. S. and Gottschling, D. E. (1994) 'TLC1: template RNA component of *Saccharomyces cerevisiae* telomerase', *Science*, 266(5184), pp. 404-9.
- Song, X., Leehy, K., Warrington, R. T., Lamb, J. C., Surovtseva, Y. V. and Shippen, D. E. (2008) 'STN1 protects chromosome ends in *Arabidopsis thaliana*', *Proc Natl Acad Sci U S A*, 105(50), pp. 19815-20.
- Sreesankar, E., Senthilkumar, R., Bharathi, V., Mishra, R. K. and Mishra, K. (2012) 'Functional diversification of yeast telomere associated protein, Rif1, in higher eukaryotes', *BMC Genomics*, 13, p. 255.
- Stellwagen, A. E., Haimberger, Z. W., Veatch, J. R. and Gottschling, D. E. (2003) 'Ku interacts with telomerase RNA to promote telomere addition at native and broken chromosome ends', *Genes Dev*, 17(19), pp. 2384-95.
- Stewart, J. A., Wang, F., Chaiken, M. F., Kasbek, C., Chastain, P. D., 2nd, Wright, W. E. and Price, C. M. (2012) 'Human CST promotes telomere duplex replication and general replication restart after fork stalling', *EMBO J*, 31(17), pp. 3537-49.

Strandberg, T. E., Strandberg, A. Y., Saijonmaa, O., Tilvis, R. S., Pitkala, K. H. and Fyhrquist, F. (2012) 'Association between alcohol consumption in healthy midlife and telomere length in older men. The Helsinki Businessmen Study', *Eur J Epidemiol*, 27(10), pp. 815-22.

Sugiyama, T. and Kantake, N. (2009) 'Dynamic regulatory interactions of rad51, rad52, and replication protein-a in recombination intermediates', *J Mol Biol*, 390(1), pp. 45-55.

Sun, J., Yang, Y., Wan, K., Mao, N., Yu, T. Y., Lin, Y. C., Dezwaan, D. C., Freeman, B. C., Lin, J. J., Lue, N. F. and Lei, M. (2011) 'Structural bases of dimerization of yeast telomere protein Cdc13 and its interaction with the catalytic subunit of DNA polymerase  $\alpha$ ', *Cell Res*, 21(2), pp. 258-74.

Sun, J., Yu, E. Y., Yang, Y., Confer, L. A., Sun, S. H., Wan, K., Lue, N. F. and Lei, M. (2009) 'Stn1-Ten1 is an Rpa2-Rpa3-like complex at telomeres', *Genes Dev*, 23(24), pp. 2900-14.

Surovtseva, Y. V., Churikov, D., Boltz, K. A., Song, X., Lamb, J. C., Warrington, R., Leahy, K., Heacock, M., Price, C. M. and Shippen, D. E. (2009) 'Conserved Telomere Maintenance Component 1 Interacts with STN1 and Maintains Chromosome Ends in Higher Eukaryotes', *Mol Cell*, 36(2), pp. 207-18.

Sweeney, F. D., Yang, F., Chi, A., Shabanowitz, J., Hunt, D. F. and Durocher, D. (2005) 'Saccharomyces cerevisiae Rad9 acts as a Mec1 adaptor to allow Rad53 activation', *Curr Biol*, 15(15), pp. 1364-75.

Symington, L. S. (2002) 'Role of RAD52 epistasis group genes in homologous recombination and double-strand break repair', *Microbiol Mol Biol Rev*, 66(4), pp. 630-70.

Theobald, D. L. and Wuttke, D. S. (2004) 'Prediction of multiple tandem OB-fold domains in telomere end-binding proteins Pot1 and Cdc13', *Structure*, 12(10), pp. 1877-9.

Tong, A. H. and Boone, C. (2006) 'Synthetic genetic array analysis in Saccharomyces cerevisiae', *Methods Mol Biol*, 313(1), pp. 171-92.

Tong, A. H., Evangelista, M., Parsons, A. B., Xu, H., Bader, G. D., Pagé, N., Robinson, M., Raghibizadeh, S., Hogue, C. W., Bussey, H., Andrews, B., Tyers, M. and Boone, C. (2001) 'Systematic genetic analysis with ordered arrays of yeast gene deletion mutants', *Science*, 295(5550), pp. 2364-8

Tran, P. T., Erdeniz, N., Dudley, S. and Liskay, R. M. (2002) 'Characterization of nuclease-dependent functions of Exo1p in Saccharomyces cerevisiae', *DNA Repair (Amst)*, 1(11), pp. 895-912.

Tsubouchi, H. and Ogawa, H. (2000) 'Exo1 roles for repair of DNA double-strand breaks and meiotic crossing over in Saccharomyces cerevisiae', *Mol Biol Cell*, 11(7), pp. 2221-33.

van den Bosch, M., Bree, R. T. and Lowndes, N. F. (2003) 'The MRN complex: coordinating and mediating the response to broken chromosomes', *EMBO Rep*, 4(9), pp. 844-9.

- Verde, Z., Reinoso-Barbero, L., Chicharro, L., Garatachea, N., Resano, P., Sanchez-Hernandez, I., Rodriguez Gonzalez-Moro, J. M., Bandres, F., Santiago, C. and Gomez-Gallego, F. (2015) 'Effects of cigarette smoking and nicotine metabolite ratio on leukocyte telomere length', *Environ Res*, 140, pp. 488-94.
- Walker, J. R., Corpina, R. A. and Goldberg, J. (2001) 'Structure of the Ku heterodimer bound to DNA and its implications for double-strand break repair', *Nature*, 412(6847), pp. 607-14.
- Walne, A. J., Bhagat, T., Kirwan, M., Gitiaux, C., Desguerre, I., Leonard, N., Nogales, E., Vulliamy, T. and Dokal, I. S. (2013) 'Mutations in the telomere capping complex in bone marrow failure and related syndromes', *Haematologica*, 98(3), pp. 334-8.
- Wan, M., Qin, J., Songyang, Z. and Liu, D. (2009) 'OB fold-containing protein 1 (OBFC1), a human homolog of yeast Stn1, associates with TPP1 and is implicated in telomere length regulation', *J Biol Chem*, 284(39), pp. 26725-31.
- Wang, F., Stewart, J. A., Kasbek, C., Zhao, Y., Wright, W. E. and Price, C. M. (2012) 'Human CST has independent functions during telomere duplex replication and C-strand fill-in', *Cell Rep*, 2(5), pp. 1096-103.
- Watson, J. D. (1972) 'Origin of concatemeric T7 DNA', *Nat New Biol*, 239(94), pp. 197-201.
- Weinert, T. A. and Hartwell, L. (1989) 'Control of G2 delay by the rad9 gene of *Saccharomyces cerevisiae*', *J Cell Sci Suppl*, 12, pp. 145-8.
- Weinert, T. A. and Hartwell, L. H. (1988) 'The RAD9 gene controls the cell cycle response to DNA damage in *Saccharomyces cerevisiae*', *Science*, 241(4863), pp. 317-22.
- Weischer, M., Nordestgaard, B. G., Cawthon, R. M., Freiberg, J. J., Tybjaerg-Hansen, A. and Bojesen, S. E. (2013) 'Short telomere length, cancer survival, and cancer risk in 47102 individuals', *J Natl Cancer Inst*, 105(7), pp. 459-68.
- Wotton, D. and Shore, D. (1997) 'A novel Rap1p-interacting factor, Rif2p, cooperates with Rif1p to regulate telomere length in *Saccharomyces cerevisiae*', *Genes Dev*, 11(6), pp. 748-60.
- Wu, Y., Kantake, N., Sugiyama, T. and Kowalczykowski, S. C. (2008) 'Rad51 protein controls Rad52-mediated DNA annealing', *J Biol Chem*, 283(21), pp. 14883-92.
- Wu, Y. and Zakian, V. A. (2011) 'The telomeric Cdc13 protein interacts directly with the telomerase subunit Est1 to bring it to telomeric DNA ends in vitro', *Proc Natl Acad Sci U S A*, 108(51), pp. 20362-9.
- Xu, D., Muniandy, P., Leo, E., Yin, J., Thangavel, S., Shen, X., Li, M., Agama, K., Guo, R., Fox, D., 3rd, Meetei, A. R., Wilson, L., Nguyen, H., Weng, N. P., Brill, S. J., Li, L., Vindigni, A., Pommier, Y., Seidman, M. and Wang, W. (2010) 'Rif1 provides a new DNA-binding interface for the Bloom syndrome complex to maintain normal replication', *EMBO J*, 29(18), pp. 3140-55.



Xue, Y., Rushton, M. D. and Maringele, L. (2011) 'A novel checkpoint and RPA inhibitory pathway regulated by Rif1', *PLoS Genet*, 7(12), p. e1002417.

Yu, T. Y., Kao, Y. W. and Lin, J. J. (2014) 'Telomeric transcripts stimulate telomere recombination to suppress senescence in cells lacking telomerase', *Proc Natl Acad Sci U S A*, 111(9), pp. 3377-82.

Zappulla, D. C., Goodrich, K. J., Arthur, J. R., Gurski, L. A., Denham, E. M., Stellwagen, A. E. and Cech, T. R. (2011) 'Ku can contribute to telomere lengthening in yeast at multiple positions in the telomerase RNP', *RNA*, 17(2), pp. 298-311.

Zubko, M. K., Guillard, S. and Lydall, D. (2004) 'Exo1 and Rad24 differentially regulate generation of ssDNA at telomeres of *Saccharomyces cerevisiae* cdc13-1 mutants', *Genetics*, 168(1), pp. 103-15.

Zubko, M. K. and Lydall, D. (2006) 'Linear chromosome maintenance in the absence of essential telomere-capping proteins', *Nat Cell Biol*, 8(7), pp. 734-40.